LEABHARLANN CHOLÁISTE NA TRÍONÓIDE, BAILE ÁTHA CLIATH | TRINITY COLLEGE LIBRARY DUBLIN
Ollscoil Átha Cliath | The University of Dublin

Terms and Conditions of Use of Digitised Theses from Trinity College Library Dublin

Copyright statement

All material supplied by Trinity College Library is protected by copyright (under the Copyright and Related Rights Act, 2000 as amended) and other relevant Intellectual Property Rights. By accessing and using a Digitised Thesis from Trinity College Library you acknowledge that all Intellectual Property Rights in any Works supplied are the sole and exclusive property of the copyright and/or other IPR holder. Specific copyright holders may not be explicitly identified. Use of materials from other sources within a thesis should not be construed as a claim over them.

A non-exclusive, non-transferable licence is hereby granted to those using or reproducing, in whole or in part, the material for valid purposes, providing the copyright owners are acknowledged using the normal conventions. Where specific permission to use material is required, this is identified and such permission must be sought from the copyright holder or agency cited.

Liability statement

By using a Digitised Thesis, I accept that Trinity College Dublin bears no legal responsibility for the accuracy, legality or comprehensiveness of materials contained within the thesis, and that Trinity College Dublin accepts no liability for indirect, consequential, or incidental, damages or losses arising from use of the thesis for whatever reason. Information located in a thesis may be subject to specific use constraints, details of which may not be explicitly described. It is the responsibility of potential and actual users to be aware of such constraints and to abide by them. By making use of material from a digitised thesis, you accept these copyright and disclaimer provisions. Where it is brought to the attention of Trinity College Library that there may be a breach of copyright or other restraint, it is the policy to withdraw or take down access to a thesis while the issue is being resolved.

Access Agreement

By using a Digitised Thesis from Trinity College Library you are bound by the following Terms & Conditions. Please read them carefully.

I have read and I understand the following statement: All material supplied via a Digitised Thesis from Trinity College Library is protected by copyright and other intellectual property rights, and duplication or sale of all or part of any of a thesis is not permitted, except that material may be duplicated by you for your research use or for educational purposes in electronic or print form providing the copyright owners are acknowledged using the normal conventions. You must obtain permission for any other use. Electronic or print copies may not be offered, whether for sale or otherwise to anyone. This copy has been supplied on the understanding that it is copyright material and that no quotation from the thesis may be published without proper acknowledgement.

Effect of intranasal administration of Semliki Forest virus recombinant particles expressing interferon-beta on the progression of experimental autoimmune encephalomyelitis

A thesis submitted to the University of Dublin, Trinity College

for the Degree of Doctor of Philosophy

by

Kathrina Quinn

Department of Microbiology,

Moyne Institute of Preventive Medicine,

Trinity College, Dublin

April 2006

TRINITY COLLEGE
13 NOV 2006
LIBRARY DUBLIN
THESIS
7983

For my parents

This thesis is submitted by the undersigned to the University of Dublin, Trinity College for the examination of Doctorate of Philosophy. The work herein is entirely my own work and has not been submitted as an exercise for a degree to any other university. The librarian of Trinity College Dublin has my permission to lend or copy this thesis upon request.

Kathrina Quinn

Kathrina Quinn

Firstly I would like to sincerely thank my supervisor Prof. Greg Atkins for all his help and support throughout my project. Even when times were tough, Greg was always available to offer reassurance and advice, and comfort when I was feeling a bit tearful over accidentally defrosted –70°C freezers and missing mouse orders… his office door was always open. I must also acknowledge the kindness of his wife, Chris, for welcoming me into her home for the summer barbecue every year. I would also like to sincerely thank Prof. Brian Sheahan for all his help with the pathological analysis of my perfused sections, and for instilling in me a true appreciation for histology which I will always have. Your help and advice was invaluable.

To my co-supervisor, Dr. Sareen Galbraith, I express my deepest appreciation. Sareen, you always steered me in the right direction, offering much needed technical advice and helping me, without hesitation, when I needed someone to hold my mice, edit my reports and listen to my talks. Not only are you a fantastic scientist and teacher, you are also a very precious friend and someone that I hope I will always be in contact with.

Dot, you're a star! Always keeping me updated on the lab goings on when I am not around and filling me up with chocolate when I am! I am going to miss our chats. Thanks so much for looking after me for the last four years. Will you come to America with me?? Speaking of shining stars, another huge thank you to Alex-Whelan Buckley without whose expertise in all things immunohistochemical, I would have been lost.

I would like to say a big thank you to the post docs in our lab – Dr. Marina Fleeton and Dr. Barbara Kelly. Marina, if my knowledge of immunology is ever as vast as yours, I will be a very happy camper! Thanks for all the advice both technical and personal. I wish you all the best both in your career as a scientist and as a mother. Barbara, what can I say??? I am so glad that we had the opportunity to become such great friends and create a little scandal and mayhem whenever we could. I will always remember your help with my viva talk but mostly I will our girly chats, your good advice and all the crazy nights out together like the trip to France, Christopher's viva night, the MicroSoc BBQ…. the list is endless but long may they last! Hope to see you in D.C… While I am acknowledging our fabulous post docs, I must also mention Dr. Margaret Morris-Downes, the queen of EAE, for all her help and advice in setting up the disease model.

To Paddy, Joe and the rest of the staff in the prep room, without you I seriously think the Moyne would fall down. Thank you for providing me with autoclaved glassware and CO_2 cylinders at a moment's notice and for never minding when I let the DI H_2O overflow….

I don't even know where to begin in acknowledging all the other Ph.D students who have passed through the lab during my time here...it was a complete privilege to work with each and everyone of you. I guess the best place to begin is at the very start. Christopher, again what can I say.. thanks for always, always being there, whether I was having a crisis at work or just in general, even now when you are far away, you are still helping me. You are a truly great friend and one I hope I keep forever. I wish you and Ana all the very best in the future. Jamie and Alan, thank you both for making my time in the lab so full of fun and booze!! There was never a dull moment with you guys in the lab, between pub crawls and parties, conferences and general impromptu sessions, I will certainly never forget our trip to Edinburgh...Another big thank you to Alan for helping me set up the EAE model.

Gowda, thank you for being such a gentleman and for always telling me that I was the most cool headed person in the lab, even though we both know that it's not true!! Every time I hear Punjabi MC, I think of you dancing on a table in the Pembroke at our first lab Christmas party. Frances, I am so glad to have shared the Ph.D experience with you, from start to finish. It was great to be able to confide in someone who understood exactly how I was feeling. I consider you a lot more than a lab colleague, I consider you a great friend. Sara, again I am stuck for words, you are like a breath of fresh air, always so kind and helpful to me and others. It was a complete pleasure to share a lab with you. Thank you so much for always being on hand to mail, photocopy, collect or check something for me when I wasn't in Dublin. Keep in touch!! A big thank you to Jerry also for his infectious laugh. John, I didn't forget you!! How could I when you give so much of yourself to make others happy. You are a true gent and so easy going and thoughtful. Last but certainly not least, are the most recent additions to the lab, Guniz and Frank. Guniz, you know I think the world of you. I was so happy to see you returning to the lab to pursue your Ph.D after the summer months you spent with us (at least we didn't scare you off!!). You add a sense of calm and serenity to the lab that is sometimes badly needed… don't ever change. Unfortunately Frank, I can't say the same about you!! You are the opposite but in the best possible way, so much fun to be around and always so obliging, I just wish you were around when I was in the lab. Keep up the dancing, and the sleeping on couches/floors… I certainly will!!

A huge thank you to everyone in the Moyne but in particular to Jenny and David (who technically is not in the Moyne!). Jenny, I am so glad to still be in contact with you after two years and am looking forward to catching up soon. I really missed my gig buddy when you left the Moyne but soon realized that no matter how far you go, true friends always seem close by. David, though I have only gotten to know you well over the last

year or so, I treasure every single drinking session we had together, particularly the trip to France and your wedding!! I wish you and Sorcha all the happiness and success in your lives together. You make a great couple.

It is easy to forget the friends who were not based in the Moyne… Liz and Connie, I bet you feel like you have done a Ph.D after listening to me banging on about it for the last four years. What did I do to deserve such loyal friends?? Thanks for all the coffee breaks and the listening. Eleanor, Fiona and Ailbhe (and Baby the fish), thanks a million for all the pep talks and gossip, living with you guys was fantastic, you were the best housemates a girl could ask for. Miss you loads!

Lisa, Morgan and baby Sienna Rose…. you were a very welcome distraction in my life from all things scientific, thank you so much for knowing absolutely nothing about EAE but listening to me all the same. You were, and are, a great support to me.

To my sister Sinead, what can I say?? Thanks for all the visits and the treats. I loved the way I could disappear to Brussels for a short break and return to Dublin more exhausted, but relaxed than when I left. You always seem to be able to make me completely forget my worries by introducing me to new experiences… like skiing… where admittedly you fared a lot better on the slopes than me! Thanks for the phone calls and for always being there.

To Mum and Dad, your constant support, encouragement and love is endless. I am blessed to have such supportive parents who are always there for me, emotionally and (sometimes!!!) financially. Constantly listening, worrying and advicing, without understanding a word of my thesis, you showed a huge interest in my work and always knew the right things to say. I owe you both so much, and more.

Multiple sclerosis (MS) is an autoimmune demyelinating disease of the CNS, characterized by the presence of sclerotic lesions throughout the brain. MS is thought to be a CD4+ T helper 1 disease caused by the infiltration of autoaggressive T cells which upregulate T helper-1 cytokines such as TNF-α and IFN-γ. Much success has been achieved in the treatment of Relapsing Remitting Multiple Sclerosis (RRMS). It is thought that the antiproliferative activity of IFN-β may inhibit the expansion of the autoaggressive T cells in MS, therefore limiting disease progression.

Semliki Forest Virus (SFV) is an arthropod-borne Alphavirus which has been engineered as a vector system for delivery to the CNS. This expression system is based on the full-length cDNA clone of SFV, in which the coding region of the 26S structural genes has been deleted and replaced with a multiple cloning site (MCS) to allow insertion of a heterologous gene. The non-structural coding region is preserved for production of the non-structural P1-4 replicase. A two-helper system provides the structural genes necessary for packaging of the recombinant virion. These genes, the capsid and spike genes are supplied *in trans* from two separate helper RNA molecules, which decreases the possibility of wild type virus production. When all three RNAs are *in vitro* transcribed and electroporated into BHK-21 cells, recombinant particles expressing the heterologous gene are produced. On infection, these SFV particles undergo one round of infection and replication resulting in transient expression of the gene of interest.

Recombinant Semliki Forest virus (rSFV) particles have been successfully developed as a treatment for Experimental Autoimmune Encephalomyelitis (EAE), which is an animal model of MS. EAE is induced in mice by immunization with myelin antigens such as myelin basic protein (MBP), proteolipid protein (PLP) and myelin oligodendrocyte glycoprotein (MOG) resulting in the production of auto-reactive T lymphocytes. Like MS, EAE is characterized by cellular infiltration of these autoreactive T cells and other immune cells into the CNS leading to an inflammatory, demyelinating response. Variations on the type of animal strain, immunizing antigen and immunization protocol used, results in either acute or chronic relapsing forms of EAE. Initial studies examined the feasibility of using the rSFV split helper system as a CNS vector through the administration of an EGFP expressing recombinant vector. This vector showed good penetration of the CNS, subsequent to which, an SFV vector expressing IL-10 was constructed and used

successfully in the treatment of EAE. This study continues to examine the efficacy of rSFV vectors in the treatment of EAE through the intranasal administration (i.n.) rSFV particles expressing IFN-β. Two different SFV vectors were chosen for cloning of IFN-β, pSFV1 and pSFV10-E. IFN-β was cloned from SFV-infected mouse brain by RT-PCR into pSFV1, and then subcloned into pSFV10-E. Recombinant SFV particles expressing IFN-β (rSFV-IFN-β) were prepared from both rSFV-IFN-β vectors. Expression studies using immunohistochemistry and viral inhibition assay confirmed increased expression of IFN-β *in vitro*. Expression levels were greater with rSFV10-E-IFN-β particles, than with rSFV1-IFN-β, due to the presence of a translational enhancer sequence upstream of the cloned gene that gives increased protein production. *In vivo* expression was confirmed following intranasal inoculation, by excision and homogenization of CNS tissue and detection of IFN-β levels in the tissue homogenate supernatant by ELISA. High-level expression was seen in both the olfactory bulbs and the spinal cord of rSFV-IFN-β treated animals. rSFV-IFN-β particles were then administered i.n. to C57/Bl6 mice that had been induced for EAE using the encephalogenic peptide MOG 35-55. Progression of EAE was measured by clinical score, weight loss, and pathology. Inhibition of disease with rSFV-IFN-β particles was dependent on the number and timing of treatments. Fewer treatments, given before the effector stage, led to improvement in clinical and pathology scores, decreased number of B lymphocytes in the CNS lesions, decreased ability of splenocytes to secrete interferon-gamma (IFN-γ) in response to MOG 35-55 and increased numbers of CD8+ cells in splenocyte populations. Treatment with empty rSFV particles moderately exacerbated EAE, as did continuous treatment with rSFV-IFN-β particles. Co-treatment with rSFV-IL-10 particles showed no significant improvement in disease severity, despite showing favourable T cell responses. Co-treatment with a vaccine adjuvant, Cholera Toxin (CT) showed more promising results. Animals experienced lower mean EAE scores than the controls during the treatment period. Despite the beneficial effect of CT, rSFV-IFN-β treatment alone still proved to be the best treatment option. It is concluded that the timing and frequency of intranasal administration of rSFV-IFN-β particles are critical to disease outcome with treatment prior to the effector stage being the most effective.

Abstracts

Quinn, K., S.E. Galbraith, B. J. Sheahan and G. J. Atkins. Treatment of experimental autoimmune encephalomyelitis using Semliki Forest virus vectors expressing interferon-β (2005). *Multiple Sclerosis* Vol 11-Supplement 1:S48

Presentations

1. Treatment of experimental autoimmune encephalomyelitis using Semliki Forest virus vectors expressing interferon-β. **Quinn, K.**, S.E. Galbraith, B. J. Sheahan and G. J. Atkins. Oral presentation at the 154th meeting of the Society for General Microbiology. University of Bath, England. 31st March 2004

2. Treatment of experimental autoimmune encephalomyelitis using Semliki Forest virus vectors expressing interferon-β. **Quinn, K.**, S.E. Galbraith, B. J. Sheahan and G. J. Atkins. Oral Presentation at the 4 th Symposium on Semliki Forest Virus. Tallinn, Estonia. 4th October 2004

3. Treatment of experimental autoimmune encephalomyelitis using Semliki Forest virus vectors expressing interferon-β. **Quinn, K.**, S.E. Galbraith, B. J. Sheahan and G. J. Atkins. Oral Presentation at the 2nd Annual Meeting of the British Society for Gene Therapy. Hulme hall, Manchester, England. 4th April 2005

4. Treatment of experimental autoimmune encephalomyelitis using Semliki Forest virus vectors expressing interferon-β. **Quinn, K.**, S.E. Galbraith, B. J. Sheahan and G. J. Atkins. Oral Presentation at the 6 th Symposium on Semliki Forest Virus. Trinity College, Dublin. 10th September 2005

5. Treatment of experimental autoimmune encephalomyelitis using Semliki Forest virus vectors expressing interferon-β. **Quinn, K.**, S.E. Galbraith, B. J. Sheahan and G. J. Atkins. Poster presentation at the 21th Congress of the European Committee for Treatment and Research in Multiple Sclerosis. Thessaloniki, Greece. 29th September 2005

a.a. – amino acid

Ab - antibody

Ag - antigen

APC- antigen presenting cells

ATCC – American type culture collection

BBB – blood brain barrier

BHK – baby hamster kidney

BDNF – brain derived neurotrophic factor

bp – base pair

BSA – bovine serum albumin

C – capsid

cDNA – complimentary DNA

CMV - cytomegalovirus

CNS - central nervous system

Con A- concanavalin A

CPE – cytopathic effect

CSF – cerebrospinal fluid

CT – Cholera toxin

CT-A – CT subunit A

CT-B - CT subunit B

CTL- cytotoxic T lymphocyte

CTLA4 - cytotoxic T lymphocyte–associated antigen 4

DAB – diaminobenzidine

DAPI – 4, -6, diamidino-2-phenylindole

DC – dendritic cells

DMA – disease modifying agents

DMEM – Dulbecco's minimal essential medium

DMSO - dimethylsulfoxide

DNA – deoxyribonucleic acid

dNTP – deoxynucleoside triphosphates

d.p.i - days post infection

dsDNA - double stranded deoxyribonucleic acid

dsRNA – double stranded ribonucleic acid

DTH – delayed-type hypersensitivity

DTT – Dithiotreitol

EAE – experimental autoimmune encephalomyelitis

EBV – Epstein barr virus

ECACC – European collection of animal cultures

EDSS - expanded disability status scale

EDTA - ethylenediaminetetra-acetic acid

EEE – eastern equine encephalitis

EGFP – enhanced green fluorescent protein

ELISA – enzyme linked immunosorbent assay

ER – endoplasmic reticulum

FACS – fluorescence activated cell sorter

FCS – foetal calf serum

FDA – food and drug authority of America

FMDV – foot and mouth disease virus

g - gravitational force

GFAP - glial fibrillary acidic protein

GA - glamiramer acetate

GLAST -

GLT - glutamate transporter

GM-CSF - granulocyte macrophage colony stimulating factor

h - hour

HBSS – Hank's Balanced Salt Solution

H&E – haematoxylin and eosin

hepes – N-2-hydroxyethyl-piperazine-N'-2-ethanesulphonic acid

HHV – human herpesvirus

HSV - herpes simplex virus

HIV – human immunodeficiency virus

HLA – human leukocyte antigen

H_2O_2 - hydrogen peroxide

h.p.i. – hours post infection

HRP – horseradish peroxidase

i.c. – intra-cranial

ICAM – intercellular adhesion molecule

I.E. – immediate early

IFA - incomplete freund's adjuvant

IFN – interferon

Ig – immunoglobulin

IL – interleukin

i.m. – intra-muscular

i.n. – intra-nasal

i.p. – intra-peritoneal

IU – infectious unit

i.v. – intra-venous

IVIG – intravenous immunoglobulin

LB – L broth

LIV – Louping Ill virus

LPS - lipopolysaccharide

LT - lymphotoxin

mAb – monoclonal antibody

MAG – myelin-associated glycoprotein

MBP – myelin basic protein

MCP – macrophage chemoattractant protein

MCS – multiple cloning site

MEM – minimal essential medium

MHC – major histocompatibility complex

MIP - macrophage inflammatory protein

MMP –matrix metalloproteinase

MOG – myelin oligodendrocyte glycoprotein

m.o.i. - multiplicity of infection

MRI – magnetic resonance imaging

mRNA – messenger RNA

MS – multiple sclerosis

NCS – normal calf serum

NK – Natural Killer cells

NO – nitric oxide

NP - nucleoprotein

NsP – non-structural protein

NTR – non-translated region

OAS - oligoadenylate synthetase

OCBs – oligoclonal bands

ORF – open reading frame

PBMC – Peripheral blood mononuclear cells

PBS – phosphate buffered saline

PCR – polymerase chain reaction

p.d.i – post disease induction

PFA - paraformaldehyde

p.f.u. – plaque forming units

PKR - protein kinase R

PLP – proteolipid protein

PML – progressive multifocal leukoencephalopathy

PNS – peripheral nervous system

PPMS – primary-progressive MS

PT – pertussis toxin

PRMS – progressive-relapsing MS

RANTES – regulated on activation, normal T-cell expressed and secreted

RBC – red blood cell

RBS – ribosomal binding site

RNA – ribonucleic acid

RNase – ribonuclease

r.p.m. – revolutions per minute

rIFN- recombinant IFN

rrIFN –recombinant rat IFN

RRMS – relapsing-remitting MS

rSFV – recombinant SFV

RT – room temperature

RT-PCR – reverse transcriptase- polymerase chain reaction

sBHK - 'Swedish' BHK

s.c. – subcutaneous

SCH – spinal cord homogenate

SCID – severe combined immunodeficient

SFV – Semliki Forest Virus

SIN – sindbis virus

SIV – simian immunodeficiency virus

SPMS – secondary-progressive MS

TGF – transforming growth factor

Th – T helper

TLR – toll like receptor

TNF – tumour necrosis factor

TRITC – rhodamine isothiocyanate

Tris - Tris-(hydroxymethyl)-aminomethane

tRNA – transfer RNA

VCAM – vascular cellular adhesion molecule

VEE – Venezulan equine encephalitis

VSV – vesicular stomatitis virus

Table of Contents

Declaration		**(i)**
Acknowledgements		**(ii)**
Summary		**(iii)**
Publications and presentations		**(iv)**
Abbreviations		**(v)**
Index of figures		**(vi)**
Index of tables		**(vii)**
1.	**General Introduction**	**1**
1.1	**Semliki Forest Virus**	**1**
1.1.1	Semliki Forest Virus - background	1
1.1.2	SFV virion	1
1.1.3	SFV genome	4
1.1.4	The life cycle of SFV	5
1.1.4.1	Viral entry	5
1.1.4.2	Viral replication	5
1.1.4.3	Processing of the structural proteins	6
1.1.4.4	Viral assembly, maturation and release	8
1.1.5	Effects of replication on infected cells	11
1.1.6	Immune response to SFV infection	12
1.1.7	SFV strains and CNS pathogenesis	13
1.2	**Semliki Forest Virus expression systems**	**16**
1.2.1	Background to SFV expression systems	16
1.2.2	SFV vectors in vaccine development	20
1.2.3	SFV vectors in tumour therapy	21
1.2.4	SFV as a vector for the CNS	22

1.3 Components of the Central Nervous System **24**
1.3.1 Neurons 24
1.3.2 Astrocytes 27
1.3.3 Microglial cells 28
1.3.4 Myelin 28
1.3.5 Oligodendrocytes 29
1.4 Multiple Sclerosis **30**
1.4.4 Background and classification of disease 30
1.4.2 Etiology of disease 32
1.4.3 Epidemiology 34
1.4.4 Immunology 36
1.4.5 Symptoms 40
1.4.6 Diagnosis 40
1.4.7 Disease modifying drugs in the treatment of MS 42
1.4.8 Immunosuppressive treatment 44
1.5 Experimental Autoimmune Encephalomyelitis **45**
1.5.1 EAE as a model of MS 45
1.5.2 The role of T and B lymphocytes in EAE 48
1.5.3 Role of cytokines in MS and EAE 50
1.5.4 The immunomodulatory effect of IFN-β on MS and EAE 53
1.5.5 Treatment of EAE with IFN-β 55
1.5.6 Treatment of EAE with viral vectors 57
1.5.7 Cholera toxin as an adjuvant in the treatment of EAE 59
1.6 Aims of study **60**

2. Cloning of IFN-β into SFV vectors and *in vitro* expression in different cell lines

2.1 Introduction **61**
2.2 Materials and methods **63**
2.2.1 Materials 63
2.2.1.1 SFV expression vectors 63
2.2.1.2 Cell lines 63
2.2.1.3 Animals 63

2.2.1.4 Molecular reagents 63
2.2.1.5 Particle production 64
2.2.1.6 Antibodies 64
2.2.1.7 Microscopy 65
2.2.1.8 Miscellaneous 65
2.2.2 Methods 65
2.2.2.1 Cell culture 65
2.2.2.2 Virus growth 66
2.2.2.3 Plaque assay 66
2.2.2.4 Virus infection 67
2.2.2.5 RNA extraction 67
2.2.2.6 RT-PCR 67
2.2.2.7 Preparation of IFN-β insert 69
2.2.2.8 Growth of recombinant SFV plasmids 70
2.2.2.8.1 Preparation of competent *E.coli* DH5α cells 70
2.2.2.8.2 Transformation of bacterial cells 70
2.2.2.8.3 Isolation of DNA from *E.coli* DHα cells 70
2.2.2.9 Linearization of SFV vectors for cloning 71
2.2.3 Insert of IFN-β into pSFV1 71
2.2.3.1 Ligation reaction 71
2.2.3.2 Screening for IFN-β insert 74
2.2.3.3 Sequencing of rSFV1-IFN-β 74
2.2.4 Insert of IFN-β into pSFV10-E 74
2.2.4.1 DNA amplification and ligation of IFN-β 74
2.2.5 Expression of IFN-β *in vitro* 76
2.2.5.1 *In vitro* SP6 RNA transcription 76
2.2.5.2 Electroporation 77
2.2.5.3 Immunohistochemistry 77
2.2.6 rSFV particle production and titration 78
2.2.6.1 Linearization of rSFV and helper plasmids for rSFV particle production 78
2.2.6.2 *In vitro* transcription 80
2.2.6.3 Electroporation 80
2.2.6.4 Harvesting rSFV particles 81

2.2.6.5 Titration of viral particles 81
2.2.7 Viral inhibition assay 82
2.3 Results 85
2.3.1 Cloning and expression of murine IFN-β in pSFV1 85
2.3.2 Cloning and expression of IFN-β in pSFV10-E 92
2.3.3 *In vitro* transcription, particle production and titration 99
2.3.4 Qualitative comparison analysis of IFN-β expression levels from rSFV-IFN-β vectors 103
2.3.5 Development of viral inhibition assay to quantify secretion of biological active IFN-β from rSFV-IFN-β vectors 103
2.3.6 Quantitative comparison of IFN-β expression in BHK-21 and murine L929 cell lines by viral inhibition assay 108
2.4 Discussion 110

3. *In vivo* expression and continuous treatment of EAE with rSFV- IFN-β vectors

3.1 Introduction 112
3.2 Materials and methods 115
3.2.1 Materials 115
3.2.1.1 Mice 115
3.2.1.2 Particle production 115
3.2.1.3 EAE induction 115
3.2.1.4 Splenocyte stimulation assays 115
3.2.1.5 Enzyme Linked Immunosorbant Assay 115
3.2.1.6 Histopathological studies 116
3.2.1.7 Miscellaneous 116
3.2.2 Methods 116
3.2.2.1 Particle production 116
3.2.2.2 Intranasal inoculation with rSFV-IFN-β particles 116
3.2.2.3 Protein assays 117
3.2.2.4 Detection of IFN-β in tissue homogenates 117
3.2.2.5 EAE induction 117

3.2.2.6 Treatment with IFN-β particles 118
3.2.2.7 Paraffin embedding and sectioning for pathology 118
3.2.2.8 Haematoxylin and eosin staining for routine histology 119
3.2.2.9 Pathological analysis 119
3.2.3.0 Preparation and freezing of splenocytes 119
3.2.3.1 Splenocyte stimulation assay 120
3.2.3.2 T cell responses *ex vivo* 120
3.2.3.3 Detection of cytokines in brain homogenates 120
3.3 Results 121
3.3.1 Duration of IFN-β expression *in vivo* following i.n. administration of rSFV-IFN-β particles 121
3.3.2 Effect of continuous rSFV-IFN-β treatment on the course of EAE through the induction, effector and recovery stages 125
3.3.3 Effect of continuous rSFV-IFN-β treatment on MOG 35-55 T cell responses *ex vivo* 129
3.3.4 Pathological analysis 132
3.3.5 Cytokine production in brains of EAE animal following rSFV-IFN-β treatment 132
3.4 Discussion 136

4. Treatment of the effector stage of EAE with rSFV-IFN-β vectors

4.1 Introduction 139
4.2 Materials and methods 143
4.2.1 Materials 143
4.2.1.1 Mice 143
4.2.1.2 Particle production 143
4.2.1.3 EAE induction 143
4.2.1.4 Histopathological studies 143
4.2.1.5 Antibodies 143
4.2.1.6 Morphometrics analysis 143
4.2.1.7 Splenocyte stimulation assay 145
4.2.1.8 Enzyme Linked ImmunoSorbant Assay 145

4.2.1.9 FACS analysis 145
4.2.2.0 Miscellaneous 145
4.2.2 Methods 146
4.2.2.1 Particle production 146
4.2.2.2 Treatment of EAE induced in C57/Bl6 mice with rSFV10-E-IFN-β particles during the effector stage 146
4.2.2.3 Treatment of EAE induced in C57/Bl6 mice with rSFV10-E-IFN-β particles before and during the effector stage 146
4.2.2.4 Treatment of EAE induced in C57/Bl 6 mice with rSFV10-E-IFN-β particles before the effector stage 147
4.2.2.5 EAE induction in SJL mice and treatment with rSFV-IFN-β particles on days 5,8,11,12 147
4.2.2.6 Paraffin embedding and sectioning for pathology 148
4.2.2.7 Haematoxylin and eosin staining for routine histology 148
4.2.2.8 Pathological analysis 148
4.2.2.9 Immunohistochemistry on spinal cord sections to detect infiltrating cells 148
4.2.3.0 Staining of spinal cord sections to detect demyelination 149
4.2.3.1 Morphometric analysis to quantify infiltrating T and B lymphocytes 149
4.2.3.2 Splenocyte stimulation assay and T cell responses *ex vivo* 149
4.2.3.3 Classification of leucocytes into MHC class II restricted CD4+ T cells, class I restricted CD8+ T cells and B cells by FACS analysis 150
4.3 Results 151
4.3.1 Effect of four rSFV10-E-IFN-β treatments during the effector stage 151
4.3.2 Effect of four rSFV10-E-IFN-β treatments before the effector stage 151
4.3.3 Summary of EAE treatments 155
4.3.4 Effect of four rSFV10-E-IFN-β treatments on MOG 35-55 T cells responses *ex vivo* 157
4.3.5 Correlation between clinical and pathological scores 161
4.3.6 Relative severity of EAE lesions in the spinal cords of rSFV-IFN-β treated and TNE treated animals on day 22 post induction 161
4.3.7 Characterization of the EAE lesion 161
4.3.8 Morphometrical analysis of T and B lymphocyte populations 166
4.3.9 FACS analysis to distinguish lymphocytes into MHC class II restricted CD4+ T cells, class I restricted CD8+ T cells and B cells 166

4.4.0 The effect of four rSFV10-E-IFN-β treatments before the effector stage on EAE induced in SJL mice 169

4.4 Discussion 171

5. The effect co-administered rSFV-IFN-β and rSFV-IL-10 vectors, or rSFV-IFN-β and Cholera Toxin on the course of EAE

5.1 Introduction 175

5.2 Materials and methods 177

5.2.1 Materials 177

5.2.1.1 SFV expression vectors 177

5.2.1.2 Molecular reagents 177

5.2.1.3 Cell culture 178

5.2.1.4 Particle production 178

5.2.1.5 Antibodies 178

5.2.1.6 Mice 178

5.2.1.7 EAE induction 178

5.2.1.8 Histopathological studies 178

5.2.1.9 Splenocyte stimulation assays 178

5.2.1.10 FACS analysis 179

5.2.1.11 Enzyme Linked ImmunoSorbant Assay 179

5.2.1.12 Miscellaneous 179

5.2.2 Methods 179

5.2.2.1 Insert of murine IL-10 into pSFV10-E 179

5.2.2.1.1 Growth of recombinant rSFV1-IL-10 181

5.2.2.1.2 PCR 181

5.2.2.1.3 Linearisation of pSFV10-E for cloning 181

5.2.2.1.4 Preparation of the IL-10 insert 183

5.2.2.1.5 Ligation reaction 183

5.2.2.1.6 Screening for IL-10 insert 184

5.2.2.2 Expression of IL-10 *in vitro* 184

5.2.2.3 rSFV10-E-IL-10 particle production and titration 184

5.2.2.4 Quantification of IL-10 expression from rSFV10-E-IL-10 particles 185

5.2.2.5 EAE induction 185
5.2.2.6 Intranasal treatment of EAE with rSFV10-E-IFN-β and rSFV10-E-IL-10 particles, and whole Cholera toxin 186
5.2.2.7 Histopathological studies 186
5.2.2.8 Splenocyte stimulation assay and serum cytokine levels 186
5.2.2.9 FACS analysis 187
5.3 Results 188
5.3.1 Cloning and expression of IL-10 in pSFV10-E 188
5.3.2 Co-administration of rSFV10-E-IFN-β and rSFV10-E-IL-10 particles in the treatment of EAE 195
5.3.3 Specific T cells responses to MOG 35-55 *ex-vivo* after rSFV-IFN-β and rSFV-IL-10 treatment 195
5.3.4 Co-administration of rSFV10-E-IFN-β particles and cholera toxin in the treatment of EAE 198
5.3.5 Specific T cells responses to MOG 35-55 *ex-vivo* after treatment with rSFV10-E-IFN-β particles and CT 198
5.3.6 Summary of EAE treatments 201
5.3.7 Detection of IFN-γ in the serum of rSFV10-E-IFN-β, rSFV10-E-IL-10 and CT treated animals 201
5.3.8 Pathological analysis of mice treatment with combined treatment 201
5.3.9 FACS analysis to distinguish lymphocytes into MHC class II restricted CD4+ T cells, MHC class 1 restricted CD8+ T cells and B cells 205
5.4 Discussion 208

6. General discussion 213

7. References 232

Chapter 1 – General Introduction

1.1	Structure of the SFV virion	3
1.2	SFV replication and transcription	7
1.3	Processing of structural proteins and viral release	9
1.4	The SFV split helper expression system	18
1.5	Production of recombinant SFV particles	19
1.6	Structure of a neuron	25
1.7	Demyelination within the CNS	26
1.8	Classification of Multiple Sclerosis	31
1.9	Epidemiology of Multiple Sclerosis	35
1.10	Immunopathogenesis of MS and EAE	38
1.11	Differentiation of naïve Th0 cells into Th1 and Th2 cells	39

Chapter 2 – Cloning of IFN-β into SFV vectors and *in vitro* expression in different cell lines

2.1	Coding region of murine IFN-β	68
2.2	SFV expression vectors used for cloning of IFN-β	72
2.3	Strategy for cloning of IFN-β into pSFV	73
2.4	Strategy for cloning of IFN-β into pSFV10-E	75
2.5	Maps of SFV helper plasmids	79
2.6	The antiviral effects of IFN-β	84
2.7	Gel analysis of RT-PCR amplified IFN-β	86
2.8	Preparation of pSFV1 plasmid and IFN-β PCR product for ligation	87
2.9	IFN-β insert in pSFV1 plasmid	88
2.10	IFN-β coding region in pSFV1-IFN-β sequence analysis	89
2.11	Expression of rSFV1-IFN-β in BHK-21 cells	91
2.12	PCR amplification of IFN-β gene from pSFV1-IFN-β plasmid	93
2.13	Preparation of pSFV10-E and IFN-β insert for ligation	94
2.14	Cloning of IFN-β into pSFV10-E	95

2.15 IFN-β coding region in pSFV10-E-IFN-β sequence analysis 96
2.16 Expression of rSFV10-E-IFN-β in BHK-21 cells 98
2.17 Linearization of rSFV-IFN-β and helper plasmids for high titre particle production 100
2.18 *In vitro* transcription of rSFV-IFN-β and helper plasmids 101
2.19 Titration of rSFV-IFN-β particles using indirect immunofluorescence 102
2.20 Comparison of *in vitro* expression of IFN-β using two different rSFV-IFN-β particle vectors 105
2.21 Measurement of viable L929 cells post treatment with rSFV-IFN-β supernatant samples and SFV-A7 challenge 106
2.22 Comparison of *in vitro* expression of IFN-β from two different rSFV-IFN-β particle vectors in different cell lines 109

Chapter 3 – *In vivo* expression and continuous treatment of EAE with rSFV- IFN-β vectors

3.1 Levels of IFN-β present in olfactory bulbs post i.n. inoculation with rSFV-IFN-β particles 122
3.2 Levels of IFN-β present in brains post i.n. inoculation with rSFV-IFN-β particles 123
3.3 Levels of IFN-β present in the spinal cord post i.n. inoculation with rSFV-IFN-β particles 124
3.4 Effect of nine rSFV1-IFN-β treatments on EAE score and weight 126
3.5 Effect of nine rSFV10-E-IFN-β treatments on EAE score and weight 127
3.6 The effect of MOG 35-55 stimulation on production of IFN-γ and IL-10 130
3.7 The effect of MOG 35-55 stimulation on production of IFN-γ and IL-10 from splencytes *ex vivo* after continuous treatment with rSFV10-E-IFN-β particles 131
3.8 A typical grade 3 EAE lesion on sagital section of spinal cord 133
3.9 Levels of IFN-γ and IL-10 in brains of EAE mice treated with rSFV-IFN-β 135

Chapter 4 – Treatment of the effector stage of EAE with rSFV-IFN-β vectors

4.1	The effect of four rSFV10-E-IFN-β treatments during the effector stage on EAE score and weight	152
4.2	The effect of five rSFV10-E-IFN-β treatments before and during the effector stage on EAE score and weight	153
4.3	The effect of four rSFV10-E-IFN-β treatments before the effector stage on EAE score and weight	154
4.4	Production of IFN-γ and IL-10 in response to MOG 35-55 stimulation day 22 p.d.i	158
4.5	Production of IFN-γ and IL-10 in response to MOG 35-55 stimulation day 15 p.d.i	159
4.6	Production of IL-4 and IL-12 in response to MOG 35-55 stimulation day 15 p.d.i	160
4.7	Comparison of a type 2 with a type 4 EAE lesion in a spinal cord section	163
4.8	Characterization of a typical EAE lesion on sequential sagital sections of spinal cord	164
4.9	Comparison of B lymphocytic infiltration in similar spinal cord lesions	167
4.10	FACS analysis of lymphocytes from rSFV10-E-IFN-β particle treated animals in the recovery stage	168
4.11	Induction and treatment of EAE induced in SJL mice with rSFV-IFN-β	170

Chapter 5 - The effect co-administered rSFV-IFN-β and rSFV-IL-10 vectors, or rSFV-IFN-β and Cholera Toxin on the course of EAE

5.1	Strategy for insert of IL-10 into pSFV10-E	180
5.2	IL-10 coding gene sequence	182
5.3	PCR amplification of IL-10 gene from pSFV1-IL-10	189
5.4	Quantification of pSFV10-E and IL-10 PCR product for ligation	190
5.5	Insert of IL-10 into pSFV10-E	191
5.6	IL-10 coding region in pSFV10-E-IL-10 sequence analysis	192
5.7	Expression of rSFV10-E-IL-10 in BHK-21 cells	193

5.8 Comparison of *in vitro* expression of IL-10 from rSFV10-E-IL-10 particles in different cell lines 194

5.9 Co-administration of rSFV10-E-IFN-β and rSFV10-E-IL-10 particle vectors in the treatment of EAE 196

5.10 The effect of MOG35-55 stimulation on production of IFN-γ and IL-10 from splenocytes *ex vivo* 197

5.11 Co-administration of rSFV10-E-IFN-β particles and cholera toxin in the treatment of EAE 199

5.12 The effect of MOG35-55 stimulation on production of IFN-γ and IL-10 from splenocytes of CT treated animals *ex vivo* 200

5.13 Levels of IFN-γ in serum taken from rSFV10-E-IFN-β, rSFV10-E-IL-10 and CT treated animals 203

5.14 FACS analysis of lymphocytes from rSFV10-E-IFN-β and rSFV10-E-IL-10 treated EAE animals 206

5.15 FACS analysis of lymphocytes from rSFV10-E-IFN-β and Cholera toxin treated EAE animals 207

Index of tables

Chapter 2 - Cloning of IFN-β into SFV vectors and *in vitro* expression in different cell lines

Table 2.1 Concentration of IFN-β (units of activity /ml) in the supernatant samples of rSFV-IFN-β infected cells 107

Chapter 3 – *In vivo* expression and continuous treatment of EAE with rSFV- IFN-β vectors

Table 3.1 Analysis of EAE mice after nine rSFV-IFN-β particle treatments 128

Table 3.2 Comparison of clinical and pathological scores 134

Chapter 4 – Treatment of the effector stage of EAE with rSFV-IFN-β vectors

Table 4.1 Table of antibodies used and recommended dilutions 144

Table 4.2 Comparison of rSFV10-E-IFN-β treatment regimes in the treatment of EAE 156

Table 4.3 Correlation between clinical scores and pathology of rSFV10-E-IFN-β treated mice 162

Chapter 5 - The effect co-administered rSFV-IFN-β and rSFV-IL-10 vectors, or rSFV-IFN-β and Cholera Toxin on the course of EAE

Table 5.1 Analysis of treatment with rSFV10-E-IFN-β, rSFV10-E-IL-10 and CT 202

Table 5.2 The effect of treatment with rSFV10-E-IFN-β particles, rSFV10-E-IL-10 particles and CT on clinical score and pathology score of EAE mice 204

Chapter 1

General Introduction

1.1 Semliki Forest Virus

1.1.1 Semliki Forest Virus - background

SFV is an enveloped positive sense single stranded RNA virus of the genus *Alphavirus* of the family *Togaviridae.* Within the alphavirus genus there are three main members - the VEE/EEE group, the SIN group and the SF group to which SFV belongs. The SF group is mostly Old World in its distribution and has been isolated from Africa, the USSR and India (Strauss and Strauss, 1994). SFV was first isolated from mosquitoes in Uganda in 1944 (Smithburn and Haddow, 1944) followed by subsequent isolations in 1948 in Kumba, Nigeria (Macnamara, 1953) and in 1959 in Namancurra, Mozambique (McIntosh *et al.*, 1961). These isolates have given rise to a variety of strains of SFV with differing levels of virulence. SFV has been linked to human disease on only two occasions. In the first case, reported in 1979, a 26-year-old laboratory worker in Germany with a 1-year history of "purulent bronchitis," working with the Osterrieth strain of SFV, developed fever and headache followed by seizures, coma, and died of encephalitis. SFV was isolated from CSF and from brain with no viral antibody detected until time of death 1 week later (Willems *et al.*, 1979). In 1987 SFV was isolated from serum samples of French soldiers serving in the Central African Republic with fever, persistent myalgias, and arthralgias (Mathiot *et al.*, 1990). No further fatal infections have been reported although a small number of documented laboratory infections have occurred since. SFV is considered to be a minor human pathogen causing a mild or sub clinical infection in man.

1.1.2 SFV virion

SFV is a relatively small virus, measuring about 65 nm in diameter. The virus structure contains one single stranded plus sense RNA encapsidated within 240 copies of a capsid protein (C) in T=4 icosahedral symmetry (Choi *et al.*, 1991; Fuller *et al.*, 1995). This nucleocapsid is surrounded by a lipid bilayer envelope in which multiple copies of three envelope glycoproteins, E1 and E2 and E3 are embedded (Garoff and Simons, 1974). Each glycoprotein has molecular mass of approximately 50kDA. E1, E2 and E3 form a stable heterodimer and three E1-E2-E3 heterodimers interact to form the spike complex found on the virus surface. The glycoproteins, like the nucleocapsid, form an icosahedral lattice with T=4 and there are 240 heterodimers on the surface of the virus, assembled into 80 spikes (Vogel *et al.*, 1986). Figure 1.1 illustrates the structure of the SFV virion.

The structural proteins are initially translated as a polyprotein NH_2-C-p62(E3/E2)-6K-E1-COOH that is processed co-and post-translationally to produce the mature products, the capsid C protein, the envelope glycoproteins, E1, p62 (E2 and E3), and the 6K protein. The capsid protein consists of 267 a.a. and is 30kDa in size. It contains an N-terminal RNA-binding domain and a conserved chymotrypsin-like serine protease COOH terminal domain, which facilitates capsid autocleavage from the nascent viral polypeptide (Melancon and Garoff, 1987; Owen and Kuhn, 1997). Once synthesized the C protein folds to act as a protease cleaving itself off the nascent chain (Hahn and Strauss, 1990; Melancon and Garoff, 1987). This reveals an N-terminal signal sequence that is recognized by the signal recognition particle targeting the nascent chain-ribosome complex to the ER membrane (Bonatti, 1982; Garoff *et al.*, 1978) where it is later cleaved to the three structural membrane proteins p62, 6K and E1 (Garoff *et al.*, 1990; Liljestrom and Garoff, 1991; Melancon and Garoff, 1986).

The spike complex on the virus surface is composed of three E1-E2-E3 heterodimers. 240 heterodimers interact to form 80 spikes (Garoff *et al.*, 1974). The E1 spike protein is composed of 438 a.a. and has a molecular weight of 49kDA. It contains a hydrophobic transmembrane domain of 23 a.a. which separates the N-terminal glycosylated ectodomain from two C-terminal residues situated on the inside of the viral membrane. The highly conserved hydrophobic domain of the E1 protein is thought to be responsible for the membrane fusion activity of the viral spike (Bron *et al.*, 1993; Levy-Mintz and Kielian, 1991). Cross-linking studies suggest that E1-E1 interactions are responsible for maintaining spike stability (Wahlberg *et al.*, 1992).

The p62 protein is a precursor of the E2/E3 proteins. On formation of a heterodimer with E1 via its E3 domain, the p62/E1 complex undergoes transport via the Golgi apparatus to a compartment just before the cell surface where p62 is cleaved into the mature E2 and E3 proteins (de Curtis and Simons, 1988; Sariola *et al.*, 1995). This cleavage event is mediated by a host cell furin endoprotease and activates the host cell binding function of the virion as well as the membrane fusion potential of E1.

The E2 glycoprotein has a molecular weight of 52kDA and consists of 422 a.a. E2 has a large N terminal ectodomain (Simons and Garoff, 1980), a transmembrane region and a 31 amino acid long C-terminal tail region. The tail resides inside the virus

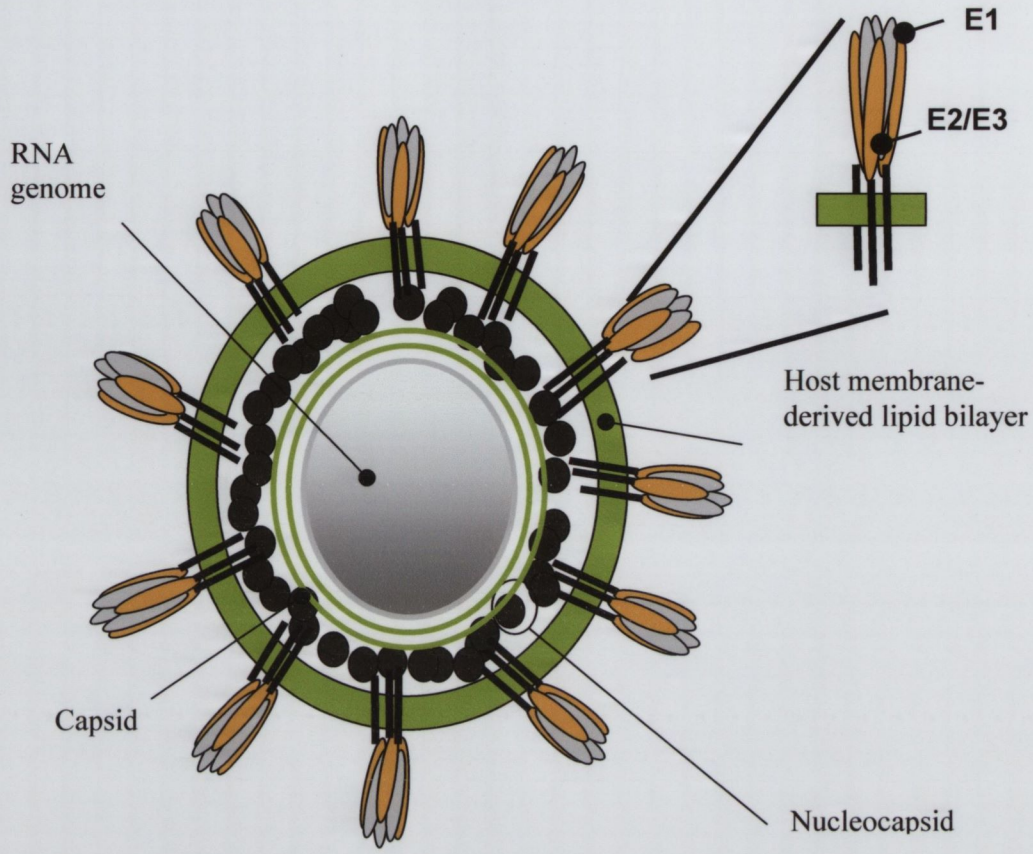

Figure 1.1 Structure of the SFV virion.

The SFV virion consists of a nucleocapsid containing a ssRNA molecule of positive polarity, encapsidated within 240 copies of the C protein. The host-derived lipid bilayer contains 80 spikes, each of which is composed of three copies of the E1, E2 and E3 glycoproteins. Only the C terminal tail of the E2 glycoprotein is in contact with the nucleocapsid core.

membrane and plays a role in the interactions with the nucleocapsid as the receptor binding subunit (Metsikko and Garoff, 1990; Skoging *et al.*, 1996; Suomalainen and Garoff, 1992). The function of the small 66 a.a. long E3 glycoprotein is relatively unknown. One role of the E3 moiety is that its N terminal end acts as a signal peptide for p62 during virus maturation (Lobigs *et al.*, 1990).

Relatively little is known about the function of the small hydrophobic protein of 6kDA, the 6K protein. This protein forms a heterotrimer with the p62/E1 complex prior to their exit from the golgi apparatus and is transported to the cell surface before it dissociates (Lusa *et al.*, 1991; Venien-Bryan and Fuller, 1994). To date the 6K is thought to be an important but nonessential component in the assembly and budding of the alphavirus particle (Loewy *et al.*, 1995).

1.1.3 SFV genome

The SFV virus genome is approximately 11.4 kb in size and consists of a single strand of positive RNA which is 5′ capped with 7-methylguanosine and 3′ capped with a poly A tail which encodes nine functional proteins; the four nsPs 1-4 which are concerned with viral RNA synthesis and the structural proteins which consist of the 6K protein, the capsid protein (C) and the envelope proteins (E1, E2 and E3). The first 5′ two-thirds of the RNA genome code for the non-structural genes responsible for transcription and replication (Takkinen, 1986), while the 3′ terminal one- third end codes for the structural genes (Garoff *et al.*, 1980). The nsPs are translated initially from the genomic 42S RNA as one or two polyproteins, p123 and p1234, which undergo cotranslational cleavage to give the nsP1, nsP2, nsP3 and nsP4 proteins. The newly synthesized non-structural proteins are responsible for the replication of the plus strand (42S) genome into full length minus strands which serve as templates for the production of new 42S genomes (Sawicki and Sawicki, 1980). These molecules also serve as templates for the synthesis of 26S RNA which is initiated from the 26S promoter on the 42S minus strands. The structural proteins are translated in the following order: C, p62, 6K and E1 (Kaariainen *et al.*, 1975; Keranen and Kaariainen, 1975). The E2 and E3 glycoproteins are derived from the post-translation cleavage of the p62 polyprotein (de Curtis and Simons, 1988; Sariola *et al.*, 1995) .

1.1.4 The Life Cycle of Semliki Forest Virus

1.1.4.1 Viral entry

The virus infects the cell by receptor mediated endocytosis (DeTulleo and Kirchhausen, 1998) and an acid triggered fusion step. Several proteins have been suggested as functional receptors for SFV, including the HLA but it is thought that, consistent with its broad host range that SFV can utilize a number of surface receptors (Helenius *et al.*, 1978). Membrane fusion is mediated by the viral spike protein, a heterodimer of the three envelope proteins E1-E2-E3 (Wahlberg *et al.*, 1992). The E2 subunit of the SFV spike has been shown to interact with the cell surface to facilitate viral entry (Dubuisson and Rice, 1993). On entry into the endosome of a new host cell, the low pH environment, a pH 6.2 or below, results in E1-E2 heterooligomeric dissociation (Wahlberg *et al.*, 1989; Wahlberg and Garoff, 1992) as well as conformational changes within individual E1 and E2 subunits (Kielian and Helenius, 1985). E2 dissociation stimulates E1 homotrimerisation at the centre of the spike. This E1 homotrimer directly mediates fusion of the viral membrane with the endosomal membrane (Bron *et al.*, 1993; Wahlberg *et al.*, 1992). In addition to its low pH requirement SFV fusion is also characterized by a need for cholesterol and sphingolipid (Nieva *et al.*, 1994; Phalen and Kielian, 1991). Uncoating of the nucleocapsids by ribosomes is followed by release of the viral RNA into the cytoplasm (Singh and Helenius, 1992).

1.1.4.2 Viral replication

Replication of the viral RNA takes place in the cytoplasm, more specifically in the 0.6 –2.0μm wide cytopathic vacuoles derived from endosomes and lysosomes (Froshauer *et al.*, 1988; Peranen and Kaariainen, 1991). Early infection begins with translation of the 5′ ORF which constitutes the first two-thirds of the genome length and codes for a non structural polyprotein p1234 (Kaariainen *et al.*, 1975; Takkinen, 1986). This polyprotein is produced upon readthrough of an arginine codon (CGA) where there is no termination at this position. After translation this precursor protein is autoproteolytically cleaved into the four nonstructural proteins nsP1, nsP2, nsP3, ns P4 which make up the viral replicase (Hardy and Strauss, 1988; Keranen and Ruohonen, 1983; Lehtovaara *et al.*, 1980). Protein nsP1 encodes a methyl transferase which is responsible for virus specific capping activity (Ahola and Kaariainen, 1995; Ahola *et al.*, 1997) as well as initiation of minus strand

synthesis (Hahn *et al.*, 1989). The nsP2 protein performs helicase and protease function during viral replication (Gomez de Cedron *et al.*, 1999). NsP3 is a phosphoprotein of which little is known. When the SFV gene for nsP3 is expressed alone in BHK cells, the nsP3 protein is localized to numerous vesicle like structures and large vacuoles indicating that the protein may function as an anchoring protein for the RNA replication complex of SFV (Peranen, 1991; Peranen *et al.*, 1988). It is also thought to play a role in RNA synthesis (Lastarza *et al.*, 1994). The nsP4 protein is responsible for cleavage of the nascent p1234 polyprotein into its four subcomponents (Takkinen *et al.*, 1991; Takkinen *et al.*, 1990) and also possesses a GDD sequence motif typical of RNA-dependent RNA polymerases indicating its role in RNA polymerase activity (Argos, 1988). Once the nsPs are synthesized, they are responsible for the replication of full length minus-strand 42S RNA, an event that occurs exclusively during the first 3-4 hours after infection (Sawicki *et al.*, 1978; Sawicki and Sawicki, 1980). The minus strand RNA also serves as a template for the synthesis of a subgenomic 26S RNA molecule (Gomatos *et al.*, 1980). This 4073 long RNA is colinear with the last one-third of the genome, is capped and polyadenylated, and serves as mRNA for translation of a single ORF encoding the structural polyprotein precursor (Garoff *et al.*, 1980). Its synthesis is internally initiated at the 26S promoter on the 42S minus strand (Sawicki *et al.*, 1978). The process of SFV replication and transcription is shown in figure 1.2.

1.1.4.3 Processing of the structural proteins

The structural proteins are initially translated from the 26S subgenomic RNA as a structural polyprotein in the following order, C-p62-6K-E1. The capsid protein, upon synthesis, is cotranslational cleaved off the nascent polypeptide by its own C-terminal serine protease activity (Garoff *et al.*, 1978; Melancon and Garoff, 1987). The C protein associates with the large ribosomal subunit to form nucleocapsids (Soderlund, 1973; Ulmanen *et al.*, 1976). Within the nsP2 gene, an encapsidation signal is responsible for viral RNA packaging (Frolova *et al.*, 1997; White *et al.*, 1998). Following cleavage of the capsid protein, the nascent chain reveals an N-terminal signal which directs cotranslational translocation of the the p62 ectodomain into the ER lumen (Garoff *et al.*, 1990; Melancon and Garoff, 1987). The N terminal signal sequence remains uncleaved and is also transferred into the lumen where it is glycosylated and then cleaved off the nascent peptide chain by signal peptidases to the protein, p62. Other signal peptidase sequences are

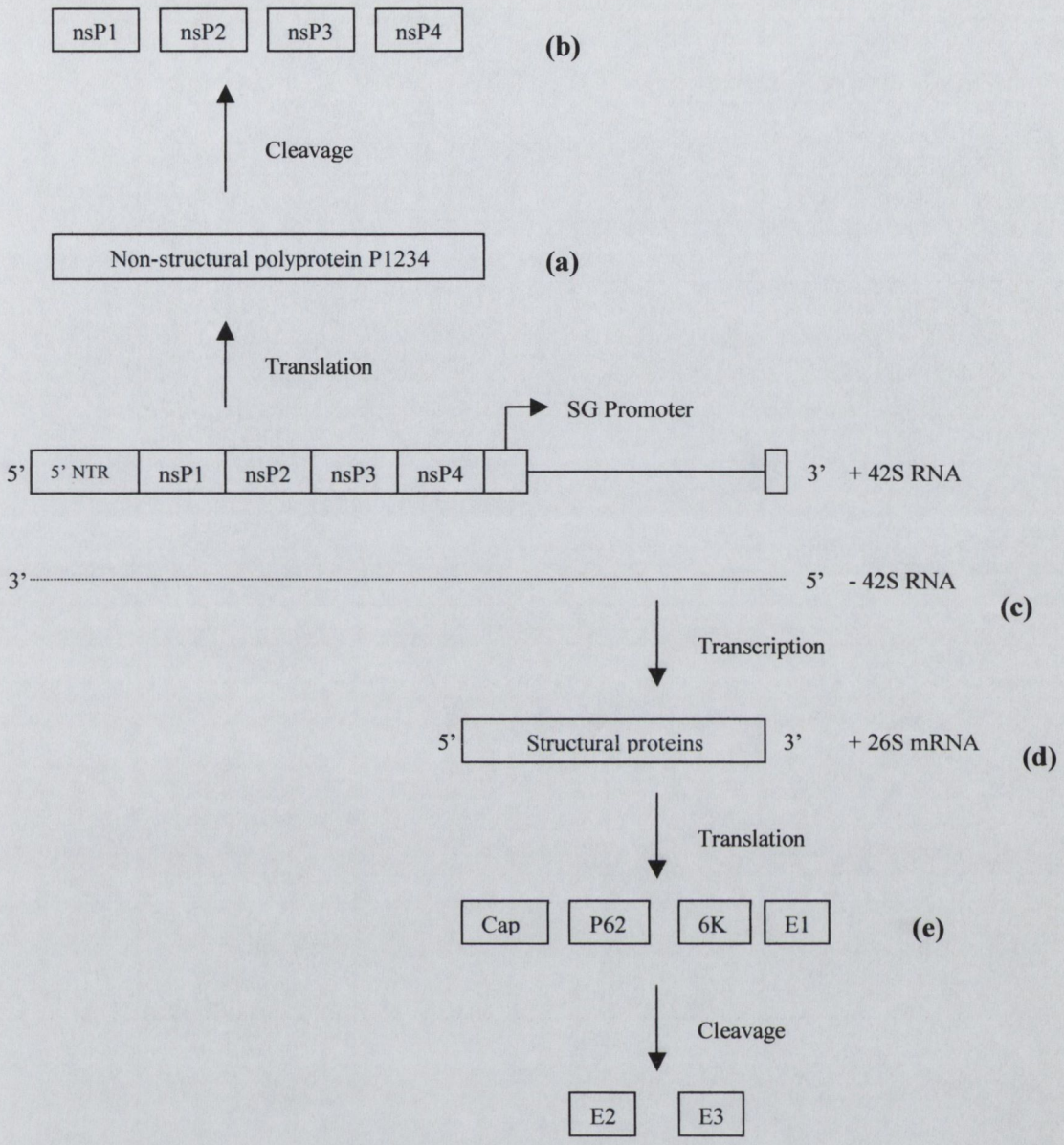

Figure 1.2 SFV replication and transcription

The 5′ two-thirds of the SFV genome encode the nsPs which are translated as the polyprotein P1234 (a). The polyprotein is subsequently processed to the non-structural proteins, nsP1-nsP4, through the action of the nsP2 and nsP4 autoproteases (b). These nsPs are responsible for replication of the full length minus-strand 42S RNA (c) from which the structural proteins are subsequently transcribed and translated as a polyprotein (d). The structural polyprotein undergoes post-translational cleavage to release the capsid protein C, the envelope glycoproteins E1, E2 and E3, and the 6K protein (e). (Adapted from Strauss & Strauss, 1994).

located at the COOH-terminus of the p62 and 6K proteins, to promote 6K and E1 translocation, respectively (Liljestrom and Garoff, 1991; Melancon and Garoff, 1986). Subsequent cleavage by host cell peptidases generates p62, 6K and E1 proteins (Barth *et al.*, 1995).

1.1.4.4 Viral assembly, maturation and release

In the ER heterodimers are rapidly formed between the p62 protein and E1 protein (Barth *et al.*, 1995; Garoff *et al.*, 1994). The 6K protein forms a complex with the low pH resistant p62/E1 heterodimers (Lusa *et al.*, 1991). These trimeric complexes are transported via the Golgi apparatus to the cell surface where the 6K protein dissociates. The 6K protein is not needed for the heterodimerization of the p62 and E1 spike membrane proteins in the endoplasmic reticulum, nor is it needed for their transport out to the cell surface (Liljestrom *et al.*, 1991). Studies suggest that the protein exerts its function late in the assembly pathway, possibly during virus budding (Loewy *et al.*, 1995; McInerney *et al.*, 2004). At a compartment after the trans-Golgi network, but prior to its arrival at the cell surface, the p62 precursor is cleaved after its residue 66 into the mature E2 and E3 moieties by host furin like proteases (de Curtis and Simons, 1988; Sariola *et al.*, 1995). This cleavage, though not required for virus budding, is necessary for host cell binding function of the virion. Cleavage of p62 renders the viral spike sensitive to low pH, facilitating the formation of the E1-E2 heterodimers, and leading to the assembly of fully infectious virions (Lobigs and Garoff, 1990; Salminen *et al.*, 1992). E3 remains transiently associated with the viral spike (Lobigs *et al.*, 1990).

Genomic RNA and C proteins are rapidly associated into nucleocapsids. Budding of virus particles occurs at the plasma membrane, driven by interactions between the capsid proteins of the nucleocapsid and the cytoplasmic tail of E2 (Garoff and Simons, 1974; Skoging *et al.*, 1996; Suomalainen and Garoff, 1992). This has been suggested by studies where amino acid substitutions in the E2 cytoplasmic tail showed that a single tyrosine residue directly interacts with the nucleocapsid and drives the budding process (Skoging *et al.*, 1996). Figure 1.3 illustrates the processing of structural proteins and the release of virions from the host cell.

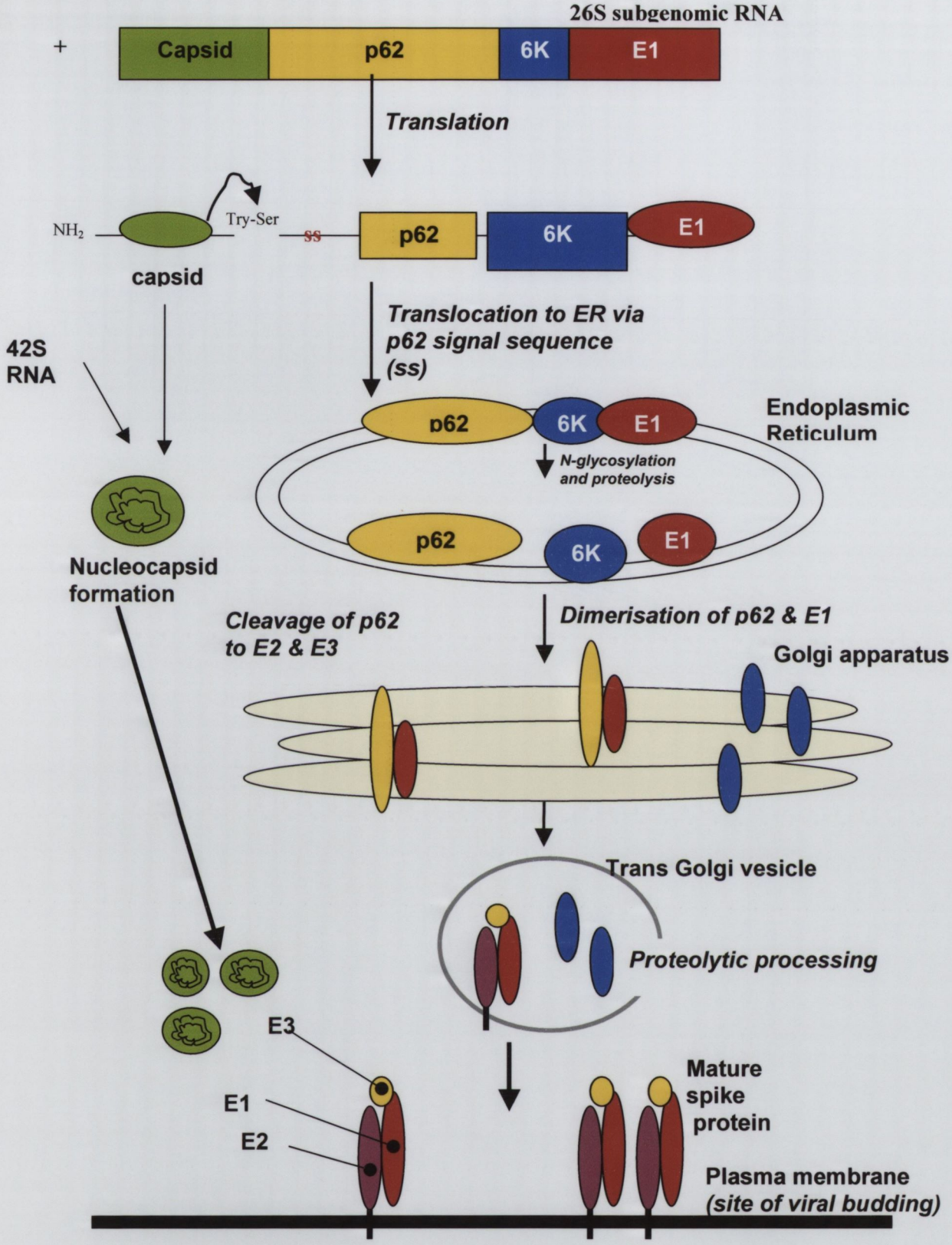

Figure 1.3 Processing of SFV structural proteins and viral release

Capsid protein is released cotranslationally by autoproteolysis, and assembles with genomic RNA to form nucleocapsids. The p62, 6K and E1 proteins are translocated to the

ER. A NH_2-terminal sequence in p62 is thought to be the translocation signal. Co-translational cleavage of the remaining polypeptide occurs in the ER, as well as N-glycosylation and further proteolytic processing. P62 is further cleaved into E2 and E3 subunits during transport to the Golgi apparatus. E2 associates with E1 to form heterodimers necessary for viral infectivity. Interaction of capsid proteins with the COOH-terminal of E2 drives the budding process, and releases infectious progeny. Adapted from Ph.D thesis entitled 'Analysis and development of the recombinant Semliki Forest virus vector as a cancer gene therapy agent' (Marie Murphy, 2001)

1.1.5 Effect of SFV replication on infected cells

SFV usually infects oligodendrocytes and neurons both in tissue culture (Atkins *et al.*, 1990; Gates *et al.*, 1985) and in the animal (Atkins, 1983; Balluz *et al.*, 1993; Fazakerley *et al.*, 1993). Death of most cells following SFV infection results from induction of apoptosis or programmed cell death (Glasgow *et al.*, 1997; Scallan *et al.*, 1997). Some cell types are naturally resistant to apoptosis such as fully differentiated macrophages, muscle cells and neurons, and are killed by necrosis (Atkins *et al.*, 1990; Glasgow *et al.*, 1997). Infection of vertebrate cells leads to inhibition of host-cell protein synthesis and cell death. In contrast, infection of invertebrate cells leads to a persistence infection, with no significant cell damage. Many studies have shown that the viral structural proteins are not involved in mechanisms that inhibit host protein synthesis therefore the cytopathic effects observed in infected cells are mediated by viral RNA replication only (Liljestrom and Garoff, 1991). Deletion of part of the nsP2 region has been shown to affect apoptosis (Glasgow *et al.*, 1998), reconfirming that the apoptotic characteristic of SFV lies within its non-structural region (Barr *et al.*, 2000).

In SFV structural proteins are produced in very high amounts during the first 24 hours of infection, and about 10^4 p.f.u are released per infected BHK-21 cell. After 6 hours of infection, only viral proteins are produced, with host cell synthesis being completely shut down (Liljestrom and Garoff, 1991). Extensive cytopathic effect is observed in infected cells, characterized by cell rounding, shrinkage, and cytoplasmic blebbing (Levine *et al.*, 1993). Apoptosis has been shown to occur independently of p53 expression in SFV infected cells. Human H358a lung carcinoma cells, containing a homozygous deletion of the p53 gene, readily undergo apoptosis upon infection (Glasgow *et al.*, 1998). One possible mechanism for induction of apoptosis is activation of double stranded RNA dependent PKR (Favre *et al.*, 1996; Grandgirard *et al.*, 1998) which has been shown to mediate a number of pro-apoptotic effects in a virally-infected cell, including the inhibition of protein synthesis and upregulation of the Fas/TNFR pathways (Balachandran *et al.*, 1998). The overexpression of the anti-apoptotic Bcl-2 oncoprotein has been shown to restrict SFV multiplication and delay the onset of apoptosis in the rat prostate cancer cell line AT3-Bcl-2 (Scallan *et al.*, 1997). AT3-Bcl-2 cell monolayers survived infection with both A7 and L10 strains of SFV, allowing persistently infected cells lines to be mainitained. Although there is a delay in SFV replication in Bcl-2-overexpressing cells, SFV is capable of overcoming this, and induces apoptosis by

caspase-mediated proteolytic cleavage of the Bcl-2 protein, thereby inhibiting its pro-survival functions (Grandgirard *et al.*, 1998; Murphy *et al.*, 2001).

1.1.6 Immune response to SFV infection

Previous studies have shown that both humoral neutralizing and non-neutralizing antibodies, and T-cell mediated immunity play a role in SFV infection (Allner *et al.*, 1974; Amor *et al.*, 1996b; Bradish *et al.*, 1975; Bradish *et al.*, 1979; Gates *et al.*, 1984; Jagelman *et al.*, 1978). Complete recovery from infection appears to be assisted by both T- and B-lymphocytes. Neutralizing antibody is detectable at three days following intraperitoneal infection with the avirulent A7 strain, and peaks at 7 days. The presence of antibody coincides with the disappearance of the viremia which peaks two days and disappears at three days (Allner *et al.*, 1974). To further verify the importance of the humoral response, treatment of mice with cyclophosphamide increases the duration of viremia, depresses neutralizing antibody synthesis and enhances mortality (Bradish *et al.*, 1975). Cyclophosphamide is a known inhibitor of both B and T lymphocyte function. The role of T- lymphocytes in immunity to SFV infection has been studied using nude (nu/nu, T-lymphocyte- deficient) mice. Lesions in the brains of these mice are less severe than in the normal immunocompetent mice after SFV infection but the virus persists in the brain (Bradish *et al.*, 1979; Jagelman *et al.*, 1978). Efficient clearing of virus and neutralizing antibody synthesis could be restored to the nude mice by transfer of spleen cells from immunocompetent but uninfected mice .

More recent studies using the avirulent A7(74) strain of SFV in the infection of immunocompetent, nu/nu mice and SCID mice have further confirmed the role of the immune response in protection and pathogenesis from SFV infection (Amor *et al.*, 1996b). Immunocompetent Balb/c mice remained healthy and showed transient viremia and infectious virus from days 2-7 with antibodies detectable by day 5. SCID mice exhibited severe paralysis and died. The average day of death was day 23 and no antibodies were detectable. Nu/nu mice experienced a transient infection and produced antiviral IgM but not IgG. Transfer of immune serum from immunocompetent mice and nu/nu mice to SCID mice decreased mortality and delayed the onset of paralysis. Transfer to infected SCID mice of a non-neutralizing IgG anti-E2 mAb did not affect the viremia but reduced brain virus titres indicating that IgG antibodies including non-neutralizing antibodies reduce and clear infectious virus, but IgM antibodies clear the viremia.

Neutralizing and non-neutralizing antibodies can also protect mice from lethal challenge with a virulent strain (Boere *et al.*, 1983). Neutralizing and non-neutralizing monoclonal antibody to E2 envelope protein protected mice from lethal challenge, with the neutralizing antibody being 100 fold more effective. The presence of T and B cells epitopes in the E2 envelope have been used to design effective peptide vaccines (Fernandez *et al.*, 1993; Snijders *et al.*, 1992).

The cytokine profile in the CNS following SFV infection is complex and has shown no clear bias towards either a Th1 or Th2 response (Morris *et al.*, 1997). Following infection of Biozzi ABH mice with the A7(74) strain of SFV, both MHC class I and class II expression was induced in the CNS. MHC class 1 expression was observed on meningeal, ependymal, choroid plexus, endothelial and microglial cells, and MHC class II expression on activated microglial cells, astrocytes and cells associated with blood vessels such as pericytes, leading to upregulation of an array of Th1/Th2 cytokines. Proinflammatory Th1 cytokines such as TNF-α, IFN-γ, IL-1α and IL-2 were present at the same time points as Th2 cytokines IL-10, IL-6 and TGF-β when the cytokine profile was examined following infection. The genetic background of the mice also influences the severity of clinical disease and the pattern of cytokine production following SFV infection (Mokhtarian *et al.*, 1996). SFV caused a more acute encephalomyelitis in C57/Bl6 mice than in SJL mice where the B6 mice showed higher levels of IL-4 and lower levels of TNF-α, IL-6, IL-1β and IL-2, despite having similar T cell proliferation and antibody responses.

1.1.7 SFV strains and CNS pathogenesis

For many years SFV has been exploited as a model of viral neuropathogenesis. The original isolate of SFV, L10 which was isolated by Smithburn and Haddow in 1944 is neurovirulent in mice causing lethal encephalitis by infection of the central nervous system when given intraperitoneally, subcutaneously or intranasally (Bradish *et al.*, 1971). Although serologically indistinguishable from L10, another strain of SFV, A7 differs markedly in its virulence for mice. This avirulent strain was isolated from mosquitoes in Mozambique (McIntosh *et al.*, 1961). A7 does not kill adult mice when given by these routes but induces immunity to virulent SFV challenge and demyelination of the CNS in infected mice (Atkins, 1983; Bradish and Allner, 1972). Interestingly A7, though attenuated, multiplies at least as efficiently as L10 in standard cultured cells such as BHK

cells (Atkins, 1983; Glasgow *et al.*, 1997). Most SFV strains are derived from these isolates and are all lethal for neonatal mice. Four mutant strains were derived from the virulent L10 strain by chemical mutagenesis - M4, M103 and M136 (Barrett *et al.*, 1980), and M9 (Atkins and Sheahan, 1982). M4 and M103 produced a transient viremia that did not enter the brain or spinal cord. M136 shows more similarity to the wild type virus, its viremia reached the brain but at lower titres. The M9 mutant has a defect in efficiency of viral RNA synthesis. These defects allow the survival of the majority of mice following peripheral infection. The avirulent A7(74) strain was derived from A7 by further selection for avirulence (Bradish *et al.*, 1971). The prototype strain from which the original infectious cDNA clone, pSP6-SFV4, (Liljestrom *et al.*, 1991) was constructed appears to be derived from the L10 strain though it is thought to have lost some of its virulence due to repeated passages in cell culture (Glasgow *et al.*, 1991). The virus produced by transcription of this infectious clone is called SFV4. This SFV4 strain of SFV is lethal when 10^6 p.f.u. is given intranasally to adult mice resulting in 100% death. The virus is less virulent, killing 70-80% mice when the same dose of virus is given intraperitoneally.

The most important difference between virulent and avirulent strains is their ability both to multiply in neurons and to cause extensive neuronal damage by rapid spread. In primary CNS cell culture derived from rats, L10 multiples more rapidly in neurons than avirulent strains, but infection with both virulent and avirulent strains causes depletion of oligodendrocytes (Atkins *et al.*, 1990). Experiments utilizing SFV4 and A7 showed that infection of cultured neurons was 10-fold higher for virulent strains then avirulent strains (Glasgow *et al.*, 1997). Little difference is found for infection of glial cells. In the CNS, both L10 and A7(74) strains infect neurons and oligodendrocytes, but differ in respect to the kinetics of viral spread and subsequent neuronal damage (Fazakerley *et al.*, 1993; Smyth *et al.*, 1990). It is thought that virulent strains of SFV spread rapidly in the CNS by axonal transport (Kaluza *et al.*, 1987). Avirulent strains, following intraperitoneal infection, cross the blood brain barrier by infection of the vascular endothelial cells (Dropulic and Masters, 1990; Soilu-Hanninen *et al.*, 1994) but fail to spread as rapidly in the neurons (Fazakerley *et al.*, 1993). A7(74) infection remains in small, delimited foci surrounding cerebral capillaries whereas L10 initiates an effective infection from small perivascular foci to a disseminated infection. Virulent strains cause more extensive damage to neurons in the CNS (Atkins *et al.*, 1985). Multiplication of avirulent strains is

much slower in the CNS due to their partially restricted ability to multiply in neurons (Balluz *et al.*, 1993; Fazakerley *et al.*, 1993; Gates *et al.*, 1985).

While virulent strains such as L10 and SFV4 induce fatal encephalitis 5-6 days after infection avirulent strains such as A7 and M9 induce immune mediated demyelination (Atkins *et al.*, 1985; Balluz *et al.*, 1993). Both virulent and avirulent strains of SFV have the capability to induce demyelination, the consequences of which are obscured by death for virulent strains. The virulence of the L10 strain is due to its ability to exceed a lethal threshold of damage to neurons before immune intervention can occur. The avirulent A7 and M9 strains do not cause extensive neuronal damage, but do induce immune-mediated CNS demyelination believed to be induced by phagocytosis of myelin debris from infected oligodendrocytes and the presentation of antigens derived from such debris to T-helper lymphocytes (Atkins *et al.*, 1985; Atkins *et al.*, 1990; Gates *et al.*, 1985). M9-SFV infection of SJL mice evokes an inflammatory reaction mediated by the pro-inflammatory cytokines, IFN-γ and TNF-α where cytokine mRNA can persist for up to a year after infection in the brains of the animals. Inflammatory lesions associated with cytokine mRNA expression were detected in SJL mice at 90 d.p.i. suggesting that secretion of the these negative regulatory cytokines may have a role in the progression of the disease (Donnelly *et al.*, 1997). Similarly type 1 IFN-γ responses are believed to play an important role in the neuropathogenesis of avirulent A7 (Keogh *et al.*, 2002; Keogh *et al.*, 2003). Further studies show that demyelination following an SFVA7(74) infection can be as a result of a T-cell mediated mechanism instead of direct viral damage (Amor *et al.*, 1996b; Fazakerley and Webb, 1987). From day 14 post infection demyelinating lesions were present throughout the CNS of the immunocompetent Balb/c mice only, no lesions were present in the athymic nu/nu or immunodeficient SCID mice (Amor *et al.*, 1996b). Previous studies have shown that CD8+ T cells in particular are important mediators of demyelination (Gates *et al.*, 1984; Morris *et al.*, 1997; Subak-Sharpe *et al.*, 1993). Myelin debris, released by destruction of oligodendrocytes, is phagocytosed by mononuclear cells and is subsequently presented to the immune system, which in turn leads to degradation of myelin by activated $CD8^+$ T cells.

1.2 Semliki Forest Virus expression system

1.2.1 Background to SFV expression systems

Many characteristics of SFV make it a good vector for rapid gene delivery. The genome is of positive polarity and therefore functions as mRNA giving very rapid foreign gene expression. The RNA genome has its own replicase which allows very efficient replication resulting in a high copy number of mRNA, the translation of which is not limited by processing. Replication takes place in the cytoplasm so there is no risk of integration into the chromosome. SFV induces apoptosis of infected cells therefore the virus genome does not persist in host tissue (Glasgow *et al.*, 1997; Grandgirard *et al.*, 1998; Scallan *et al.*, 1997). A very late onset of cytopathogenic effects allows for an extensive time frame (4 h to 24 h after infection) where a very high expression level of the structural proteins is combined with negligible morphological changes. SFV also has a broad host range, infecting most types of cell lines, for example, mammalian, avian and insect cells (Clark *et al.*, 1973; Griffin, 1986; Leake *et al.*, 1977; L'Heritier, 1970; Stollar, 1980). Its low pathogenicity in humans makes it safe to work with.

The original SFV infectious clone was generated from a strain derived from the original isolate, L10, by cloning viral cDNA under the control of a prokaryotic DNA-dependent RNA polymerase promoter, SP6 to allow viral mRNA to be transcribed *in vitro* (Liljestrom and Garoff, 1991). The RNA transcripts are fully infectious, and transfection of cells by electroporation with this RNA is sufficient to initiate intracellular replication and propagation of progeny virus particles. The original SFV vector system was developed from this first full length infectious clone by adding a second subgenomic promoter either up stream or downstream of the structural genes together with the foreign gene of interest (Raju and Huang, 1991). Thus, the structural proteins, as well as the foreign protein are efficiently transcribed from the subgenomic promoter. Despite leading to high protein expression upon replication, these vectors give rise to infectious virus, and high levels of structural protein synthesis may also potentially generate immune responses against the vector, making the system unsafe for *in vivo* studies. A suicide particle vector system was developed to allow foreign sequences to be encapsidated into infectious virions (Liljestrom and Garoff, 1991). The viral structural genes were deleted and replaced with a short polylinker sequence to facilitate insertion of the heterologous gene under the control of the 26S SG promoter, colinear with the last one-third of the genome. The vector still retains its

viral replicase which will initiate RNA synthesis from any subgenomic promoter on a minus strand molecule. To facilitate packaging, the system employs a helper vector. This helper clone has much of its nonstructural coding region deleted and also contains a deletion in its own packaging signal. The helper RNA itself cannot be packaged but can provide structural proteins along with *cis*-acting 5' and 3' replication signals for the recombinant vector RNA. Co transfection of the helper and recombinant vector result in the packaging of vector RNA into particles and subsequent release from the cells. This system limits production of fully infectious virus particles since the helper virus lacks a packaging signal and the vector lacks the structural protein genes. To further increase biosafety of this vector, a split-helper system was developed in which two separate helper plasmids supply the genes encoding the capsid and envelope proteins, and a further mutation in the helper capsid, an S219A substitution prevents production of infectious virus by abolishing self-cleavage ability (Smerdou and Liljestrom, 1999). The SFV genome and its split-helper system are illustrated in figure 1.4. These changes allow production of replication deficient SFV particles. Recombinant particles are produced when all three RNA species are electroporated into the same BHK cells. After infection or inoculation, these particles undergo one round of replication resulting in transient expression of the gene of interest. No infectious virus is produced. The processes involved in the production of rSFV particles are shown in figure 1.5.

Recent modifications to the alphavirus expression system have included taking advantage of a translational enhancer (Cenh) sequence, located in the N-terminal region of the C-protein (Sjoberg *et al.*, 1994). This enhancer, which appears to be active only in the context of the alphaviral replicon, has been mapped to the first 102 nucleotides in SFV C-protein (Sjoberg and Garoff, 1996). This C-enh induced up to 10-fold more β-galactosidase expression when LacZ was cloned in-frame at the 3' end of the capsid gene. The autoproteolytic activity of the C-protein enables it to cleave itself from the nascent fusion protein chain during translation. Alternatively, the inclusion of only the first 48 a.a. of the C-protein results in high-level synthesis of uncleaved fusion proteins. This C-enh is included upstream of the envelope protein genes in the "split" helper system in order to produce equal levels of capsid and spike proteins following transfection (Smerdou and Liljestrom, 1999).

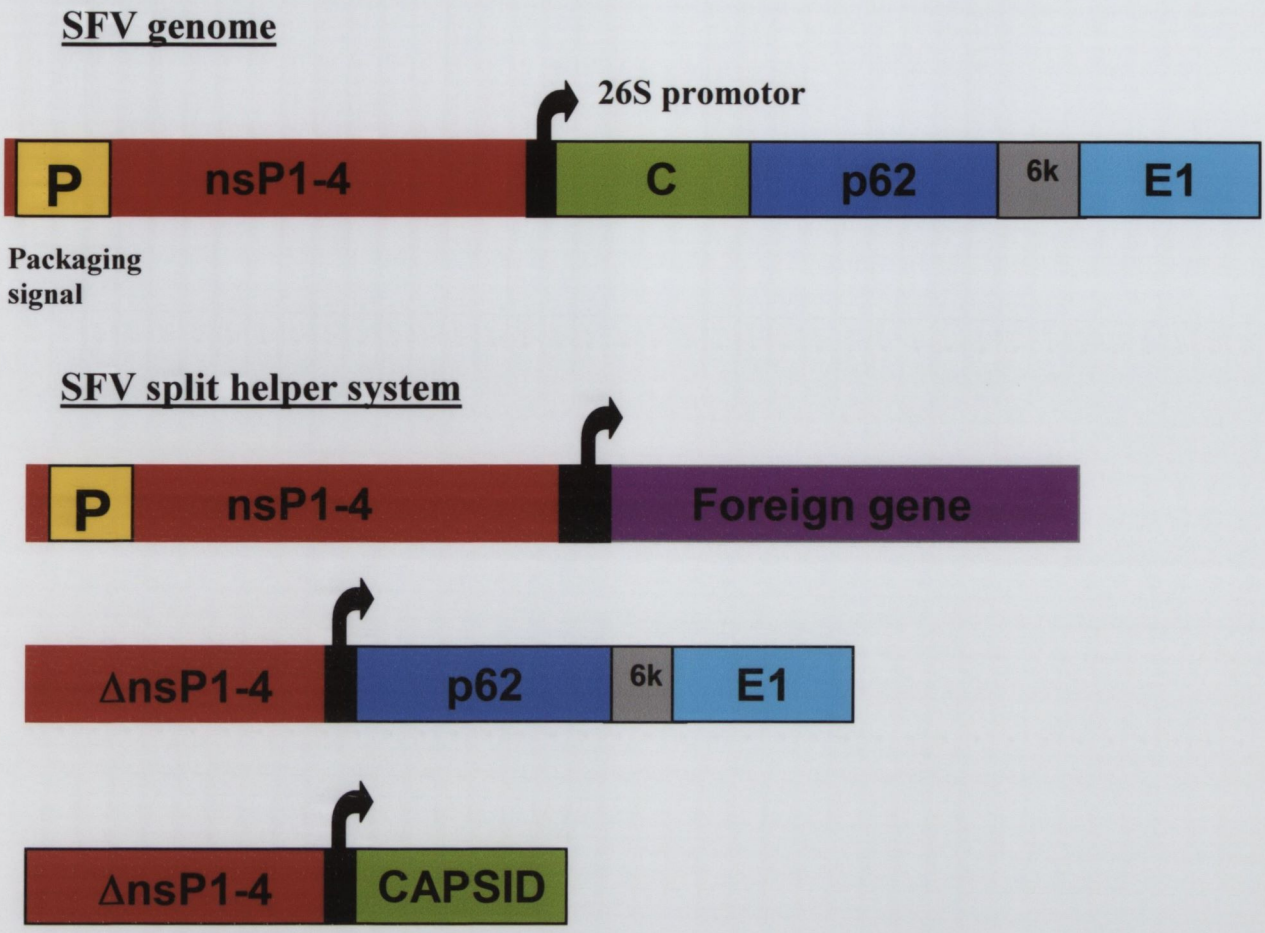

Figure 1.4 The SFV split helper expression system

The SFV split helper system consists of a recombinant SFV vector expressing a foreign gene of interest in replace of its structural genes. Two separate helper plasmids supply the structural genes *in trans,* the helper spike and the helper capsid. The helper molecules lack the viral non-structural sequences (nsP1-nsP4), and are dependent on the replicase of the rSFV vector for amplification *in vitro*. This system allows production of replication deficient viral particles only, as the infecting rRNA lacks the structural genes necessary to form infectious virus. To further increase biosafety, the helper capsid plasmid contains another deletion which abolishes its self cleavage ability. This system allows production of recombinant virions expressing the foreign gene which undergo one round of replication resulting in transient expression.

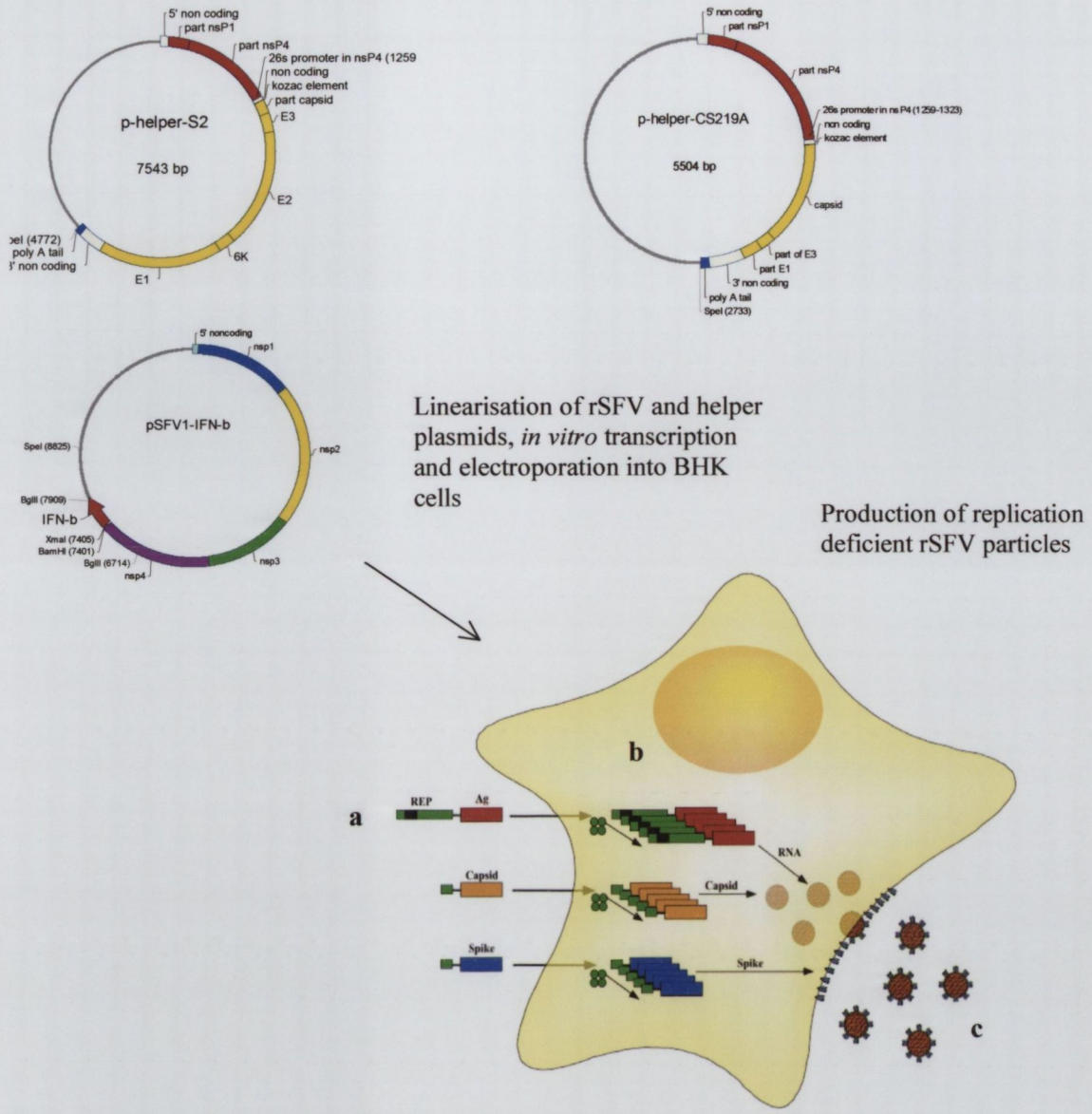

Figure 1.5 Production of recombinant SFV particles

The rSFV vector and its helper plasmids are linearised, *in vitro* RNA transcribed and all three RNAs are co-transfected by electroporation into BHK cells (a). Upon co-transfection, rSFV particles expressing the heterologous protein are assembled (b) and released from the cells by budding (c). Replication deficient rSFV particles are formed as the rSFV vector lacks its structural genes, which are supplied *in trans* by the helper spike and helper capsid. A further mutation in the helper capsid prevents production of wild–type infectious virions by abolishing self-cleavage function. These recombinant particles give high-level expression of the heterologous protein on infection.

1.2.2 SFV vectors in vaccine development

SFV vectors have been shown to be successful in inducing humoral and cell-mediated immunity against several diseases. Their strong protective efficacy makes them ideal candidates for development of prototype vaccines. Previous studies have shown that the administration of rSFV RNA by intramuscular (i.m.), intravenous (i.v.) or subcutaneous (s.c.) routes led to significant levels of antigen-specific CTL responses and increased numbers of specific CD8+ T cells, as detected by tetramer binding (Colmenero *et al.*, 2001). The distribution of antigen-specific CTLs correlated with the *in vivo* distribution pattern of rSFV, with a highest frequency in the spleen or local lymph node, depending on the injection route. Berglund *et al.* 1998 exploited the immunogenicity of rSFV vectors in a vaccination against influenza, by administering an SFV DNA vector expressing Lac Z, and rSFV suicide particles expressing Lac Z and comparing the protection they elicit to that of a conventional DNA CMV expression system. Mice immunized with such vectors developed humoral and cellular immune responses at higher levels than mice that received the conventional vaccine vector, and acquired protective immunity to lethal influenza challenge. Further vaccine studies used rSFV as a prototype influenza vaccine from which to express the NP of influenza (Berglund *et al.*, 1999). Mice immunized with rSFV-NP vectors developed antigen specific IgG levels and induction of CTL memory cells that were protective against challenge with infectious influenza. rSFV vectors have also been used as a prototype vaccine against LIV, a member of the tick-borne flavivirus, which predominantly causes disease in sheep. SFV vectors expressing the LIV envelope proteins prME and NS1 have elicited significant protection against LIV infection in both mouse and sheep models (Fleeton *et al.*, 1999; Morris-Downes *et al.*, 2001). Immunization of mice with the rSFV-prME construct elicited complete protection when animals were subsequently challenged intraperitoneally. In a sheep model rSFV-LIV particles generated a robust immune response giving complete protection following challenge by s.c. route. rSFV-LIV vector vaccines have proved to induce a better protective response than a commercially available formaldehyde inactivated virus preparation or a standard naked DNA vaccine (Fleeton *et al.*, 2000). Many studies have been done on the use of rSFV as a vaccine against HIV, with initial studies using an SIV challenge model (Hanke *et al.*, 2003; Mossman *et al.*, 1996; Nilsson *et al.*, 2001; Nordstrom *et al.*, 2005). rSFV vectors expressing SIV envelope protein gp160 showed protection against lethal challenge with SIV in macaques when administered together with

a gp120 subunit vaccine (Mossman *et al.*, 1996). In HIV SFV particle vectors expressing HIVA, an immunogen derived from HIV –1 clade A was shown to be highly immunogenic for HIV T-cell-mediated immune responses and induced T cell memory that lasted for 6 months (Hanke *et al.*, 2003).

1.2.3 SFV vectors in tumour therapy

Many features of the SFV expression system make it an attractive option for cancer gene therapy. One of the most attractive features of the system is its ability to induce apoptosis in infected cells (Allsopp *et al.*, 1998; Glasgow *et al.*, 1997), independently of p53 (Glasgow *et al.*, 1998). When a recombinant, replication deficient SFV vector was used to express the LacZ marker gene product in seven human prostate cell lines, as well as in human prostate tissue explants, flow cytometry revealed that 40-60% of PPC-1 prostate cancer cells died 24-72 h after infection (Hardy *et al.*, 2000). SFV vectors have also been administered intratumorally to study therapeutic efficacy in tumour models such as a human lung carcinoma model, a rat prostate cancer cell line, a murine sarcoma model and a murine colon carcinoma model (Chikkanna-Gowda *et al.*, 2005; Murphy *et al.*, 2000; Murphy *et al.*, 2001; Smyth *et al.*, 2005). SFV vectors expressing EGFP were used to treat the human lung carcinoma model, by intratumoral injection, that had been implanted as xenografts into nude mice (Murphy *et al.*, 2000). rSFV-EGFP suicide particles induced apoptosis in H358a cells, which are human non-small cell lung carcinoma cells deleted in p53, resulting in inhibition of tumour growth and in some cases complete tumour regression. The murine sarcoma virus transformed Balb/3T3 cell line, K-Balb and the murine colon carcinoma CT26 cell line both underwent apoptosis and expressed viral antigen when infected with both SFV4 infectious virus and rSFV vector expressing the p62 –6K structural genes (Smyth *et al.*, 2005). The K-Balb tumour model showed greater inhibition and overall antitumoral effect when immunized with SFV4 virus. No significant difference was observed in CT26 tumours between rSFV replication deficient particles and SFV4-treated groups, but prior immunization considerably enhanced the antitumoral response in both groups.

The apoptotic characteristic of the vector lies within the non-structural region of the SFV (Barr *et al.*, 2000), which is maintained in the vector. This allows for insertion of genes in place of the structural region, which could modify or enhance its pro-apoptotic or anti-tumor properties. Administration of SFV vectors expressing the IL-12 subunits, p35

and p40 have been shown to be particularly effective in inducing an antitumoral response and regression of many tumour models (Asselin-Paturel *et al.*, 1999; Chikkanna-Gowda *et al.*, 2005; Colmenero *et al.*, 2002; Ren *et al.*, 2003; Rodriguez-Madoz *et al.*, 2005; Yamanaka *et al.*, 2002; Zhang *et al.*, 1997). IL-12 is an immunomodulatory cytokine, which plays a key role in the induction of T-helper1 responses. Administration of high titre rSFV10-E-IL-12 particles intratumorally to treat implanted K-Balb tumours in Balb/c mice demonstrated complete tumour regression in comparison to control or rSFV10-IL-12 treated groups (Chikkanna-Gowda *et al.*, 2005). Treatment also proved effective in the CT26 tumour model and in a metastatic (4T1) tumour model by inhibition of primary tumour growth and lung metastases. Histological and immunohistochemical studies revealed tumour necrosis in addition to aggressive influx of CD4+ and CD8+ T cells and other immune cells. Some work has been done on enhancing the p53-independent apoptotic characteristic of SFV by expression of the Bax gene (Hoffman *et al.*, 2001). This pro-apoptotic member of the Bcl 2 superfamily enhanced the cytopathic and anti-tumor potential of the vector, while counteracting the anti-apoptotic *Bcl*-2 gene.

1.2.4 SFV as a vector for the CNS

The easy and fast generation of alphaviruses and their preferential transduction of neurons in cell and tissue culture make them an increasingly used gene transfer system. Recombinant SFV particles have been shown to efficiently deliver genes into dispersed primary neurons in culture (Olkkonen *et al.*, 1993). In this study two canine kidney cell membrane–associated reporter genes, the rab8, a small GTPase involved in post-Golgi vesicle transport and the VIP21, a membrane protein involved in the trans Golgi network were expressed by the original recombinant SFV suicide particle vector system in cultured rat hippocampal neurons. Expressed proteins were first detected in the neurons 3-4 h post infection. The infection rate was impressively high with 50-60 % of the cells expressing the reporter genes after 6 h infection at a multiplicity of one. SFV vectors also efficiently and preferentially infect neurons in organotypic slices prepared from the hippocampus of 6 day old rats (Ehrengruber *et al.*, 2001; Ehrengruber *et al.*, 1999). When the pyramidal cell layer, an area known to contain large numbers of glia and microglia, was transfected with recombinant SFV suicide vectors expressing the reporter genes, Lac Z and EGFP, 60 and 90% of positive cells were identified as neurons and pyramidal cells respectively. The time course of EGFP expression in cultured slices was transient and showed a peak at 1-2

d.p.i indicating that rSFV may be preferred for rapid, high level and neuron–specific transgene expression. *In vivo* studies using the SFV-Lac Z vector caused local high level galactosidase expression after injection into the striatum and amygala of rat brain. Maximal transgene expression was obtained at 1-2 d.p.i and galactosidase levels declined thereafter (Lundstrom, 1999).

More recently two novel vector systems based on the avirulent A7(74) strain have been developed and used to express the fluorescent reporter gene, EGFP. One of these vectors, VA7 is derived from the full length cDNA clone of the avirulent A7(74) strain (Vaha-Koskela *et al.*, 2003). This replication-proficient expression vector has a second subgenomic promoter inserted in the viral 3' NTR through which a heterologous gene is expressed. This VA7 vector expressing EGFP efficiently transduced pyramidal cells, interneurons, and glial cells in cultured rat hippocampal slices. The number of EGFP-expressing neurons in hippocampal slices increased with prolonged time post infection. Mice infected intraperitoneally with the recombinant virus remained completely asymptomatic but showed CNS expression of EGFP as evidenced by immunohistochemistry. Another vector, the replication deficient SFV(A774nsP)-GFP was constructed which encoded EGFP downstream from nsP1-4 region of the avirulent SFV strain A7(74) with preliminary results showing that this vector only infected neurons at 31°C and not at 37°C . When rat hippocampal slices and dissociated mixed glial cells were infected with both the SFV(A774nsP)-GFP and VA7-EGFP, and incubated at 37°C, virtually no neurons were transduced. At 31° C, 33% of the cells infected with SFV(A774nsP)-GFP in slices were neurons, and 94% of cells infected in dissociated cells were neurons. 94% of cells infected with VA7-EGFP in slices were neurons at the same temperature (Ehrengruber *et al.*, 2003). These results show that in addition to the developmental age, the temperature determines which cell type becomes infected by A7(74). This data suggests that A7(74) is avirulent in adult animals because it does not readily replicate in mature neurons at body temperature, whereas it still does so at lower temperatures.

Most recently the split helper SFV suicide expression system has been used to express EGFP *in vivo*. Intranasal administration of recombinant SFV particles, expressing the reporter gene, EGFP, showed that high level EGFP expression could be detected in incoming axons from receptor cells in the olfactory epithelium that terminate in the glomerular area of the olfactory bulbs. Expression occurred in the olfactory bulb as early

as one day after intranasal inoculation and continued for up to 10 days, with no detectable pathological damage. In some cases expression lasted for up to 14 days. Viral RNA could be detected only in the nasal passage of infected animals and persisted for 7 days suggesting that only the expressed protein enters the CNS (Jerusalmi *et al.*, 2003).

1.3 Components of the Central Nervous System

1.3.1 Neurons

Neurons are the basic functional units of the nervous system. They respond to physical and chemical stimuli, conduct electrochemical impulses and release specific chemical regulators. Although neurons vary considerably in size and shape, they generally have three principle regions: a cell body, dendrites and an axon. The cell body contains the nucleus and densely staining areas of rough ER known as Nissel bodies. Dendrites are thin-branched processes that extend from the cytoplasm of the cell body and transmit electrical impulses to the cell body. The axon is a longer process that conducts impulses away from the cell body. The structure of a neuron is shown in figure 1.6. There are two main types of neurons: sensory or afferent neurons which conduct impulses from sensory receptors into the CNS and motor or efferent neurons which conduct impulses out of the CNS to effectors organs (muscles and glands). A nerve is a bundle of axons located outside the CNS. Some axons in the CNS and the PNS are surrounded by a myelin sheath. Schwann cells form the myelin sheaths in the PNS and the myelin sheaths in the CNS are formed by oligodendrocytes. Each Schwann cell wraps only 1 mm of axon leaving gaps of exposed axon between adjacent Schwann cells called nodes of Ranvier. Unlike Schwann cells oligodendrocytes have extensions that form myelin sheaths around several axons. Areas of the CNS that contain a high concentration of axons form the white matter. In MS or EAE myelin loss results from damage to oligodendrocytes or myelin itself. The process of demyelination is seen in Figure 1.7. Myelin damage is accompanied by a decrease in conduction velocity and a loss of cell-cell interactions between the axon and myelinating glial (Fox, 1996). Active lesions in the brains of MS patients contain both damaged and transected axons (Ferguson *et al.*, 1997; Trapp *et al.*, 1998). Areas of demyelination are populated by mononuclear cells such as phagocytic macrophages (Lucchinetti *et al.*, 1996; Rodriguez and Scheithauer, 1994).

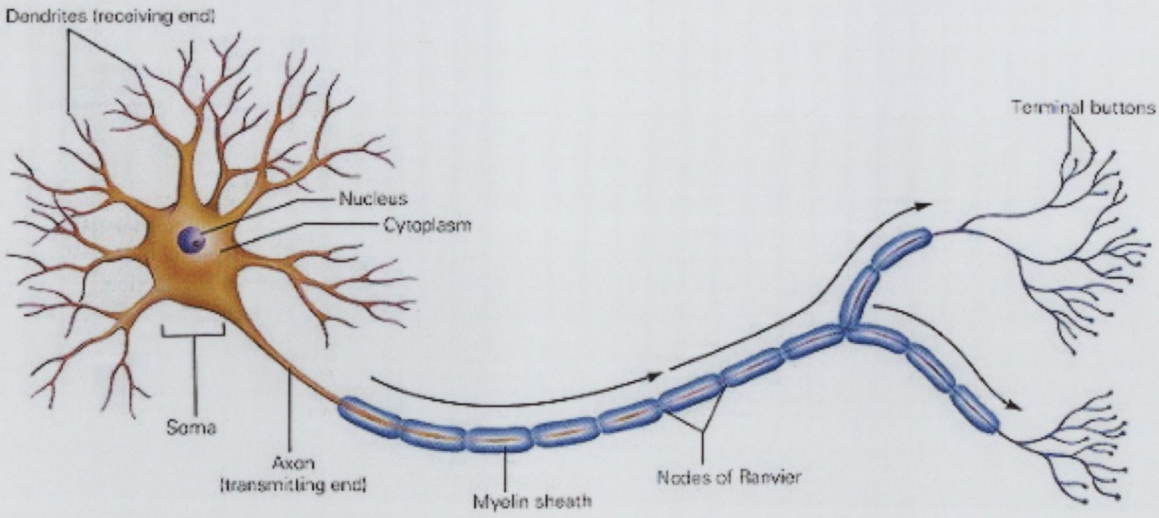

Figure 1.6 Structure of a neuron

A neuron generally consists of three principle regions: a cell body, dendrites and an axon. The cell body or the soma is the enlarged portion of the neuron that contains the nucleus. It serves as a nutritional centre where macromolecules are produced. It also contains densely staining areas of rough ER known as Nissel bodies. Dendrites are thin, branched processes that extend from the cytoplasm of the cell body. They transmit electrical impulses to cell body. The axon is a longer process that conducts impulses away from the cell body. The axon is surrounded by a myelin sheath, which is composed of successive wrappings of the cell membrane of Schwann cells (in the PNS) or oligodendrocytes (in the CNS). Gaps of unmyelinated, exposed axon in the myelin sheath are called the nodes of Ranvier. These gaps transmit nerves impulses along the axon to the terminal buttons. Adapted from Human Physiology, The Nervous System, Stuart Ira Fox, 2002.

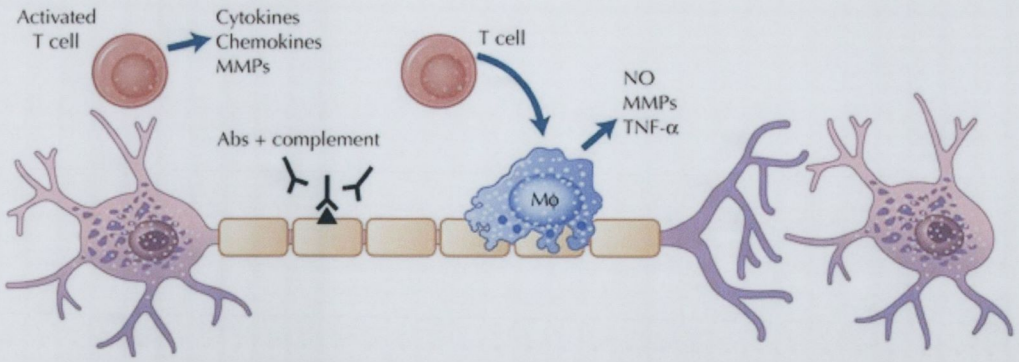

Figure 1.7 Demyelination within the CNS

In MS or EAE lesions, demyelination of the myelin sheath surrounding the axons of the neuron occurs when activated autoimmune T cells cross the BBB and release pro-inflammatory cytokines, chemokines and MMPs. Release of Th1 cytokine, IFN-γ, activates the resident macrophages in the CNS, the microglial cells, which through their role as APCs and their ability to produce TNF-α and NO result in demyelination. TNF-α causes direct damage to the myelin-producing oligodendrocytes. NO is also shown to cause damage to oligodendrocytes and to lipid and protein components of myelin sheath. Release of chemokines such as MIP-1 and RANTES attract antigen-specific T cells and other nonspecific macrophages through the BBB, and then stimulate these leucocytes to release proteases which can cleave myelin proteins such as MBP into peptides. MMPS also attract autoreactive lymphocytes across the extracellular matrix into the CNS and mediate degradation of myelin components. Myelin autoantibodies play a significant role in the demyelinating process. They are produced by infiltrating plasma cells and B cells. Release of Th2 cytokines such as IL-10 are thought to contribute to demyelination by enhancing proliferation of these B cells leading to antibody and complement mediated demyelination. http://mult-sclerosis.org.

1.3.2 Astrocytes

Astrocytes are the most abundant glial cell in the mammalian brain and out number neurons 10 to 1. Protoplasmic astrocytes are found predominantly in grey matter and fibrous astrocytes are localized primarily in the white matter, having long thin ramified process. They can be distinguished from other CNS cells by their expression of GFAP, an astrocyte–specific intermediate filament. Astrocytes influence the formation and maintenance of the BBB *in vitro*, both by production of soluble mediators and by cell-to-cell contact. *In vivo* astrocyte foot processes are in close apposition to the surface of the microvascular endothelium of the BBB, thus astrocytes contribute to the both the structural and functional integrity of the BBB. Glutamine synthetase is an enzyme that has been localized to astrocytes and which helps to regulate levels of the neurotransmitter glutamate and prevent chronic glutamate toxicity through the astrocyte glutamate transporters GLAST and GLT-1. Astrocytes also produce a glial reaction in response to neurological insult characterized by astrocytic proliferation, morphologic changes and enhancement of GFAP expression. This reaction is termed astrogliosis and may be detrimental by inhibiting neuronal function through the formation of glial scarring creating a physical barrier to the regrowth of axons (Peterson and Remington, 2000).

Astrocytes have the capacity to respond to or secrete many immunomodulatory cytokines/chemokines, including IL-1, IL-4, IL-6, IL-10 and IL-12: GM-CSF, IFN-γ TGF-β (Barna *et al.*, 1990; Giulian and Lachman, 1985; Yong *et al.*, 1991). It is through their ability to respond to these cytokines that astrocytes contribute to the inflammatory response typical of MS and EAE. In addition astrocytes are capable of expressing a variety of immunologically relevant proteins such as class I and class II MHC antigens, complement and adhesion molecules (Shrikant and Benveniste, 1996; Traugott and Lebon, 1988)). One of the main immunomodulatory cytokines that astrocytes produce is IL-6 (Van Wagoner *et al.*, 1999). This cytokine has a number of pro- and anti–inflammatory effects in the CNS. In the presence of the IL-6R, IL-6 can upregulate chemokine production such as RANTES, MCP-1 and adhesion molecule, ICAM-1, on endothelial cells. On the other hand it can inhibit TNF-α expression and induce the expression of soluble TNF-α receptors and IL-1R antagonist (Benveniste *et al.*, 1995; Tilg *et al.*, 1994). *In vivo* and *in vitro* studies also show a role for IL-6 in neuronal survival, protection and differentiation (Gadient and Otten, 1997). Astrocytes also secrete an IL-3 like factor that induces growth of brain tissue macrophages and GM-CSF, a cytokine necessary for growth and

differentiation of macrophages leading to accumulation of macrophages at the site of inflammation (Frei *et al.*, 1985; Frei *et al.*, 1992).

1.3.3 Microglial cells

Microglial cells are the resident macrophages found in the CNS. They reside in the brain parenchyma, are derived from bone marrow and populate the brain early in development. They are a homologous group of cells and differ slightly in their morphology depending on what part of the brain they are found. Following tissue injury or infection in the brain, microglial activation generally precedes any other response. Activated microglia change their immunophenotype, upregulating molecules such as MHC class I and class II. In immune mediated responses such as MS and EAE, they also express B7 molecules (De Simone *et al.*, 1995; Windhagen *et al.*, 1995). Activated microglia also release IL-1a and TNF-α and acquire a phenotype consistent with the respiratory burst reaction of activated monocytes in which molecules of the cyclo-oxygenase pathway are upregulated and oxygen free radicals are released. One of the main roles of microglial cells is in tissue damage demyelination (Benveniste, 1997; Dijkstra *et al.*, 1992; Hendriks *et al.*, 2005). They scavenge myelin debris by phagocytic uptake facilitated by clathrin coated pits, via Fc receptor binding on the surface of microglia-macrophage cells (Raine and Scheinberg, 1988). Through their role as APCs they can also present myelin debris to autoreactive T cells (Matsumoto *et al.*, 1992).

1.3.4 Myelin

Myelin is a lipid protein membrane primarily found in the white matter of the CNS and in the peripheral nerves containing large motor axons. It consists of 70% lipid and 30% protein. The major glycolipid in myelin is galactocerebroside. The lipid molecules are arranged such that the hydrophilic portions provide the interface between the aqueous layers, and acyl chains produce the hydrophobic core. The myelin sheath is arranged in concentric layers and the myelinated segments of nerve are separated by regularly spaced nodes of Ranvier. The major protein of CNS myelin is proteolipid protein (PLP). PLP plays an important role in oligodendrocyte development. Absence of PLP results in premature cell death and hypomyelination. Mice containing PLP point mutations exhibit axial body tremors followed by tonic seizures and subsequent death. Myelin basic protein (MBP) is present in both the PNS and in the CNS compact myelin. MBP exists in multiple

isoforms that are derived from exon splicing and post translational modifications such as phosphorylation and methylation. Unlike other myelin proteins it is not a transmembrane protein. Shiverer mice, which lack functional MBP, show intention tremor, convulsions and premature death. Myelin associated glycoprotein (MAG) is a member of the Ig superfamily and contains five extracellular Ig-like domains and an intracellular domain that can that be modified via phosphorylation and alternative messenger RNA splicing. There are two isoforms: 64 kDa and 60kDa. MAG is phosphorylated by protein kinase C in cultured oligodendrocytes which has been found to be involved in oligodendrocyte differentiation and process formation. MAG also contains an RGD (Arg-Gly-Asp) sequence that is known to play an important role in attachment to the integrin family. Myelin oligodendrocyte glycoprotein (MOG) is classified as a minor myelin glycoprotein in comparison to the other myelin proteins. It is found on the outer surface of oligodendrocytes and myelin sheaths (Dangond, 2002). Due to its easy accessibility, MOG has been implicated as a target Ag for Ab-mediated attack in diseases of the CNS. Anti-MOG antibody has also been found in the serum of MS patients (Angelucci *et al.*, 2005; Berger *et al.*, 2003; Egg *et al.*, 2001).

1.3.5 Oligodendrocytes

Oligodendrocytes are the cells of the CNS responsible for production and maintenance of myelin sheaths of the axons in the CNS, where one cytoplasmic process provides myelin for one internode of an axon. Unlike their counterparts, the Schwann cells, which are responsible for myelination in the PNS, oligodendrocytes can extend multiple processes, ensheathing multiple nerves. Myelination begins with contact between the oligodendrocyte and axonal membranes, followed within the cytoplasmic space by a compaction process that results in the apposition of the two opposing bilayers (Dangond, 2002). Oligodendrocytes are susceptible to damage via a number of immune or toxic mechanisms present within the MS lesions. These factors include cytokines such as TNF-α and IFN-γ, the generation of reactive oxygen or nitrogen species, the production of excitatory amino acids such as glutamate and the release of proteolytic and lipolytic enzymes. Pathological studies have shown the presence of preserved oligodendrocytes in actively demyelinating lesions. These cells may either be myelinating cells that have not been affected by the demyelinating process or mature oligodendrocytes that have survived the loss (Bruck *et al.*, 1994; Ozawa *et al.*, 1994; Prineas *et al.*, 1989).

1.4 Multiple Sclerosis

1.4.1 Background and classification of disease

MS is a chronic inflammatory demyelinating disease of the CNS which is characterized by the presence of sclerotic lesions throughout the brain and spinal cord. It is thought to be an immune mediated disease triggered by an unknown exogenous reagent in subjects with a specific genetic background. MS can be classified into four main types of disease in humans – relapsing-remitting MS (RRMS), secondary-progressive MS (SPMS), primary-progressive MS (PPMS), progressive-relapsing MS (PRMS) (Lublin and Reingold, 1996). A fifth type is Benign MS. The five main types of disease are showed in Figure 1.8. MS symptoms generally appear in people aged 20 to 40 years, and women are more likely than men to have the disease. RRMS accounts for 85-90% of MS at onset and it is characterized by self-limited attacks of neurological dysfunction. These attacks develop acutely, evolving over days to weeks while in between attacks the patient is neurologically and symptomatically stable (Weinshenker *et al.*, 1989a; Weinshenker *et al.*, 1989b). The first clinical progressive MS, SPMS, begins as RRMS but at some point, changes such that the attack rate is reduced and the course becomes characterized by a steady deterioration in function, unrelated to acute attacks. The course of disease in over 90% of RRMS patients ultimately changes to SPMS in a 26 year follow up (Weinshenker *et al.*, 1989b). PPMS usually occurs after the age of 40 years and is only slightly more common in women than men with a ratio of about 1.3:1. PPMS is a progressive disease from onset, with occasional plateaus but no distinct relapses, and affects primarily the spinal cord (Andersson *et al.*, 1999; McDonnell and Hawkins, 1996). PRMS also begins with a progressive course, although these patients experience occasional attacks while accumulating significant disability in the interval between attacks (Andersson *et al.*, 1999). Benign MS is characterized by mild to moderate symptoms, which do not worsen or lead to permanent disability. It is present in 20 to 40 percent of people with MS (Edan and Sabouraud, 1991; Weinshenker, 1995).

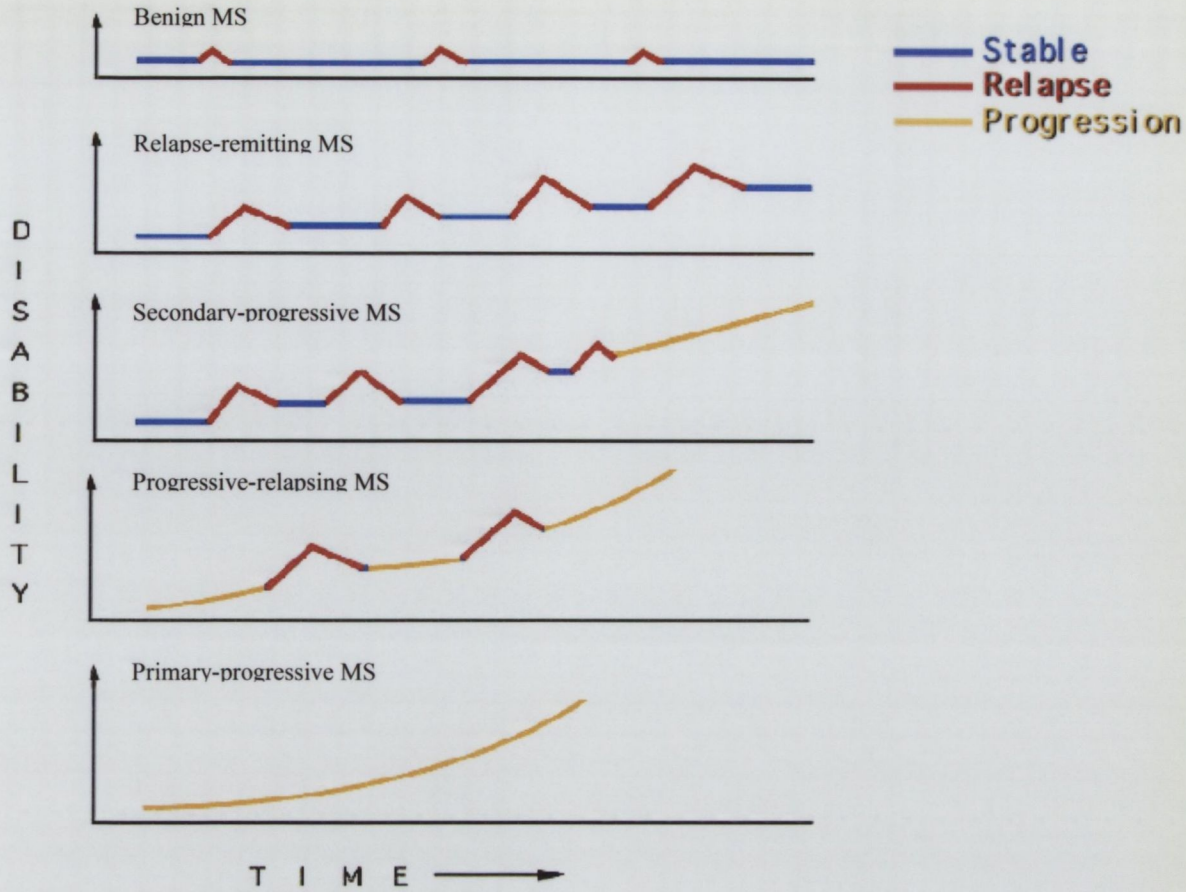

Figure 1.8 Classification of MS

MS can be classified into five main types of disease: benign, relapsing-remitting, secondary progressive, primary progressive and progressive relapsing MS. Benign MS is considered to be a precursor to RRMS, in which patients present with underlying symptoms and infrequent relapses but full diagnosis cannot be made yet. It is characterized by mild to moderate symptoms which do not worsen or lead to permanent disability. The second type of disease, RRMS accounts for 85-90% of MS at onset, where patients experience recurrent attacks followed by periods of total remission. Disability may accumulate after each new attack, and eventually clinical presentation may become that of SPMS. In this third type of MS, patients have a relapsing disease that develops into a continuous progressive disease accompanied by constant deterioration in neurological function. PRMS is the least common type of disease. Patients with PRMS experience occasional attacks while accumulating significant disability in the interval between attacks. The fifth and most severe type of disease, PPMS is progressive from disease onset. Patients experience acute onset of symptoms which do not significantly improve with time. http://womenshealth.med.miami.edu

1.4.2 Etiology of disease

The cause of MS is still unknown, though genetic, immunogenic and environmental factors, as well as exogenous infectious agents and diet are all thought to contribute to disease pathogenesis. To date, there has been no conclusive evidence that suggests MS is a genetic disease. There is however evidence that points to a genetic link. Half-sibling and adoption studies confirm that genetic and not environmental factors are responsible for familial aggregation (Ebers *et al.*, 1995; Sadovnick *et al.*, 1996). The combined results of several of the larger population based twin studies demonstrated that a monozygotic twin of an MS patient is at a higher risk (25-30% concordance) of developing MS than a dizygotic, same sex twin (2-5 % concordance). Linkage analysis in families with more than one member affected has revealed an association of the MHC alleles with increased risk of developing the illness. Extended MHC haplotype analysis concluded that Class II DR2 haplotype conferred true susceptibility to the disease rather than just being a marker of risk (Hauser *et al.*, 1989; Hillert and Olerup, 1993; Olerup and Hillert, 1991). These MHC molecules may fail to negatively select autoreactive T cells within the embryonic thymic microenvironment or may encode a class II recognition molecule with a propensity to bind peptide antigens of myelin and stimulate encephalolithic T cells. The frequent occurrence of MS in some ethnic populations than in others, irrespective of geographic location, further provides evidence for a genetic link. For example populations of northern latitudes have a higher incidence of disease than those of Asian and African origins (Compston, 1997; Ebers and Sadovnick, 1994; Oksenberg, 1996; Poser, 1995). Studies done on resistant ethnic groups, such as gypsies in Bulgaria, who reside within these high risk areas have suggested a genetic resistance to the disease (Milanov *et al.*, 1997).

MS is in general a temperate disease with a population prevalence that decreases with decreasing latitudes (Kurtzke and Delasnerie-Laupretre, 1996). This characteristic, geographic distribution may implicate a pathogen that is unevenly distributed as a causative agent of MS. Migratory studies show that children born to parents who have migrated from a high risk to a low risk area appear to have a lower life time risk than their parents (Martyn and Gale, 1997). Conversely migration of parents from a low-risk to a high-risk area confers a higher risk in the children. Consistent patterns suggest that children of a critical age, believed to be between 13-20, with a genetic predisposition to an infectious agent, are more at risk of acquiring MS (Gale and Martyn, 1995). Clusters of outbreaks of MS, such as those described in the Faroe Islands, also empathize the potential

role of an infectious agent. It is believed that British troupes introduced MS during their five year occupation from 1941 to 1944. By 1991, 42 cases of MS were documented amongst native Faroese. Prior to these patients, no single resident patient who had experienced clinical onset in this century prior to July 1943 could be found (Kurtzke *et al.*, 1993). To date no environmental agent can satisfactorily account for the worldwide distribution of MS.

In some studies a role for different viral and bacterial infections in MS has been shown. Since initial exposure to numerous viruses, bacteria and other microbes occurs during childhood, and since viruses are well recognized as causes of demyelination and inflammation, it is possible that a virus or other infectious agent is the triggering factor in MS (Allen and Brankin, 1993; Atkins *et al.*, 2000). Viruses commonly implicated in the pathogenicity of MS are HSV, HHV-6, retroviruses, EBV, rubella virus, measles virus, mumps virus and the varicella zoster virus. Higher antibody titres against each of these have been detected in the serum and CSF of MS patients when compared to control individuals (Granieri and Casetta, 1997). The association between MS and dual infection with retrovirus and EBV has also been evaluated (Haahr and Munch, 2000). Herpes viruses are thought be involved in the acute attack stage of RRMS (Berardelli, 1997). HHV- 6 is highly neurotropic and has a tendency to reactivate itself in response to stress or infection with another agent. Primary infection with HHV-6 usually occurs during the first two years of life, consistent with the epidemiological evidence of childhood exposure to the causative agent (Berti *et al.*, 2000; Goodman *et al.*, 2003). One bacterial agent *Chlamydia pneumoniae* has also been implicated through the finding of a secondary infection in already injured brain tissue (Sriram *et al.*, 1998).

Looking at all the evidence so far MS appears to have both strong genetic and epidemiological links. Other exogenous factors such as geographical, ecological and socio-cultural factors also have an important impact on disease development and progression. Low temperature and high levels of humidity may have direct effects on the immune system, leaving those living in such areas predisposed to more frequent respiratory tract infections (Lauer, 1995). Lack of vitamin D has been implicated in MS development as areas which receive minimal sunlight in the winter experience higher incidence of disease (Embry *et al.*, 2000). Studies have shown that the consumption of animal fat correlates with the geographical distribution of MS. In contrast polyunsaturated omega 6 fatty acids are shown to have a beneficial effect on severity of relapses (Lauer,

1997). Various studies have supported the idea that people of higher socio-economic class tend to be more likely to develop MS compared with the average population (Granieri, 2000). The theory that MS is an immune response to an infectious agent could explain the lower incidence of MS among children with low socio-economic level who are in general infected earlier (Poskanzer *et al.*, 1981). A strong association of MS risk has also been implied in individuals born or living in urban areas (Kurtzke and Page, 1997).

1.4.3 Epidemiology

MS frequency is positively correlated with latitude in both hemispheres (Kurtzke, 1980; Kurtzke and Delasnerie-Laupretre, 1996). In both the northern and southern hemispheres, the prevalence of MS decreases with decreasing latitude (Figure 1.9). A high prevalence of MS is found in Caucasians of Northern European origin where the lifetime risk of disease can be as high as 0.2- 0.3% and the population prevalence is 1 in 1000 (Robertson *et al.*, 1996; Weinshenker, 1996). High incidence rates of disease are found in Scandinavia, Iceland, the British Isles, Ireland and the countries settled by their inhabitants and descendants (Compston, 1997; Martyn and Gale, 1997; Poser, 1995), for example in the United States, Canada, Australia and New Zealand the prevalence is higher among Caucasians than in other racial groups. Even within the US, distinctions exist in the prevalence of MS between populations living north and south of the 37th parallel (Hogancamp *et al.*, 1997). The highest reported prevalence of MS, estimated at 250 cases per 100,000 population, occurs in the Orkney Islands north of Scotland (Swingler and Compston, 1986). MS is uncommon in Japan (2 per 100,000) and other Asian nations, in sub-Saharan Africa, the Indian subcontinent and in the native populations of the Americas (Oksenberg and Barcellos, 2000).

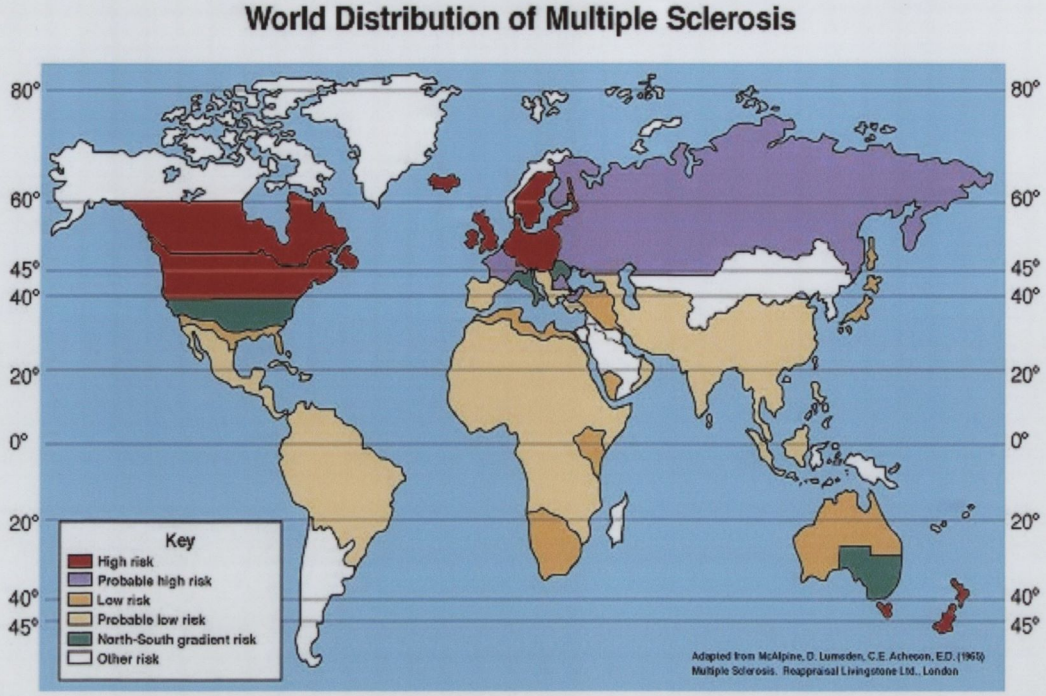

Figure 1.9 Epidemiology of Multiple Sclerosis

Studies have shown that the MS is positively correlated with latitude in both hemispheres. In both the northern and southern hemispheres, the prevalence of MS decreases with decreasing latitude. North America and Northern European countries have the highest incidence of disease in the world. The highest number of reported cases, estimated at 250 cases per 100,000 population, occurred in the Orkney Islands north of Scotland. Adapted from McAlpine, D. Lumsden, CE, Acheoon, ED (1965) http://medstat.med.utah.edu.

1.4.4 Immunology

The view that MS is an immune mediated disease has been based largely on the presence of activated myelin reactive T cells, plasma cells and macrophages, the pathological appearance of the lesions and the presence of abnormally elevated immunoglobulins levels in CSF. Activated MHC class II restricted CD4+ T lymphocytes are believed to be the major mediators of disease (Martin and McFarland, 1995). These T cells become activated within a genetically susceptible host immune system upon encountering a common environmental antigen (Figure 1.10). The activation of these T cells may be facilitated by superantigens or by a process of molecular mimicry in which foreign epitopes are recognized by normally harmless self reactive T cells clones (Gran *et al.*, 1999; Hemmer *et al.*, 1997). These activated T cells can then migrate to the CNS and mount inflammatory responses to myelin epitopes. Selective expression of adhesion molecules, chemokines and matrix metalloproteinases are required for adhesion and transmigration of these cells across the blood brain barrier. Increased frequencies of PLP reactive T cells have been found in the blood and CSF of MS patients compared to MS controls (Markovic-Plese *et al.*, 1995; Sun *et al.*, 1991b). Similar levels of MBP reactive T cells were found in the blood of both MS and normal individuals, however the IL-2 receptor, a hallmark of activated T cells was expressed on MBP reactive T cells from MS patients only (Zhang *et al.*, 1994). In general T cells are classified according to the cytokine profiles they produce upon activation (Abbas *et al.*, 1996) (Figure 1.11). These CD4+ cells are of the Th1 phenotype due to their production of Th1 cytokines such as IFN-γ, TNF-α, LT and IL-2 (Martin and McFarland, 1995). Release of such cytokines allows recruitment of other effector cells such as CD8+ T cells, monocytes and B cells to the site of inflammation. Mechanisms of myelin destruction and axonal damage are multifaceted and can be caused by direct effect of proinflammatory cytokines, digestion of surface myelin antigens by macrophages or direct injury to tissue by T cells.

The detection of elevated levels of intrathecal CSF Ig is still used to support the diagnosis of MS in some cases. These Igs separate into a distinctive pattern of bands known as oligoclonal bands (OCBs) and can be detected in more than 90% of patients with clinical definite MS (Andersson *et al.*, 1994). Relatively little research has been performed regarding the B lymphocyte population in MS. Elevated numbers of autoreactive B cells from MS patients secreting antibodies to MBP, MOG, PLP and MAG have been found in the CSF of MS patients compared to the peripheral blood of the same MS patients and in

control subjects (Sun *et al.*, 1991a; Sun *et al.*, 1991b). The demyelination observed during MS is believed to be a consequence of a synergy between autoimmune T and B cells through CD40L-CD40L interactions (Gerritse *et al.*, 1996; Laman *et al.*, 1998).

Some controversy surrounds the belief that MS is an autoimmune CD4+ Th1 disease. For example we are led to believe that CD4+ cells are the main effector cells in MS lesions, however MHC class 1 CD8+ cells outnumber the CD4+ cells in all stages of lesion development (Gay *et al.*, 1997). These CD8+ cells are expressed on all different cells types including glia and neurons and are thought to possess cytotoxic T cell properties involved in tissue injury (Huseby *et al.*, 2001; Sun *et al.*, 2001). CD4+ Th1 cells have also been shown to be neuroprotective, producing neurotrophins, such as BDNF. Class II-restricted CD4+CD25+ regulatory cells can also inhibit encephalitogenic inflammation in MS lesions (Calopa *et al.*, 1995). This indicates that CD4+ cells may have a protective effect in MS, depending on the stage of the lesion.

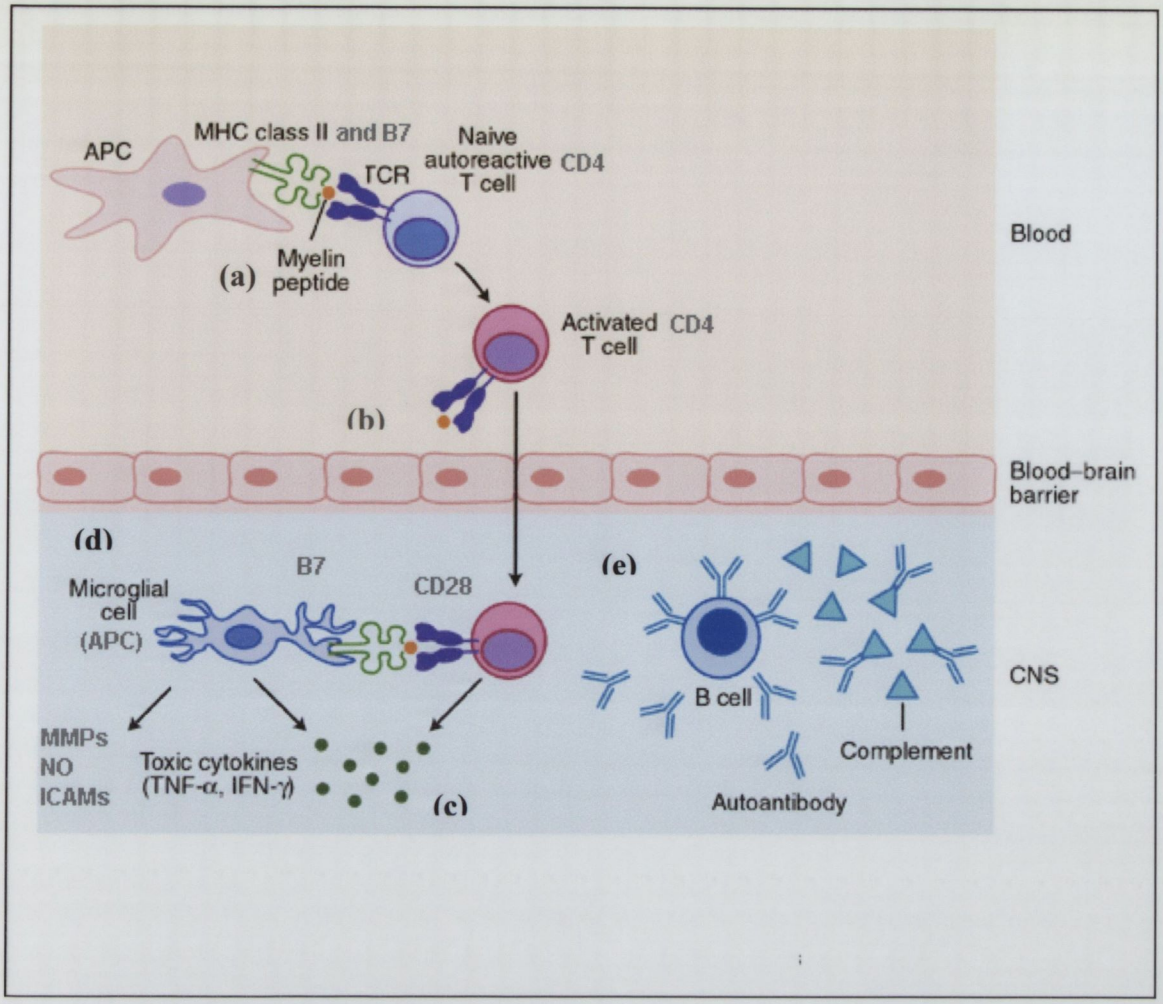

Figure 1.10 Immunopathogenesis of MS and EAE

APCs such as peripheral blood macrophages or B cells expressing MHC class II molecules, present foreign antigen, infectious agent in the case of MS, and myelin antigen in the case of EAE to myelin reactive CD4+ T cells **(a)**. These CD4+ cells require a costimulatory signal that is provided by the interaction of B7 and CD28 molecules for activation **(b)**. These activated T cells can then migrate across the BBB into the CNS and mount inflammatory responses to myelin epitopes. Selective expression of adhesion molecules, chemokines and MMPs are required for adhesion and transmigration of these cells across the blood brain barrier. Once in the perivenular space they may release pro-demyelinating cytokines such as TNF-α, and pro-inflammatory cytokines such as IFN-γ that lead to activation of microglial cells **(c)**. These activated microglial cells release MMPs, oxygen free radicals and other agents which result in demyelination and tissue damage **(d)**. They also engulf myelin debris and present the fragments to activated T cells in their role as APCs. B cells are activated by Th2 cytokines. Production of autoantibodies through the action of complement leads to demyelination **(e)**. Adapted from the Expert Reviews in Molecular Medicine © 2005 Cambridge University Press.

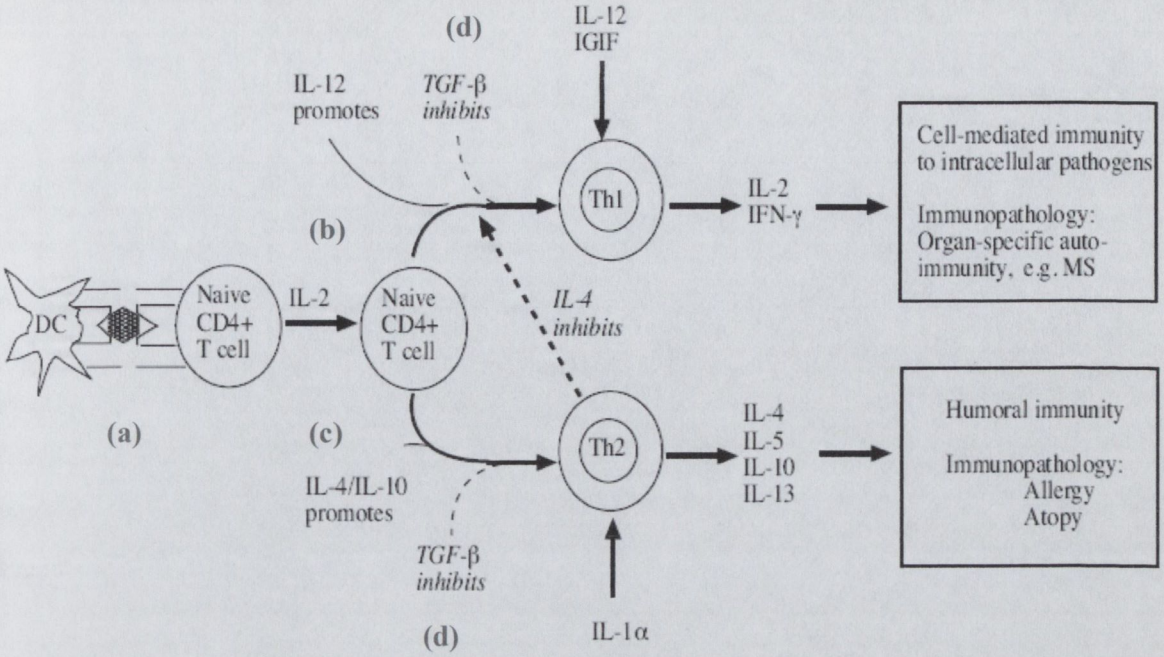

Figure 1.10 Differentiation of naïve Th0 cells into Th1 and Th2 cells

On activation of native CD4+ T cells, the integrated signals from peptide–MHC complexes and costimulatory molecules on the surface of APCs, such as DCs co-determine whether T cells will go on to develop as Th 1 cells and support cell mediated inflammatory response, or as Th2 cells and support the humoral response **(a)**. IL-2 (also known as T cell growth factor) is produced by activated T cells and is necessary for the proliferation and differentiation of T cells, B cells, and for monocyte and macrophage activation. IL-2, together with IL-12, supports differentiation of Th0 cells into the Th1 phenotype **(b)**. On the other hand IL-4 and IL-10 promote Th2 differentiation **(c).** IL-4, in particular, is a strong inducer of Th2 differentation and can, in turn, inhibit Th1 differentiation. A third type of Th cell, the Th3 cell exists (not shown). These Th3 cells are thought to originate in the intestinal mucosa and mainly produce the modulatory cytokine TGF-β. TGF-β inhibits both Th1/Th2 differentation (d). Adapted from F Dangond. Multiple sclerosis. eMedicine Web site: Neurology. Available at: http://www.emedicine.com.

1.4.5 Symptoms

Common symptoms of MS include sensory disturbances in the limbs, optic nerve dysfunction, ataxia, and vertigo or motor dysfunction. Less common, initial symptoms include bowel and bladder problems. Symptoms are typically separated in time, usually by weeks, months and years. Transient symptoms known as paroxymal attacks are commonly experienced in MS especially in the early days of the disease (Mitchell, 1993). These attacks are brief and intense lasting seconds to minutes, with a tendency to reoccur in a stereotypical matter for each individual. Pain is not usually a presenting symptom of MS but frequently develops over the course of the disease. Fatigue is one of the most common symptoms and includes both physical exhaustion and mental cognitive slowing leading to reduced motivation levels.

Optic neuritis or inflammation of the optic nerve may occur as an isolated episode, as a prelude to developing MS or during MS disease progression. Approximately 50% of MS patients will at some point develop optic neuritis. Vision loss typically occurs over a 1 week period. Motor symptoms include weakness and spontaneous paroxymal spasms of limbs and tend to begin asymmetrically and, except for patients with primary progressive MS, reach maximum severity acutely indicating the presence of an exacerbation. Sensory dysfunction is the most common symptom attributed to MS with practically all patients having experienced some degree of numbness, tingling, 'pins and needles' or loss of vibration.

1.4.6 Diagnosis

Diagnosis of MS is difficult and typically made by exclusion with heavy reliance on clinical history and neurological symptoms using the criteria specified by Kurtzke's Expanded Disability Status Scale (EDSS) (Kurtzke, 1983). This scale is used as a disease progression measure by assigning a severity scale between 0-9.5 to patients' clinical status, 10 being death due to MS. Although the scale is not linear with relation to the natural progression rate of MS patients its widespread use and ease of implementation allows its use as a standardization measure for clinical trials. General standard diagnostic protocol involves the isolation of immunoglobulin OCBs from the CSF of potential MS patients. A normal CSF IgG is typically less than 4.7 mg/dl (less than 12% of total protein) and the normal IgG index is less than 0.8. Most MS patients exhibit an elevated IgG index higher than 1.7. Optic neuritis is one of the most common early onset symptoms and can be

diagnosed by funduscopy. In general the timing of optic neuritis development gives some indication as to the risk of developing clinical definite MS. Some studies suggest that the earlier the age at which optic neuritis develops, the higher the risk for developing MS (Rizzo and Lessell, 1988). The presence of OCBs in patients with optic neuritis also correlates with a significantly greater risk of developing MS. The combination of both OCBs levels and MRI investigations are valuable tools in disease diagnosis (Paolino *et al.*, 1996; Soderstrom *et al.*, 1998). MS lesions are present in both white and grey matter but grey matter lesions are much less obvious and generally do not appear on MRI due to the relatively small amount of myelin present and a less intense inflammatory reaction. Lesions range from acute plaques with active infiltrates and macrophages loaded with lipid and myelin degeneration products, to plaques that are active only at their margin to chronic, inactive demyelinated shrunken glial scars. Plaque reactivation can be seen on MRI during acute attacks. Four different patterns of demyelination in active MS lesions based on a variety of modern staining and labeling techniques have been identified and used to classify the stage of disease the patient is experiencing (Lucchinetti *et al.*, 1996). Three of these patterns are seen in exacerbating remitting MS while the fourth is seen only in primary progressive MS. MRI is an important tool for assessing inflammatory activity in the CNS. MS lesions appear as ovoid T2 hyperintensities around the ventricles, usually in an orientation perpendicular to the ventricles. T2 images on a MRI show inflammation and represent a combination of tissue edema and gliosis (Gilman, 1998). T1 images are more useful for detecting acute MS lesions and chronic inactive lesions and for evaluating brain atrophy (axonal loss) (Barkhof *et al.*, 2000). An acute MS lesion enhances with contrast on a T1 scan. The chronic, inactive lesions on a T1 scan appear as hypointensities (black holes) (van Walderveen *et al.*, 1995). More recently gadolinium enhancement has been used to enhance signals on T1 weighted scans (Miller *et al.*, 1988). This MRI technique is extremely useful in identifying new or reactivated MS lesions in which blood-brain barrier disruption, inflammation and edema are the main features (Katz *et al.*, 1993; Nesbit *et al.*, 1991). Inflammatory MRI lesions usually precede the onset of clinical symptoms.

1.4.7 Disease modifying drugs in the treatment of MS

There are currently four disease–modifying agents (DMAs) or therapies available on the market for the treatment of RRMS: IFNβ-1a (Rebif), IFNβ1-a (Avonex), IFNβ-1b (Betaseron) and glatiramer acetate (Copaxone). The DMAs are all approved by the FDA and are considered the first line of therapy for RRMS, showing both clinical safety and efficacy. Three pivotal trials in MS have established the efficacy of IFNs in MS: IFN-β multiple sclerosis study group, Multiple Sclerosis Collaborative Research Group (MSCRG) and the Prevention of Relapses and disability by Inteferon-β1a Subcutaneously in Multiple Sclerosis (PRISMS) study (Ebers, 1998; Jacobs *et al.*, 1996; Sibley, 1993). All were randomized, placebo controlled double-blinded trials involving patients with RRMS. In 1993, Betaseron was the first disease–modifying agent to show therapeutic efficacy in MS. This is a non-glycosylated form of IFN-β produced by *E.coli*. In a trial consisting of three treatment arms, placebo and IFN-β given at 50μg and 250μg subcutaneously, the relapse rates were 1.27, 1.17 and 0.84 respectively. The two IFN-β doses had a statistically significant dose related effect on the reduction of the relapse rate. Treatment also decreased the EDSS in the 250μg treated group compared to the control and significantly reduced the MRI lesion area (Paty and Li, 1993). Avonex was the second agent to gain FDA approval. This form of IFN-β is produced in mammalian COS cells and is glycosylated. In the Avonex trial, 172 out of 301 patients completed the two years of protocol where patients received 30μg of IFNβ-1a intramuscularly once a week. The annual relapse rate was reduced by 18% compared to controls in the intent-to-treat analysis. For patients who finished the trial, the annual relapse rate was significantly reduced by 32% and the number and volume of contrast enhancing lesions were significantly reduced by IFNβ-1a at years one and two. Rebif was the third agent to receive FDA approval. Patients were randomized to receive placebo, 22μg or 44μg IFN-β1a given subcutaneously. The relapse rates were reduced by 27% and 33% respectively by the two doses compared to placebo, and the number of T2 lesions were reduced by 67% and 78% with the lower and higher doses.

Long-term efficacy of IFNs in MS is difficult to assess. There are no long term, placebo controlled double blinded trials of IFNs in MS usually due to high percentage of withdrawal. The London, Ontario cohort of patients in IFN-β MS study has the longest follow up of 12-year data (Rice, 2001). Of the 31 patients enrolled in the pivotal trial, 61% were still on IFNβ-1b and 39% had withdrawn. Patients who continued treatment had a

decrease in T2 burden of disease compared to untreated, age matched controls. Similar results were seen in the long term follow up with Rebif in MS, 7-8 year data (Li *et al.*, 2004).

Two large studies have provided conflicting results on the efficacy of IFNs in SPMS. Kappos *et al.* 1998 found that therapy significantly delayed the time to confirmed progression of disability for 9-12 months and also reduced the relapse rate, the T2 lesion volume and contrast enhancing lesions. In a North American study group similar effects were seen on relapse rate and MRI measures in SPMS, but did not reduce time to confirmed disease progression (Panitch *et al.*, 2004). This was explained by the fact that the European trial had fewer numbers of relapse free patients than the North American group, with these patients experiencing more frequent relapses in the prior 2 years (mean of 1.7 versus 0.82). Hence more patients had more active diseases in this trial, therefore, IFN therapy was shown to be beneficial in delaying disability progression (Kappos *et al.*, 2004). The NA trial suggests little utility in treating SPMS without relapses. In PPMS there is no clear evidence for the efficacy of IFNs on disability progression.

In general IFNs have been shown to be well tolerated by MS patients (Walther *et al.*, 1996). The most common side effects include local site injection reactions, fever, chills, headache and myalgias ("flu like symptoms"). The use of acetaminophen or ibuprofen prior to IFN injection is usually helpful in decreasing " flu like symptoms. Treatment with IFN has also led to leukopenia and elevated liver transaminases. These lab abnormalities are usually transient and stabilize over time. Development of autoimmunity is rare with IFN-β. IFN therapy has been associated with early thyroid dysfunction especially in patient with pre-existing thyroiditis (Diago *et al.*, 1999). However thyroid dysfunction is often subclinical and spontaneous resolution occurs in most patients without the need for withdrawing IFN therapy.

There have been continued attempts at improving the efficacy of IFNs by using them in combination with other agents such as statins, immunosuppressive agents and IVIG. Two of the agents which have received most attention are glatiramer acetate (Copaxone), which is itself an FDA approved DMA, and natalizumab (Tysabri), a human IgG4K mAb with short segments of murine protein at the antigen recognition site. Glamiramer acetate (GA) is a mixture of randomly arranged polypeptides composed of 4 a.a. and is thought to suppress inflammation by inducing a Th2 cell response (Aharoni *et al.*, 1997; Arnon and Aharoni, 2004; Duda *et al.*, 2000). Its immunomodulatory effects are

believed to occur both in the periphery and in the CNS. The therapeutic efficacy of GA has been established by a large, multi-center, phase III trial where 251 randomly assigned patients receiving GA had a two year relapse rate of 1.19, compared with 1.68 for patients receiving placebo (Johnson *et al.*, 1995). There was a 29% reduction in the relapse rate over two years. The combination of IFNs with GA remains speculative. It is possible that such a combination would restrict the entry of GA-specific T cell to the CNS due to a decrease in BBB permeability caused by the IFNs, thereby limiting the effectiveness of GA in MS. Lublin *et al.* 2001 reported that the combination of Avonex and glatiramer acetate is safe. Results from *in vitro* studies do not necessarily suggest antagonistic effects of IFNs and GAs on T cells. Clinical trials using the two agents in combination are ongoing. Combinational treatment with natalizumab has produced the most controversial result to date. In a trial of 1196 patients, one of which had experienced an exacerbation in the prior year during therapy with Avonex, were treated with Avonex in combination with natalizumab. Combined treatment was shown to reduce relapse rate by 53% compared to Avonex alone (Rudick *et al.*, 2006). Unexpectedly, a form of encephalitis caused by the JC polyoma virus called progressive multifocal leukoencephalopathy (PML) developed in two patients in the combined treatment group after 28 and 37 natalizumab infusions. After the PML cases arose, administration of the drug was put on hold as well as important clinical trials of natalizumab in PPMS. Since PML was only seen in patients receiving both Avonex and natalizumab, it is possible that the effects of IFN on T cell migration synergized with those of natalizumab resulted in poor immune surveillance of the CNS (Kuruganti *et al.*, 2002; Yong *et al.*, 1998). This could have allowed the emergence of opportunistic infections such as PML.

1.4.8 Immunosuppressive treatment

Other agents are also available for treating MS usually when there are frequent relapses or rapidly progressive disease despite treatment with the DMAs. These agents are mostly immunosuppressive in their action and include glucocorticoids, azathioprine, methotrexate, cyclophosphamide and mitoxantrone. These ancillary treatments can be used alone but are usually given in combination with the DMAs. Glucocorticoid treatment consisting of a high-dose IV methylprednisolone injection, alone or followed by oral prednisone is an example of acute therapy administered to patients experiencing acute relapses of MS. This regime results in an enhanced rate of recovery from the relapse and

reduced MRI contrast enhancing lesions (Beck *et al.*, 1993; Milligan *et al.*, 1987). Long term treatment with glucocorticoids, however, does not provide the sustained effect that is seen with the IFNs (Lubetzki *et al.*, 1996). The use of chronic treatment is limited by the potential of side effects such as hypertension, glucose intolerance, obesity, osteoporosis and cataract formation. Azathioprine and methotrexate have long been used to treat MS, particularly prior to the advent of the first approved DMA. They are mild chemotherapeutic agents (Goodkin *et al.*, 1995; Palace and Rothwell, 1997; Yudkin *et al.*, 1991). More cytotoxic agents such as cyclophosphamide and mitoxantrone are useful in treating rapidly progressive disease (Gonsette, 1996; Hartung *et al.*, 2002; Weiner *et al.*, 1993), however the efficacy is short lived. Long-term use of these agents is associated with risk of developing secondary malignancies. Mitoxantrone is the only FDA-approved immunosuppressive agent that is efficacious in both RRMS and SPMS (Hartung *et al.*, 2002). Statins have also received much attention recently as a combination agent (Neuhaus *et al.*, 2005; Neuhaus *et al.*, 2004). Statins are inhibitors of the 3-hydroxy-3-methyl-glutaryl coenzyme A reductase and are widely used as lipid-lowering drugs. Statins have been shown to ameliorate or even prevent disease expression in several EAE or animal models of MS by causing a shift from pro-inflammatory to anti-inflammatory conditions (Aktas *et al.*, 2003; Youssef *et al.*, 2002).

1.5 Experimental Autoimmune Encephalomyelitis

1.5.1 EAE as a model of MS

EAE is a well-characterized animal disease used extensively as a model system to study MS. Like MS, EAE is an inflammatory, demyelinating disease of the CNS whose development and course varies according to several genetic and environmental determinants. Unlike MS, the etiology of EAE has been clearly defined as an autoimmune disease caused by myelin specific CD4+ T-cells (Pettinelli and McFarlin, 1981; Zamvil *et al.*, 1985). Similar to what is seen in MS, there is a clear relationship between the animals MHC class background and disease susceptibility (Greer *et al.*, 1996). The EAE model shares major clinical, genetic and pathological similarities with MS which renders it one of the best available tools for studying the mechanisms of the disease at the cellular and molecular levels.

In 1933, Rivers *et al.* 1933 published the first convincing description of EAE. Rivers and his colleagues administered a series of rabbit brain tissue, alternating between i.m. r aqueous emulsions of ground rabbit brain and alcohol-ether extracts of rabbit brain, to half grown rhesus monkeys thrice weekly over a period of months (Rivers *et al.*, 1933). After 44-86 injections the monkeys became sick with an inflammatory demyelinating disease. The next major advance came with the introduction of Freund's adjuvant (Freund and Dermott, 1942). The basic idea for Freund's adjuvant came from Louis Dienes, a colleague of Freund. He observed that injecting a protein such as egg white into a tuberculous focus, even one that contained killed tubercle, greatly augmented the magnitude of the antibody response to the egg white. More important the injection led to the appearance of a tuberculin – type reaction to egg white in immunized animals when egg white and tubercle bacilli were injected subcutaneously. Freund's insight was to incorporate the tubercle bacilli in oil and to add an emulsifying agent so that water soluble antigens could be incorporated into a water- in-oil emulsion. In 1947, Freund reported EAE in guinea pigs after a single injection of brain and mycobacteria in water. The ability to induce EAE by administration of spinal cord homogenate led researchers to suspect myelin as a major encephalitogenic component of the homogenate (Waksman and Morrison, 1951). In 1954 and 1956 it was shown that the myelin proteins, MBP and PLP could also induce EAE (Kies *et al.*, 1956; Waksman *et al.*, 1954). Although myelin and its components could induce disease, the precise mechanism of demyelination was not known until the 1970s and 1980s. In 1977, Panitch and McFarlin successfully induced EAE in naïve Lewis rats by transfer of splenocytes from disease donors. In 1981, this study was repeated in mice showing that lymph node cells from MBP–sensitized SJL/J mice were capable of transferring disease into naïve recipients (Pettinelli and McFarlin, 1981). These observations also implicated T cells in disease mediation. Administration of monoclonal antibodies against specific populations of lymph node cells was shown to prevent the induction of EAE.

The type of EAE induced is dependent on the immunization protocol, the animal strain and the antigen used, and can occur in two different types of disease, a chronic relapsing form and a single acute episode. Immunization of animals with SCH (Baker *et al.*, 1990; Lublin *et al.*, 1981) is one of the most common ways to induce EAE but purified myelin antigens such as myelin basic protein (MBP), proteplipid protein (PLP), myelin oligodendrocytes glycoprotein (MOG) and myelin associated glycoprotein (MAG) are also

frequently used. As previously found MBP protein was one of the first myelin protein to be implicated in EAE induction (Levine *et al.*, 1972; Martenson *et al.*, 1972; Raine *et al.*, 1977). It has since been shown that EAE can be induced with peptides containing specific encephalitogenic epitopes of MBP (Amor *et al.*, 1996a; Jansson *et al.*, 1991; Sakai *et al.*, 1988; Takacs *et al.*, 1997). Similarly PLP protein was originally showed to induce EAE (Endoh *et al.*, 1986; Hauser *et al.*, 1989; Yoshimura *et al.*, 1985). In more recent studies encephalitogenic peptides of the protein have been used for induction (Amor *et al.*, 1993; Amor *et al.*, 1996a; Kuchroo *et al.*, 1991; Takacs *et al.*, 1997). A MAG peptide, consisting of 97-112 residues, has also been showed to successfully induce clinical and histological signs of acute EAE in AB/H mice (Maatta *et al.*, 1998; Morris-Downes *et al.*, 2002a).

Due to its easy accessibility on the extracellular surface of oligodendrocytes and myelin sheaths, high levels of anti-MOG antibodies have been found in the serum of EAE animals suggesting an important role for MOG in autoimmunity as a target of antibody mediated demyelination (Gunn *et al.*, 1989; Ichikawa *et al.*, 1996; Linington and Lassmann, 1987). Experimental models showed that treatment with monoclonal antibodies to MOG augmented EAE (Linington *et al.*, 1993; Linington *et al.*, 1988). Many studies have examined the induction of EAE with recombinant MOG peptide (Amor *et al.*, 1994; Bernard *et al.*, 1997; Okuda *et al.*, 1998). Amor *et al.*, 1994 showed that recombinant MOG protein and MOG molecules, composed of synthetic 15-mer peptides, could induce EAE in Biozzi AB/H (H-2dq1) and SJL (H-2S) mice. Recombinant MOG, which corresponded to the Ig-like domain of MOG protein, induced clinical and histological signs of EAE in both AB/H and SJL mice. At least three of the MOG epitopes within residues 1-22, 43-57, and 134-148 induced clinical and histologic EAE in AB/H mice, whereas only the sequence 92-106 was encephalitogenic in SJL mice. EAE induced in C57/Bl6 mice with MOG 35-55 peptide is a well characterized model of EAE (Costa *et al.*, 2003; Jerusalmi *et al.*, 2003; Mendel *et al.*, 1995; Slavin *et al.*, 1998). EAE can also be induced by adoptive transfer of CD4+ activated cells specific for myelin components such as MBP and PLP (Mokhtarian *et al.*, 1984; van der Veen *et al.*, 1989).

Considerable variations in the susceptibility of various animals to EAE have been described. These variations are largely due to genetic background and especially to the MHC genes of the strain of mice (Andersson and Karlsson, 2004; Bernard, 1976; Gasser *et al.*, 1973). In mice, different MHC haplotypes typically associate with different regions of experimental antigens (epitopes) leading to effective disease induction. Some epitopes are

effective in inducing EAE in a number of different strains despite haplotype differences, for example the region 89-101 of MBP (Issazadeh *et al.*, 1997). EAE pathology varies considerably between species. In mice, the EAE lesion is characterized by perivascular lymphocytic and monocytic infiltrates, white matter demyelination, and some limited remyelination (Raine, 1983; Raine, 1984).

1.5.2 The role of T and B lymphocytes in EAE

The principle of EAE immunology is the same as that of MS. When CD4+ cells specific for a particular peptide antigen recognize that antigen presented by competent antigen presenting cells such as monocytes or B cells, the T cells become activated and proliferate. CD4+ T cells capable of recognizing myelin proteins such as MBP, PLP or MOG are activated in the periphery and then migrate to the CNS where they cause autoimmune inflammation (Figure 1.10). As stated before CD4+ T helper 1 cells are believed to be the major effector cells in EAE, initiating and perpetuating the disruptive inflammatory process (Pettinelli and McFarlin, 1981; Zamvil *et al.*, 1985). T cells require two signals from the APC: the first is antigen-specific and is delivered by the recognition of the antigen peptide–MHC complex on the APC by the T cell receptor, the second signal, termed costimulatory, is delivered by the contact between several soluble or membrane-bound molecules. Two of the most important costimulatory molecules are CD28 and CTLA4, which are found on the surface of T cells. These molecules bind to B7-1 (also called CD80) and B7-2 (also called CD86) expressed on the surface of APCs cells. This B7-CD28-CTLA4 costimulatory system plays a critical role in EAE (Cross *et al.*, 1995; Khoury *et al.*, 1995; Oliveira-dos-Santos *et al.*, 1999; Perrin *et al.*, 1995). Once activated the CD4+ cells release cytokines, chemokines and adhesion molecules that attract myelin-specific and nonspecific immune cells to the site, and alter adhesion molecule expression on endothelial cells allowing migration of inflammatory cells across the BBB (Kubes and Ward, 2000; Zang *et al.*, 2004). Upon entry the CD4+ cells are reactivated by antigenic costimulation and differentiate into two distinct populations (Abbas *et al.*, 1996) (Figure 1.11). The Th1 cells produce IL-2, TNF-β and IFN-γ and mediate activation of macrophages and induction of delayed hypersensitivity responses. Th2 cells produce IL-4, IL-5, IL-10 and IL-13 and have been shown to suppress cell mediated immunity and supports B cell function. The autoreactive Th1 cells induce EAE whereas the secretion of Th2 cytokines from the Th2 cells suppresses development of EAE and aids recovery from

disease. CD4+ cells can also play a regulatory role in disease. The CD4+CD25+ regulatory T cells have been shown to suppress autoreactive antigen specific T cell activity in EAE (Furtado *et al.*, 2001; Kohm *et al.*, 2002; McGeachy *et al.*, 2005). They are thought to be the main IL-10 producing cells during recovery phase of disease (Zhang *et al.*, 2004). CD8+ cells can also play either an effector or regulator role in EAE. CD8+ cells can enhance the encephalitogenic response in EAE causing damage to tissue through demyelination and axonal injury (Huseby *et al.*, 2001; Sun *et al.*, 2001) or else play a role in preventing relapses (Koh *et al.*, 1992). CD8+ knockout mice experienced a milder acute EAE, reflected by fewer deaths, but more chronic EAE, reflected by a higher frequency of relapse. In other studies no requirement was found for CD8+ cells in the immunoregulation of EAE in the Lewis rat (Lohse *et al.*, 1995; Sedgwick, 1988). Others found that CD8+ cells were major participants in resistance to a second induction of EAE but were not essential for spontaneous recovery from the first episode of the disease (Jiang *et al.*, 1992).

The role of B cells in EAE, unlike MS, is not well established. On one hand EAE has been successfully induced in B cell knockout animals, suggesting that B cells are not critical for disease expression (Hjelmstrom *et al.*, 1998; Wolf *et al.*, 1996). Neither B cells nor antibody production were required to induce EAE with MBP or MOG. In contrast B cells have been shown to have an aggressive effector role in EAE (Lyons *et al.*, 1999; Willenborg and Prowse, 1983) where MOG primed serum from wild type mice was found to reconstitute the ability for clinical and histological EAE to be induced in MOG-immunized B cell-deficient mice (Lyons *et al.*, 2002). Other authors have shown that B cell knockout mice develop a severe form of EAE as shown by Fillatreau *et al.*, 2002, where B cells regulate immunity by provision of IL-10. In the absence of IL-10 production by B cells, the pro-inflammatory type 1 immune response persisted and mice did not recover. This suggests a protective regulatory role for B cells. Similarly the humoral response can play both an effector and protective role in disease. Autoantibodies play a major role as effectors of tissue damage through activation of complement leading to the destruction of myelin sheaths (Sun *et al.*, 1991a; Sun, 1993). Antibodies against the myelin antigens have been found in the serum of EAE animals (Cross *et al.*, 2001; Morris-Downes *et al.*, 2002b; Wang and Fujinami, 1997). Some autoantibodies are believed to play a regulatory role in EAE, as well as a pathogenic role (Morris-Downes *et al.*, 2002b). They can also promote remyelination (Miller *et al.*, 1997; Miller and Rodriguez, 1995). The mechanism by which autoantibodies may enhance myelin repair is unknown. They

may stimulate oligodendrocytes to differentiate or produce myelin, or promote oligodendrocyte survival factors by astrocytes or microglia.

1.5.3 Role of cytokines in MS and EAE

Cytokines serve as signaling molecules produced by both T and B lymphocytes and macrophages in EAE and also by cells of the CNS such as astrocytes and microglia. They function as regulators of both adaptive and innate immunity. All cytokine receptors are transmembrane proteins which translate the extracellular cytokine signal into an intracellular signal that lead to a cellular response. The cytokine binding to its receptor initiates this process by triggering a cascade of signaling events that lead to effector responses of the cell. Expression of the cytokines associated with the Th1 phenotype, IL-2, TNF-α/β and IFN-γ correlates with disease activity. Expression of cytokines from the Th2 cells IL-4, IL-5, IL-10 and IL-13 are involved mostly in disease recovery. These Th2 cytokines promote humoral responses but it is only in the context of EAE or MS that they are seen as anti-inflammatory. It is through these cytokines and other pro- and anti-inflammatory cytokines that demyelinating disease is mediated. In contrast to the animal model, the study of the role of cytokines in MS is limited to indirect measurement of cytokines produced by peripheral blood cells or measurement of serum or CSF.

IFN-γ is a type II IFN involved in the regulation of nearly all phases of immune and inflammatory responses, including the activation, growth and differentiation of T cells, B cells, macrophages, NK cells and other cell types such as endothelial cells and fibroblasts. The main sources of IFN-γ are CD8+, CD4+ and NK cells. One of the main roles of IFN-γ is enhancement of MHC class II expression on many cells types including microglia (Colton *et al.*, 1992), astrocytes (Fierz *et al.*, 1985) and endothelial cells (Dore-Duffy *et al.*, 1996). IFN-γ also stimulates secretion of other pro-inflammatory cytokines from cells. Upon IFN-γ stimulation, macrophages produce TNF-α and IL-1, as well as nitric oxide (Billiau *et al.*, 1998). IFN-γ has been found in both acute MS and EAE plaques (Brosnan *et al.*, 1995; Cannella *et al.*, 1991; Cannella and Raine, 1995; Traugott and Lebon, 1988). Similarly elevated IFN-γ levels have been found in both the serum and CSF of MS patients experiencing acute exacerbation (Calabresi *et al.*, 1998; Hohnoki *et al.*, 1998). IFN-γ has also been shown to induce clinical exacerbations when administered systemically to patients with MS or directly into the spinal cord in EAE (Panitch *et al.*, 1987a; Panitch *et al.*, 1987b; Simmons and Willenborg, 1990). Recent experiments have challenged the

assumption that IFN-γ mediates a critical effector function in disease through the successful induction of EAE in IFN-γ knockout mice (Ferber *et al.*, 1996; Krakowski and Owens, 1996; Willenborg *et al.*, 1996). In at least three case studies, more severe disease was seen in the IFN-γ knockout mice than in the wild type counterparts. Similarly the injection of neutralizing antibodies to IFN-γ has been shown to exacerbate disease, while the administration of rat IFN-γ has been found to have a protective effect in a rat model of EAE (Duong *et al.*, 1994; Duong *et al.*, 1992; Lublin *et al.*, 1993; Voorthuis *et al.*, 1990). IFN-γ may act paradoxically to suppress disease development either during the priming of encephalitogenic effectors or at a downstream event critical to the formation of demyelinating plaques.

The other pro-inflammatory cytokines, TNF-α, LT-α (TNF-β) and IL-2 are produced during the course of EAE *in vivo* and by encephalitogenic T-cells *in vitro*. Most studies have found little difference between the biologic effects of soluble TNF-α and LT-α. LT-α is synthesized by B and T lymphocytes whereas TNF-α is derived predominantly from activated monocytes, macrophages and dendritic cells (DCs). Both have been implicated in EAE disease exacerbation and play an important role in tissue damage (Dick *et al.*, 1996; Korner and Sedgwick, 1996; Martin *et al.*, 1995; Ruddle *et al.*, 1990). Like IFN-γ, TNF-α has also been found in MS brain plaques (Cannella and Raine, 1995; Hofman *et al.*, 1989; Sun *et al.*, 2004) and elevated levels have also been found in the CSF and serum of MS patients experiencing acute disease (Hauser *et al.*, 1990; Hohnoki *et al.*, 1998; Maimone *et al.*, 1991). Injections of TNF-α resulted in a significant prolongation of clinical EAE and more severe cellular inflammation in the spinal cords compared to controls (Kuroda and Shimamoto, 1991; Simmons and Willenborg, 1990). IL-2 is also known as a T cell growth factor and T cells are its main source of production. It exerts autocrine and paracrine actions on T cells and neighbouring cells. It is necessary for proliferation and differentiation of T cells and B cells, and for monocyte and macrophage activation. IL-2 also stimulates T cells to produce IFN-γ.

The production of IL-12 has been found to be critical in every EAE model thus far examined (Constantinescu *et al.*, 1998; Leonard *et al.*, 1995; Segal *et al.*, 1998; Segal and Shevach, 1996). Increased expression of mRNA encoding the IL-12 subunit, IL-12p40, has also been found in acute MS plaques and in unstimulated PBMCs from patients with both RRMS and SPMS (Windhagen *et al.*, 1995). IL-12 is a powerful pro-inflammatory cytokine by virtue of its ability to differentiate naïve cells into Th1 cells (Bright *et al.*,

1998; Leonard *et al.*, 1997). It is a potent inducer of the Th1 cell differentiation through the production of IFN-γ from stimulation of lymphocytes and NK cells (Bliss *et al.*, 1996; Trinchieri, 1998). In recent studies. however, Cua *et al.*, 2003 showed that IL-12 related cytokine, IL-23, is more critical for EAE induction than IL-12 which is not required in the pathogenesis of EAE. Further investigation on the immunomodulatory action of IL-12 in this disease model found that IL-12 suppresses MOG35-55 induced EAE when administered during the early induction phase of disease through the induction of IFN-γ (Gran *et al.*, 2004).

In previous studies Th2 cytokines have been shown to down-regulate adoptive transfer of experimental autoimmune encephalomyelitis (Young *et al.*, 2000). IL–4 and IL-10 are the most studied classical Th2 cytokines involved in both MS and EAE. IL-4 drives the differentiation of naïve CD4+ cells to Th2 cells and is thought to play a regulatory role in EAE due to its prominent expression in the CNS during the remission phases of EAE (Begolka *et al.*, 1998; Khoury *et al.*, 1992). IL-10 suppresses cytokine production by Th1 cells and inhibits NO production and antigen presentation of macrophages (Sagawa *et al.*, 1996). It can also stimulate or enhance proliferation of B cells (Itoh and Hirohata, 1995). Its main function is to inhibit IL-12 production by macrophages (Trinchieri, 1998).

In vivo administration of IL-4 reduces disease severity in some cases, often through generation of TGF-β secreting cells and induction of oral tolerance to peptide (Inobe *et al.*, 1998; Inobe *et al.*, 1996; Piccirillo and Prud'homme, 1999). Studies of IL-4 in MS have been limited. While IL-4 is important in EAE induction, it is not essential. EAE has been successfully induced in IL-4 knockout mice immunized with either SCH or MOG (Falcone *et al.*, 1998; Liblau *et al.*, 1997). A slight prolongation of disease in the IL-4 knockout mice indicated a role in disease termination. While IL-4 may reduce disease severity, its absence does not alter the course of EAE. The absence of IL-10, however, has been shown to result in a more severe form of EAE. IL-10 knockout mice with a C57/Bl6 background were more susceptible to disease and developed a more severe form of EAE than IL-4 knockout or wild type mice. Spontaneous recovery from EAE occurred in normal and IL-4 knockout mice, but not in mice deficient in IL-10 (Bettelli *et al.*, 1998; Samoilova *et al.*, 1998). Direct injection of IL-10 or overexpression of IL-10 in transgenic mice also gave resistance to induction of EAE after immunization (Bettelli *et al.*, 1998; Cua *et al.*, 1999; Mathisen *et al.*, 1997; Rott *et al.*, 1994; Xiao *et al.*, 1998). These results strongly suggest

that IL-10 plays a crucial role in the recovery of autoimmune encephalomyelitis. Similarly in MS studies, unalleviated levels of IL-10 have been found in the serum of patients compared to the levels of Th1 cytokines (Hohnoki *et al.*, 1998). Other studies have shown elevated IL-10 mRNA in CSF cells of MS patients with stable disease or just after relapse. IL-10 also inhibits macrophage costimulatory activity by selectively inhibiting the upregulation of B7 (CD80) expression (Ding *et al.*, 1993). In contrast other studies suggest that exogenous administration of IL-10 *in vivo* can have no effect at all (Santambrogio *et al.*, 1995).

1.5.4 The immunomodulatory effect of IFN-β on MS and EAE

IFN-β is a type 1 IFN which is secreted from fibroblasts in response to viral infection. It is a globular protein consisting of 5 α-helices and has a calculated MW of 20kDa, though it often runs on SDS PAGE gels with a MW closer to 25kDa due to glycosylation. dsRNA is one of the primary intracellular signals for IFN production during viral infection. Cellular response to IFN-β is mediated by the IFN receptor, which is found on many different cell types. IFN, acting through the STAT1 and STAT2 activation pathway is known to upregulate or downregulate a wide variety of genes involved in the antiviral immune response. Firstly IFN induces two proteins, (2′-5′) –oligoadenylate synthetase (OAS) and dsRNA dependent protein kinase R (PKR) (Clemens *et al.*, 1993; Pestka *et al.*, 1987). (2′-5′)–OAS catalyses the polymerization of ATP and the resultant oligomers activate a cellular Rnase that cleaves viral RNAs and thereby inhibiting viral translation of proteins. PKR inactivates eIF-2, a viral transcription-initiating factor by phosphorylation preventing viral protein synthesis.

The immunomodulatory effects of IFN-β are believed to inhibit the inflammatory responses in MS at several steps. The antiproliferative effect of IFN-β has dose dependently reduced *in vitro* mitogen-induced proliferation of T cells from both patients with MS and healthy individuals, in turn, downregulating the release of IFN-γ (Furlan *et al.*, 2000; Noronha *et al.*, 1993). IFN-β stimulates the secretion of anti-inflammatory cytokines such as IL-4 and IL-10 (Chabot and Yong, 2000; Ersoy *et al.*, 2005; Rudick *et al.*, 1998). IFN-β can also alter the MHC class II molecules in MS by inhibiting the effects of IFN-γ on MHC class II expression in macrophages and monocytes (Jiang *et al.*, 1995; Ling *et al.*, 1985; Porrini and Reder, 1994). There is also some evidence that IFN-β promotes the proliferation of MHC class I CD8+CD28- T suppressor cells which is

thought to have therapeutic consequences, possibly through their ability to upregulate TGF-β production. TGF-β inhibits the migration of lymphocytes into the CNS *in vivo* (Fabry *et al.*, 1995). CD8+CD28- have been shown to limit inflammation but their activity is reduced in MS and EAE (Antel *et al.*, 1986; Najafian *et al.*, 2003; Noronha *et al.*, 1990; Noronha *et al.*, 1992). *In vitro* stimulation with IFN-β enhances Ts activity in cells taken from MS patients, however, not to the same level as normal controls (Javed and Reder, 2005). One of the most important effects of IFN-β in the treatment of MS is its ability to downregulate the anti-inflammatory reaction mediated by Th1 cytokines leading to a shift towards a Th2 profile. *In vitro* IFN-β significantly enhances secretion of the immunomodulatory cytokine IL-10 by human monocytes (Porrini *et al.*, 1995) as well as T cells (Rep *et al.*, 1996), and also induces IL-10 mRNA (Goodkin *et al.*, 1996). IL-10 induction by IFN-β therapy has also been shown *in vivo* (Chabot and Yong, 2000; Rep *et al.*, 1999). IFN-β exerts inhibitory effects on IL-2, IL-12 and both LT-α and TNF-α (Arnason, 1996; Karp *et al.*, 2000; Noronha *et al.*, 1993). IFN-β is thought to suppress IL-12 production by inhibition of IFN-γ priming of IL-12 production, or through induction of immunomodulatory cytokines such as IL-10 from T cells and monocytes (Byrnes *et al.*, 2002). IFN-β also interferes with T cell/BBB adhesion by enhancing the expression and release of soluble adhesion molecules which can bind T cells and block their ability to adhere to the BBB (Bitsch *et al.*, 2004; Calabresi *et al.*, 1997a; Calabresi *et al.*, 2001; Calabresi *et al.*, 1997b).

There are many mechanisms by which IFN-β also beneficially modulates the course of EAE. These mechanisms are similar to those which modulate MS, as EAE has always been accepted as a model for the human disease both in clinical manifestation and immunology of disease. IFN-β therapy also leads to a shift in favour of a Th2 response in EAE (Luca *et al.*, 1999; Yasuda *et al.*, 1999). More recently IFN-β has been shown to modulate the IL-10/IL-12 circuit complex in EAE, by downregulating the DC expression of IL-12 and upregulating production of anti-inflammatory IL-10 (Tuohy *et al.*, 2000). Some studies have shown that treatment modulates inflammatory events at the level of the cerebral endothelium (Floris *et al.*, 2002), by decreasing the expression of adhesion molecules, ICAM -1 and VCAM-1 on brain capillaries leading to a marked reduction in perivascular infiltrates. One study found that IFN-β knockout mice experienced augmented and chronic EAE which in part was modulated by augmented macrophage and microglial mac-1 expression and activation (Teige *et al.*, 2003).

Two classes of accessory molecules have been shown to be modulated by IFN-β treatment and conceptually contribute to its therapeutic effect. These are the CD28-B7 and the CD40-CD40 ligand signaling pathways previously discussed. In MS patients the numbers of B7-1 (CD80) and B7-2 (CD 86) lymphocytes are significantly increased during active disease but not in stable disease. From EAE studies CD80 expression on APCs induces Th1 cell responses upon binding to the CD28 T cell receptor, whereas CD 86 enhances Th2 responses (Kuchroo *et al.*, 1995). Treatment of MS patients with IFN-β markedly reduced the number of circulating B7-1 (CD80) expressing B cells and increased the B7-2 (CD86) monocyte numbers (Genc *et al.*, 1997). Similarly the suppressive effect of IFN-β on CD80 (B7-1) costimulatory molecule expression on B cells also leads to induction of disease anergy in EAE and increased expression of the CTLA4 molecule which induces Th2 responses (Hallal *et al.*, 2003). IFN-β also inhibits CD40-mediated IL-12 secretion by human APCs, independent of the T cell response, leading to downregulation of both IL-12 and IL-12 induced IFN-γ (Byrnes *et al.*, 2002; McRae *et al.*, 1998).

1.5.5 Treatment of EAE with IFN-β

To date the treatment of EAE with IFN-β has yielded both positive and negative effects. Original studies described how naturally derived rat fibroblast IFN had a suppressive effect on EAE in Lewis rats when administered during the induction phase of disease (Abreu, 1982; Abreu, 1985) but Ruuls *et al.* 1996 was the first to administer IFN–β during the paralytic phase of disease which was more relevant for the treatment of MS. Treatment with recombinant rat IFN-β (rrIFN-β) dose dependently inhibited disease activity, with a subcutaneous dose of 300,000U/day giving total prevention provided treatment was continued for three weeks. Discontinuation of treatment led to worsening of disease. This result correlates with IFN-β therapy in RRMS where IFN-β is most effective in preventing relapses and reducing severity of the lesion when high doses are administered frequently, on a long term basis (Barbero *et al.*, 2006; Barbero *et al.*, 2004). When the same EAE rat model was treated with 300,000U/day two days prior to disease induction and for ten days after, treatment enhanced disease severity despite showing a dramatic rrIFN-β mediated reduction in effector cells which gradually increased again as the animals entered the remission phase (van der Meide *et al.*, 1998). Together these studies show that rrIFN-β prevents disease activity only when administered prior to and

during the effector and remission phases of EAE, and that exposure to rrIFN-β in the induction phase and discontinuation of treatment in the effector stage phase leads to exacerbation of clinical disease. Like in MS, the beneficial effects of rrIFN-β are short-lived and sustained only upon continuous exposure. IFN-β has also been shown to be effective in murine EAE models when administered either subcutaneously or intraperitoneally (Yasuda *et al.*, 1999; Yu *et al.*, 1996). Treatment of EAE induced in (SWR×SJL) F_1 mice with PLP139-151 with high dose IFN-β from the first day of disease onset and every other day after by subcutaneous injection delayed disease progression and significantly delayed disease compared to the control animals but no effect was seen on proliferative response to the priming of lymph nodes with PLP139-151 *ex vivo* (Yu *et al.*, 1996). Likewise in another study improvement in disease did not lead to IFN-β inhibition of proliferative antigen specific responses (Tuohy *et al.*, 2000). Continuous IFN-β treatment of EAE induced in SJL mice with MBP also reduced disease severity but in this study IFN-β effectively inhibited the T cell response to MBP stimulation (Yasuda *et al.*, 1999). The successful or unsuccessful proliferative response of IFN-β treated lymphocytes to priming antigen obviously does not always correlate with an improvement or exacerbation in clinical disease. Even when IFN-β was ineffective in treating EAE induced in mice with PLP peptide, it still inhibited PLP139-151 specific proliferative responses (Luca *et al.*, 1999).

Recent studies have shown that IFN-β is more effective when administered in combination with another protein, for example with early pregnancy factor, a secreted protein with immunosuppressive and growth factor properties (Zhang *et al.*, 2000) or with glucocorticoid such as methylprednisolone which is administered to patients experiencing acute relapses of MS (Schmidt *et al.*, 2001) or with minocycline, an tetracycline analogue (Giuliani *et al.*, 2005).

1.5.6 Treatment of EAE with viral vectors

Due to the presence of the BBB, the CNS is not easily accessible to systemically delivered macromolecules with therapeutic activity such as growth factors, cytokines or enzymes. In EAE and MS the target lesions occur throughout the CNS and due to limited parenchymal diffusion, protein would have to be delivered by multiple, invasive injections. Injection of naked plasmid DNA exhibits exceedingly low and transient expression in the CNS (Croxford *et al.*, 1998). Currently the most efficient method for transferring potential therapeutic agents is through the use of modified viruses as biological vector systems because of their natural propensity to transfer their own genome into the cells that they infect. Viruses which have been used in animal models of CNS gene therapy include retroviruses (including lentivirus), HSV, adenoviruses and adeno-associated viruses (Baker and Hankey, 2003; Lai and Brady, 2002; Martino *et al.*, 2000a; Prud'homme, 2000). More recently alphaviruses have been used as potential tools in neurobiology and gene therapy of the CNS (Ehrengruber, 2002; Jerusalmi *et al.*, 2003; Lundstrom, 1999; Lundstrom and Ehrengruber, 2003; Nygardas *et al.*, 2004). Viral vectors are advantageous due to their ability to achieve transgene expression in a high proportion of target cells, for example, intracisternal or intraventricular delivery of replication deficient adenoviral and herpes simplex viral vectors showed significant and efficient transduction of the ependymal cell layer that surrounds the brain ventricles and spinal canal (Broberg *et al.*, 2001; Cua *et al.*, 2001; Furlan *et al.*, 2001a; Furlan *et al.*, 2001b).

Most work has been done on the treatment of EAE with HSV and adenoviral vectors using both replication competent and defective viruses (Broberg *et al.*, 2001; Cua *et al.*, 2001; Furlan *et al.*, 1998; Guy *et al.*, 1998; Martino *et al.*, 2000b; Poliani *et al.*, 2001). Overall viral vector expression of IL-4 had been found to be one of the most consistent inhibitors of EAE. IL-4 has been administered by both replicative and nonreplicative HSV vectors through i.c. inoculation to different strains of mice and still proves successful in inhibition of EAE (Broberg *et al.*, 2001; Furlan *et al.*, 1998; Furlan *et al.*, 2001b; Poliani *et al.*, 2001; Shaw *et al.*, 1997). When directly compared, viral vector treatment with IL-4 is more efficient than with IL-10 (Broberg *et al.*, 2001; Shaw *et al.*, 1997; Willenborg *et al.*, 1995). Results for IL-10 have been notably variable. CNS delivery of high titre adenoviral vector expressing human IL-10 inhibited CNS infiltration and development of relapsing murine EAE when administered during remission (Cua *et al.*, 2001). However when another adenoviral vector expressing IL-10 was administered,

albeit at lower titres, treatment was clinically ineffective compared to a retroviral vector expressing the same cytokine, despite high level IL-10 expression from both. An alphaviral vector expressing IL-10 has shown promising results in the treatment of EAE induced in C57/Bl 6 mice with MOG 35-55 (Jerusalmi *et al.*, 2003). Mice showed reduced clinical and pathological severity when administered during the effector stage of disease.

While viral vectors are excellent for the transfer of gene products into the CNS, there may be consequences of such direct infection. Viral vectors have the potential to mount host cell immune responses to themselves therefore causing additional damage to the CNS. Advanced vector systems are now derived from viral genomes which have been deleted of all sequences encoding viral structural proteins. The only viral nucleic acid remaining encodes sequences required for replication and packaging into virions. Despite these precautions, some viral vectors are still capable of inducing inflammatory and immune responses (Bowers *et al.*, 2003; Castro *et al.*, 2001). Recombinant replication-deficient HSV vectors have been found to harbour virtually intact genomes that contain ORFs that, when expressed at low levels, are capable of augmenting the potential for antigen processing and MHC class 1 presentation (Johnson *et al.*, 1992; Krisky *et al.*, 1998). Replication competent SFV has never been detected in studies using SFV replication defective vectors, however i.n. administration of rSFV-EGFP particle vectors has been shown to exacerbate disease severity in the treatment of EAE (Jerusalmi *et al.*, 2003).

There is only one previous study where EAE has been treated with a viral vector expressing IFN-β. In this study EAE was induced in Biozzi ABH mice with SCH and treated with a retroviral vector expressing murine IFN-β (Triantaphyllopoulos *et al.*, 1998). DNA–cationic liposomes were used to express the retroviral-IFN-β construct. A single injection of these liposomes on day 12 after disease induction by direct i.c. inoculation reduced disease severity significantly in comparison to the controls.

1.5.7 Cholera toxin as an adjuvant in the treatment of EAE

CT is a major enterotoxin produced by *Vibrio Cholerae* and is composed of a monomeric A subunit (CT-A) that is covalently linked to a pentameric B subunit (CT-B). CT is used as a potent mucosal immunogen as well as a potent mucosal adjuvant that stimulates strong responses to mucosally codelivered Ags (Lavelle *et al.*, 2004; Lavelle *et al.*, 2003; Williams *et al.*, 1999). Its adjuvant effect is characterized by the induction of Ag-specific serum IgG1 and IgG2b and mucosal IgA and enhancement of CD4+ and to a less extent CD8+ cells (Lavelle *et al.*, 2004; Williams *et al.*, 1999). A number of studies reported that mucosally delivered CT stimulates a mixed Th1/Th2 response but with a bias towards Th2 (Lavelle *et al.*, 2003; Xu-Amano *et al.*, 1994). CT can also promote isotype differentiation in B cells leading to increased IgA formation (Lycke and Strober, 1989).

Recent studies have shown that oral administration of CT-B–autoantigen conjugates prevented autoimmune diseases such as EAE by inducing functional tolerance (Sun *et al.*, 1996; Sun *et al.*, 2000). In these studies CT-B was conjugated to minute amounts of MBP. Treatment was effective in suppressing IL-2 production and proliferative responses of lymph node cells to MBP. Most importantly, low-dose oral CT-B-MBP treatment greatly reduced the level of leukocyte infiltration into spinal cord tissue compared with treatment with repeated feeding of large doses of MBP (Sun *et al.*, 1996). Treatment also dramatically reduced the number of leukocytes staining for CD4+, CD8+, IL-2R and MHC class II in the spinal cord while inducing TGF-β secreting cells and suppressing chemokine expression (Sun *et al.*, 2000). CT-B has also been conjugated to PLP-139-151 protein in the treatment of EAE induced in SJL mice (Yuki *et al.*, 2001). Mice that were intranasally immunized 5 times with 70μg rCT-B-PLP peptide hybrid protein showed a significantly suppressed development of EAE and an inhibition of both PLP-peptide-specific DTH responses and leukocyte infiltration into the spinal cord. Treatment of EAE with whole CT alone also showed promising results (Yura *et al.*, 2001). EAE was induced in C57/Bl 6 mice with MOG 35-55 and mice were treated with 64μg of whole CT, given intranasally. Mice received 32μg CT in 10μl PBS per nostril on day 7 p.d.i. Treatment induced a suppressive effect on the clinical score of EAE, as well as its related disease mortality, which was accompanied by lower IL-12 and IFN-γ expression in the CNS compared to PBS treated animals.

1.6 Aims

In this project the potential of the rSFV split helper expression system in the treatment of EAE, through the expression of immunomodulatory cytokines, was investigated. The main aims of this study were:

- Cloning of murine IFN-β into rSFV vectors, pSFV1 and pSFV10-E
- Preparation of high titre rSFV particle vectors and performance of *in vitro* expression studies in different cell lines to ensure expression, secretion and biological activity of IFN-β from rSFV particle vectors
- *In vivo* expression study following i.n. inoculation of rSFV-IFN-β particle vectors to examine the expression and duration of IFN-β within the CNS
- Induction and treatment of MOG induced EAE in C57/Bl 6 mice with rSFV-IFN - β by i.n. inoculation
- Monitoring of clinical disease according to a standard neurological scale and severity of the lesion according to a semi quantitative grading system
- Measurement of immunological responses through *ex vivo* stimulation of T cells with MOG peptide and measurement of Th1/Th2 cytokines
- Characterisation by the EAE lesion through immunohistochemical labeling and morphometrical analysis to enumerate infiltrating lymphocyte populations
- FACS analysis to distinguish splenic lymphocytes into B cells, CD4+ cells and CD8+ cells
- Examination of the effects of co-treatment with rSFV-IFN-β particles and either rSFV-IL-10 particle vectors or whole CT on the course of EAE

Chapter 2

Cloning of IFN-β into SFV vectors and in vitro expression in different cell lines

2.1 Introduction

Previous studies investigated the use of SFV-A7(74) vectors expressing EGFP as delivery systems for the CNS (Ehrengruber *et al.*, 2003; Vaha-Koskela *et al.*, 2003). A replication competent vector, VA7 was shown to efficiently transduce pyramidal cells, interneurons, and glial cells in cultured rat hippocampal slices. Upon i.p. infection with this recombinant virus, mice remained completely asymptomatic but showed CNS expression of EGFP as shown by immunohistochemistry (Vaha-Koskela *et al.*, 2003). A replication deficient SFV(A774nsP)-GFP vector was also constructed and was shown to efficiently transfect neurons in dissociated CNS cells. Transfection was much more efficient at 31°C than at 37°C (Ehrengruber *et al.*, 2003). Recent work has resulted in the development of the SFV split helper particle vector system for delivery of therapeutic genes to the CNS. Intranasal administration of recombinant SFV particles expressing the marker gene, EGFP, and monitoring of fluorescence within the CNS showed a high level of EGFP protein expression in the olfactory bulbs. Expression occurred in the olfactory bulb as early as 1 day after i.n. inoculation and remained for up to 10 days with no detectable damage (Jerusalmi *et al.*, 2003).

Due to its ability to penetrate the CNS, the SFV split helper system was used in the treatment of a CNS autoimmune disease, EAE, an animal model of MS. An SFV vector expressing the Th2 cytokine IL-10, a cytokine shown to be beneficial in the treatment of EAE, was constructed and high levels of IL-10 expression was found in the olfactory bulbs of mice up to seven days following i.n. administration. When used to treat EAE induced in C57/Bl 6 mice, the rSFV-IL-10 vector was shown to significantly reduce disease severity and retard the onset of disease, leading to milder and less frequent brain and spinal cord lesions (Jerusalem *et al.*, 2003).

According to clinical trial studies, IFN-β has been shown to favorably alter the disease course in relapsing-remitting MS patients (Jacobs *et al.*, 1996; Patty and Li, 1993). IFN-β has also been shown to be effective in the treatment of EAE (Yasuda *et al.*, 1999; Yu *et al.*, 1996). IFN-β is a type 1 interferon which is secreted from fibroblasts in response to viral infection. The antiviral effects exhibited by IFN-β are due to its ability to induce cellular proteins such as (2′-5′) OAS and dsRNA dependent PKR which result in inhibition of viral mRNA translation (Clemens *et al.*, 1993; Pestka *et al.*, 1987). These antiviral effects are shown in Figure 2.6. As well as antiviral effects IFN-β also possesses antiproliferative and immunomodulatory effects. The antiproliferative activity is not well

understood but it is thought that both the OAS-Rnase L and PKR- eIF2α pathways play a role. High levels of synthetase and Rnase L have been found in growth arrested cells. The antiproliferative activity of IFN-β is what is thought to inhibit the expansion of autoaggressive T cells in RRMS therefore limiting disease progression (Furlan *et al.*, 2000; Noronha *et al.*, 1993). The immunomodulatory function of IFN-β is multifaceted and also believed to play an important role in MS and EAE. IFN-β is known to enhance expression of the class 1 MHC antigen molecules and in turn inhibit Class II molecules in a variety of cell type, rendering effector cells more susceptible to lysis by cytotoxic T cells (Jiang *et al.*, 1995; Ling *et al.*, 1985; Porrini and Reder, 1994). IFN-β also inhibits production of Th1 cytokines including IFN-γ, IL-12 and TNF-α, the cytokines believed to be upregulated in MS and EAE and enhances IL-10 and TGF-β (Luca *et al.*, 1999; Rep *et al.*, 1999). The ability of IFN-β to cause a shift in cytokine profile from Th1 to Th2 is an important therapeutic factor, given that MS is generally believed to be a Th1 disease (Martino and Hartung, 1999) and EAE is a classical Th1 MHC class II restricted CD4+ disease (Pettinelli and McFarlin, 1981).

One previous study has utilized a viral vector expressing IFN-β encapsidated in a DNA-liposome complex to treat EAE induced in Biozzi ABH mice by injection of SCH with much success (Triantaphyllopoulos *et al.*, 1998). This chapter describes how IFN-β was cloned into two different SFV vectors systems (pSFV1 and pSFV10-E), one of which gives enhanced protein expression (pSFV10-E) and *in vitro* expression studies have been carried out in BHK-21 cells and mouse L929 cells. This new vector, pSFV10-E contains a translational enhancer sequence which allows increased expression of heterologous protein as seen in previous studies (Chikkanna-Gowda *et al.*, 2005; Daemen *et al.*, 2002; Rodriguez-Madoz *et al.*, 2005). rSFV10-E particle vectors expressing IL-12 produced up to 1 log more heterologous protein than the original SFV expression system rSFV10 in the treatment of metastatic cancer in mice (Chikkanna-Gowda *et al.*, 2005). The effect that these rSFV-IFN-β vectors have on the course of EAE will be addressed in subsequent chapters.

2.2 Materials and methods

2.2.1 Materials

2.2.1.1 SFV expression vectors

The SFV expression vectors, pSFV1, pSFV10-E, pSFV1-EGFP and the split-helper vectors pSFV-Helper S2 and pSFV-Helper CS219A were a gift from Prof. P. Liljeström, Microbiology and Tumorbiology Centre, Karolinska Institute, Stockholm, Sweden.

2.2.1.2 Cell lines

The BHK-21 cell line was obtained from the American Type Culture Collection (ATCC). The BHK cell line, Swedish BHK 'sBHK' was a gift from Prof. P. Liljeström (Karolinska Institute, Stockholm). The murine cell line, L929 was obtained from the European Collection of Cell Cultures (ECACC). BHK medium, DMEM medium, newborn calf serum (NCS), fetal calf serum (FCS), tryptose phosphate broth, HEPES, and trypsin EDTA were all from Gibco (UK). Penicillin-streptomycin-L-glutamine solution was from Sigma (UK). Dulbecco's phosphate buffered saline (PBS) was from Invitrogen (UK).

2.2.1.3 Animals

Specific pathogen free female six to eight week old Balb/c mice were obtained from the Bioresources Unit, TCD and maintained under pathogen-free conditions with food and water provided in accordance with the principles set down in SI 17/94 of the European European Communities regulations 1994 for care and use of laboratory animals.

2.2.1.4 Molecular reagents

Trizol reagent for RNA extraction from tissue was purchased from Sigma (UK). The following primers used for RT-PCR and PCR amplification were from MWG Biotech AG (Germany) :

Mouse GAPDH F 5'-ACCACCATGGAGAAGGCTG-3'

Mouse GAPDH R 5'-CTCAGTGTAGCCCAGGATGC-3'

Mouse IFN-β F 5'AATCCCGGGGCACCATGAACAACAGGTGGA-3'

Mouse IFN-β R 5'-GCGCCCGGGTCTTCAGTTTTGGAAGTTTCT-3'

Mouse IFN-β F 5'-AATCCCGGGATGAACAACAGGTGGA-3' (pSFV10-E cloning)

Sequencing primers for the SFV nsP 4 region were from Invitrogen (UK)

Nsp4 F 5'- GCGAAGCTTGCTAACAGTGAAGACAAGC-3'

Nsp4 R 5'-GCCAAGCTTGCTGATGAGTTGCTGCATCT-3'

The following restriction enzymes EcoR1, BanII, Xma1, BglII, Spe1 and Nru1 and Quick T4 Ligase and its 10X ligase buffer were from New England Biolabs (NEB) (MA, USA). Oligo (dT) primers, ImProm-II reverse transcriptase (RT), reverse transcriptase reaction buffer, dNTP mixture, $MgCl_2$, recombinant Rnasin ribonuclease inhibitor, Taq DNA polymerase, Mg^{2+} free polymerase reaction buffer, high efficiency T4 DNA Ligase, ligase buffer, nuclease free water, and lambda DNA marker were from Promega (Wisconsin, USA). The 500bp DNA molecular weight markers was from Roche. A 100 bp DNA marker was from NEB. The PCR cleanup, nucleotide extraction and gel extraction kits were from Qiagen Ltd. (West Sussex, UK). Plasmid purification kits for mini- preps were from Qiagen Ltd. SP6 RNA polymerase, cloned FPLC pure, $m^7G(5')ppp(5')G$, sodium and nucleoside 5'-triphosphate mix were from Amersham Pharmacia Biotech (Uppsala, Sweden).

2.2.1.5 Particle production

A Sorvall RC 5C plus centrifuge with a SS-34 rotor, and a Beckman ultracentrifuge were used for all spins during particle production. Ultracentrifuge tubes and the SW28 rotor and swing buckets were from Beckman-Coulter Instruments Inc. (CA, USA). Sucrose was from BDH Ltd (Poole, UK). A Bio-Rad gene pulser was required for electroporation. Electroporation cuvettes were from BTX (San Diego, USA). TNE buffer: 50mM Tris, 0.1M NaCl and 0.1mM EDTA were dissolved in 800ml distilled water, pH adjusted to 7.4 with HCL and volumize to 1 liter. Infection medium for titration was prepared as follows: 500ml MEM from Gibco (UK) was supplemented with 13.3ml of 7.5% BSA prepared in PBS.

2.2.1.6 Antibodies

The rabbit anti-mouse IFN-β polyclonal antibody was purchased from PBL (USA). The normal goat serum (NGS), the biotinylated goat anti-rabbit secondary antibody, the Vectastain Elite ABC kit and the hard set mounting medium with DAPI came from Vector laboratories Inc. (CA, USA). The standard IFN-β ($1x10^6$ U/ml) came from PBL (USA).

The rat anti-mouse IFN-β monoclonal antibody was from US biologicals (USA). The anti-SFV nsP4 antibody was donated by Dr. Marina Fleeton, Virology group, Dept. of Microbiology, Trinity College, Dublin. Streptavidin-FITC was purchased from Dako (Denmark). The diaminobenzidine substrate (DAB) came from Sigma (UK). Hydrogen peroxide (H_2O_2), Harris's haematoxylin and DPX were purchased from BDH Ltd., UK. Sodium chloride was from Sigma (UK) and 1M hepes came from Gibco (UK). 4% (w/v) paraformaldehyde (PFA) was made by adding 20g of PFA to 500ml PBS.

2.2.1.7 Microscopy

A Nikon Eclipse E400 Epifluorescence microscope was used for both bright field and fluorescent microscopy. The following Nikon filters were used for fluorescence detection: GFP filter at 460-500 nm and DAPI filter at 340-380 nm,

2.2.1.8 Miscellaneous

The CellTiter 96 one solution cell proliferation assay kit was from Promega (UK). The 96 well culture plates were from Sarstedt (Denmark). A Multiskan RC reader from ThermoLabsystems was used to read 96 well culture plates at 492nm. Solvents were mainly from BDH Ltd,UK. All other chemicals were of AnalaR or molecular biology grade as required and were purchased from Sigma or BDH Ltd. Ampicillin and trypan blue were from Sigma (UK), noble agar was from Difco (Detroit, USA), 10X MEM medium was from Gibco (UK), crystal violet was from ClinTech. (Essex, UK), sodium bicarbonate and formalin neutral buffered were from BDH Ltd., UK and lysing matrix D tubes were from Q-Biogen (UK). Biopulverizer tubes and the FastPrep Instrument (FP 120) were from Anachem

2.2.2 Methods

2.2.2.1 Cell culture

The BHK-21 cell line was used for SFV A7 virus growth, plaque assay and expression studies. Cells were cultured in 75 cm^3 tissue culture flasks containing BHK-21 medium, supplemented with 5% (vol/vol) NCS, 5% (vol/vol) tryptose phosphate broth, 100 U/ml penicillin, 100 μg/ml streptomycin in 200 mM L-glutamine, and maintained at 37°C in a humidified atmosphere of 5% CO_2. Cells were seeded at 1 x 10^5 ml^{-1} for

growing (ATCC recommendation) in a total volume of 15ml medium, and passaged when confluent as follows: Cell monolayers were washed twice with PBS, pH 6.7 and incubated with 0.25% (wt/vol) trypsin/EDTA at 37°C until detachment was evident (1-3 min), the flask was tapped to complete detachment and medium added to terminate trypsinization. Cells were then split and returned to the incubator. For recombinant particle production and titration, the sBHK cell line was used. sBHK were grown in 150 cm^3 culture flasks under the same conditions as above, in BHK-21 medium supplemented with 5% (vol/vol) FCS and 2% (vol/vol) 1M Hepes in addition to tryptose phosphate broth, L-glutamine and antibiotics. Cells were propagated in the same manner as above. For titration experiments, sBHK cells were seeded at 1 x 10^5 ml^{-1} in a total volume of 2 ml per well in 6-well dishes. The murine L929 cell line was used in the viral inhibition assay and was grown in DMEM medium supplemented with 10% FCS and 1% penicillin-streptomycin in 75 cm^3 culture flasks. Conditions and method of growth were the same as above.

2.2.2.2 Virus growth

A working stock of avirulent A7 strain of SFV was obtained by infecting BHK-21 cells with a seed-stock of A7 in a 75 cm^3 flask for 1 h, with rocking movements every 15 min to achieve a homogenous infection. The virus inoculum was removed from the monolayer and cells were given fresh BHK medium and incubated at 37°C in a humidified atmosphere of 5% CO_2 until full CPE was observed (approximately 24 h). To harvest the virus, supernatant was removed, centrifuged at 3000rpm (2730g) for 10 min to remove cellular debris, filtered through 0.2 μm filters, and stored in 0.5 ml aliquots at –70°C. Virus titre was established by plaque assay.

2.2.2.3 Plaque assay

BHK-21 cells were seeded at a concentration of 1x10^5 ml^{-1} in a total volume of 2 ml per 60 mm plate and then infected with varying dilutions of A7 for 1 h in a humidified atmosphere of 5% CO_2, 37°C with rocking movements every 15 min. The virus inoculum was removed from the monolayer and cells were given 3 ml of medium containing a 50:50 solution of overlay medium and 1.8% (wt/vol) noble agar, and incubated at 37°C in a humidified atmosphere of 5% CO_2 for approximately 48 h. Cells were then fixed in formalin neutral buffered, and stained with crystal violet. Viral titre was measured by counting plaques, and expressing the number as plaque forming units/ml (p.f.u. /ml).

2.2.2.4 Virus infection

For virus infection, 14 Balb/c mice were inoculated intraperitoneally (i.p.) using 10^6 p.f.u. of A7 virus in 500µl of PBS. Mice were anaesthetised with halothane, ligatured at the neck, and brains and spleens were removed at days 2, 4 and 7 post infection.

2.2.2.5 RNA extraction

Total RNA was isolated from the mouse brains by homogenising 100 mg tissue per 1ml of Trizol reagent in a Biopulverizer tube using a FastPrep Instrument (FP 120) for 45s at a pulse of 5.5 and then incubated on ice for 10 min. The mixture was then centrifuged (14000rpm (10,000g), 10 min, 4°C) and supernatant transferred to a microcentrifuge tube. After 5 min incubation at RT, 200 µl of chloroform (per ml of Trizol used) was added to the tube, and the mixture was centrifuged (14000rpm (10,000g), 10 min, 4°C). The colourless aqueous phase was transferred to a new tube, mixed with 500 µl of isopropanol (per ml of Trizol), and incubated at RT for 10 min. The mixture was centrifuged (14000rpm (10,000g), 10 min, 4°C), the supernatant was removed and the pellet washed with 1 ml of 75% ethanol (-20°C) by vortex. The mixture was centrifuged again (14000rpm (10,000g), 10 min, 4°C), ethanol was removed and RNA resuspended in 20 µl of nuclease-free water before storage at -70°C.

2.2.2.6 RT-PCR

Oligonucleotide primers were designed to clone murine IFN-β (GenBank database) from cDNA. The forward primer incorporated the first 16 nucleotide bases of the coding sequence of murine IFN-β and also incorporated the native SFV ribosome-binding site (RBS) sequence, and both forward and reverse primers contained a XmaI restriction site, to facilitate ligation with pSFV1 (Figure 2.1). The sequence of primers used in IFN-β amplification is indicated with the XmaI sites in *italics*, the RBS sequence underlined, and the IFN-β start codon in bold:

Mouse IFN-β F 5'AAT*CCCGGG*<u>GCACC</u>**ATG**AACAACAGGTGGA-3'

Mouse IFN-β R 5'GCG*CCCGGG*TCTTCAGTTTTGGAAGTTTCT-3'

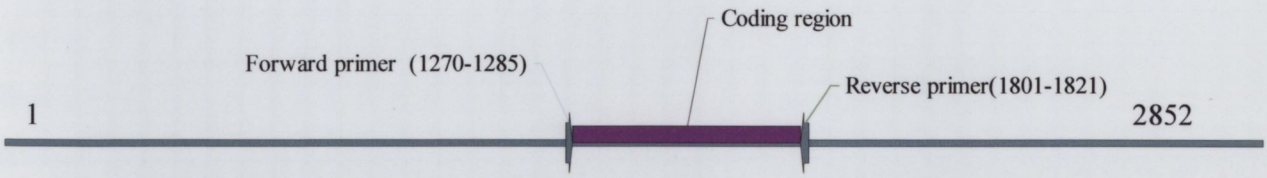

2852 bp

Full length interferon-beta

Sequence of the coding region within the full length IFN-β gene

atgaacaaca ggtggatcct ccacgctgcg ttcctgctgt gcttctccac cacagccctc tccatcaact ataagcagct ccagctccaa gaaaggacga acattcggaa atgtcaggag ctcctggagc agctgaatgg aaagatcaac ctcacctaca gggcggactt caagatccct atggagatga cggagaagat gcagaagagt tacactgcct ttgccatcca agagatgctc cagaatgtct ttcttgtctt cagaaacaat ttctccagca ctgggtggaa tgagactatt gttgtacgtc tcctggatga actccaccag cagacagtgt ttctgaagac agtactagag gaaaagcaag aggaaagatt gacgtgggag atgtcctcaa ctgctctcca cttgaagagc tattactgga gggtgcaaag gtaccttaaa ctcatgaagt acaacagcta cgcctggatg gtggtccgag cagagatctt caggaacttt ctcatcattc gaagacttac cagaaacttc caaaactgaa ga

Figure 2.1 Coding region of murine IFN-β

The full length murine IFN-β gene is 2852 bp long of which the coding region covers 552bp and codes for 184aa. The coding region alone was amplified. This region does not contain the TATA promoter, enhancer consensus sites, a primary transcript, a polyA tail (supplied by vector) or N-linked glycosylation sites. The forward primer was designed to include the first 16 nucleotides of this region, an Xma1 restriction site as well as the native SFV ribosome-binding site. The reverse primer was designed to include the final 21 nucleotides of the coding region of the IFN-β gene, and an Xma1 restriction site. The restriction sites, Ban II and Bgl II, on the coding sequence of IFN-β at positions 123bp and 495bp respectively were used for analysis of PCR product and correct orientation.

First strand cDNA was synthesized from 1μg of RNA tissue in a 20μl reaction using oligo (dT) primers and Promega Improm-II reverse transcriptase as per manufacturers instructions. Each reaction contained 5mM $MgCl_2$, 1X reverse transcription buffer (10mM Tris-HCl [pH 9.0], 50mM KCl, 0.1% Triton X-100), 1mM dNTP, 1U recombinant Rnasin ribonuclease inhibitor, 15U high concentration AMV reverse transcriptase, and 0.5μg oligo (dT) primers. The reaction was incubated at 25°C for 5 min, 37°C for 60 min and 70°C for 15 min. A 20μl aliquot of the cDNA product was incorporated in a 100μl PCR reaction with the following final concentrations: 20μl cDNA reaction, 0.2mM dNTPs, 2mM $MgCl_2$, 1X Mg^{2+} free polymerase reaction buffer, 1μM forward and reverse primers and 5.0U of Taq DNA polymerase. Samples were incubated for 2 min at 95°C, followed by 30 cycles of denaturation at 95°C for 30 sec, annealing at 55°C for 30 sec and extension at 72°C for 4 min. A final extension time of 5 min at 72°C was used and 5μl of the amplified products (5μl DNA, 2μl loading dye, 15μl 1X TBE) were analysed on 2% wt/vol agarose gel stained with ethidium-bromide (0.5g agarose, 25ml 1X TBE and 10% ethidium bromide). Attempts to amplify IFN-β using different annealing temperatures were performed, for example 58°C and 61°C but 55°C gave the best result. Negative control reaction mixes using PBS mock infected brains were analysed for each RT-PCR reaction set. Internal controls for the reaction included reaction mixes lacking RNA or the RT enzyme. Oligonucleotide primers that produce a 508bp product of the GAPDH protein were used to demonstrate the integrity of the DNA. Six RT-PCR reactions were performed in total.

2.2.2.7 Preparation of the IFN-β insert

Following PCR amplification, IFN-β products were purified using the Qiagen PCR purification protocol, eluted in 30μl nuclease free water and then digested with Xma1 to create the necessary 'sticky' ends. Digestion mixtures were as follows: 10μl IFN-β DNA, 28μl H_2O, 5μl buffer 4 (NEB), 5μl BSA (10X) and 20U Xma1. These digestion reactions were pooled (6x50μl) and further purified by gel extraction from a 2.0 % gel using the Qiagen gel extraction protocol. Digested, gel extracted IFN-β was analysed by electrophoresis of a 2μl aliquot on a 2.0% (w/v) agarose gel.

2.2.2.8 Growth of recombinant SFV plasmids

2.2.2.8.1 Preparation of competent *E. coli* DH5α cells

Escherchia coli strain DH5α cells were used for transformation of recombinant SFV and 'helper' SFV plasmids. 50ml of LB broth was inoculated with a colony of *E. coli* cells and cells were grown up with vigorous shaking at 37°C until a density of 5 $\times 10^7$ cell/ml (optical density at 360nm of 0.3) was reached. The culture was centrifuged at 3000rpm (2730g) for 5 min at 4°C. The bacterial pellet was resuspended in 20ml of 100mM $CaCl_2$ and incubated on ice for 30 min. The cell suspension were centrifuged at 3000rpm (2730g) for 5 min and the pellet resuspended in 2ml $CaCl_2$ and stored for 12-24 h at 4°C. 15% (vol/vol) 80% glycerol was added to the competent bacterial cell suspension, which were then aliquoted and stored at -70°C.

2.2.2.8.2 Transformation of bacterial cells

Competent DH5α cells were transformed with SFV recombinant plasmids (pSFV1, pSFV10-E and pSFV1-EGFP) and helper SFV plasmids (pSFV-Helper S2 and pSFV-Helper CS219A). Up to 25ng of DNA was added to 50μl of competent cells, tubes were mixed and incubated on ice for 30 min. The cells were then heat shocked for 2 min at 42°C and cooled on ice for 1-2 min before 800μl of SOC medium was added to the suspension. Tubes were warmed to 37°C and grown for 45 min on a shaker to allow the cells to recover and not express antibiotic resistance. Transformed colonies were then plated onto L agar containing 100μg/ml ampicillin and incubated overnight at 37°C.

2.2.2.8.3 Isolation of DNA from *E.coli* DH5α cells

Two conical flasks of 50 ml L-broth containing 100μg/ml ampicillin were inoculated with a transformed *E.coli* colony and grown overnight on a shaker at 37°C. Plasmids were then extracted from this broth culture using the Qiagen midi prep kit as per manufacturer's instructions. DNA was eluted from the midi prep column in 1ml nuclease free water and plasmid concentration was assessed by mixing a 1μl aliquot of plasmid DNA with 2μl loading buffer and 9μl 1X TBE and running this on a 0.8% (w/v) agarose gel (0.2g agarose, 2.5μl ethidium bromide (10mg/ml) in 25ml 1X TBE). The concentration of plasmid was estimated from this gel by comparing band intensity with

that of the Lambda molecular weight marker [10µl Lambda (Hind111 & EcoR1), 20µl loading buffer, 90µl 1X TBE].

2.2.2.9 Linearization of SFV vectors for cloning

The 11.3 kbp plasmid, pSFV1, and the 10.7 kbp plasmid, pSFV10-E, contain the following MCSs, BamH1-Xma1-Sma1 and HindIII, Xma1, Xho1, Spe1, Not1, NspV and Bln1 respectively, for use in the construction of recombinant plasmids and an ampicillin resistance site for bacterial screening (Figure 2.2). Plasmids was grown in *E.coli* DH5α competent cells and purified using the QIAGEN midi-prep plasmid purification kit. Prior to cloning, both plasmids were digested with Xma1, which linearises the circular plasmid, in six reaction mixtures as follows: 10µl plasmid, 5µl 10X Buffer 4 (NEB), 5µl 10X BSA, 2µl Xma1 and 28µl H_20 and was purified using the Qiagen nucleotide removal kit. The plasmid was analysed by electrophoresis of a 1µl aliquot on a 0.8% (w/v) agarose gel. Verification that the plasmids pSFV1 and pSFV10-E were correct was shown by digestion with EcoR1 which cuts the plasmids three times, generating three fragments.

2.2.3 Insert of IFN-β into pSFV1

Figure 2.3 depicts the cloning strategy for IFN-β cloning into pSFV1.

2.2.3.1 Ligation reaction

Linearised pSFV1 and IFN-β product were mixed at a ratio of 1:10 in a 20µl ligation mixture containing 1 unit Quick T4 Ligase and 10X ligase buffer (NEB) and incubated for 5 min at RT. This ligation mixture was transformed into *E.Coli* DH5α cells as previously described in section 2.2.2.8.2 and then the bacterial mixture was plated out on agar plates containing 100µg/ml ampicillin. Plates were incubated overnight at 37°C to allow colony growth. To confirm the presence of insert in the vector, colonies were inoculated into 10ml L broth containing 100µg/ml ampicillin and incubated on a shaker at 37°C overnight. Plasmids were purified from broth culture using the Qiagen mini-prep procedure, and size compared to pSFV1 by agarose gel electrophoresis.

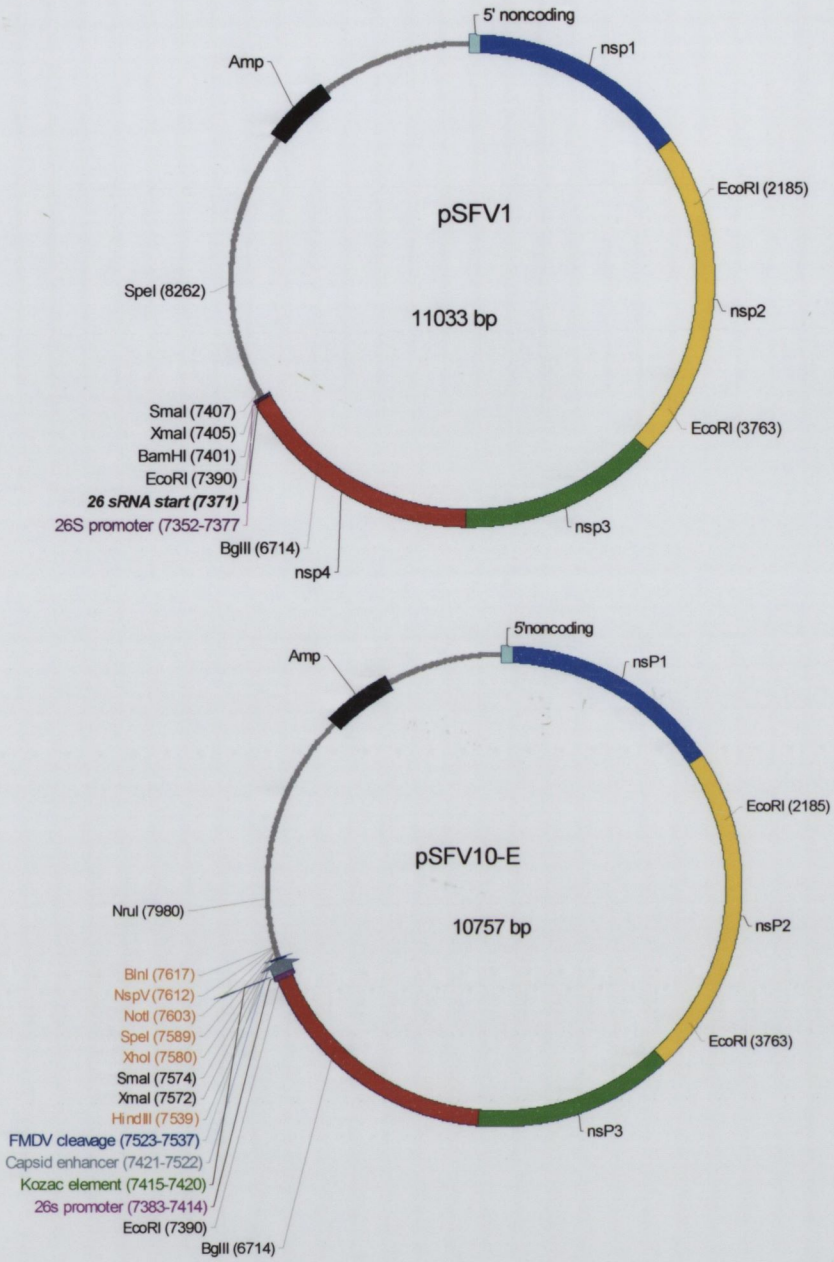

Figure 2.2 SFV expression vectors used for cloning of IFN-β

The cloning vector, pSFV1, contains a cassette of three restriction sites, BamH1-Xma1-Sma1 for cloning, downstream of its 26S promoter. pSFV10-E contains more restriction sites in its MCS for ease of cloning. pSFV10-E also contains a capsid translational enhancer sequence and a 2A autoprotease from FMDV downstream of its 26S promoter. The capsid enhancer sequence is composed of the N terminal 34 a.a. sequence of the SFV capsid gene and forms a fusion protein with the foreign gene of interest upon translation. The FMDV 2A autoprotease cleaves the N–terminal capsid residues from the gene of interest allowing high level expression of the gene of interest.

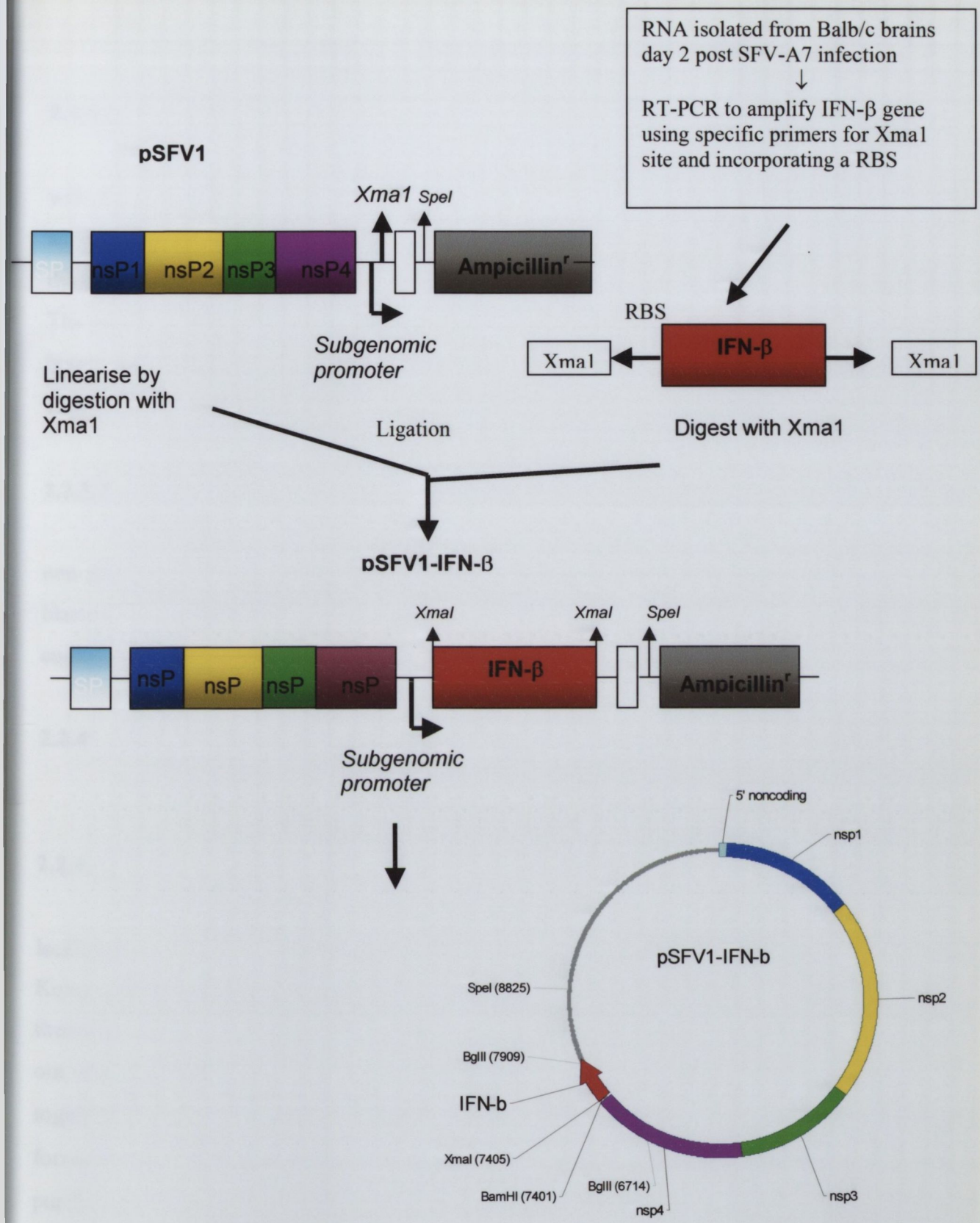

Figure 2.3 Strategy for cloning of IFN-β into pSFV1

IFN-β was isolated by RT-PCR from brain RNA day two post infection with A7. The gene was then cloned into the Xma 1 restriction site of the pSFV1 expression vector.

2.2.3.2 Screening for IFN-β insert

Plasmid mini preps were screened for the presence of IFN-β insert by digestion with XmaI, and digests were run on a 2.0% (w/v) agarose gel. Digestions were carried out as follows: 5μl DNA, 2μl 10X BSA, 2μl buffer 4, 1μl XmaI and 10μl H_2O. 2μl loading dye was added to the mixture after digestion and ran on a 2% gel with a 500bp ladder. The positive clone found was digested with BglII restriction enzyme to confirm that the insert was in the right clockwise orientation (2μl pSFV1-IFN-β, 5μl buffer 2, 1μl Bgl II, 12μl H_2O).

2.2.3.3 Sequencing of rSFV1-IFN-β

The positive clone was confirmed by sequencing with SFV primers coding for the non-structural protein 4 region (Lark sequencing, UK). The resulting sequence was blasted against the NCBI database, and then compared to the original sequence for the coding region of IFN-β obtained from the GenBank database.

2.2.4 Insert of IFN-β into pSFV10-E

See Figure 2.4 for cloning strategy of IFN-β into pSFV10-E.

2.2.4.1 DNA amplication and ligation of IFN-β gene

The IFN-β gene was amplified from pSFV1-IFN-β using a new forward primer lacking the ribosomal binding site and the existing reverse primer. pSFV10-E contains a Kozac element sequence upstream from its MCS. This region serves as a RBC and therefore one does not have to be incorporated into the forward primer. PCR was carried out under the same conditions as before, this time using 2μl pSFV1- IFN-β in the reaction together with 0.2mM dNTPs, 2mM $MgCl_2$, 1X Mg^{2+} free polymerase reaction buffer, 1μM forward and reverse primers and 5.0U of Taq DNA polymerase. IFN-β products were purified using Qiagen PCR purification protocol, eluted in 30μl nuclease free water and then digested with XmaI to create the necessary 'sticky' ends as in section 2.2.2.7. These digestion reactions were pooled and further purified using the Qiagen gel extraction kit from 2.0% agarose gel. The concentration of XmaI linearised pSFV10-E and XmaI digested IFN-β were analysed by electrophoresis of 1μl aliquots on a 2.0% (w/v) agarose gel. Linearised pSFV10-E and IFN-β insert product were mixed at a ratio of 1:20 in a

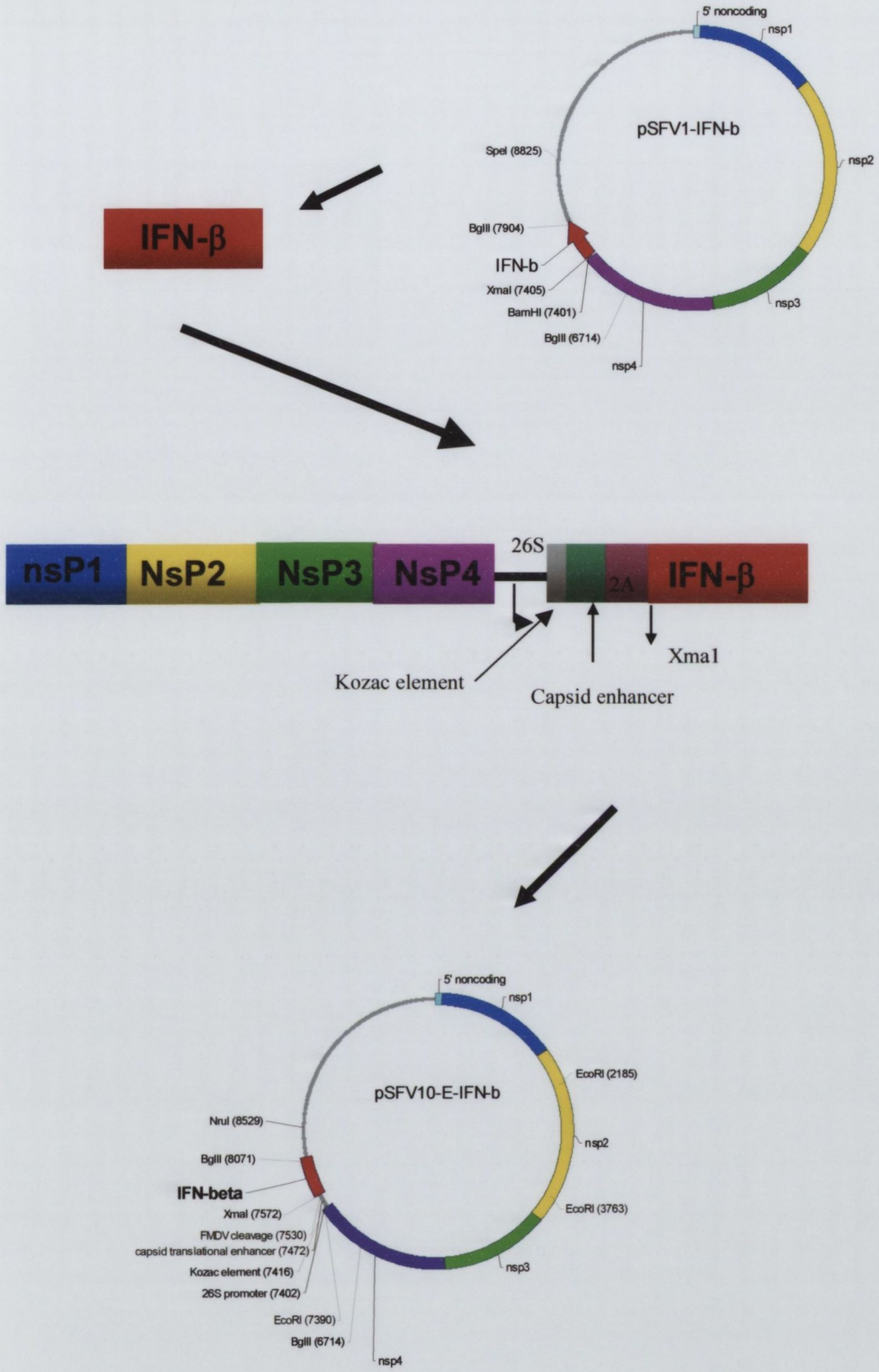

Figure 2.4 Cloning of IFN-β into pSFV10-E

IFN-β was amplified from pSFV1-IFN-β and cloned into pSFV10-E vector using the Xma1 restriction site.

20µl ligation mixture containing 1 unit Quick T4 Ligase and 10X ligase buffer (NEB) and incubated for 5 min at RT. Positive clones were confirmed using the same SFV nsP4 sequencing primers as before and correct orientation confirmed by digestion with Bgl 11.

2.2.5 Expression of IFN-β *in vitro*

Expression of IFN–β from both rSFV-IFN-β vectors was detected by electroporating 1.5µg of *in vitro* transcribed linearised plasmid into BHK-21 cells and carrying out immunohistochemical labelling to detect IFN-β expression. Further expression studies were performed to quantify expression and secretion of biological active IFN-β from both rSFV-IFN-β particle vector by viral inhibition assay.

2.2.5.1 *In vitro* SP6 RNA transcription

rSFV1-IFN-β and rSFV10-E-IFN-β vectors were linearised with Spe1 and Nru1 restriction enzymes respectively and 1.5µg of linearised DNA was *in vitro* transcribed to produce RNA for electroporation. Standard reaction mixtures contained 1.5µg DNA template, 1X SP6 buffer [40mM N-2-hydroxyrthyl-piperazine-N'-2-ethansulphonic acid-KOH (Hepes-KOH), pH 7.4, 6mM MgOAc, 2mM spermidine-HCL], 1mM $m^7G(5')ppp(5')G$, 5 mM dithiotreitol, 1mM each rATP, rCTP, rUTP, 500 µM rGTP, 10U recombinant Rnasin and 0.5U SP6 polymerase. The reactions were incubated at 37°C for 1 h 50 min and transcripts were analysed by electrophoresis on a 0.6% (w/v) agarose gel and quantified by comparison with 5 and 10µl volumes lambda marker (5µl marker, 55µl 1X TBE and 40µl loading dye).

2.2.5.2 Electroporation

BHK-21 cells were propagated as described in section 2.2.2.1. For electroporation, BHK-21 cells were grown in 75 cm^3 tissue culture flasks until ~ 80% confluent. Cell monolayers were washed twice with PBS, incubated with 0.25% (w/v) trypsin/EDTA at 37°C until detachment was evident, the flask tapped to complete detachment and 6ml medium added to terminate trypsinization and to resuspend the cells. Cells were centrifuged (1500rpm (1365g), 10 min), and pellet resuspended in 6ml PBS. The cells were centrifuged (1500rpm (1365g), 10 min) and resuspended in a final volume of 700µl PBS. *In vitro* transcribed SFV RNA was then added to suspended cells, and the mixture incubated on ice for 15 min in a 0.4µm electroporation cuvette. The cells were then electroporated at 0.85 kV and 25µF capacitance, using a BioRad Gene Pulser 11. Following pulse, cells were replaced on ice for a further 15 min, before resuspension in 20ml BHK medium at 37°C. The cells were immediately placed into 6-well plates, each containing one 22x22 mm glass coverslip, and maintained at 37°C in a humidified atmosphere of 5% CO_2 for 18-24 h. Linearised empty SFV plasmids were *in vitro* transcribed and electroporated into BHK-21 cells as negative controls. PBS mock electroporated cells were also included.

2.2.5.3 Immunohistochemistry

After incubation medium was removed from the wells containing the coverslips and the cells were washed twice with 2 ml PBS. The cells were then fixed on the glass coverslips by adding 1ml 4% paraformaldehyde (w/v) to each well for 20 min. After removal of paraformaldehyde and two washes with PBS, the coverslips were transferred to a metal coverslip holder using forceps. The cells were then permeablized in Acetic Acid: Ethanol (1:2) at -20°C for 5 min, and endogenous peroxidase activity was blocked with 3% (vol/vol) H_2O_2 in PBS for 10 min. Five min washes were done twice with PBS between each step. After washing the coverslips were transferred to a humidity chamber (HC) where cells were incubated in normal goat serum (15µl per 1ml PBS, 150µl per slide) for 20 min at 37°C to block non specific binding sites. Serum was removed and cells were incubated with rabbit anti-mouse IFN-β antibody (1:100 dilution in PBS) in the HC for 40 min at 37°C to detect IFN- β expression. Cells were washed with 0.05 % (v/v) tween-80 in PBS twice, followed by PBS washes as described above and then incubated with biotinylated goat anti rabbit secondary antibody (1:200 dilution in goat serum blocking buffer) for 30 min at RT. Following two PBS-tween 80 washes VECTASTAIN Elite ABC reagent (20µl

reagent A and 20 µl reagent B in 1ml PBS) was added for 30 min at RT in HC (150µl per slide). Cells were washed in PBS for 5 min, incubated in DAB for 2 min, and washed in running tap water for 5 min. Cells were then counterstained in haematoxylin harris for 10 sec, washed in water, then dipped 3 times in ammonia water (2ml NH_3 in 500ml H_2O). Following in a series of ethanol washes (75%, 90%, and 100%) to dehydrate the cells, they were cleared in 3 xylene washes and mounted on slides in DPX.

2.2.6 rSFV particle production and titration

The helper capsid, CS219A and helper spike, S2 plasmids are required to package the recombinant SFV vector after transcription and replication in rSFV particle production (Figure 2.5). These helper plasmids supply the necessary structural proteins *in trans*, allowing packaging of replication deficient viral particles. The main steps in particle production are linearization of the helper and recombinant plasmids, *in vitro* transcription, transfection by co-electroporation into sBHK cells, harvesting and titration of the viral particles .

2.2.6.1 Linearisation of rSFV and helper plasmids for rSFV particle production

For production of each batch of high titre rSFV particles, 9µg of each linearised helper capsid, helper spike and rSFV DNA is required. The helper capsid, helper spike, rSFV1 and rSFV1-IFN-β are all linearised by digestion with SpeI restriction enzyme. rSFV10-E and rSFV10-E-IFN-β are linearised with NruI restriction enzyme. Helper plasmids and rSFV plasmids were grown up by transformation of *E.coli* DH5α cells with 25-50ng of each plasmid. DNA extraction was carried out according to Qiagen Midi prep protocol. Plasmids were quantified by running 1µl DNA with 2µl loading dye and 10µl 1X TBE on a 0.8% gel against the lambda marker (90µl TBE, 20µl loading dye, 10µl marker). 15µg of each plasmid was digested to compensate for any loss of DNA. Multiple digestions were carried out for each plasmid in 100µl volumes. SpeI digestions contained 10-15µg DNA, 10µl 10X buffer 4 (NEB), 1µl 100X BSA, 25-35U SpeI (10U/µl) and nuclease free H_20 to volumise. NruI digestions contained 10-15µg DNA, 10µl 10X NruI unique buffer, 25-35U NruI (10U/µl) and nuclease free H_20 to volumize. Digestions were incubated at 37°C for 2 h. 1µl linearised DNA was run on a 0.8% gel to quantify (1µl DNA, 9µl 1X TBE and 2µl loading dye) and then nucleotide clean up performed using Qiagen protocol.

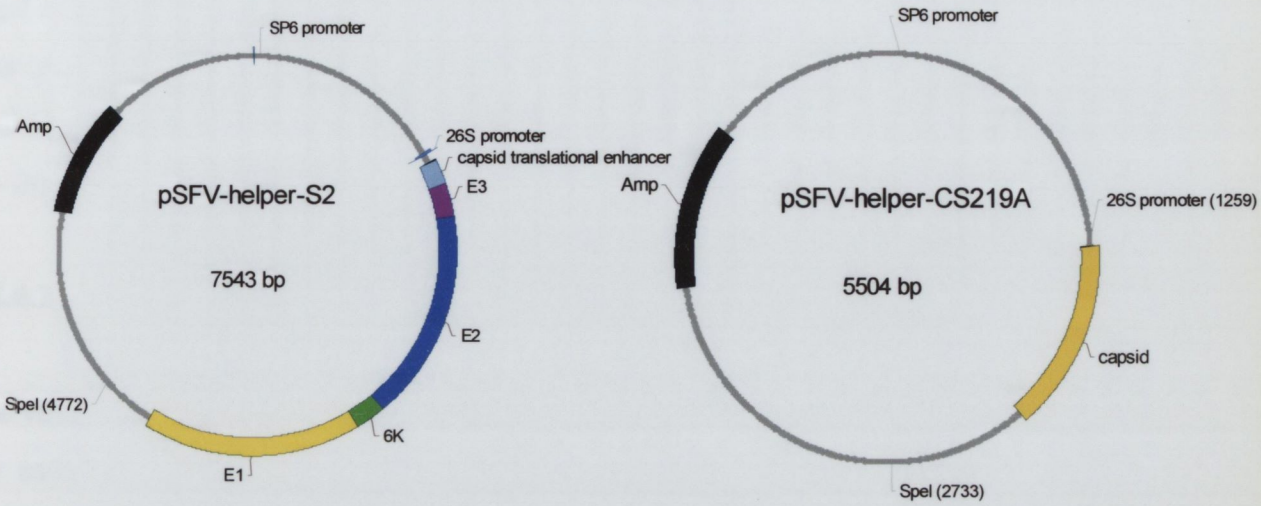

Figure 2.5 Maps of SFV helper plasmids

The helper plasmids, pSFV-helper S2 and pSFV-CS219A supply the packaging system that rSFV vectors require for production of recombinant particles. These plasmids contain the complete 26S viral sub-genomic RNA sequence as well as the 3′ and 5′ replication signals necessary for genomic RNA replication. They do not encode the viral replicase. The helper S2 plasmid supplies the envelope proteins and also contains an engineered capsid translational enhancer sequence upstream of its envelope proteins to ensure comparable levels of expression from both the envelope and capsid proteins. The helper plasmid, CS219A, supplies the capsid gene and naturally possesses the enhancer sequence. Both plasmids contain a unique Spe1 site for linearization. The SP6 promoter drives *in vitro* transcription of the helper plasmids.

The recommended DNA concentration per column is 10μg, digestions containing in excess of this amount were divided and applied to two columns. Plasmids were eluted in 30μl nuclease free H_20 and pooled. 1μl plasmid (1μl plasmid, 15μl TBE, 4 μl loading dye) was quantified against 5 and 10μl volumes of the lambda marker (5μl marker, 55μl 1X TBE and 40μl loading dye) on a 0.8 % agarose gel. Linearised, cleaned up plasmids were stored at –20°C until use.

2.2.6.2 *In vitro* transcription

Each standard *in vitro* transcription reaction mixture contained 1.5μg DNA template in a volume of 50μl together with all the other reagents required, as seen in section 2.2.5.1. For each batch of high titre particles, the volume of the reaction mixture was increased six times to allow *in vitro* transciption of 9μg DNA template. Reactions were carried out in volumes of 300μl for each helper plasmid, and rSFV vector as described above, with the same concentration of the necessary reaction reagents described above, in increased volumes. 1μl of RNA for each plasmid was run on a 6.0% agarose gel with the same lamba marker as described in section 2.2.5.1.

2.2.6.3 Electroporation

Three T150cm^3 culture flasks of sBHK cells were required for production of each batch of particles. Cells were cultured as described in section 2.2.2.1. After trypsinization with 2ml trypsin the cells were aspirated 10 times to ensure a single celled suspension. 18 ml of medium was added to each flask and cell suspension was aspirated again. The cell suspensions from each flask were pooled together in one flask giving a total volume of 60ml. The mixture was then divided equally into two sterile 50ml falcon tubes and the volume was made up to 50ml in each tube with culture medium. The tubes were then centrifuged at 1500rpm (1365g) for 8 min at RT. The medium was decanted and the cell pellet was resuspended by flicking. 25ml of PBS was added to each tube and the cell suspension was aspirated until no clumps were visible. The volume was brought up to 50ml with PBS and the tubes were centrifuged again at 1500rpm (1350g) for 8 min. After centrifugation the PBS was decanted and the cells were again resuspended by flicking. 3.9ml of PBS was added to one tube. After aspiration the cell-PBS mixture was transferred to the second tube where these cells were resuspended in the cell mixture. At this point all three RNAs (helpers and rSFV RNA) were added to the cell mixture and aspirated to ensure

a uniform mix. 800µl of the RNA/cell/PBS mix was added to six individual electroporation cuvettes and each cuvette was pulsed under the same conditions described in section 2.2.5.2. After electroporation, the cell suspension from three of the cuvettes were resuspended in 50ml of culture medium, giving two 50ml volumes in total. The cells were added very quickly to allow recovery and transferred to two separate T150cm^3 flasks and incubated at 33°C, 5% CO_2 for 36-40 h.

2.2.6.4 Harvesting rSFV particles

After incubation, medium containing viral particles was pooled in a glass bottle on ice, transferred to sterile screw cap sorvall centrifuge tubes in equal 30ml volumes and clarified three times by centrifugation at 4°C in a Sorvall SW34 rotor for 15 min at 18000rpm (25,261g). After the last centrifugation the supernatant was pooled again and transferred in 20ml volumes to three 50ml Beckman ultracentrifuge tubes. A 5ml 20% (w/v) sucrose cushion was added to each tube by carefully placing the pipette at the bottom of each tube and releasing the sucrose slowly. The tubes were now topped up with the remaining supernatant and placed in the rotor buckets. Each bucket was weighed and additional medium was required when needed to balance. The particles were concentrated by ultracentrifugation through this sucrose cushion in a Beckman SW28 rotor at 25000rpm (125,892g) for 2h 15 min at 4°C. Virus pellets were resuspended in 300µl TNE buffer and left to incubate on ice for 2 h. After incubation the resuspended pellet was transferred to a glass bijou and another 300µl TBE was added to each tube to ensure all particles had been carried over to the bijou, bringing the volume up to 1.8ml. 50µl aliquots were made and snap frozen in liquid N_2 and stored at –70°C until use.

2.2.6.5 Titration of viral particles

To determine the titre of the stocks, sBHK cells were seeded at 1 x 10^5 cells per well of a six well plates in a total volume of 2 ml. Each well contained a 22x22 mm coverslip on which the cells would adhere. Plates were incubated overnight at 37°C. The medium was removed and the cells were washed twice with PBS containing Ca^{2+} and Mg^{2+}. The cells were infected with serial dilutions of viral particles, performed in infection medium in 500µl volumes and rocked gently. Plates were incubated at 37°C for 1 h and were rocked every 10 min. 2.5ml of fresh medium was added on top of the virus inoculum and the plates were incubated overnight. After 18-24 h the medium was removed and the cells were

washed twice with PBS as before and then fixed for 20 min in 4% PFA. After fixation the cells were washed again and then monitored for expression of IFN-β as seen in section 2.2.5.3 but by indirect immunofluorescence. rSFV-IFN-β particles were titrated with rabbit anti mouse IFN-β antibody as described before and all steps remained the same until addition of streptavidin-FITC. After the secondary antibody step, streptavidin-FITC was diluted 1:100 in high salt NaCl-Hepes buffer (0.5M NaCl, 10mM Hepes) and 100µl was added to each coverslip and incubated for 30 min at RT. After incubation the cells were washed twice in NaCl–Hepes buffer for 5 min, dipped in DI H_20 before being mounted onto clean slides with Vectashield hard set mounting medium with DAPI. Empty particles were titrated in the same way using a rabbit anti-mouse antibody specific for the nsP4 region of SFV. Particle titres were obtained by examining cells microscopically for the presence of fluorescence using a specific FITC filter. Particle titres were calculated at a magnification of x 400 and expressed as IU/ml.

2.2.7 Viral inhibition assay to quantify expression of biologically active IFN-β from SFV vectors

There was no ELISA available for quantification of IFN-β expression from rSFV-IFN-β vectors. A viral inhibition assay was developed which is based on the protective effects that IFN-β elicits on infection (Figure 2.6). BHK-21 and L929 cells were cultured as described in section 2.2.2.1 and seeded at a concentration of 1×10^6 cells per well of 6 well plates in 2ml volume. BHK- 21 cells were infected with rSFV-IFN-β particles, and rSFV1 and rSFV10-E empty particles at MOI 1, 10, 100 and incubated at 37°C, 5% CO_2 for 24 h. The supernatant of cells infected at an MOI 1 were harvested at additional time points 12, 36, 48 and 60 h post infection. L929 cells were also infected with rSFV-IFN-β and empty particles at MOI 1,10,100 and harvested 24 h post infection. All supernatant samples were then centrifuged at 14,000 rpm (10000g) for 5 min at 4°C to remove cell debris, aliquoted and frozen at –70°C until they were assayed for the presence of IFN-β as previously described (Miller and Anders, 2003), with minor alterations to the protocol. Murine L929 cells were seeded in a 96 well plate, $3x10^4$ cells per well in 100µl culture medium and grown overnight at 37°C. Standard IFN-β ($1x10^6$ units /per ml) was serially ten fold diluted in DMEM and 50µl of each dilution was added to duplicate wells, at a starting concentration no greater than 50U/well. Supernatant samples were serially two fold diluted

and 50µl added to duplicate wells. A rat anti mouse IFN-β monoclonal antibody (US Biologicals) was added to each well, both control and sample wells, at a concentration of 1.25ng/well. The plate was incubated at 37°C for 18-24 h, then the samples were removed and the cells were washed twice with PBS. The cells were then infected with SFV A7 (MOI 1) for 1h. The virus inoculum was removed and 100µl fresh medium was added to each well. The plate was incubated for 48h at 37°C. 10µl MTS was added to the medium in each well after 48 h and absorbance was read at 492nm (Buttke *et al.*, 1993). Internal controls for this inhibition assay included infected, untreated and mock infected L929 cells.

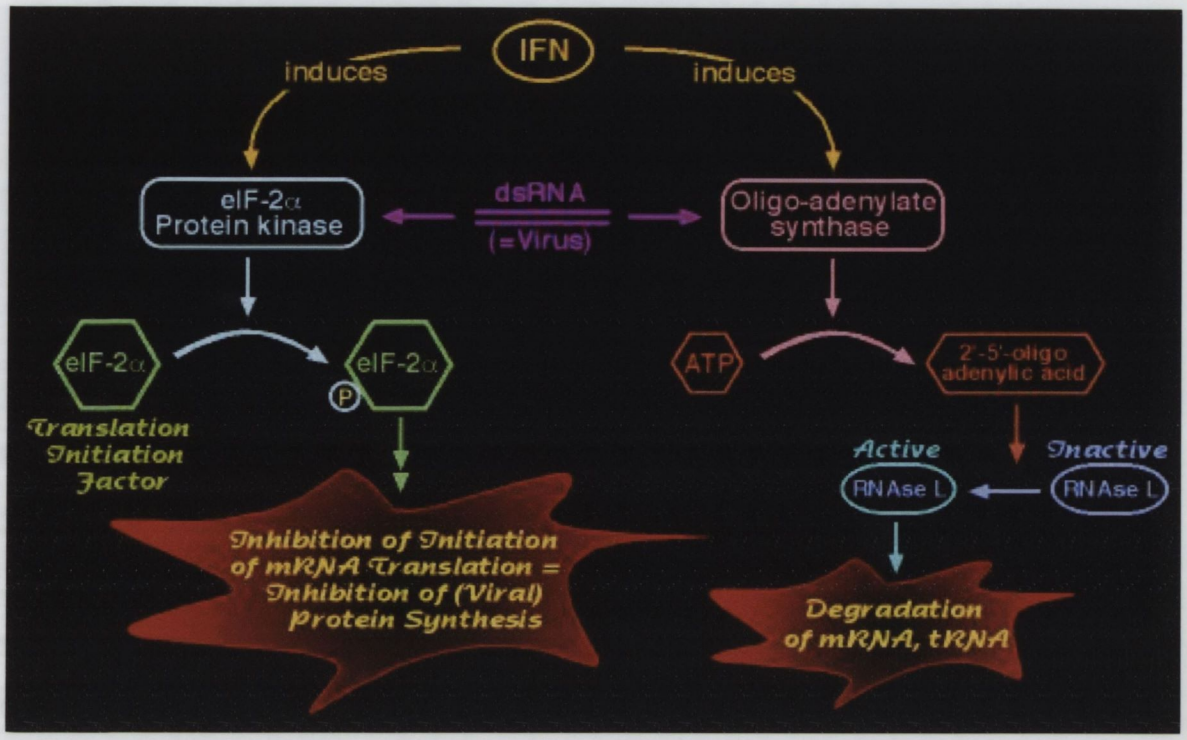

Figure 2.6 The antiviral effects of IFN- β

IFN-β is generally produced in response to viral infection. The two best known IFN-β-induced proteins are (2′-5′) OAS and dsRNA dependent PKR. Together these enzymes inhibit viral mRNA translation through the activation of cellular Rnase and through the degradation of viral RNAs, leading to inhibition of viral protein synthesis. http://www-biology.ucsd.edu/labs/david.

2.3 Results

2.3.1 Cloning and expression of murine IFN-β into pSFV1

RNA was extracted from the brains and spleens of SFV A7 infected Balb/C mice days two, four and eight post infection. The IFN-β gene (552 bp + 6 random bp + 12 bp for Xma1 sites + 5bp for ribosomal binding site = 575 bp) was amplified from RNA extracted from the brains at two days post infection by RT-PCR (Figure 2.7A). The IFN-β PCR product was digested with Ban II to ensure correct product and yielded two fragments of 137 bp and 438bp (Figure 2.7B). Minimal levels of IFN-β RNA were found in the brain and spleen four and eight days post infection. PCR amplified, Xma1 digested IFN-β (552 bp + 5bp RBS + 6bp= 563bp) was cloned into Xma1 linearised pSFV1 (Figure 2.8B). pSFV1 was digested with Eco1 prior to linearisation and ligation to ensure correct plasmid. EcoR1 cuts the plasmid three times and generates three fragments, 1578bp, 3627bp and 5828bp (Figure 2.8A). Transformation of ligation mixture yielded one positive rSFV-IFN-β clone (Figure 2.9A). Correct orientation of the clone was confirmed by restriction digestion with Bgl 11, an enzyme unique to pSFV1 and to the IFN-β insert. Bgl 11 cuts rSFV-IFN- β twice, resulting in two fragments, one 1190 bp in size, the other 10406 (Figure 2.9B). Sequencing using SFV primers coding for the non-structural protein 4 region confirmed correct orientation of IFN-β within the plasmid and sequence homology of 100% when compared to the original mouse IFN-β coding region sequence from GenBank database (Figure 2.10). IFN-β expression was confirmed in BHK-21 cells transfected by electroporation with *in vitro* transcribed rSFV-IFN-β RNA using immunohistochemistry. Diffuse brown cytoplasmic staining was evident in rSFV10-E-IFN-β electroporated BHK-21 cells 24 h post electroporation (Figure 2.11A). No staining was evident in the PBS electroporated cells or rSFV10-E electroporated cells (Figure 2.11B&C).

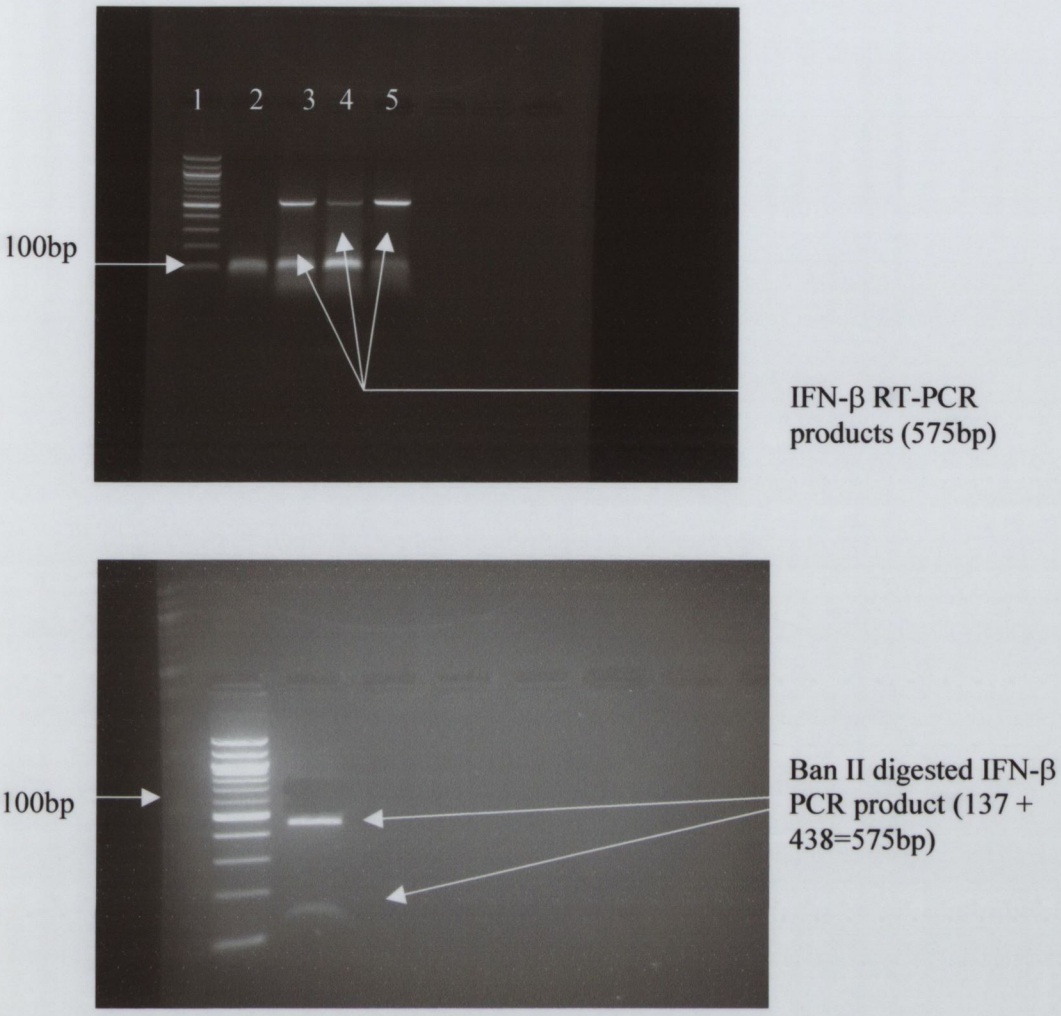

Figure 2.7 Gel analysis of RT- PCR amplified IFN-β

Total RNA was extracted from the brains of Balb/c mice infected i.p. with SFV-A7 at 2, 4 and 7 days post infection. The integrity of the RNA was checked by RT-PCR using primers specific for mouse β actin and GAPDH (not shown). The PCR amplified IFN-β gene was analysed by electrophoresis of a 5μl volume on a 2% (wt/vol) agarose gel (A) and further confirmed by restriction digestion with Ban II (B).

(A) Lane 1: 100bp DNA ladder, Lane 2: H_2O, Lanes 3-5: PCR amplified undigested IFN-β (552bp + 6 random bp + 6 bp x 2 for restriction sites + 5 bp for RBS = 575bp)

(B) Lane 1: 100bp DNA ladder, Lane 2: Ban II digested IFN-β PCR product (137bp + 438 bp fragments =575bp)

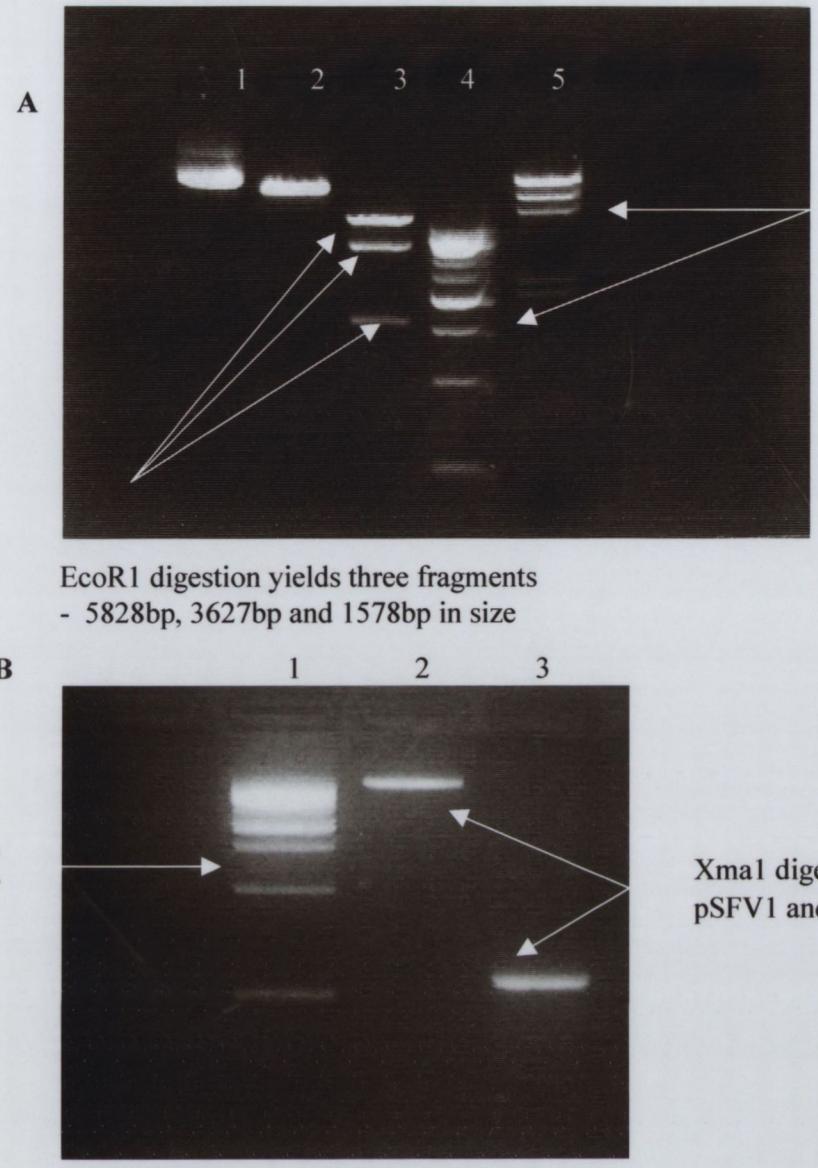

Figure 2.8 Preparation of pSFV1 plasmid and IFN-β PCR product for ligation

To ensure correct plasmid for cloning, the pSFV1 plasmid was digested with EcoR1 restriction enzyme, generating three fragments of 1578bp, 3627bp and 5828bp in size, as seen on a 1.0% agarose gel (A). Both pSFV1 and the IFN-β PCR product were digested with Xma1 restriction enzyme to give correct sticky ends for ligation. Equal volumes of linearised pSFV1 and Xma1 digested IFN-β were run on a 2.0% agarose gel to allow a ratio to be established for the ligation reaction (B).

(A) Lane 1: Undigested pSFV1, Lane 2: Xma1 digested pSFV1, Lane 3: EcoR1 digested pSFV1, Lane 4: 500bp DNA ladder, Lane 5: Lamdba- Hind III DNA ladder

(B) Lane 1: 500bp DNA ladder, Lane 2: 1μl of Xma1 digested pSFV1, Lane 3: 1μl of Xma1 digested IFN-β (552bp + 5bp RBS + 6bp Xma1 site= 563bp)

A

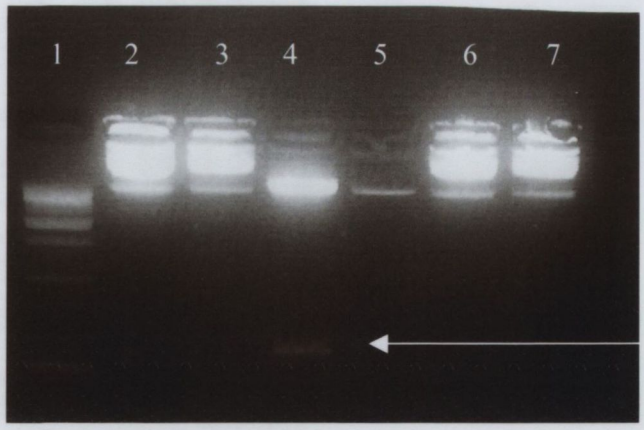

IFN-β band of 552bp in size present after Xma1 digestion

B

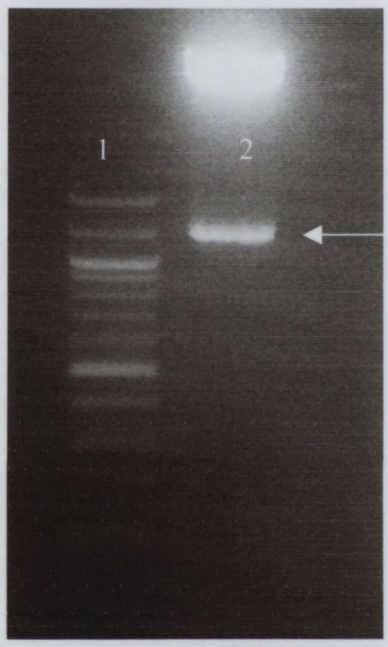

Band 1190bp in size present after Bgl 11 digestion of pSFV1-IFN-β

Figure 2.9 IFN-β insert in pSFV1 plasmid

To confirm whether IFN-β had been successful cloned into the Xma1 site in the MCS of pSFV1, 5µl of each plasmid prep was screened for insert by digestion with Xma1. Each digestion was run on a 2% agarose gel along with the appropriated sized DNA ladder marker. One positive clone was found after screening of the first thirty preps (A). The insert was found to be in the correct orientation after digestion with Bgl 11 which yielded a fragment 1190 bp in size, shown on a 1.5 % agarose gel (B)

(A) Lane 1: 500bp DNA ladder, Lanes 2&3 : Xma1 digested mini preps with no IFN-β, Lane 4: Presence of IFN-β insert, Lanes 5-7: Xma1 digested mini preps with no IFN-β

(B) Lane 1: 100bp DNA ladder, Lane 2: Bgl 11 digested pSFV1-IFN-β to ensure correct orientation (1190bp + 10,406bp = 11,596bp)

CLUSTALW Result

[clustalw.aln][clustalw.dnd][readme]

```
 CLUSTAL W (1.83) Multiple Sequence Alignments


Sequence type explicitly set to DNA
Sequence format is Pearson
Sequence 1: IFN             552 bp
Sequence 2: Seq_query       552 bp
Start of Pairwise alignments
Aligning...


Sequences (1:2) Aligned. Score: 43.6594
Sequences (2:2) Aligned. Score: 43.6594
Guide tree        file created:   [clustalw.dnd]
Start of Multiple Alignment
There are 1 groups
Aligning...
Group 1: Sequences:   2      Score:10488
Alignment Score 3958
CLUSTAL-Alignment file created  [clustalw.aln]

clustalw.aln

CLUSTAL W (1.83) multiple sequence alignment


IFN             ATGAACAACAGGTGGATCCTCCACGCTGCGTTCCTGCTGTGCTTCTCCACCACAGCCCTC
Seq_query       ATGAACAACAGGTGGATCCTCCACGCTGCGTTCCTGCTGTGCTTCTCCACCACAGCCCTC
                ************************************************************

IFN             TCCATCAACTATAAGCAGCTCCAGCTCCAAGAAAGGACGAACATTCGGAAATGTCAGGAG
Seq_query       TCCATCAACTATAAGCAGCTCCAGCTCCAAGAAAGGACGAACATTCGGAAATGTCAGGAG
                ************************************************************

IFN             CTCCTGGAGCAGCTGAATGGAAAGATCAACCTCACCTACAGGGCGGACTTCAAGATCCCT
Seq_query       CTCCTGGAGCAGCTGAATGGAAAGATCAACCTCACCTACAGGGCGGACTTCAAGATCCCT
                ************************************************************

IFN             ATGGAGATGACGGAGAAGATGCAGAAGAGTTACACTGCCTTTGCCATCCAAGAGATGCTC
Seq_query       ATGGAGATGACGGAGAAGATGCAGAAGAGTTACACTGCCTTTGCCATCCAAGAGATGCTC
                ************************************************************

IFN             CAGAATGTCTTTCTTGTCTTCAGAAACAATTTCTCCAGCACTGGGTGGAATGAGACTATT
Seq_query       CAGAATGTCTTTCTTGTCTTCAGAAACAATTTCTCCAGCACTGGGTGGAATGAGACTATT
                ************************************************************

IFN             GTTGTACGTCTCCTGGATGAACTCCACCAGCAGACAGTGTTTCTGAAGACAGTACTAGAG
Seq_query       GTTGTACGTCTCCTGGATGAACTCCACCAGCAGACAGTGTTTCTGAAGACAGTACTAGAG
                ************************************************************
```

file://D:\CLUSTALW%20Result.htm

```
IFN             GAAAAGCAAGAGGAAAGATTGACGTGGGAGATGTCCTCAACTGCTCTCCACTTGAAGAGC
Seq_query       GAAAAGCAAGAGGAAAGATTGACGTGGGAGATGTCCTCAACTGCTCTCCACTTGAAGAGC
                ************************************************************

IFN             TATTACTGGAGGGTGCAAAGGTACCTTAAACTCATGAAGTACAACAGCTACGCCTGGATG
Seq_query       TATTACTGGAGGGTGCAAAGGTACCTTAAACTCATGAAGTACAACAGCTACGCCTGGATG
                ************************************************************

IFN             GTGGTCCGAGCAGAGATCTTCAGGAACTTTCTCATCATTCGAAGACTTACCAGAAACTTC
Seq_query       GTGGTCCGAGCAGAGATCTTCAGGAACTTTCTCATCATTCGAAGACTTACCAGAAACTTC
                ************************************************************

IFN             CAAAACTGAAGA
Seq_query       CAAAACTGAAGA
                ************

clustalw.dnd

(IFN:0.28170,Seq_query:0.28170);
```

Select tree menu ▾ Exec

Figure 2.10 IFN-β coding region in pSFV1-IFN-β sequence analysis

The IFN-β sequence obtained using SFV nsP4 sequencing primers were blasted against the original IFN-β sequence from the Genbank database. 100% identity of sequence was found with the original sequence. Further restriction analysis and *in vitro* expression studies confirmed expression.

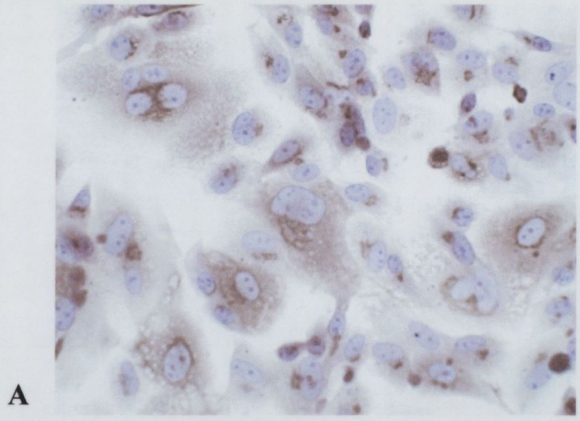

A

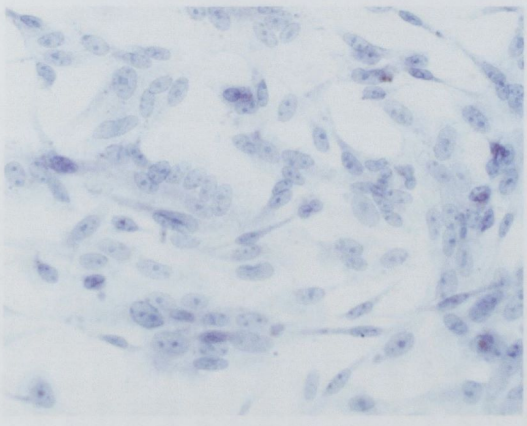

B

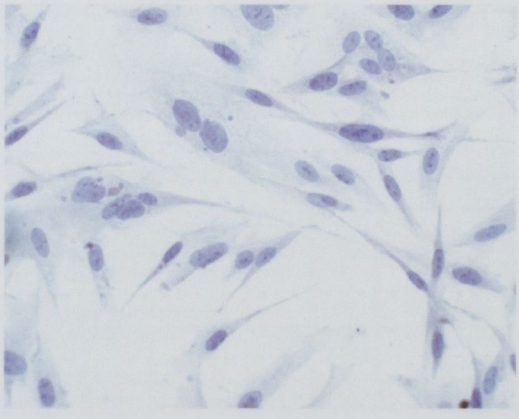

C

Figure 2.11 Expression of rSFV1-IFN-β in BHK-21 cells

Diffuse cytoplasmic staining was evident in the cells electroporated with rSFV1-IFN-β indicating the expression of IFN-β from the vector (A). No staining was evident in the cells electroporated with RNA from linearised empty SFV plasmids (B) or mock electroporated BHK-21 cells (C) which were included as negative controls. Stained cells were examined using bright field microscopy at a magnification of x400. Staining was performed twice.

2.3.2 Cloning and expression of IFN-β in pSFV10-E

IFN-β was amplified from rSFV1-IFN-β by PCR (Figure 2.12). The PCR product (552bp + 6 random bases + 12 bps for Xma1 sites=570bp) was digested with Xma1 and the resultant product (552bp + 6 bp Xma1 = 558bp) was ligated with Xma1 linearised pSFV10-E to facilitate construction of rSFV10-E-IFN-β (Figure 2.13). Prior to linearisation and ligation correct plasmid was confirmed by digestion with EcoR1. As above EcoR1 cuts the plasmid three times generating fragments of 1578, 3627 and 5552 bp in size. Four rSFV10-E- IFN-β clones were obtained by digestion of multiple plasmid preps with Xma1 (Figure 2.14A). Correction orientation of IFN-β insert within these clones was confirmed by digestion with Bgl11 an enzyme unique to both the insert and pSFV10-E. Digestion with Bgl II generated two fragments, 1357 bp and 9958 bp in size. These fragment sizes indicate that IFN-β is inserted in the correct orientation. One out of four positive clones had the insert in correct orientation (Figure 2.14B). The positive clone were sent for sequencing with SFV nsp4 primers. The resultant sequence was compared with the original coding sequence for mouse IFN-β as before. A sequence homology of 98% was obtained with the original sequence (Figure 2.15). *In vitro* expression was carried out as above by electroporation of *in vitro* transcribed rSFV10-E-IFN-β into BHK 21 cells. Diffuse cytoplasmic staining was again seen in cells electroporated with rSFV-IFN-β RNA (Figure 2.16A). No staining was seen in the control cells which were mock electroporated with PBS and with rSFV empty vector RNA (Figure 2.16 B&C).

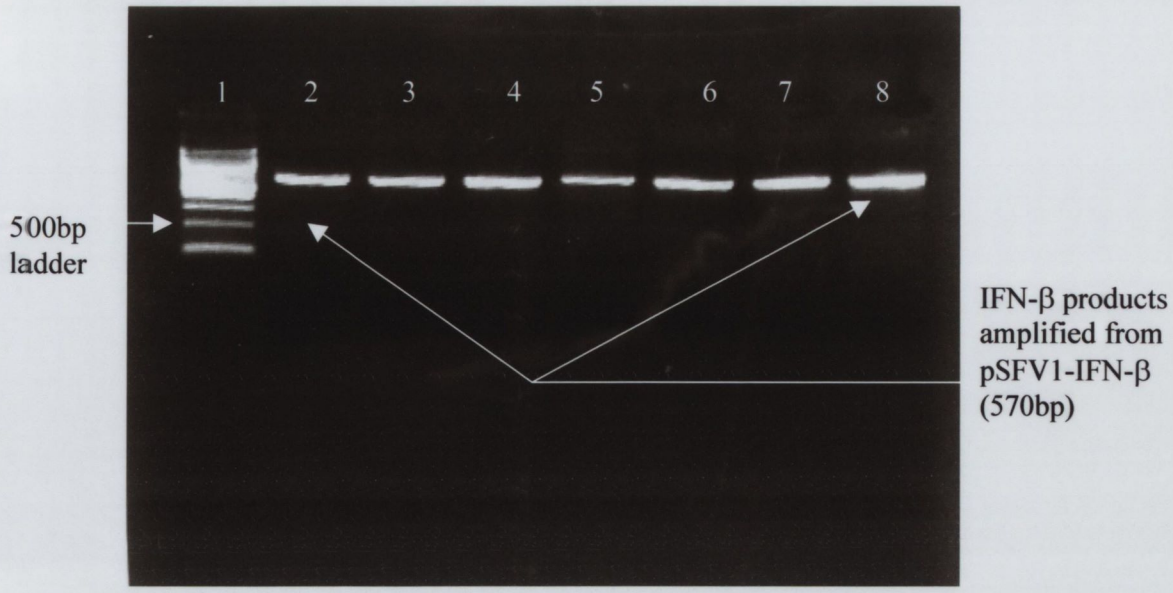

Figure 2.12 PCR amplification of IFN-β gene from pSFV1-IFN-β plasmid

IFN-β was successfully amplified from the pSFV1- IFN-β plasmid using specific IFN-β primers incorporating the Xma1 site as before. 5μl of PCR products were run on a 2.0% agarose gel along with a 100bp marker to ensure the gene was successfully amplified. H_2O control was included though not shown.

Lane 1: 100bp DNA ladder, Lanes 2-8: IFN-β PCR products amplified from pSFV1-IFN-β (552bp + 6 random bp + 6 bp X 2 Xma1 sites = 570bp)

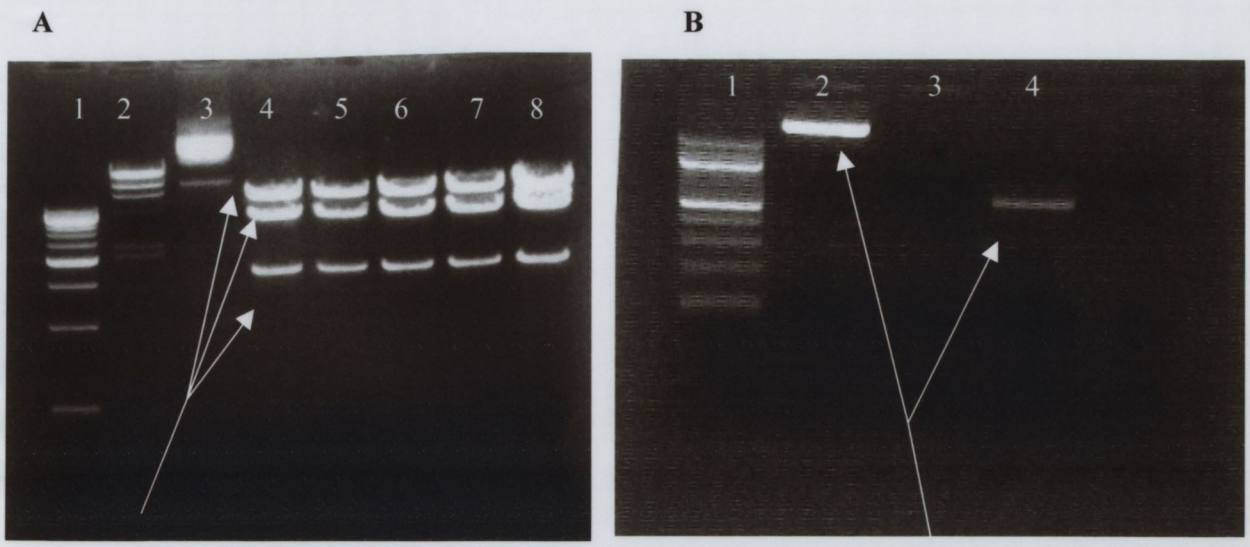

EcoR1 digestion yields three fragments – 5552bp + 3627bp + 1578bp in size

Xma1 digested pSFV10-E and IFN-β (558bp)

Figure 2.13 Preparation of pSFV10-E and IFN-β insert for ligation

Prior to ligation of pSFV10-E with IFN-β, the enhanced vector was digested with EcoR1 to ensure that the plasmid was correct. EcoR1 cuts the plasmid three times yielding three fragments of 1578bp, 3627bp and 5552 bp in size on 1.0% agarose gel (A). Both pSFV10-E and IFN-β were digested with Xma1 to give the correct sticky ends for ligation. 1µl of both Xma1 linearised pSFV10-E and Xma1 digested IFN-β were run on a 1.5% agarose gel to quantify the amount of each required for the ligation reaction.

(A) Lane 1: 500bp marker, Lane 2: Lambda-HindIII cut marker,
Lane 3: 1 µl undigested pSFV10-E, Lanes 4-8: 1µl EcoR1 digested pSFV10-E (1578 + 3627 + 5552 = 10757bp)
(B) Lane 1: 100bp marker, Lane 2: 1µl Xma1 linearised pSFV10-E, Lane 4: 1µl Xma1 digested IFN-β PCR product (552bp + 6bp for Xma1 ends=558bp)

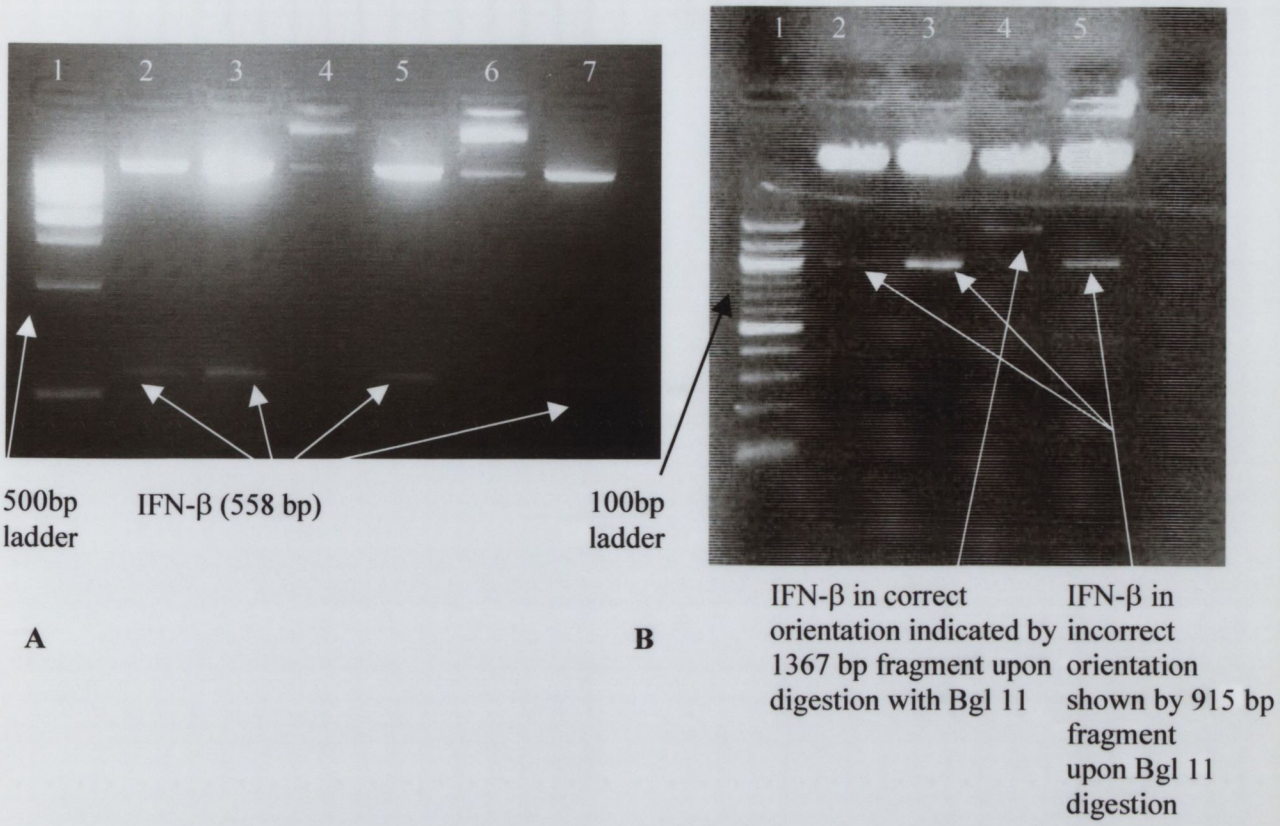

Figure 2.14 Cloning of IFN-β into pSFV10-E

IFN-β was successfully subcloned from pSFV1 into the enhanced vector pSFV10-E. Four positive clones were found, screened by digestion with Xma1 and run on a 2.0% gel to show the IFN-β band of 558bp (552bp + 6bp for Xma1 sites) (A). Upon digestion with BglII, one out of the four clones was found to be in the correct orientation. A fragment of 1357 bp was generated as shown on a 1.5% agarose gel. A fragment of 915 bp in size was generated when the insert was in an anticlockwise orientation (B).

(A) Lane 1: 500bp DNA ladder, Lane 2,3& 5: Presence of IFN-β insert in Xma1 digested mini preps, Lanes 4,6&7: Xma1 digested mini preps without IFN-β insert. Lanes 4 and 6 show incomplete digestions where plasmid is not linearised with Xma1. Enzyme may have been absent from reactions.

(B) Lane 1: 100bp DNA ladder, Lanes 2,3&5: Bgl 11 digested clones with IFN-β in anticlockwise orientation (915 bp), Lane 4:Bgl 11 digested clone with IFN-β in correct clockwise orientation (1357 bp)

Blast 2 Sequences results

Score = 1029 bits (535), Expect = 0.0
Identities = 544/552 (98%)
Strand = Plus / Minus

```
Query: 1   atgaacaacaggtggatcctccacgctgcgttcctgctgtgcttctccaccacagccctc
60
           |||||||||||||||||| ||||||  |||||||  | ||||  ||  ||||||||||||||
Sbjct: 750 atgaacaacaggtggatcntccacgntgcgttcnngntgtgnttntccaccacagccctc
691


Query: 61  tccatcaactataagcagctccagctccaagaaaggacgaacattcggaaatgtcaggag
120
           ||||||||||||||||||||||||||||||||||||||||||||||||||||||||||||
Sbjct: 690 tccatcaactataagcagctccagctccaagaaaggacgaacattcggaaatgtcaggag
631


Query: 121 ctcctggagcagctgaatggaaagatcaacctcacctacagggcggacttcaagatccct
180
           |||||||||||||||||||| ||||||||||||||||||||||||||||||||||||||
Sbjct: 630 ctcctggagcagctgaatggaaggatcaacctcacctacagggcggacttcaagatccct
571


Query: 181 atggagatgacggagaagatgcagaagagttacactgcctttgccatccaagagatgctc
240
           ||||||||||||||||||||||||||||||||||||||||||||||||||||||||||||
Sbjct: 570 atggagatgacggagaagatgcagaagagttacactgcctttgccatccaagagatgctc
511


Query: 241 cagaatgtctttcttgtcttcagaaacaatttctccagcactgggtggaatgagactatt
300
           ||||||||||||||||||||||||||||||||||||||||||||||||||||||||||||
Sbjct: 510 cagaatgtctttcttgtcttcagaaacaatttctccagcactgggtggaatgagactatt
451


Query: 301 gttgtacgtctcctggatgaactccaccagcagacagtgtttctgaagacagtactagag
360
           ||||||||||||||||||||||||||||||||||||||||||||||||||||||||||||
Sbjct: 450 gttgtacgtctcctggatgaactccaccagcagacagtgtttctgaagacagtactagag
391


Query: 361 gaaaagcaagaggaaagattgacgtgggagatgtcctcaactgctctccacttgaagagc
420
           ||||||||||||||||||||||||||||||||||||||||||||||||||||||||||||
Sbjct: 390 gaaaagcaagaggaaagattgacgtgggagatgtcctcaactgctctccacttgaagagc
331


Query: 421 tattactggagggtgcaaaggtaccttaaactcatgaagtacaacagctacgcctggatg
480
```

```
            ||||||||||||||||||||||||||||||||||||||||||||||||||||||||||||||||
Sbjct: 330 tattactggagggtgcaaaggtaccttaaactcatgaagtacaacagctacgcctggatg
271


Query: 481 gtggtccgagcagagatcttcaggaactttctcatcattcgaagacttaccagaaacttc
540
            ||||||||||||||||||||||||||||||||||||||||||||||||||||||||||||||||
Sbjct: 270 gtggtccgagcagagatcttcaggaactttctcatcattcgaagacttaccagaaacttc
211


Query: 541 caaaactgaaga 552
            ||||||||||||
Sbjct: 210 caaaactgaaga 199
```

Figure 2.15 IFN-β coding region in pSFV10-E-IFN-β sequence analysis

The IFN-β sequence obtained using SFV nsP4 sequencing primers was blasted against the original IFN-β sequence from the Genbank database. 98% identity of sequence was found with the original sequence. The difference between the original sequence and the sequence of the rSFV-IFN-β clone was a result of sequencing artifacts, as immunohistochemistry confirmed correct IFN-β expression from the clone upon immunolabelling with an anti-IFN-β antibody. Further restriction analysis and *in vitro* expression studies confirmed expression.

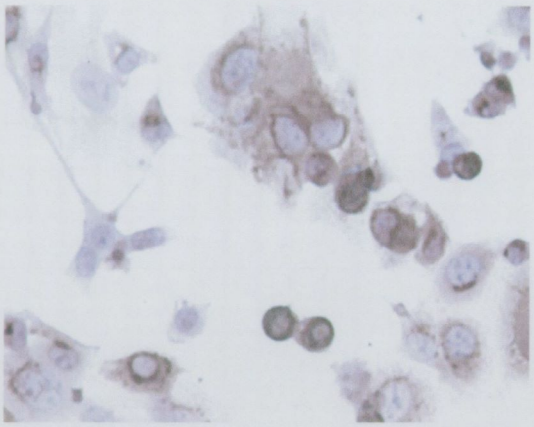

A

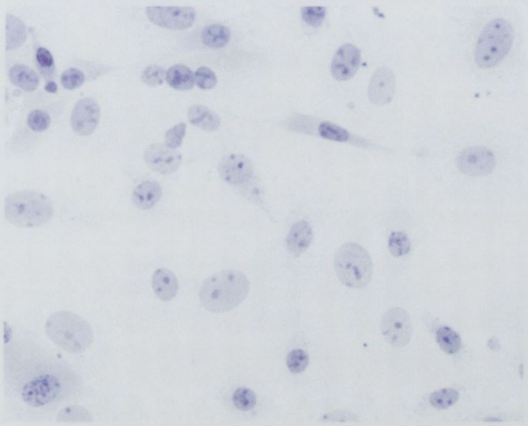

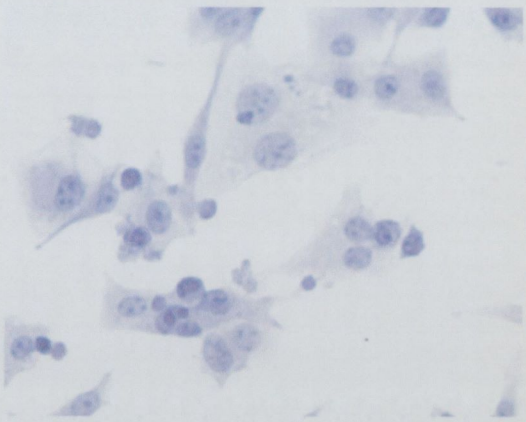

B C

Figure 2.16 Expression of rSFV10-E-IFN-β in BHK-21 cells

Diffuse cytoplasmic staining was evident in the cells electroporated with rSFV10-E-IFN-β as was seen on electroporation of BHK cells with rSFV1-IFN-β RNA (A). No staining was evident in cells electroporated with RNA from linearised empty SFV plasmids (B) or mock electroporated BHK-21 cells which were included as negative controls (C). Stained cells were examined using bright field microscopy at a magnification of x200. Staining was repeated to ensure correct expression.

2.3.3 *In vitro* transcription, particle production and titration

For immunohistochemical studies, rSFV1-IFN-β and rSFV10-E-IFN-β vectors were linearised with Spe1 and Nru1 restriction enzymes respectively, prior to *in vitro* transcription. For particle production the required helper plasmids were linearised with Spe1. All three linearised plasmids, rSFV-IFN-β, helper spike and helper capsid are shown on a 1.0% agarose gel in Figure 2.17. Figure 2.18 shows a 6.0% agarose gel of *in vitro* transcribed rSFV-IFN-β RNA and the helper plasmid RNAs ready for electroporation into BHK cells. After electroporation and harvesting of the rSFV-IFN-β particles, the actual titre of the particle batch was found by infecting sBHK cells with serial dilutions of the viral particles to be titrated followed by indirect immunofluorescence using an anti-mouse IFN-β polyclonal antibody to detect the cells expressing IFN-β. Fluorescent cells were counted and particle titres were calculated at a magnification of x 400 and expressed as IU/ml. Figure 2.19 shows pictures of IFN-β expression in sBHK after infection with rSFV-IFN-β particles using immunofluorescence. Ten fold more fluorescent cells are seen in picture (A) than (B) indicating that dilutions were performed correctly.



Figure 2.17 Linearisation of rSFV-IFN-β and helper plasmids

Linearised plasmid concentrations were calculated by comparison with the top band intensity of the lambda-HindIII DNA ladder of which the concentration was known, 0.25μg. 5μl and 10μl volumes of the plasmids were run side by side and compared with the same volumes of Lambda ladder on a 0.8% (wt/vol) agarose gel prior to *in vitro* transcription.

Lane 1&8: 5μl and 10μl λ DNA ladder (equal to 0.125 and 0.25μg DNA respectively)

Lane 2&3: 5 and 10μl of Spe1 linearised rSFV1-IFN-β, respectively

Lane 4&5: 5 and 10μl of Spe1 linearised spike, respectively

Lanes 6&7: 5 and 10μl Spe1 linearised capsid, respectively

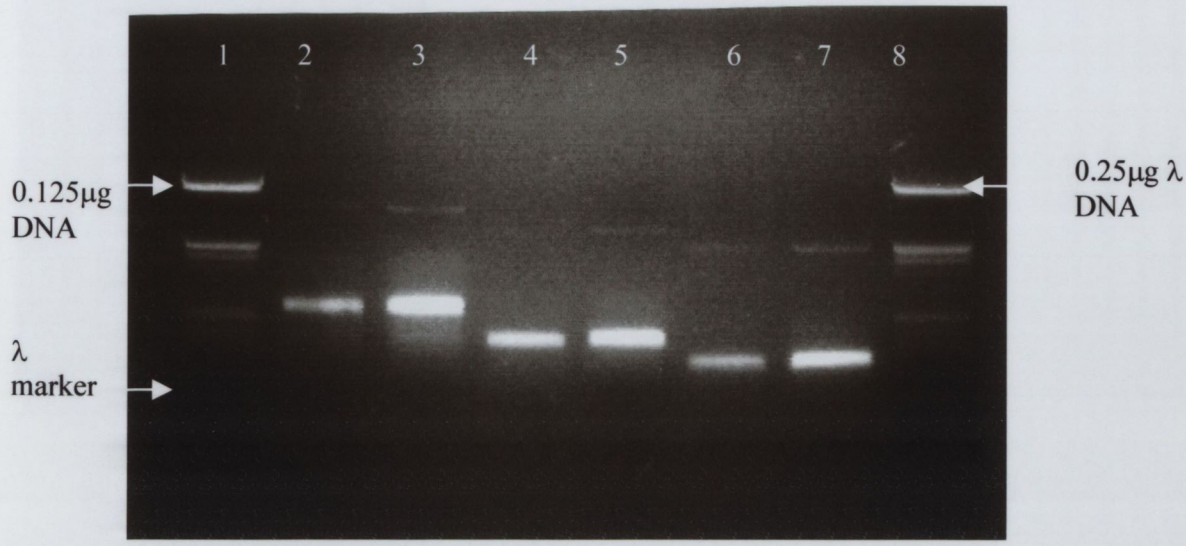

Figure 2.18 ***In vitro*** **transcription of rSFV-IFN-β and helper plasmids**

In vitro transcribed RNAs were run on a 6.0% agarose gel along with the lambda marker used previously, to quantify the amount of rSFV and helper plasmid RNA produced and to ensure that each RNA was present in equal quantities to allow for maximum efficient particle production. For this gel it is important to have bright RNA with the original template of the linearised plasmids visible above each band of RNA.

Lanes 1&8: 5 and 10μl λ DNA ladder (0.125 and 0.25μg respectively)

Lanes 2&3: 5 and 10μl rSFV1-IFN-β RNA (respectively)

Lanes 4&5: 5 and 10μl spike RNA (respectively)

Lanes 6&7: 5 and 10μl capsid RNA (respectively)

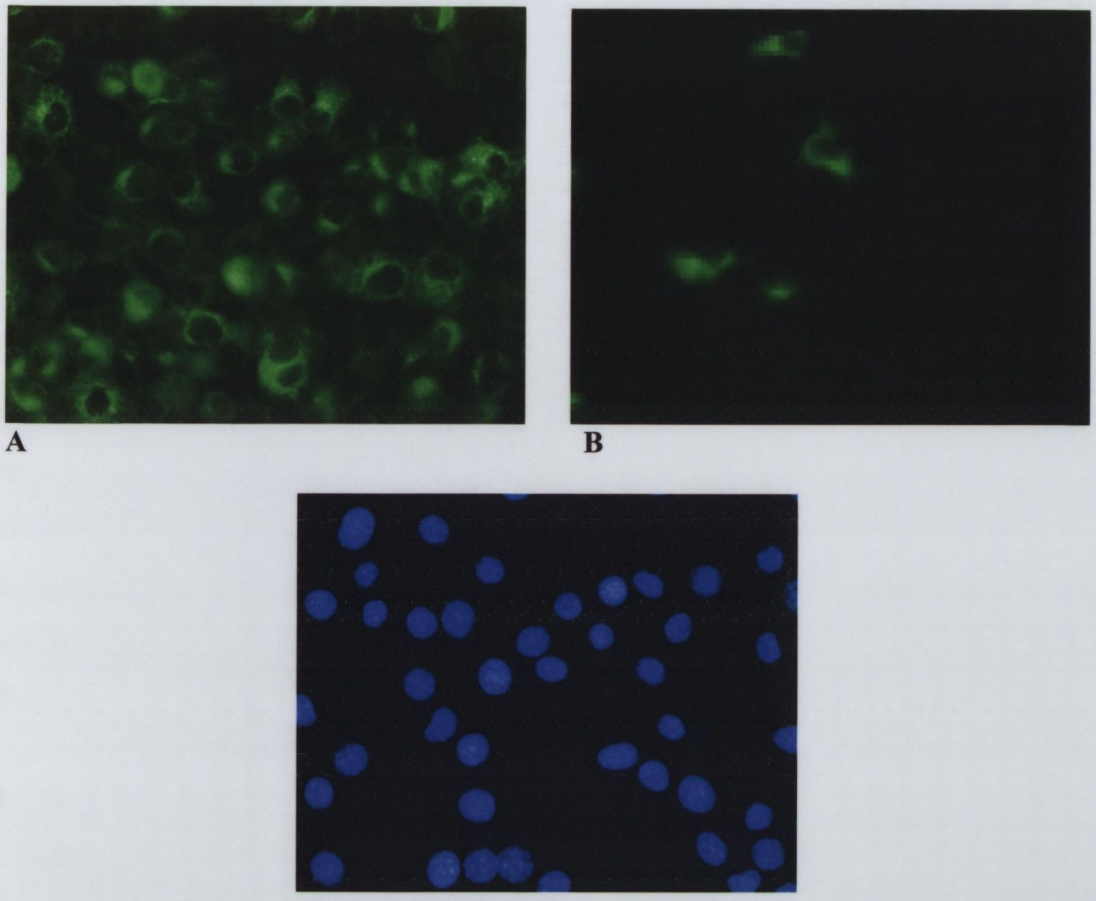

Figure 2.19 Titration of rSFV-IFN-β particles using indirect immunofluorescence

rSFV-IFN-β infected sBHK cells were labeled with a rabbit anti-mouse IFN-β polyclonal antibody, followed by a biotinylated secondary goat anti-rabbit antibody. Bound antibody was detected using streptavidin-FITC antibody and slides were examined under the fluorescent microscope at x200. At lower dilutions the number of fluorescent cells are higher than at higher dilutions as expected. There is approximately a ten fold difference between pictures (A) and (B). Cells appeared normal under the DAPI filter (C). No fluorescence was seen in PBS infected cells (not shown).

2.3.4 Qualitative comparative analysis of IFN-β expression levels from rSFV-IFN-β vectors

The qualitative difference in expression levels between the rSFV-IFN-β constructs was found by looking at the difference in staining intensities between rSFV1-IFN-β and rSFV10-E-IFN-β infected BHK-21 (MOI 1). The same diffuse cytoplasmic staining was evident in both rSFV1-IFN-β and rSFV10-E-IFN-β infected cells as was seen in rSFV-IFN-β electroporated cells, shown in Figure 2.20. Any difference in intensity between the figures is probably due to the fact that the cells were electroporated with rSFV-IFN-β in Figure 2.11 rather than infected, and examined at x400 instead of x200. However staining was more intense in the cells infected with rSFV10-E-IFN-β particles than rSFV1-IFN-β when examined under the bright field microscope at x200 (Figure 2.20A&B). No staining was evident in the PBS infected cells or empty vector particle infected cells as seen in figure 2.20C.

2.3.5 Development of viral inhibition assay to quantify secretion of biological active IFN-β from rSFV-IFN-β vectors

There was no ELISA available to quantify expression of IFN-β from rSFV-IFN-β so a viral inhibition assay using L929 cells was developed. BHK-21 cells were infected with rSFV- IFN-β particles at an MOI 1 and supernatant samples were collected 12, 24, 36, 48, 60 h post infection. L929 cells were incubated with the samples and then challenged with SFV-A7. This assay measures the levels of IFN-β being expressed by rSFV- IFN-β particles into the BHK supernatant by measuring the absorbance reading of viable L929 cells after challenge and comparing to the absorbance value of L929 cells which were incubated with standard IFN-β of known concentration. Initially the supernatant samples taken from rSFV-IFN-β, rSFV1-EGFP and TNE infected cells were all diluted 1: 1024 in DMEM medium, added to L929 cells and incubated for 18-24 h at 37°C. The L929 cells were then challenged with SFV-A7 at an MOI 1. The aim was to compare how much protection each sample could give against A7 challenge at the same dilution by measuring the absorbance measures of the viable cells. The rSFV-IFN-β particle samples showed higher absorbance values than the rSFV1-EGFP and mock infected controls at all time points, peaking 36 hours post infection (Figure 2.21). The rSFV10-E-IFN-β samples showed a greater protective effect than the rSFV1-IFN-β samples indicated by higher

absorbance values at time points 12, 24 and 36h post infection. Table 2.1 shows the actual IFN-β levels (units of activity/ml) expressed by both vectors and controls by comparison with the concentration of standard IFN-β known to exhibit 50% CPE after challenge with SFV-A7 virus. In this experiment the dilution of each sample was not fixed, and the dilution exhibiting 50% CPE was used to calculate the actual IFN-β levels in each sample through direct comparison with the commercial IFN-β of known concentration. High levels of IFN-β expression from both rSFV1- IFN-β and rSFV10-E-IFN-β occurred up to 36 h post infection. rSFV10-E-IFN-β gave greater expression at 12, 24 and 48 h timepoints. Levels reached 4×10^5 U/ml by 36 h post infection but dropped back to 3200U/ml by 60 h.

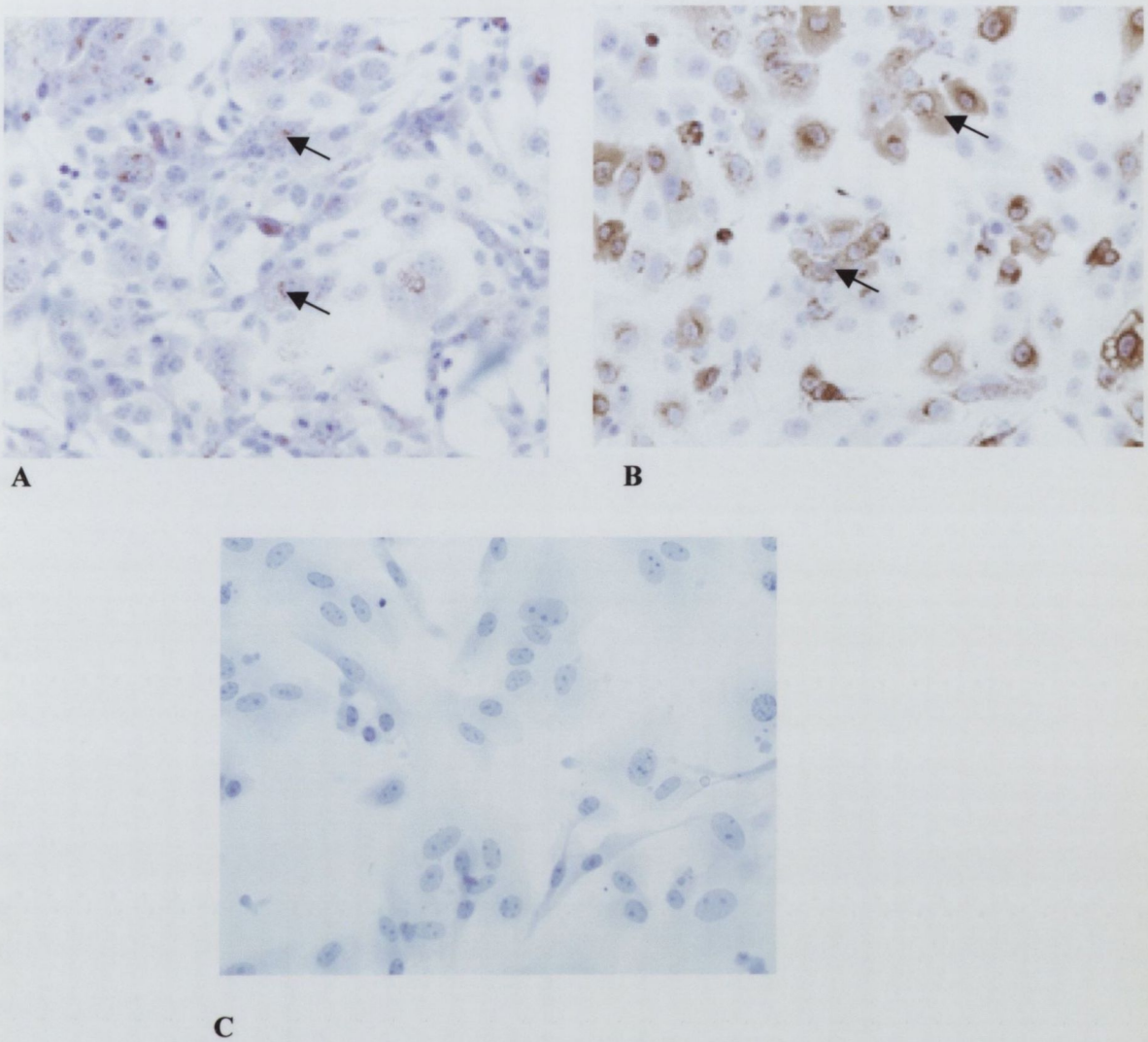

Figure 2.20 Comparison of *in vitro* expression of IFN-β using two different rSFV-IFN-β particle vectors

BHK-21 cells were infected with (A) rSFV1-IFN-β and (B) rSFV10-E-IFN-β particles (MOI 1), and mock-infected with (c) PBS and then labeled for the presence of IFN-β using immunohistochemistry. More intense staining was observed in the cells infected with rSFV10-E-IFN-β particles compared to those infected with rSFV1-IFN-β. No staining was observed in mock -infected cells (x200).

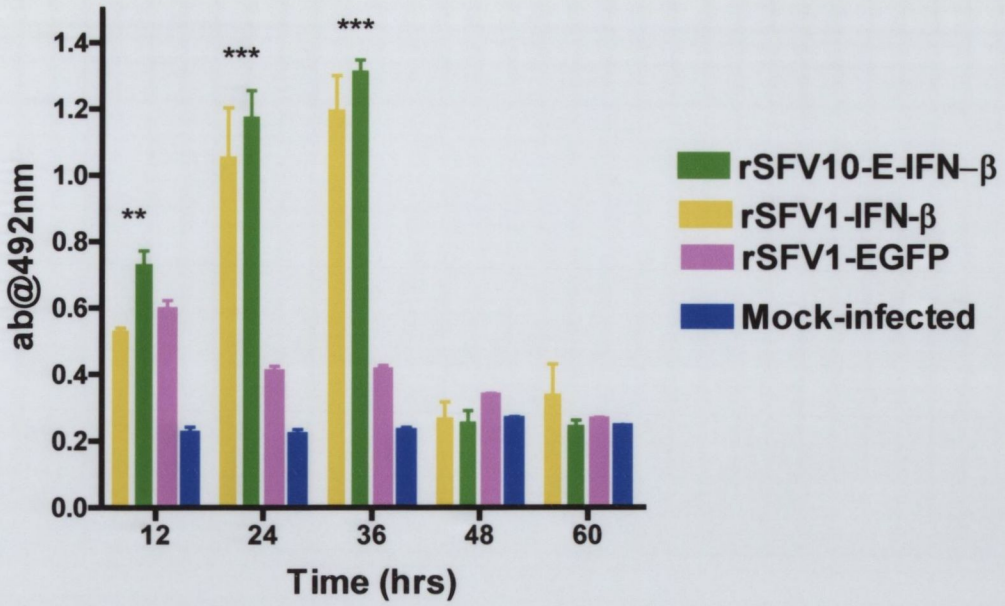

Figure 2.21 Measurement of viable L929 cells post treatment with rSFV-IFN-β supernatant samples and SFV-A7 challenge

This assay measures the number of viable L929 cells remaining after treatment with rSFV-IFN-β supernatant samples and SFV-A7 challenge. The higher the absorbance value the greater the number of viable cells remaining after SFV-A7 challenge. Overall the absorbance values of the cells which were treated with rSFV-IFN-β supernatant were significantly higher than those which received supernantant from rSFV1-EGFP and mock infected cells ($p<0.001$). At 12 h.p.i the rSFV1-EGFP supernatant sample exhibited a greater protective effect than the supernatant from the rSFV1-IFN-β infected cells but this was not significant. This graph shows a trend where rSFV10-E-IFN-β samples exhibited a greater protective effect than the rSFV1-IFN-β samples at time points 12, 24 and 36 h.p.i. Overall the greatest protective effect was seen 36 h.p.i. Two-way ANOVA analysis and Bonferroni post-tests were used for statistical comparison between the treatment groups. The experiment was carried out three times. Each bar represents the average result of the three experiments.

		Standard IFN-β	rSFV1- IFN-β	rSFV10-E-IFN-β	rSFV1-EGFP	Mock - infected
12h	dilution exhibiting 50% CPE	1:10000	1:1024	1:2048	1:2	Neat
	Abs@492nm	0.62	0.525	0.54	0.593	0.34
	IFN-β (U/ml)	1×10^6	102400	204800	200	-----
24h	dilution exhibiting 50% CPE	1:10000	1:2048	1:4096	Neat	Neat
	Abs@492nm	0.62	0.652	0.544	0.467	0.36
	IFN-β (U/ml)	1×10^6	204800	409600	100	------
36h	dilution exhibiting 50% CPE	1:10000	1:4096	1:4096	Neat	Neat
	Abs@492nm	0.62	0.6125	0.649	0.593	0.32
	IFN-β (U/ml)	1×10^6	409600	409600	100	--------
48h	dilution exhibiting 50% CPE	1:10000	1:32	1:64	Neat	Neat
	Abs@492nm	0.62	0.54	0.646	0.593	0.29
	IFN-β (U/ml)	1×10^6	3200	6400	100	-------
60h	dilution exhibiting 50% CPE	1:10000	1:32	1:32	Neat	Neat
	Abs@492nm	0.62	0.481	0.506	0.593	0.509
	IFN-β (U/ml)	1×10^6	3200	3200	100	-------

Table 2.1 Concentration of IFN-β (units of activity/ml) in the supernatant samples of rSFV-IFN-β infected cells

High levels of IFN-β expression from both rSFV1-IFN-β and rSFV10-E-IFN-β infected cells occurred up to 36 h.p.i. rSFV10-E-IFN-β infected cells gave greater expression at 12, 24 and 48 h time points. Levels reached 4×10^5 U/ml by 36 h.p.i but dropped back to 3200U/ml by 60 h. Minimal IFN-β production was seen by the rSFV1-EGFP infected cells, with levels not exceeding 100U/ml. In calculating the actual concentration of IFN-β in supernatant samples in U/ml, the dilution factor of each sample supernatant showing 50% viability according to their absorbance values was multiplied by a factor of 100. This factor of 100 is derived from the known concentration of commercial IFN-β required to show 50% viability after viral challenge. Commercial IFN-β was diluted 1:10000, from a concentration of 1×10^6 U/ml to 100U/ml, indicating that 100U/ml IFN-β is sufficient to allow 50% viability.

2.3.6 Quantitative comparison of IFN-β expression in BHK-21 and murine L929 cell lines by viral inhibition assay

BHK-21 and L929 cell lines were infected with rSFV-IFN-β particles and empty particles at MOIs of 1, 10, 100. Supernatant samples were taken 24 h post infection and assayed for IFN-β production by viral inhibition assay. Infection of the L929 cell line with rSFV-IFN-β particles exhibited greater expression of IFN-β at MOI 10 and 100 in comparison with infection of BHK 21 cells (Figure 2.22). Overall rSFV10-E expressing IFN-β showed higher levels of expression of IFN-β in both cell lines at MOI 10 and 100 with levels reaching 1×10^{8} U of activity/ml. Overall rSFV10-E-IFN-β expression gave levels up to eight times higher than those of the rSFV1-IFN-β. Infection with rSFV1 and rSFV10-E empty particle controls produced low levels of IFN-β in both cell lines at MOI 10 and 100 with levels reaching 6400U/ml but in comparison to rSFV-IFN-β infected cells, IFN-β production was minimal, up to 5×10^{4} times less. The empty particle control vectors produced low levels of IFN-β at MOI 1 (100U/ml) in L929 cells but not in BHK cells.

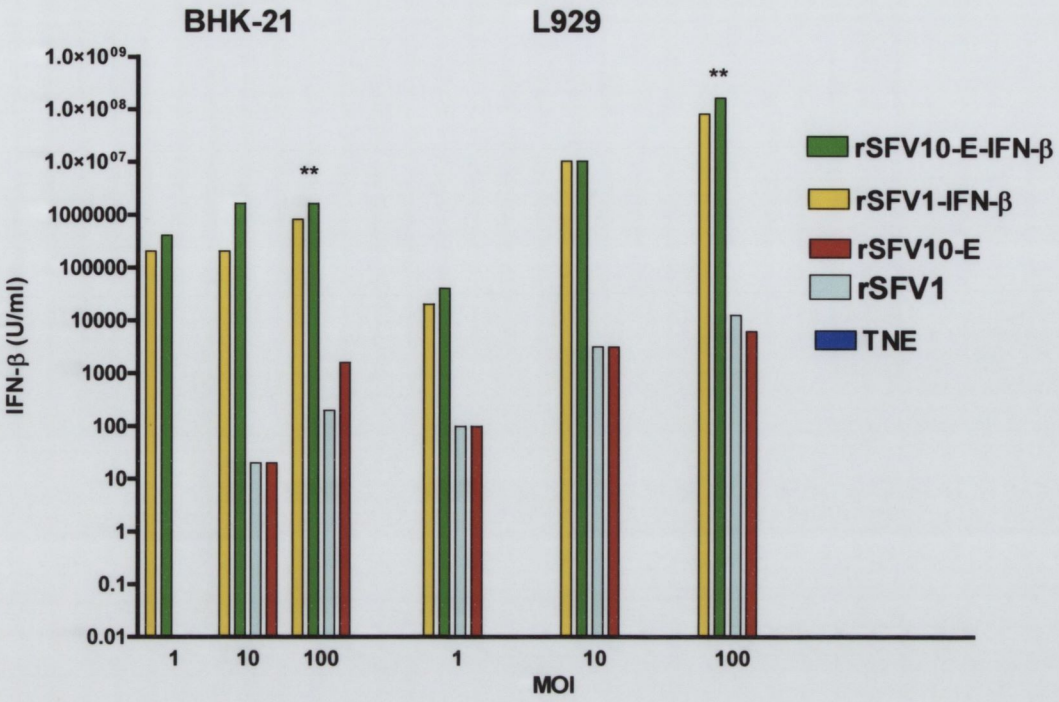

Figure 2.22 Comparison of *in vitro* expression of IFN-β from two different rSFV-IFN-β particle vectors in different cell lines

Overall rSFV-IFN-β infected L929 cells produced more IFN-β than BHK-21 cells. Both vectors produced significantly more IFN-β than the empty particle controls at MOI 100 ($p<0.01$). A trend was seen where rSFV10-E-IFN-β particles showed higher levels of IFN-β expression than rSFV1-IFN-β particles in both cell lines at MOIs 1, 10 and 100 with levels reaching 1×10^8 U/ml. Infection with rSFV1 and rSFV10-E empty particle controls produced low levels of IFN-β in both cell lines at MOIs 10 and 100 with levels reaching 6400U/ml. Both empty particle vectors produced low levels of IFN-β at MOI 1 (100U/ml) in L929 cells. This bar graph has a log scale on the y-axis and each bar represents triplicates of a single experiment which yielded the same result. Error bars cannot be calculated as this assay is not sensitive enough to detect differences between each well containing the same sample supernatant, it can only show a similar trend between the sample wells.

2.4 Discussion

One previous study used the SFV expression system to express the Th2 IL-10 cytokine to treat EAE an animal model of MS with promising results. Due to its antiproliferative ability and its previous success in the treatment of RRMS and EAE (Yasuda *et al.*, 1999; Yu *et al.*, 1996) we decided to construct an SFV vector that expresses IFN-β and examine the effects it had on EAE. IFN-β is a type I interferon and is secreted from fibroblasts in response to infection. IFN-β can also be produced by glial cells in the CNS. In this study high levels of IFN-β were detected day two post disease induction in the brains of SFV-A7 infected mice. IFN-β levels dropped as the SFV infection progressed because IFNs are one of the first cytokines to be expressed following virus infection and then they disappear very quickly (Isaacs and Lindenmann, 1957; Isaacs *et al.*, 1957). Maximal titres have been obtained from virally infected cells 12 –24 h post infection (Tovey *et al.*, 1974).

The SFV vectors chosen for cloning of IFN-β, pSFV1 and pSFV10-E have both been used extensively in vaccine and tumour therapy studies and more recently in gene therapy of the CNS. The more novel vector pSFV10-E contains a capsid translational enhancer sequence consisting of 34 a.a. of the original capsid protein, and a 2A autoprotease self-cleavage sequence from the FMDV, both located upstream from the MCS (Sjoberg *et al.*, 1994). The enhancer region drives expression of the cloned gene of interest, allowing increased expression of heterologous protein as part of a fusion protein with the capsid. The 2A autoprotease is responsible for cleaving the heterologous protein from the capsid enhancer protein. Initial IFN-β expression was detected in BHK-21 cells electroporated with rSFV-IFN-β particles using immunohistochemistry. Diffuse cytoplasmic staining was shown in electroporated cells. Qualitative comparison between expression of IFN-β from the two rSFV-IFN-β vectors was carried out using immunohistochemistry. BHK cells infected with rSFV10-E-IFN-β at an MOI of 1 showed more intense cytoplasmic staining 24 h.p.i than rSFV1-IFN-β infected cells.

A viral inhibition assay was used to verify expression and secretion of biologically active IFN-β from the rSFV-IFN-β vectors. This assay is based on the protective effect that IFNs elicit in cells when they are challenged with virus (Figure 2.6). IFN inducible cell proteins activate systems which result in inhibition of viral protein synthesis and degradation of viral mRNA and tRNA (Clemens *et al.*, 1993; Pestka *et al.*, 1987). In this assay L929 cells were treated with IFN-β containing cell supernatant from rSFV-IFN-β

infected cells, mixed with a standard amount of neutralizing anti-mouse IFN-β antibody, challenged with A7 virus and the degree of cytopathic effect is estimated by measuring cell viability. The inclusion of neutralizing anti-mouse IFN-β antibody serves as a control to ensure that it is indeed IFN-β which is exhibiting the protective effect and not other IFN types present in the cell supernatant (Meager *et al.*, 1987). Increasing levels of IFN-β are not bound by the antibody and they decrease the CPE of the SFV-A7 virus on the cells resulting in less cell death, which is determined by a MTS colorimetric assay (Buttke *et al.*, 1993). Standard IFN-β protein was included in each assay as a control. A set concentration of 100U/ml standard IFN-β was shown to exhibit 50% CPE and used as a means of comparison when analyzing the absorbance values of the sample wells. An initial study looked at the ability of the IFN-β in the supernatant sample to protect the cells from infection with A7 through their absorbance values, and showed a trend where the supernatant sample taken from rSFV10-E-IFN-β infected cells showed the highest number of viable cells after A7 challenge.

In this chapter IFN-β was successfully amplified from virally infected murine brain tissue and cloned into two SFV vectors, pSFV1 and pSFV10-E. Both rSFV-IFN-β vectors showed diffuse cytoplasmic expression of the cloned cytokine in BHK-21 cells, however, a trend was seen where infection with rSFV10-E-IFN-β particles led to greater quantitative expression of IFN-β in both BHK-21 and L929 cells at three different MOIs. This is due to the presence of the capsid translational enhancer sequence in rSFV10-E-IFN-β as previously discussed. In BHK-21 cells, IFN-β levels were highest at 36 h post infection (4 $\times 10^5$U/ml) and they dropped considerably by 48 h post infection (3200U/ml, Table 2.1). Infection of L929 cells with rSFV-IFN-β led to greater IFN-β production than infection in BHK-21 cells. Both L929 and BHK-21 cells produce some endogenous IFN-β upon infection, which is seen when these cell lines are infected with empty particle vectors. The levels produced are lower than those of rSFV-IFN-β infected cells, up to 5×10^4 times less ($p<0.01$). Previous studies have shown the ability of BHK-21 and L929 cells to produce IFN upon infection (Margolis *et al.*, 1972; Stanwick and Hallum, 1974). This study shows that IFN-β production is induced upon infection of BHK-21 and L929 cells with rSFV vector *in vitro*. This may prove problematic in *in vivo* studies if one cannot distinguish between secreted IFN-β, and endogenous IFN- β produced in response to the vector itself.

Chapter 3

In vivo expression and continuous treatment of experimental autoimmune encephalomyelitis with rSFV- IFN-β vectors

3.1 Introduction

EAE is a well-established animal model for EAE. Like MS, EAE is an inflammatory demyelinating disease of the CNS. EAE differs from MS in that it has been clearly defined as an autoimmune disease caused by myelin specific CD4+ T cells (Kuchroo *et al.*, 1991; Pettinelli and McFarlin, 1981; Zamvil *et al.*, 1985). These CD4+ T lymphocytes are of the Th 1 phenotype as defined by the specific pattern of cytokine production where the T cells secrete LT, IFN-γ and IL-2. T cell mediated immunological processes lead to the alteration of the BBB and enable recruitment of these effector cells together with other inflammatory cells, such as monocytes, components of the humoral response (B cells and complement factors) and CD8+ cells into the CNS (Kubes and Ward, 2000; Zang *et al.*, 2004).

The type of EAE induced is dependent on the immunization protocol, the animal strain and the antigen used and can occur as two different types of disease, a chronic relapsing form and a single acute episode. Immunization of animals with SCH (Baker *et al.*, 1990) is one of the methods to induce EAE but individual myelin antigens such as MBP, PLP, MOG and MAG are also frequently used (Amor *et al.*, 1993; Amor *et al.*, 1994; Amor *et al.*, 1996; Jerusalmi *et al.*, 2003; Okuda *et al.*, 1998). EAE pathology varies considerably between species. In mice, it is characterized by perivascular lymphocytic and monocytic infiltrates, white matter demyelination, and some limited remyelination (Raine, 1983; Raine, 1984).

Cytokines play an important role in the inflammation of the CNS characteristic of autoimmune disease such as MS and EAE. Two major types of Th cell responses have been described: Th1 cells produce IL-2, TNF-α and IFN-γ and Th2 cells produce IL-4, IL-5, IL-10 and IL-13. IFN-γ plays a central role in EAE as an inflammatory cytokine and is produced by the MHC class II restricted Th1 CD4+ T cells (Karpus and Swanborg, 1989; Martin and McFarland, 1995). IFN-γ in turn is a potent inducer of class II MHC antigen expression on various cells type in the CNS including APCs such as astrocytes, infiltrating macrophages and endothelial cells while blocking production of IL-10 by Th2 subset CD4+ cells (Billiau *et al.*, 1998; Colton *et al.*, 1992; Dore-Duffy *et al.*, 1996; Fierz *et al.*, 1985). The expression of Th2 cytokines such as IL-10 is associated with disease recovery (Bettelli *et al.*, 1998; Fillatreau *et al.*, 2002; Samoilova *et al.*, 1998). Anti-inflammatory Th2 and Th0 CD4+ T cells produce IL-10 and its functions include blocking activation of cytokine synthesis by Th1 cells, activated monocytes and NK cells. Much work has been

done on the treatment of different EAE models with immunodulatory cytokines such as IL-4, IL-10, IL-13, IL-23 and TGF-β (Young *et al.*, 2000). These cytokines have been administered systemically, via intramuscular injection of naked DNA plasmids (Piccirillo and Prud'homme, 1999; Piccirillo and Prud'homme, 2003; Prud'homme and Piccirillo, 2000) or via DNA and RNA viral vectors with varying degrees of success (Broberg *et al.*, 2001; Furlan *et al.*, 1998; Jerusalmi *et al.*, 2003; Shaw *et al.*, 1997). Gene therapy administration offers many advantages over traditional means of administration. After gene transfer, these mediators can be produced at relatively constant, non-toxic levels and sometimes in a tissue-specific manner, overcoming limitations of protein administration.

Previous studies have utilised viral vectors expressing cytokines to treat different models of EAE with varying degrees of success. Replicative and nonreplicative herpes simplex virus type 1 vectors have been engineered to administer IL-4 and IL-10 to treat EAE, with IL-4 treatment showing more success (Broberg *et al.*, 2001; Furlan *et al.*, 1998). Adenoviral vectors have also been used to express IL-10 in the treatment of EAE but with little success (Cua *et al.*, 2001). Retroviral vectors expressing IL-4 and IL-10 have shown more success in EAE treatment than the adenoviral vectors (Croxford *et al.*, 2001; Shaw *et al.*, 1997) where retroviral administration of IL-10 proved to be more effective than adenoviral administration. More recently the rSFV split helper expression system has been successfully used to express IL-10 in the treatment of EAE (Jerusalmi *et al.*, 2003).

Studies utilising rIFN-β protein to treat mouse EAE have yielded both positive and negative results (Luca *et al.*, 1999; Triantaphyllopoulos *et al.*, 1998; van der Meide *et al.*, 1998; Yasuda *et al.*, 1999; Yu *et al.*, 1996). As discussed in the previous chapter IFN-β exerts its therapeutic effect by decreasing MHC class II expression on APCs, inhibiting T cell activation and decreasing the release of inflammatory cytokines. Successful treatment of MS and EAE with IFN-β has been shown to be both time and dose dependent. If the long term dose of IFN-β1b received by MS patients was reduced from 250μg every 48 h to 30μg IFN-β1a every week, only 23% remained relapse free compared to 79% at the higher dose and frequency (Barbero *et al.*, 2004). Similarly, subcutaneous administration of rIFN-β dose dependently inhibited EAE in Lewis rats, provided the treatment was continued for three weeks (Ruuls *et al.*, 1996). One previous study has utilised a viral vector expressing IFN-β to treat EAE induced in Biozzi ABH mice by injection of SCH. Mice received intracranial injections of a retroviral vector expressing murine IFN-β encapsulated in a DNA-liposome complex during the effector stage and mice showed a

reduction in clinical disease (Triantaphyllopoulos *et al.*, 1998). Other studies have shown that IFN-β has no efficacy in inhibiting EAE induced in SJL mice with PLP 139-151 peptide (Luca *et al.*, 1999). IFN-γ production was inhibited and IL-4 and IL-10 production stimulated, resulting in a Th2 response, but no improvement was observed in severity of EAE.

In this chapter rSFV-IFN-β particles were used to treat a chronic model of EAE induced in C57/Bl 6 mice with MOG 35-55. A preliminary study was done to examine the duration of IFN-β expression from rSFV-IFN-β particles in the CNS following i.n. administration due to the short half life of the interferons. This allowed a treatment regime to be selected which allowed a constant level of IFN-β to persist in the CNS between treatment days over the duration of the experiment. There are three different stages of EAE – the induction, the effector and the recovery stages. Due to university ethical restrictions this EAE model was not allowed to relapse and could only be monitored for 30 days. Each disease phase was defined around this 30 day period. The induction stage occurs between days 0-11 when animals are not yet showing signs of clinical disease. During the effector stage, between days 12-17, the animals are beginning to display symptoms of clinical disease. At this point the T cell response to the encephalolithogenic peptide is fully developed but significant cell accumulation in the CNS has not occurred and the animals experience a progressive clinical disease. From approximately day 19 or 20 onwards, the animals begin to show signs of recovery. By day 30, the untreated EAE animals have almost completely recovered. Treatments were administered continuously during the induction, the effector and the recovery stages up to day 27 before the animals relapse. T cell responses were measured in response to stimulation with MOG 35-55 peptide *ex vivo* and typical EAE lesions present in the brain and spinal cord were assessed pathologically. Cytokines levels were also examined in the brains of animals post disease induction and treatment with rSFV-IFN-β particles.

3.2 Materials and methods

3.2.1 Materials

3.2.1.1 Mice

Specific pathogen free female 6-8 week old C57/Bl 6 mice were obtained from Harlan (Bicester, UK) and were maintained as described in section 2.2.1.3.

3.2.1.2 Particle Production

As described in section 2.2.1.5.

3.2.1.3 EAE induction

Encephalolithogenic MOG 35-55 peptide (MEVGWYRSPFSRVVHLYRNGK) was obtained from Genemed Synthesis Inc., CA, USA. Peptide was made with a hydroxl group. Incomplete Freund's adjuvant (IFA), *Mycobacterium tuberculosis* and *Mycobacterium butyricium* were from DIFCO (Detroit, USA). Pertussis Toxin came from CAMR (UK). A Clifton ultrasonic bath model DU-4 was obtained from Laboratory Instruments & Supplies Ltd. (Meath, Ireland).

3.2.1.4 Splenocyte stimulation assays

Lyophilized Concanavalin A (5mg/ml) was from Sigma (UK). HBSS and RPMI 1640 medium were both from Gibco (UK). RPMI culture medium was supplemented with 10% (v/v) heat inactivated FBS, 2% (v/v) Hepes, 1% (v/v) glutamine/penicillin streptomycin, 1% (v/v) non-essential amino acids and 50μm β-mercaptoethanol. All were from Gibco (UK). RBC lysis buffer was from BD biosciences. Splenocyte freezing medium was prepared from 90% heat inactivated FBS and 10% DMSO from Sigma-Aldrich (UK).

3.2.1.5 Enzyme Linked ImmunoSorbant Assay

ELISA sets for measuring IFN-γ and IL-10 were from BD Biosciences. An ELISA set for measuring murine IFN-β was from PBL (USA).

3.2.1.6 Histopathological studies

10% formal saline was obtained by diluting 38% formaldehyde solution 1:10 in 1L distilled water and adding 9 g of Sodium Chloride (Sigma). Paraformaldehyde (PFA), haematoxylin harris, eosin aqueous solution and DPX solutions were from BDH Ltd (Poole, UK).

3.2.1.7 Miscellaneous

Syringes (20ml, 10ml and 1.0ml) and needles, (21G), were from Terumo (Leuven, Belgium). 1ml insulin syringes were from BD biosciences. 0.25 M Tris-HCl buffer was prepared by dissolving 6.06g of Tris in 200ml of sterile distilled water, pH lowered to 8.0 with HCl, and final solution filter sterilized. Bradford protein reagent and BSA protein standards were from Sigma (UK). Homogenizer type RZR 1 was from Heidolph (Germany). 40μm cell strainers were from Falcon. 96 well flat bottomed ELISA plates and 24 well culture plates were from NUNC (Denmark).

3.2.2 Methods

3.2.2.1 Particle production

rSFV-IFN-β, rSFV1 and rSFV10-E particles were prepared and titrated as previously described in section 2.2.6.

3.2.2.2 Intranasal inoculation with rSFV-IFN-β particles

Five groups of nine C57/Bl mice were inoculated intranasally with 10^7 IU of rSFV1-IFN-β, rSFV10-E-IFN-β, rSFV1 and rSFV10-E particles in 20μl TNE, and with TNE alone by placing a droplet on each nostril. Three mice from each group were sampled 24, 48 and 72 h post inoculation, and their olfactory bulbs, brains and spinal cords were removed. Upon excision each tissue was pooled and homogenized in 2ml of Tris-HCl (pH 8.0) buffer in a 15ml glass tube. Homogenized solution was transferred to a fresh 15ml tube, and centrifuged (3500 rpm (3185g) 10 min, 4°C). Clear supernatant was transferred to a clean tube and stored at -70°C.

3.2.2.3 Protein assays

Bradford reagent was used to determine protein concentration of homogenised sample. The assay consists of mixing 1 part of protein sample with 30 parts of the Bradford reagent. A serial dilution of a protein standard (BSA) solution was used to generate a standard curve. To each well of a 96 well plate, 5 µl of each protein and standard were added in duplicate. 250µl of Bradford reagent was then added to each well containing protein. Samples were mixed for 30 sec, incubated at RT for 5 to 45 min, and absorbance read at 595 nm in a spectrophotometer. Concentrations were recorded as mg/ml of total protein.

3.2.2.4 Detection of IFN-β in tissue homogenates

Homogenized tissue samples were tested for the presence of IFN-β by use of a capture ELISA specific for murine IFN-β according to manufacturer's protocol and values were expressed in pg per mg of total protein. The limits of detection range from 15.6pg to 1000pg/ml. Cytokine levels were compared using the one-way analyses of variance (ANOVA) statistical test. When a statistically significant difference between groups was calculated, the Bonferroni's multiple comparison test was used to compare between individual pairs of groups. All statistical tests were calculated using Prism 4.0 (GraphPad software Inc.).

3.2.2.5 EAE induction

A total of 70 C57/Bl6 were induced with EAE. To allow for loss of adjuvant/peptide mix, enough mix for 100 mice was prepared. A working stock was of adjuvant and bacteria was prepared by dissolving 16.0mg of *Mycobacterium tuberculosis* and 2.0mg of *Mycobacterium butyricium* in 4.0ml of incomplete Freund's adjuvant (IFA). This stock was kept for 7 days at 4°C and used for a booster immunization. An enriched adjuvant was prepared by mixing 1.0ml of freshly prepared working stock with 11.5ml of IFA, twice. Each mouse was immunized with 100µg of the peptide emulsified in enriched adjuvant. 5.0mg of peptide was dissolved in 7.5ml of PBS, and mixed with 7.5ml of enriched adjuvant in a 20ml plugged syringe. This was repeated to allow enough mixture for 100 mice. Solutions were sonicated for 10 min at RT in an ultrasonic bath, and mixed with a 2ml syringe until an emulsion was formed. A CSF needle was used to fill 1ml syringes with freshly prepared emulsions. Needles were glued to a 1ml syringe prior to

use. Each mouse was immunized s.c. with 0.15ml of emulsion into the femoral region. Mice received a booster immunization 7 days later. Each animal also received 200ng of Pertussis Toxin in 0.1ml of PBS by i.p. inoculation on the first day of immunization and then 24 h later. When the immunization was repeated seven days later, animals received PT at the same times. Animals were monitored daily and disease severity graded on a neurological scale of 0 to 6 with 0.5 points for intermediate clinical findings. For ethical reasons set by the university the animals were not allowed to experience a relapse, therefore disease was monitored for thirty days only. Score design was as follows: 0, no clinical sign; 1, limp tail and feet; 2, impaired righting reflex; 3, partial hind limb paralysis; 4, total hind limb paralysis; 5, moribund; 6, death. The Mann Whitney test was used for statistical analyses (GraphPad Prism 4.0) on EAE progression after the onset of disease. Weight loss was also monitored on a daily basis.

3.2.2.6 Treatment with IFN-β particles

Groups of 14 mice were treated with rSFV1- IFN-β, rSFV10-E- IFN-β, rSFV1 or rSFV10-E particles, or TNE buffer alone. Mice received nine treatments, starting day 3 and every third day afterwards until day 27 post disease induction. In all treatments with rSFV particles, animals received 10^7 IU of rSFV particles in 20 µl TNE intranasally as described in section 3.2.2.2. Two mice from each of the five groups were sampled on days 28 and 32 post disease induction. Mice designated for pathological studies were perfused and spleens were excised.

3.2.2.7 Paraffin embedding and sectioning for pathology

Mice were anaesthetized with halothane and perfused via the left ventricle with PBS followed by 10% formal saline for 5 min. 10 mice were perfused on day 28 p.d.i. Excised brains and spinal cords were allowed to fix overnight in 10% formal saline prior to paraffin embedding. Samples were dehydrated in a graded series of alcohol washes; 50% (vol/vol) alcohol for 60 min, 70% (vol/vol) alcohol for 60 min and 90% (vol/vol) alcohol for 60 min, before being placed into 2 absolute alcohol washes, for 40 min each. Samples were then immersed in a 1:1 solution of absolute alcohol: xylene solution, for 60 min, before being washed 3 times in absolute xylene, for 40 min each. This was followed by 4 individual immersions in paraffin wax, for 40 min each. Tissues were then mounted onto

blocks prior to sectioning. Four μm thick paraffin sections were prepared using a microtome and dried overnight at 37°C in an oven.

3.2.2.8 Haematoxylin and eosin staining for routine histology

Sections of paraffin embedded brains and spinal cords were routinely stained with H&E. Dried sections were dewaxed with 3 X 10 min washes in 100% xylene and subsequently rehydrated through 100%, 95%, 70% ethanol for 5 min each followed by dH_2O. Sections were then placed in Harris's haematoxylin for 10 min, rinsed under running water until cleared, differentiated in 1% acid alcohol and blued up by dipping 3 times in 3% ammonia water. After a subsequent wash under running tap water, sections were counterstained in 1% dichromate eosin for 2 min and washed under running tap water for a further 5 min or until cleared. Stained sections were then dehydrated and mounted using DPX by covering the section with a coverslip without air bubbles. Paraffin embedding, sectioning and staining were performed by Ms. Alex Whelan-Buckley, Veterinary Pathology Laboratory, University College Dublin.

3.2.2.9 Pathological analysis

Sections of brains and spinal cords were examined blind and given an estimated score for the parameters of EAE (i.e. myelin vacuolation, axonal degeneration, leucocytic infiltration, glial activation). Axonal degeneration was determinated by examination of areas of fibres.... Lesions were graded using a semi-quantitative five point scale. Mild localized lesions received a rating of 1 and severe, diffuse lesions received a rating of 5. Grade 1 lesions were confined to the spinal cord and grade 5 lesions involved brain stem areas and spinal cord. Pathological analysis were performed by Prof. Brian Sheahan, Veterinary Pathology Laboratory, University College Dublin.

3.2.3.0 Preparation and freezing of splenocytes

Spleens were added to 5.0ml of HBSS and then filtered through a 40μm cell strainer, using the plunger of a 10ml syringe, into a 50ml sterile falcon tube. The cell strainer was further rinsed with 10ml HBSS to ensure no cellular debris remained attached, increasing the volume of the cell suspension to 15ml. The spleens were then centrifuged at 1500rpm (1365g) for 10 min at 4°C, supernatant discarded and the pellets resuspended in 2ml of RBC lysis buffer for 5 min to allow haemolysis to occur. 35ml HBSS was then

added and the tubes were centrifuged again for 10 min at 1500rpm (1365g). The pellets were resuspended in 1ml of freezing medium and passed through another 40μm strainer to remove any remaining debris. The cell suspensions were then cryopreserved under liquid nitrogen.

3.2.3.1 Splenocyte stimulation assay

Frozen splenocytes were thawed at 37°C and resuspended in 9ml RPMI 1640 medium. Cells were counted by trypan blue exclusion assay using a haemocytometer. Cells were diluted 1:10 in trypan blue and 10μl was loaded into the gap between the haemocytometer and coverslip. The clear viable cells were counted in the four main quadrants and the average number of viable cells per ml were calculated. $5x10^5$ cells were seeded per well of a 24-well plate and duplicate wells were stimulated with either 5 or 10 μg MOG 35-55 peptide. Untreated wells and wells treated with 5μg Concanavalin (Con) A were included as controls. The plate was incubated at 37°C, 5% CO_2 for 72 h. Samples were centrifuged at 14000rpm (10000g), 4°C to remove cell debris, aliquoted and frozen at –70°C until use.

3.2.3.2 T cell responses ex vivo

Levels of IFN-γ and IL-10 present in stimulated splenocyte supernatant samples were measured using the OptEIA mouse IFN-γ and mouse IL-10 ELISA sets according to the manufacturer's protocol. Two way ANOVA analysis and Bonferroni post-tests were used for statistical comparison between treatment groups.

3.2.3.3 Detection of cytokines in brain homogenates

Homogenized brain samples were tested for the presence of IFN-γ and IL-10 by use of capture ELISA kits according to the manufacturer's protocol and values were expressed in pg per mg of total protein as described in sections 3.2.2.3 and 3.2.2.4. Cytokine levels were compared using the one-way analyses of variance (ANOVA) statistical test. All statistical tests were calculated using Prism 4.0 (GraphPad Software Inc.).

3.3 Results

3.3.1 Duration of IFN-β expression *in vivo* following i.n. administration of rSFV-IFN-β particles

C57/Bl 6 mice were intranasally inoculated with rSFV10-E-IFN-β particles and rSFV10-E empty particle controls, and TNE alone. After 24, 48 and 72 h olfactory bulbs, brains and spinal cords were excised, pooled and homogenized, and levels of IFN-β in each tissue type were measured at each time point using a mouse IFN-β ELISA kit. The levels of IFN-β were expressed in pg per milligram of total protein. Bradford protein reagent was used to use to measure the levels of protein. Overall more IFN-β was present in the olfactory bulbs and the spinal cords than the brains of the animal. Animals receiving rSFV10-E-IFN-β expressed significantly more IFN-β in the olfactory bulbs 24 hrs post inoculation compared to the TNE and empty particle controls ($P<0.001$) (Figure 3.1). Little difference is seen in the levels of IFN-β present in the olfactory bulbs of each group at 48 and 72 h post inoculation. At 48 h significantly more IFN-β was present in the brains of the rSFV10-E-IFN-β treated animals than the TNE and empty particle treated ($p<0.05$) (Figure 3.2). A peak is seen in the level of IFN-β present in the cords of the rSFV10-E-IFN-β treated animals 48 h post inoculation reaching 50 pg/mg total protein ($p<0.001$), but this decreases dramatically by 72 h post inoculation to levels comparable with the empty particle treated and TNE treated animals (Figure 3.3). rSFV10-E empty particle produced low levels of endogenous IFN-β in all tissues of the CNS .

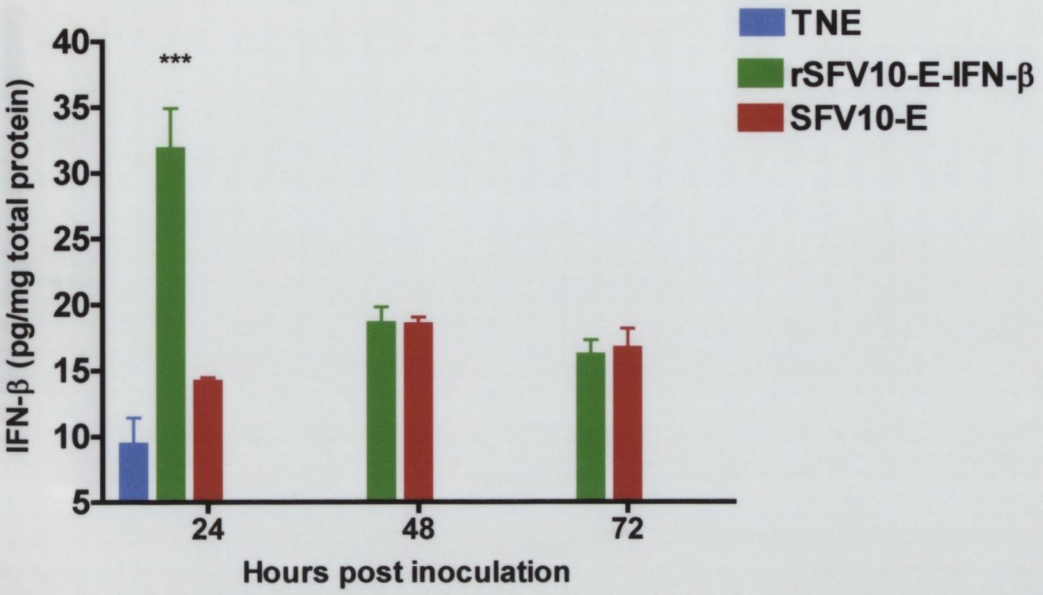

Figure 3.1 Levels of IFN-β present in the olfactory bulbs post i.n. inoculation with rSFV-IFN-β particles

Overall levels of IFN-β were expressed in pg/mg of total protein. Significantly more IFN-β was present in the olfactory bulbs of rSFV10-E-IFN-β treated animals 24 h post inoculation in comparison to the TNE and empty particle treated controls ($p<0.001$). These levels had decreased by 48 h post inoculation to 20pg/mg protein and remained low at 72 h post inoculation. rSFV10-E treated animals produced endogenous IFN-β at all time points. Statistical comparison was carried out using Two-way ANOVA and Bonferroni post-tests.

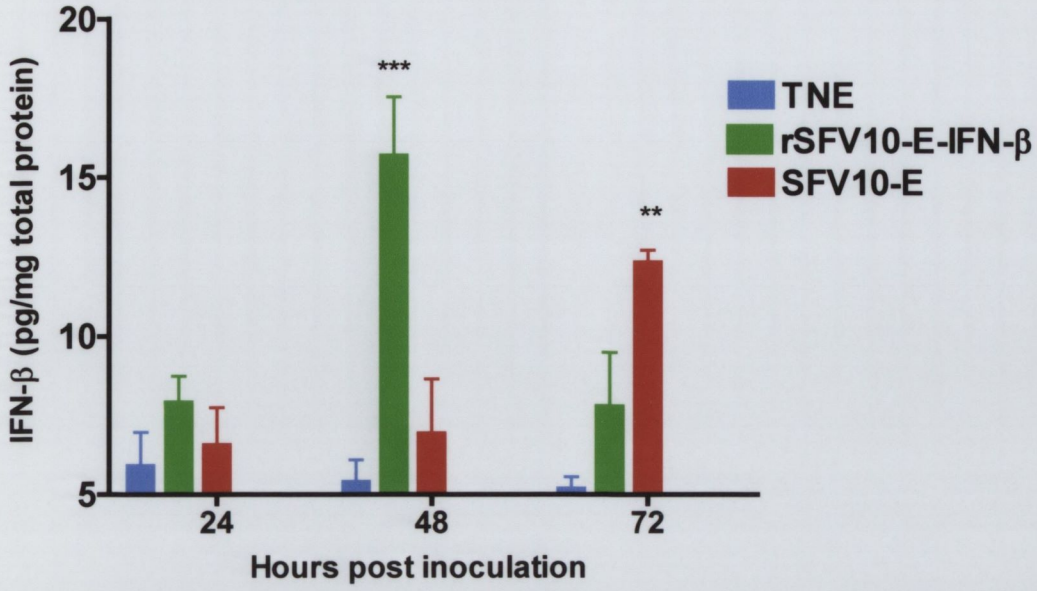

Figure 3.2 Levels of IFN-β present in the brains post i.n. inoculation with rSFV-IFN-β

Overall levels of IFN-β were expressed in pg/mg of total protein. Minimal IFN-β was present in the brains of all groups 24 h post inoculation. Significantly more IFN-β was present in the brains of rSFV10-E-IFN-β treated animals 48 h post inoculation in comparison to the TNE and empty particle treated controls ($p<0.001$). The brains of empty particle control animals produced significantly more IFN-β than the rSFV10-E–IFN-β treated and TNE treated animals 72 h post inoculation ($p<0.01$). Statistical comparison was carried out using Two-way ANOVA and Bonferroni post-tests.

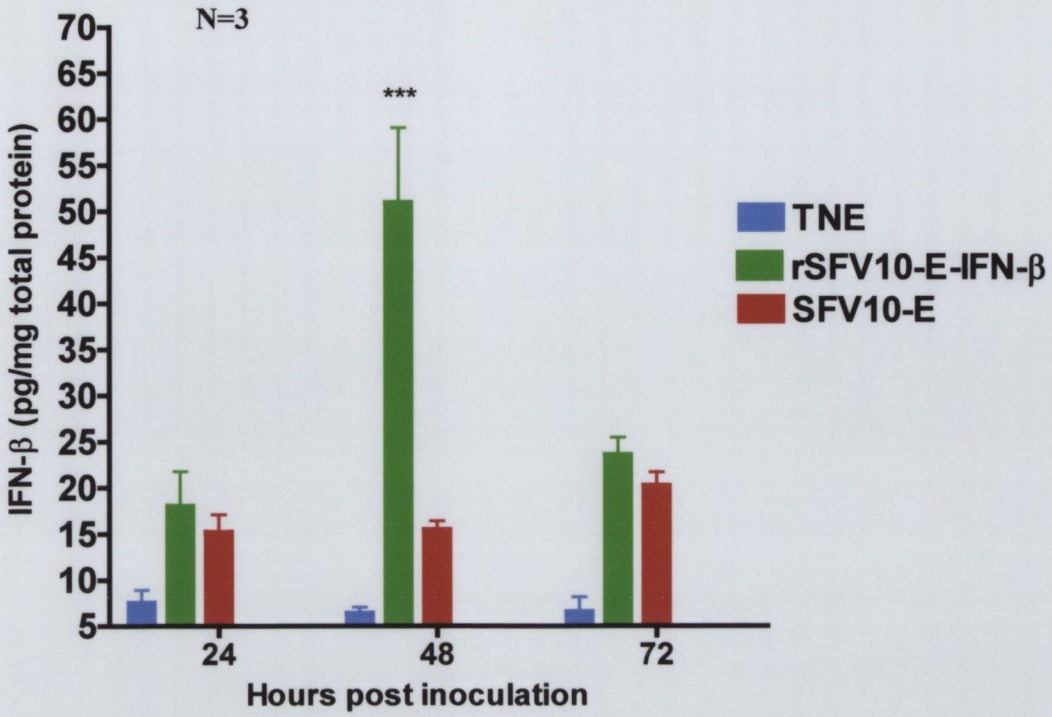

Figure 3.3 Levels of IFN-β present in the spinal cord post i.n. inoculation with rSFV-IFN-β

Overall levels of IFN-β were expressed in pg/mg of total protein. Background levels of IFN-β were present in the cords of TNE animals at all times. Significantly more IFN-β was present in the spinal cords of the rSFV10-E-IFN-β treated animals 48 h post inoculation compared to the control animals ($p<0.001$). This level had dropped by 72 h to a level similar to the empty particle controls. Statistical comparison was carried out using Two-way ANOVA and Bonferroni post-tests.

3.3.2 Effect of continuous rSFV-IFN-β treatment on the course of EAE throughout the induction, effector and recovery stages

EAE was induced in C57/Bl 6 mice by s.c. injection with MOG 35-55 peptide as described in section 3.2.2.5. Mice received intranasally administered rSFV1-IFN-β, rSFV10-E-IFN-β particles, rSFV1, rSFV10-E empty particles and TNE buffer alone at nine time intervals (days 3, 6, 9, 12, 15, 18, 21, 24, 27). Treatment with rSFV-IFN-β particles did not ameliorate paralytic disease as expected but enhanced severity compared to TNE controls. Treatment with both rSFV1-IFN-β and rSFV10-E-IFN-β increased disease clinical score significantly compared to TNE buffer alone ($p<0.05$) (Figures 3.4A and 3.5A) from day 19 onwards. These results were confirmed by analysis of weight gain where rSFV1-IFN-β and rSFV10-E-IFN-β treated animals experienced significantly greater weight loss overall ($p<0.05$ and $p<0.0001$ respectively) than the TNE control animal (Figures 3.4B and 3.5B). In the study using rSFV1-IFN-β, TNE and empty particle controls experienced similar start weights. In the rSFV10-E-IFN-β study, the rSFV-IFN-β and the empty particle groups experienced similar start weights. Empty particle controls also exacerbated disease compared to the TNE controls. rSFV10-E particles significantly enhanced disease severity compared to the TNE controls ($p<0.05$). rSFV-IFN-β and empty particle treated animals all experienced a similar degree of disease severity and earlier disease symptoms compared to the TNE treated animals. rSFV10-E-IFN-β treated animals experienced a marginally less severe disease than the rSFV1-IFN-β treated animals in comparison to the TNE animals. Table 3.1 summarizes the main findings from the treatment regimes. All rSFV-IFN-β and empty particle treated groups experience a similar maximum EAE score of 2.8-3.2 with the TNE animals experiencing a score 2.3.

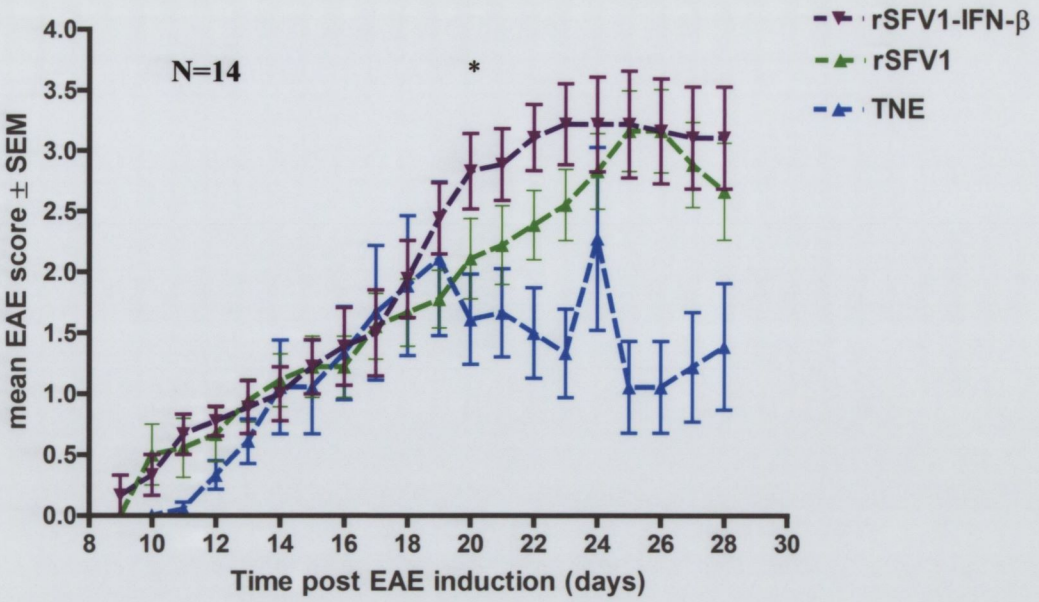

A

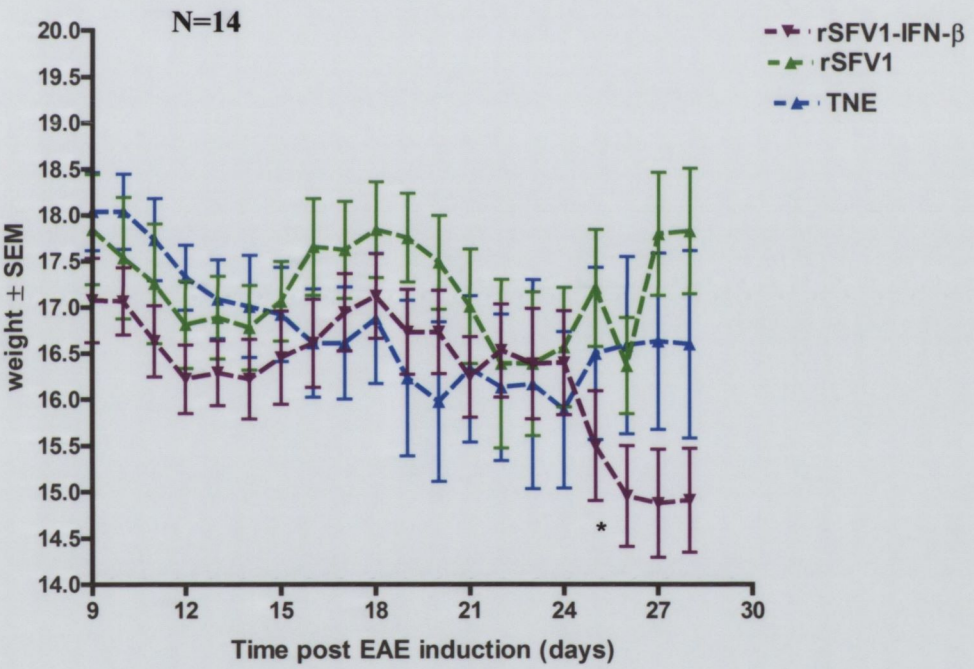

B

Figure 3.4 Effect of nine rSFV1-IFN-β treatments on EAE score and weight

Continuous treatment with rSFV1-IFN-β exacerbated the disease model significantly compared to TNE controls as indicated by higher average clinical scores ($p<0.05$) from day 19 onwards and weight loss ($p<0.05$). TNE and empty particle controls experienced similar start weights. rSFV empty particles also exacerbated disease severity compared to the TNE controls. Statistical analysis was performed using the non-parametric Mann-Whitney test, using Graph Prism 4.0 software.

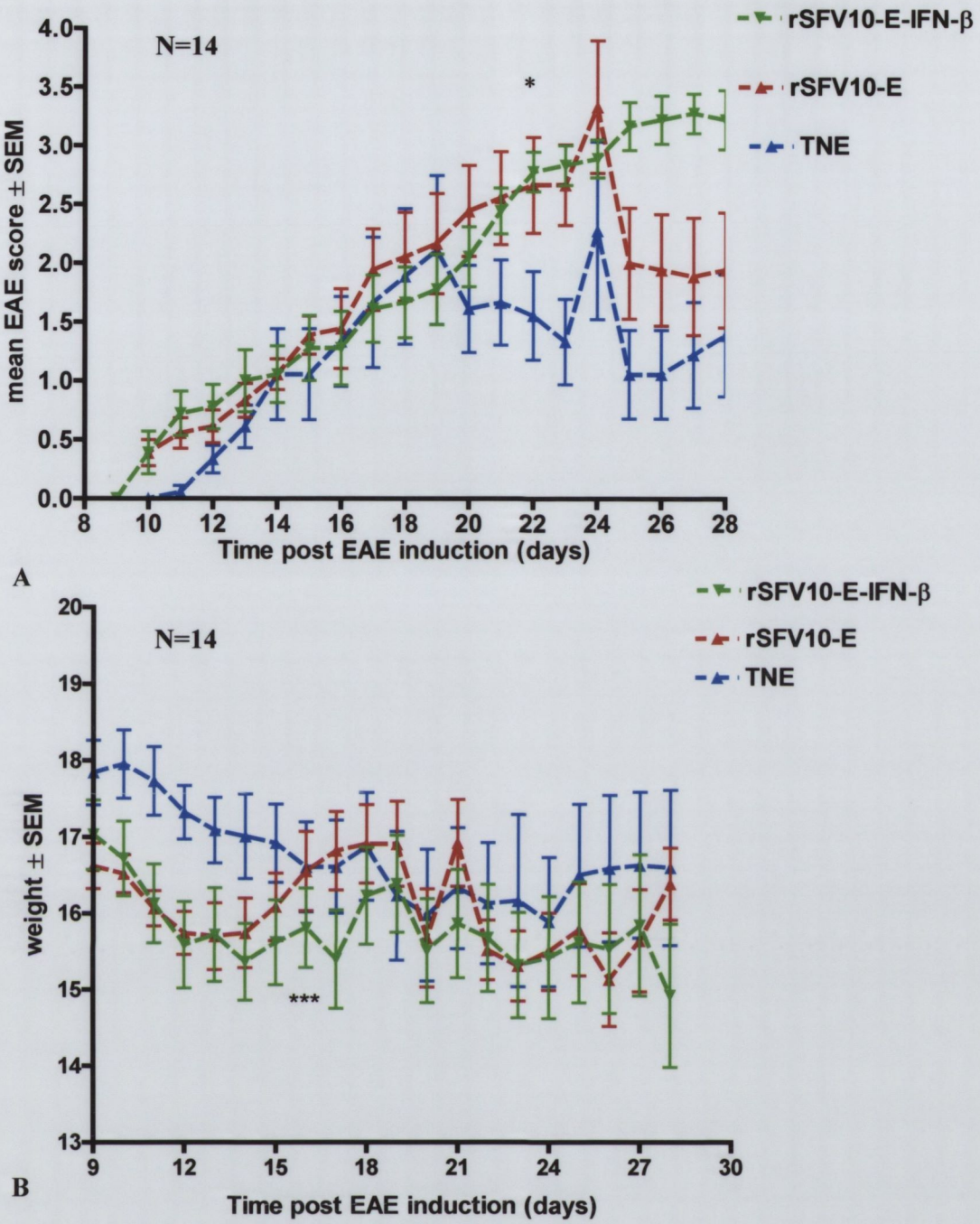

Figure 3.5 Effect of nine rSFV10-E-IFN-β treatments on EAE score and weight

Continuous treatment with rSFV10-E-IFN-β exacerbated the disease model significantly indicated by higher average clinical scores ($p<0.05$) from day 19 onwards, and weight loss ($p<0.0001$) compared to the TNE treated controls (A) and (B). The rSFV-IFN-β and the empty particle groups experienced similar start weights. Treatment with empty particle control also exacerbated clinical disease ($p<0.05$) and resulted in greater weight loss. Statistical analysis was performed using the nonparametric Mann-Whitney test, using Graph Prism 4.0 software.

Group	Maximum EAE score (mean ± SEM)	Day of onset (mean ± SEM)	EAE mice	P value vs TNE control	P value vs empty particle controls
rSFV1-IFN-β	3.2 ± 0.4	13.9± 0.46	9/14	0.0315*	n.s.
rSFV10-E-IFN-β	3.2 ± 0.5	15.2 ± 0.93	10/14	0.04*	n.s.
rSFV1	3.2 ± 0.3	13.4± 0.78	9/14	n.s.	n.a.
rSFV10-E	2.8 ± 0.3	14.0 ± 0.65	12/14	0.04*	n.a.
TNE	2.3 ± 0.7	16.6 ± 1.09	9/14	n.a.	0.04*

n.s., not significant

n.a., not applicable

** EAE score significantly worse compared to the TNE control

Table 3.1 Analysis of EAE mice after nine rSFV-IFN-β particle treatments

Mice received nine rSFV-IFN-β particles treatments on days 3, 6, 9, 12, 15, 18, 21, 24, 27 p.d.i. Both the rSFV1-IFN-β and the rSFV10-E-IFN-β particles made clinical disease significantly worse than treatment with TNE alone, with rSFV1-IFN-β making the disease marginally worse than rSFV10-E-IFN-β. Both empty particle vectors enhanced disease severity compared to TNE controls. rSFV10-E exacerbated disease to a significant level ($p<0.05$). Animals receiving either rSFV-IFN-β particles or empty particles reached a similar degree of disease severity and showed symptoms of clinical disease at an earlier time than the TNE controls.

3.3.3 Effect of continuous rSFV-IFN-β treatment on MOG35-55 T cell responses *ex vivo*

Three animals from each group were perfused day 28 post disease induction for pathological analysis. Their spleens were excised prior to perfusion, harvested and cultured in the presence or absence of MOG35-55 peptide (5 or 10 μg/ml), and in 5μg Con A as a positive control, for 72 h to analyze responsive IFN-γ or IL-10 producing T cells. Minimal levels of IFN-γ were produced in the absence of peptide. Overall stimulation of splenocytes with MOG 35-55 peptide resulted in greater production of IFN-γ in rSFV-IFN-β treated and empty particle treated animals than in TNE animals in response to stimulation with MOG peptide with levels reaching 3000 pg/ml (Figure 3.6A). However, rSFV10-E-IFN-β treated animals produced significantly less IFN-γ compared to the rSFV1-IFN-β treated and rSFV10-E treated animals ($p<0.001$). IL-10 production was also measured and overall levels were lower than IFN-γ levels, not exceeding 350pg/ml (Figure 3.6B). rSFV10-E-IFN-β treated mice did produce significantly more IL-10 in response to stimulation with 10 μg MOG than the rSFV1-IFN-β treated, the empty particle treated and TNE controls ($p<0.001$), and also compared to the TNE controls in response to stimulation to 5 μg/ml MOG 35-55 ($p<0.01$). rSFV1-IFN-β treated animals produced significantly more IL-10 than TNE controls in response to stimulation with 10 μg ($p<0.01$). Splenocytes from rSFV1 treated animals did not produce much IFN-γ or IL-10 in response to MOG stimulation. Figure 3.7 shows the IFN-γ and IL-10 production from splenocytes of rSFV10-E-IFN-β and rSFV10-E treated animals only, in response to MOG stimulation.

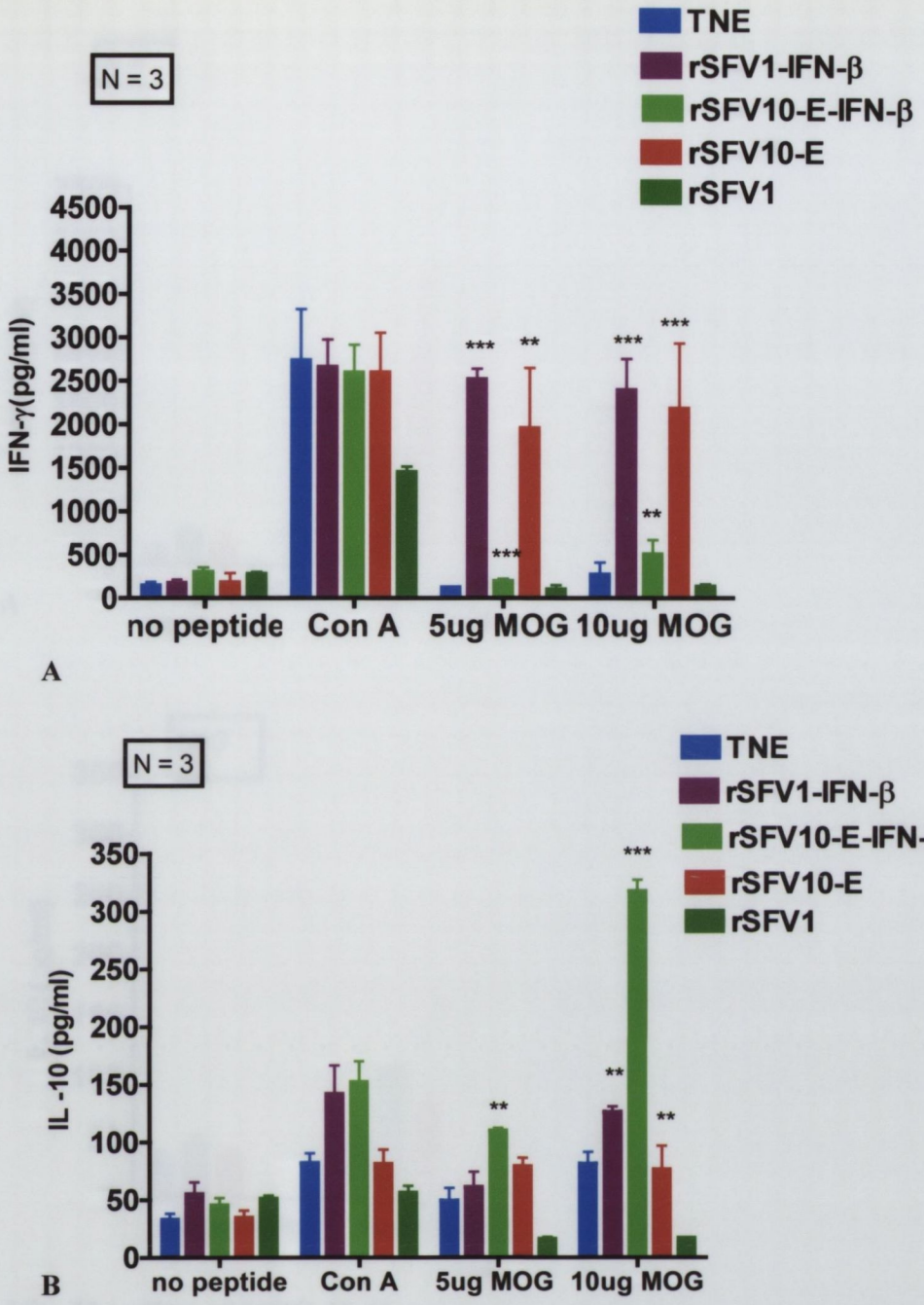

Figure 3.6 The effect of MOG 35-55 stimulation on production of IFN-γ and IL-10

Overall production of IFN-γ in response to MOG 35-55 stimulation was greater from splenocytes of rSFV-IFN-β and empty particle treated animals compared to TNE treated animals (A). This response was weaker in rSFV10-E-IFN-β treated animals compared to rSFV1-IFN-β and rSFV10-E treated animals ($p<0.01$) suggesting that rSFV10-E-IFN-β particles are downregulating the Th1 response and upregulating the Th2 response, indicated by the significantly higher IL-10 levels being produced by splenocytes in response to stimulation with 10μg MOG ($p<0.001$) (B). Statistical comparison was carried out using Two-way ANOVA and Bonferroni post-tests.

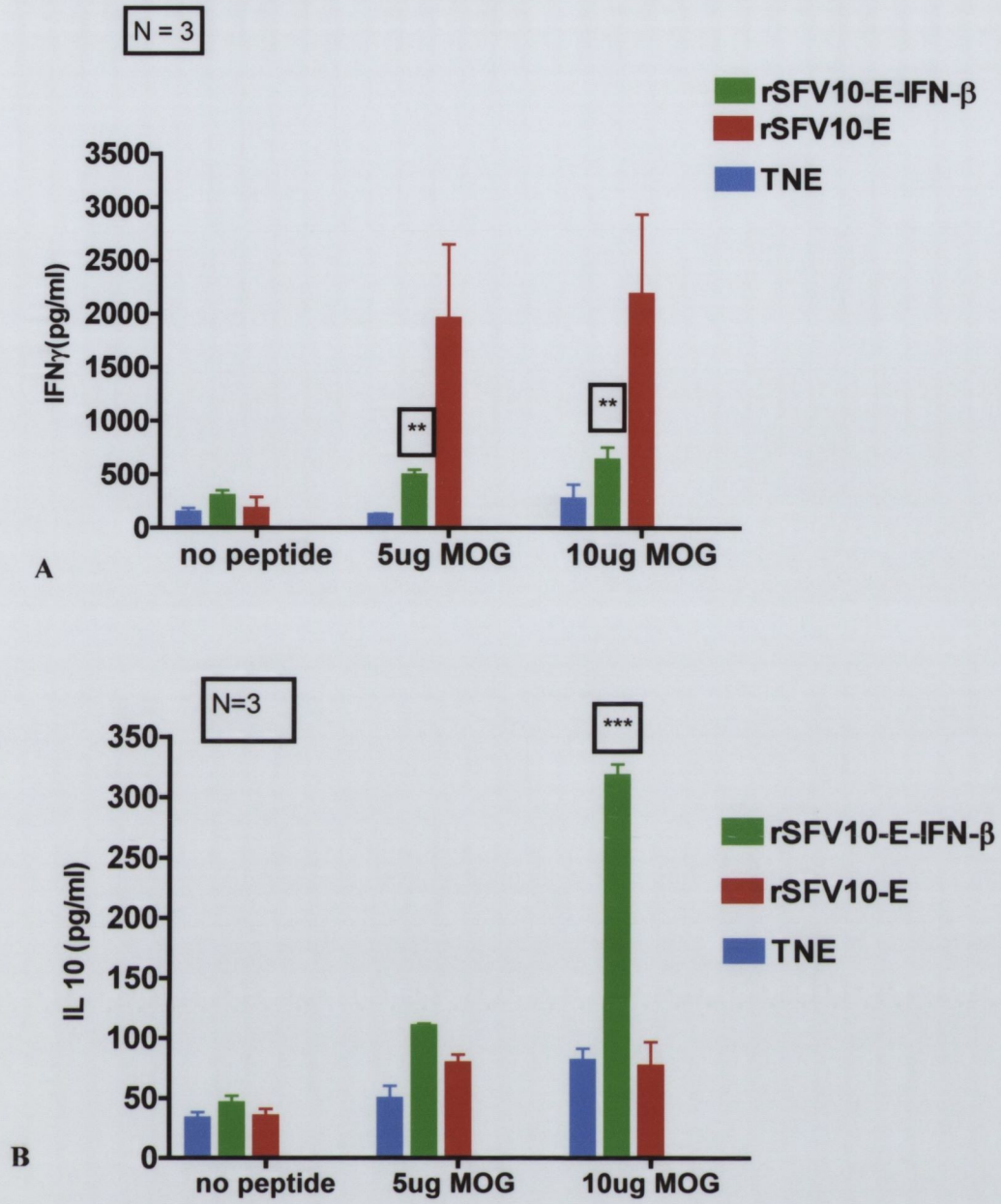

Figure 3.7 The effect of MOG 35-55 stimulation on production of IFN-γ and IL-10 from splenocytes *ex vivo* after continuous treatment with rSFV10-E-IFN-β particles

Overall production of IFN-γ in response to MOG 35-55 stimulation was greater from splenocytes of rSFV10-E-IFN-β and empty particle rSFV10-E treated animals compared to TNE treated animals. However this response was weaker in rSFV10-E-IFN-β treated animals compared to rSFV10-E treated animals ($p<0.01$). This suggests that rSFV10-E-IFN-β particles are downregulating the Th1 response while upregulating the Th2 response, shown by the significantly higher IL-10 levels being produced by splenocytes in response to stimulation with 10μg MOG ($p<0.001$). Statistical comparison was carried out using Two-way ANOVA and Bonferroni post-tests.

3.3.4 Pathological analysis

Lesions typical of EAE were found in the brains and spinal cords of animals on day 28 p.d.i and were assessed using a semi-quantitative five-point scale. A typical grade 3 EAE lesion in the spinal cord of a TNE-treated animal showing myelin vacuolation, axonal swelling, leucocytic infiltration and astrocytic swelling in the subpial white matter is illustrated in Figure 3.8. The severity of lesions correlated with the clinical scores (Table 3.2).

3.3.5 Cytokine production in brains of EAE animal following rSFV-IFN-β treatment

The level of IFN-γ and IL-10 production was minimal in the brains of animals sacrified day 32 post disease induction. Less IFN- γ was found in the brain homogenates of rSFV10-E-IFN-β treated animals than TNE treated, rSFV1-IFN-β and empty particle treated animals (Figure 3.9A). Minimal differences were seen in the levels of IL-10 found in the brain homogenates (Figure 3.9B).

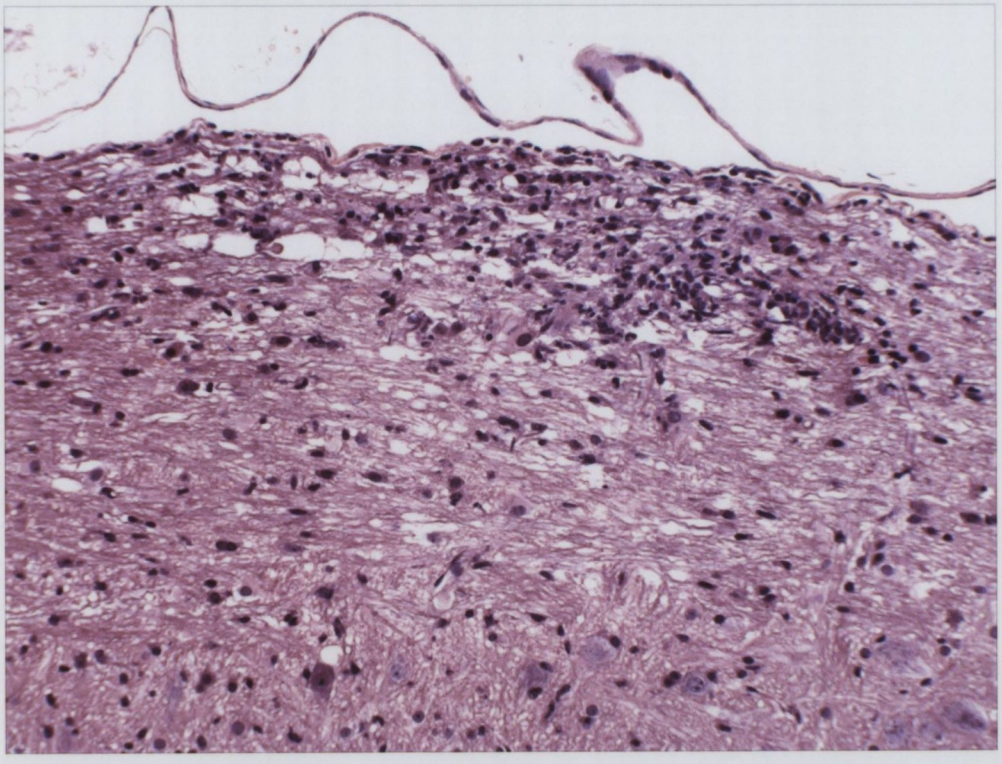

Figure 3.8 Typical grade 3 EAE lesion on sagital section of spinal cord

Following induction of EAE using MOG 35-55, mice were perfused day 28 and spinal cord sections were stained with H&E. This figure shows a longitudinal section of spinal cord showing myelin vaculoation, axonal swelling, leucocytic infiltration and astrocytic swelling in the subpial white matter (x400).

Group	Mouse No.	Clinical score	Pathology score	Total clinical score	Total pathology score
rSFV10-E-IFN-β	1	3.5	4+	6	8
	2	2.5	4+		
rSFV1-IFN-β	1	3	4+	3	7
	2	0	3+		
rSFV10-E	1	1.5	4+	4	9
	2	2.5	5+		
rSFV1	1	4	4+	6	8
	2	2	4+		
TNE	1	2.5	3+	3.5	6
	2	1	3+		

Table 3.2 Comparison of clinical and pathological scores

A trend was seen where clinical scores and pathology scores correlated at this time. Overall little difference was seen in both clinical and pathology scores between the treatment groups. Brains and spinal cords were examined blind and given an estimated score for the parameters of EAE (i.e. myelin vacuolation, axonal degeneration, leucocytic infiltration, glial activation). A semi quantitative system based on a scale of one plus for small isolated focus lesions to five plus for very diffuse and severe lesions was employed.

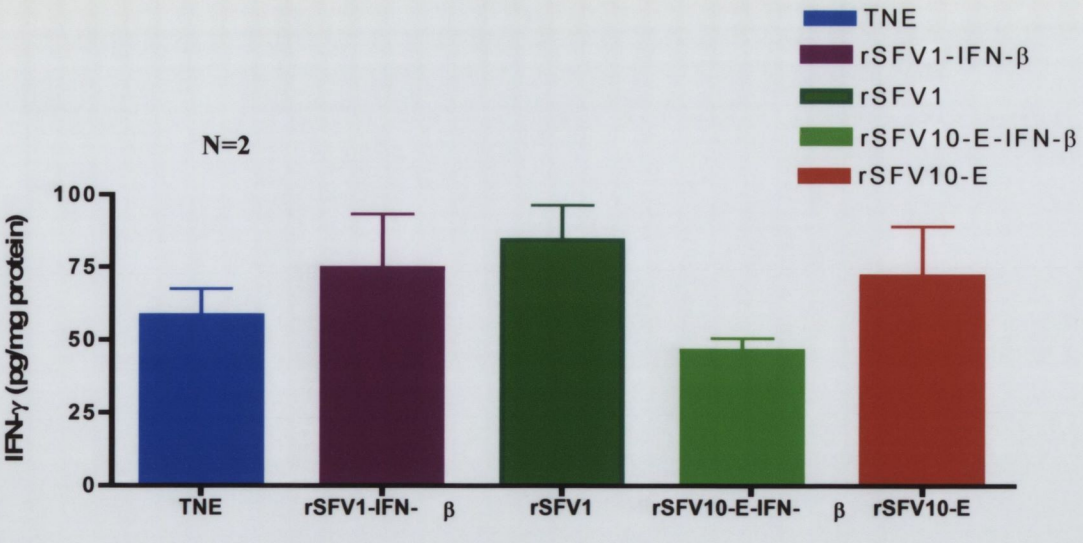

A

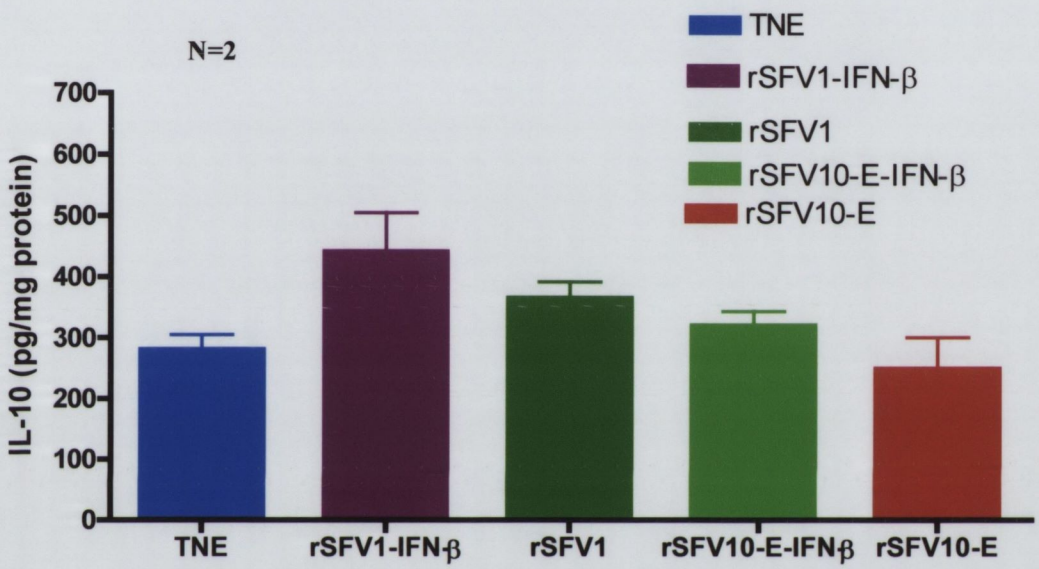

B

Figure 3.9 Levels of IFN-γ and IL-10 in brains of EAE mice

Low levels of IFN-γ were present in the brains of mice after continuous rSFV-IFN-β treatment day 32 p.d.i. A trend was seen where marginally less IFN-γ was present in the brains of the rSFV10-E-IFN-β treated animals compared to the other groups. IL-10 levels were higher than the IFN-γ levels found in the brain, reaching 500pg/ml but no significant difference was seen in levels between the groups.

3.4 Discussion

A number of previous studies have shown that recombinant IFN-β is a successful treatment for both EAE and MS when administered frequently. IFN-β1a (Rebif) and IFN-β1b (Betaseron) are the two forms of IFN-β shown to be effective in the treatment of RRMS. The efficacy of recombinant IFN-β protein in the treatment of MS is increased when high doses are administered frequently. Reduction of the dose or the number of treatments to once weekly resulted in an increase in the number and severity of relapses in patients (Barbero *et al.*, 2006; Barbero *et al.*). Similarly daily treatment of EAE in Lewis rats with s.c. injections of rrIFN-β was shown to inhibit disease activity with discontinuation of treatment leading to worsening of disease (Ruuls *et al.*, 1996). Based on these results it was decided to administer rSFV-IFN-β treatments throughout the induction, effector and recovery stages of the EAE model previously used where disease is induced in C57/Bl 6 mice with MOG 35-55.

An initial study was performed to examine the persistence of IFN-β expression from the rSFV10-E-IFN-β particle vector following i.n. administration to allow a treatment regime to be decided upon which gives constant IFN-β expression between treatments throughout the duration of the study. High levels of IFN-β were seen in the olfactory bulbs of rSFV-IFN-β treated animals 24 h post inoculation which had decreased by 72 h to levels comparable to those measured in the bulbs of the TNE and empty particle treated animals ($p<0.001$). This supports previous studies which show the high level of EGFP expression in the olfactory bulbs of mice following i.n. inoculation with rSFV-EGFP particles (Jerusalmi *et al.*, 2003). Levels of IFN-β measured in the brain were lower than in the bulbs but did peak 48 h post inoculation in the rSFV-IFN-β treated animals ($p<0.001$). By 72 h this level had dropped off with animals that received empty particles showing an increase suggesting that the presence of virally infected cells alone may be causing IFN-β production. The levels of IFN-β found in the spinal cord are comparable with those found in the olfactory bulbs but with a peak seen in rSFV-IFN-β animals 48 h post inoculation ($p<0.001$). The study suggests a persistence of IFN-β for up to two days post inoculation within the CNS with levels gradually dropping off by 72 h. This allowed a lapse of two days between treatments.

In this model multiple treatments exacerbated the severity of the disease compared to TNE controls ($p<0.05$). Frequent treatment with rSFV-IFN-β may have evoked a Th1 response, indicated by the enhanced production of IFN-γ from splenocytes of both

rSFV10-E-IFN-β and rSFV1-IFN-β treated animals in response to stimulation with the MOG 35-55 peptide *ex vivo*. This IFN-γ proliferative response was greater in rSFV-IFN-β treated animals compared to the TNE control and greatest in the rSFV1-IFN-β ($p<0.001$). The Th2 response was examined by measuring the levels of IL-10 produced in response to stimulation with MOG 35-55 *ex vivo*. A trend was seen where the levels produced were much lower than the IFN-γ levels, not exceeding 350 pg/ml. Overall rSFV-IFN-β treated animals did produce significantly more IL-10 than empty particle treated and TNE treated animals in response to a higher concentration of MOG ($p<0.01$), indicating that rSFV-IFN-β particle treated animals, the rSFV10-E-IFN-β treated in particular ($p<0.001$), do favour a Th2 response. A previous study supports our findings where IFN-β treatment of EAE induced in SJL mice with PLP 139-151 favours PLP 139-151 Th2 responses *ex vivo* despite having no inhibitory effect on disease course (Luca *et al.*, 1999).

As previously found by Jerusalmi *et al.*, 2003, the administration of empty particles increased disease severity compared to the TNE control group by increasing clinical score and weight loss. This paper suggested that disease exacerbation was due to the inflammatory response caused by the vector, however immunological studies to support this theory were not performed. Comparisons with the successful rSFV1-IL-10 treatment are difficult to make at this point as both the cytokine being expressed in this chapter and the treatment regime are very different. In this study stimulation of splenocytes from these empty particle control animals *ex vivo* with MOG peptide showed an overall increased IFN-γ response compared to splenocytes from TNE treated control animals and rSFV10-E-IFN-β treated animals ($p<0.01$), combined with a lower IL-10 response compared to the rSFV-IFN-β treated animals ($p<0.01$). This was found with regard to the rSFV10-E empty particles only. A recent study has shown that i.p. or i.v. administration of Vero cells infected with rSFV suicide particles expressing the ovalbumin gene *in vivo* led to activation of the ds RNA TLR3 (Schulz *et al.*, 2005). TLR3 signalling augments cross presentation by CD8+ dendritic cells leading to upregulation of co-stimulatory molecules and production of immunomodulatory cytokines such as IFN-γ. In this study the administration of numerous rSFV-IFN-β and rSFV empty particle treatments may have upregulated TLR 3 expression on infiltrating immune cells within the CNS leading to an upregulation of the pre-existing Th1 inflammatory response typical of EAE.

Little difference was seen in the severity of lesions in animals treated with rSFV-IFN-β, empty rSFV particles and TNE. Localized or diffuse lesions typical of EAE were

present in all mice examined. Lesions were consistently more severe in the spinal cords than in the brains. All mice exhibited medium to severe clinical signs and clinical and pathological scores correlated closely. Overall axonal degeneration was determined by loss of connection between the distal axon and the proximal axon, accumulation of organelles and mitochondria and by the presence of fragmented, phagocytosed axons.

No significant difference was seen between the levels of IFN-γ and IL-10 found in the brains of each group of animals. A trend was seen where rSFV10-E-IFN-β treated animals did have marginally less IFN-γ present in their brains. Levels of IL-10 were similar between each group, and overall were higher than the IFN-γ levels. Cytokine levels were not measured in the spinal cord but may have been higher as lesions were more severe in this tissue. The regulatory role of IL-10 has been further strengthened by findings showing that IL-10 deficient mice develop a more severe EAE and a local production of IL-10 in the brain prevented the induction of EAE (Samoilova *et al.*, 1998). Spontaneous recovery from EAE does not occur in IL-10 deficient mice suggesting that IL-10 plays a role in the recovery phase of disease. This may explain why higher levels of IL-10 are present at this later time when animals are beginning to recover. IFN-γ is produced by astrocytes in the CNS and has dual roles as a pro-inflammatory and anti-inflammatory cytokine. Overexpression of IFN-γ in the CNS of mice results in progressive demyelinating disease but on the other hand, elimination of this cytokine worsens EAE by abrogating the termination of the immune response (Krakowski and Owens, 1996; Lublin *et al.*, 1993). Immunolabelling of cytokines present in these CNS lesions would offer a more informative profile of the inflammatory response and any alterations in Th1/Th2 cytokine levels due to rSFV-IFN-β treatment.

Overall neither treatment with rSFV1-IFN-β particles nor with rSFV10-E-IFN-β inhibited disease progression in this EAE model, when administered frequently. However treatment with rSFV10-E-IFN-β particles showed more promising results with regard to upregulation of Th2 responses *ex vivo* indicated by the increased levels of IL-10 induction from rSFV10-E-IFN-β. The increased production of IFN-β from rSFV10-E-IFN-β is leading to a downregulation in the Th1 response and a tendency towards a Th2 response. The rSFV10-E-IFN-β vector was chosen as the most suitable vector to continue the work, with the theory that fewer treatments targeting the effector stage of disease may suppress disease.

Chapter 4

Treatment of the effector stage of EAE with rSFV-IFN-β vectors

4.1 Introduction

Cytokines are pleiotropic factors produced by a variety of immune cells including T cells and B cells but also by cells of the CNS such as astrocytes and microglia. They function as regulators of both adaptive and innate immunity. IFN-γ plays a central role in EAE and is produced by the CD4+ effector Th1 cells. Some functions of IFN-γ include enhancement of MHC class I and class II on different cell types and stimulation of macrophages by induction of NO synthase, TNF-α and IL-1 (Billiau *et al.*, 1998). Expression starts at onset of disease, increases during the peak of disease and decreases during disease remission. Overexpression of IFN-γ in the CNS of mice results in progressive demyelinating disease (Dandekar *et al.*, 2004; Renno *et al.*, 1998; Takacs *et al.*, 1995). Recent experiments challenge the assumption that IFN-γ mediates a critical effector function in EAE progress, for example EAE has been successfully induced in IFN-γ-/- and IFN-γ receptor knockout mice with disease being more severe in the knockout mice than in the wild type (Ferber *et al.*, 1996; Krakowski and Owens, 1996; Willenborg *et al.*, 1996). These studies suggest that IFN-γ may act paradoxically to suppress development of EAE. An alternative pro-inflammatory cytokine, IL-12, produced by cells of the innate immune system, has been shown to be critical in every EAE model thus examined (Constantinescu *et al.*, 1998; Segal *et al.*, 1998). IL-12 is produced by activated macrophages, dendritic cells and microglia in response to IFN-γ induction and is itself a potent inducer of Th1 cell differentiation leading to secretion of factors such as IFN-γ (Bliss *et al.*, 1996; Trinchieri, 1998). Generation of the effector CD4+ Th1 cells depends on the coordinated action of IL-12 and IFN-γ.

The other CD4+ MHC class II cells, the Th 2 cells produce IL-4, IL-5, IL-10 and IL-13. Expression of these cytokines is associated with disease recovery, generally through the promotion of humoral immune responses (Cua *et al.*, 1995; Falcone and Bloom, 1997; Young *et al.*, 2000). IL-4 is a classical Th2 cytokine that has been implicated as a suppressor cytokine in EAE (Begolka *et al.*, 1998; Khoury *et al.*, 1992). It is involved in the differentiation of Th0 cells into Th2 cells which in turn secrete the anti-inflammatory cytokines IL-4, IL-5 and IL-10. Though the presence of IL-4 reduces the severity of EAE, the absence of IL-4 may not alter the course of EAE. Studies have shown that IL-4 deficient mice experienced a similar, if not more severe, incidence of EAE as wild type mice. IL-4 deficient PJL mice also experienced a slight prolongation of disease indicating a role for IL-4 in disease termination (Falcone *et al.*, 1998; Liblau *et al.*, 1997).

IL-10 is another classical Th2 cytokine but in contrast to IL-4, absence of IL-10 consistently results in a more severe form of EAE. IL-10 knockout mice of the C57/Bl6 genetic background are more susceptible and develop more severe EAE than wild type mice after immunization with MOG peptide. The evidence that IL-10 knockout mice did not show spontaneous recovery like the wild type and IL-4 knockout mice suggests an important role in recovery (Samoilova *et al.*, 1998). As previously discussed IL-10 is produced by the Th0 and Th2 subsets of CD4+ murine T cells, and its main function is to inhibit IL-12 production by macrophages (Trinchieri, 1998; Trinchieri *et al.*, 2003). Recent studies has suggested that an IL-12/IL-10 immunomodulatory circuit is a key determinant of disease expression in EAE (Karp *et al.*, 2001; Segal *et al.*, 1998). Therapy is related to treatments capable of increasing IL-10 and/or decreasing IL-12. Studies have shown that IFN-β can inhibit *in vitro* secretion of IL-12 by splenic leukocytes (Byrnes *et al.*, 2001; McRae *et al.*, 1998) while at the same time maintaining the ability to induce IL-10 expression on macrophages (Rep *et al.*, 1999). Tuohy *et al.*, 2000 showed that IFN-β treatment of EAE induced in SWXJ mice with PLP 139-151 resulted in increased production of IL-10 and a concurrent decreased production of APC generated IL-12 leading to inhibition of disease progression.

The significance of B cells and antibody responses in the CNS remains controversial and depends on the experimental models used. EAE has been successfully induced in B cell deficient animals suggesting that B cells are not critical for disease expression (Hjelmstrom *et al.*, 1998; Wolf *et al.*, 1996). In other studies B cells were required for complete expression of disease (Lyons *et al.*, 1999; Willenborg and Prowse, 1983). B cells are believed to play an active role in demyelination together with autoimmune T cells, which through CD40-CD40L interactions lead to development of humoral immunity and production of autoantibodies (Gerritse *et al.*, 1996; Laman *et al.*, 1998). In contrast B cells have also been shown to be involved in regulation and recovery from acute EAE. In EAE induced with MBP peptide B cell deficient animals experienced a slower recovery compared to wild type litter mates (Wolf *et al.*, 1996). Similarly their ability to skew the T helper cells to differentiate toward a T helper 2 response in the later stages of EAE indicates their role as regulators in the recovery phase of disease (Fillatreau *et al.*, 2002). IFN-β has been shown to markedly reduce the number of circulating $CD80^+$ B cells involved in activating Th1 cells in MS and EAE, leading to improvement in clinical disease (Genc *et al.*, 1997; Hallal *et al.*, 2003).

Astrocytes provide a link between the CNS and the immune system. They are immunocompetent cells and are among the first cells to respond to CNS injury. Gliosis, characterized by the presence of reactive astrocytes, is the best-recognized cellular response to CNS injury (Eng *et al.*, 1992). Cytokines such as IL-1, IFN-γ and TNF-α are among the factors involved in the production of reactive astrocytes (Barna *et al.*, 1990; Giulian and Lachman, 1985; Yong *et al.*, 1991). Astrocytes secrete an IL-3 like factor that induces growth of brain tissue macrophages and GM-CSF, a cytokine necessary for growth and differentiation of macrophages leading to accumulation of macrophages at the site of inflammation (Frei *et al.*, 1985; Frei *et al.*, 1992).

Macrophages are essential effectors in demyelination performing a wide range of immunological functions in the process including myelin degradation through phagocytic activity, antigen presentation and production of inflammatory mediators in response to inflammatory stimuli (Dijkstra *et al.*, 1992; Hendriks *et al.*, 2005). The best indicator for active demyelination is the presence of myelin degradation products in the cytoplasm of macrophages. The expression of IFN-γ enhances the phagocytic activity of macrophages involved in tissue injury and induces class II MHC antigen expression which is generally not present on these cells (Suzumura *et al.*, 1987).

As previously described the MHC class II restricted CD4+ Th1 cells are the primary effector cells in EAE and are crucial to disease development (Pettinelli and McFarlin, 1981; Zamvil *et al.*, 1985). More recent studies have shown the role of these cells is not purely pathogenic. These cells are also potentially neuroprotective producing neurotrophins such as BDNF and also act as the key IL-10 producing cells in disease resolution (Kerschensteiner *et al.*, 1999; Kohm *et al.*, 2002; McGeachy and Anderton, 2005; McGeachy *et al.*, 2005; Zhang *et al.*, 2004). The other major T cell subset CD8+ T cells also plays a role in EAE as effectors of the encephalitogenic response causing damage to tissue through demyelination and axonal injury (Huseby *et al.*, 2001; Sun *et al.*, 2001). CD8+ T cells are also thought to play a role in recovery in EAE where less mortality but more relapses were shown in CD8+ deficient mice (Koh *et al.*, 1992). Treatment of MS with IFN-β is thought to promote proliferation of the CD8+ T cells leading to enhanced secretion of Th2 cytokines such as TGF-β (Javed and Reder, 2005). Little is known about the effect that IFN-β therapy has on CD8+ cells in EAE.

This chapter attempts to continue treatment of EAE with rSFV-IFN-β particles, this time designing regimes where fewer treatments are targeted towards the effector stage

of disease only. As explained in Chapter 3, there are three different stages of EAE – the induction, the effector and the recovery stage. During the effector stage, between days 12-17, the animals are beginning to display symptoms of clinical disease. At this point the T cell response to the encephalolithogenic peptide is fully developed and the animals experience a progressive clinical disease. In this study immunological aspects of treatment will be examined in greater detail by looking at a wider range of T cells responses and the relationship between IL-10 and IL-12 in the immunoregulation of EAE. The percentage of total splenocytes constituted by the CD4+, CD8+ and B cells in response to IFN-β treatment will also be examined, and the phenotype of the infiltrating cell populations in the acute EAE lesion will be characterized using immunohistochemistry and morphometrical analysis. Another model of EAE will be introduced where disease is induced in SJL mice using spinal cord homogenate (SCH). This model will also be treated with rSFV-IFN-β following the most successful treatment regime established in the C57/Bl6 model.

4.2 Materials and methods

4.2.1 Materials

4.2.1.1 Mice

Specific pathogen free female C57/Bl6 mice and female SJL mice aged 6-8 weeks were obtained from Harlan (Bicester UK). BALB/c male mice were obtained from the BioResources Unit, TCD. All animals were maintained as previously described in section 2.2.1.3.

4.2.1.2 Particle production

As described before in section 2.2.1.5.

4.2.1.3 EAE induction

Materials as described in section 3.2.1.3 for induction of EAE in C57/Bl6 mice. For induction of EAE in SJL mice, SCH was obtained by homogenizing spinal cord of 20 Balb/c mice, freezing it overnight at -20°C, and then freeze drying it overnight.

4.2.1.4 Histopathological studies

As described before in section 3.2.1.6.

4.2.1.5 Antibodies

Table 4.1 shows the antibodies used for both immunohistochemistry and FACS analysis and their working dilutions. NRS, NGS, biotinylated rabbit anti-rat antibody and Vector Elite ABC HRP kits (rabbit anti-rat and goat anti-rabbit) were from Vector Laboratories Inc. (CA, USA).

4.2.1.6 Morphometrics analysis

Image Pro plus software was used for analysis.

TABLE OF ANTIBODIES

Antibody	Use	Manufacturer/Source	Working dilution
Rat anti-mouse CD3	Immunohistochemistry	Novacastra	1:20
Rat anti-mouse C45R/ B220	Immunohistochemistry	BD Pharmingen	1:150
Rat anti-mouse Mac-3	Immunohistochemistry	BD Pharmingen	1.35
Rabbit anti-bovine Glial fibrillary acidic protein (GFAP)	Immunohistochemistry	Dako (Denmark)	Recommended protocol
Rat anti-mouse CD4 (L3T4)	FACS analysis	BD Pharmingen	1:100
Rat anti-mouse CD8a (Ly-2)	FACS analysis	BD Pharmingen	1:100
Rat anti-mouse C45R/B220	FACS analysis	BD Pharmingen	1:100
Rat $IgG_{2a}\kappa$ isotype control	FACS analysis	BD Pharmingen	1:100

Table 4.1. Table of antibodies used and recommended dilutions

4.2.1.7 Splenocyte stimulation assay

As described in section 3.2.1.4.

4.2.1.8 Enzyme Linked ImmunoSorbant Assay

OptEIA ELISA kits for mouse IFN-γ, IL-10, IL-4 and IL-12 (p70) were from BD Biosciences, PharMingen (USA).

4.2.1.9 FACS analysis

A Becton Dickinson FACSCalibur E4687 cytometer and WinMDI (Windows Multiple Document Interface for Flow Cytometry) software program were used in FACS studies.

4.2.2.0 Miscellaneous

Streptavidin-FITC was from Dako (Denmark), 1ml FACS tubes were from Nunc (Denmark), 96 well tissue culture plates were from Sarstedt (Denmark). FACS wash buffer was prepared from PBS + 1% NCS, FACS blocking buffer was prepared from 50% PBS: 50% FBS, $H_2O_2$was from Sigma (UK), 100% methanol was from BDH, UK. Cell marque pressure cooker and Trilogy (with EDTA) unmasking solution were from Cell Marque Corporation; Hot Springs, AR. DAB substrate was from Vector laboratories Inc. (CA,USA). Luxol fast blue solution was prepared from 1g luxol fast blue MBS diluted in 5ml 10% acetic acid and 1 L 95 % alcohol.

4.2.2. Methods

4.2.2.1 Particle production

rSFV10-E-IFN-β and rSFV10-E particles was prepared and titrated as described in section 2.2.6.

4.2.2.2 Treatment of EAE induced in C57/Bl6 mice with rSFV10-E-IFN-β particles during the effector stage

EAE was induced in 30 C57/Bl 6 mice with MOG 35–55 peptide as previously described in section 3.2.2.5. Each mouse was immunized with 100μg of the peptide emulsified in the enriched adjuvant as before. 4.5mg of peptide was dissolved in 6.75ml of PBS, and mixed with 6.0 ml of enriched adjuvant in a 20ml plugged syringe to prepare enough mix for 45 mice and allow for loss. Animals received four i.n. treatments with rSFV10-E-IFN-β particles, rSFV10-E empty particle and TNE buffer alone on days 12, 15, 16 and 17 as described in sections 3.2.2.2 and 3.2.2.6. Clinical disease was graded from day 8 onwards according to the standard neurological scale previously used. Weight was also monitored.

4.2.2.3 Treatment of EAE induced in C57/Bl6 mice with rSFV10-E-IFN-β particles before and during the effector stage

EAE was induced in 30 C57/Bl 6 mice with MOG 35–55 peptide as previously described 3.2.2.5. Each mouse was immunized with 100μg of the peptide emulsified in the enriched adjuvant as before. 4.5mg of peptide was dissolved in 6.75ml of PBS, and mixed with 6.75ml of enriched adjuvant in a 20ml plugged syringe to prepare enough mix for 45 mice and allow for loss. Animals received five i.n. treatments with rSFV10-E-IFN-β particles, rSFV10-E empty particle and TNE alone on days 5, 8, 11, 13 and 17 as previously described in sections 3.2.2.2 and 3.2.2.6. Clinical disease was graded from day 8 onwards according to the standard neurological scale previously used. Weight was also monitored.

4.2.2.4 Treatment of EAE induced in C57/Bl6 mice with rSFV10-E-IFN-β particles before the effector stage

EAE was induced in 30 C57/Bl 6 mice with MOG 35–55 peptide as previously described 3.2.2.5. Each mouse was immunized with 100μg of the peptide emulsified in the enriched adjuvant as before. 4.5mg of peptide was dissolved in 6.75ml of PBS, and mixed with 6.75ml of enriched adjuvant in a 20ml plugged syringe to prepare enough mix for 45 mice and allow for loss. Three groups of 10 animals received four i.n. treatments with rSFV10-E-IFN-β particles, rSFV10-E empty particle and TNE buffer alone on days 5, 8, 11 and 12 as described in sections 3.2.2.2 and 3.2.2.6. Clinical disease was graded from day 8 onwards according to the standard neurological scale previously used. Weight was also monitored. Three animals from each group were sampled for pathology day 22 post disease induction and pathological and immunohistochemical analysis performed on serial sections of spinal cord. A repeat experiment was performed using 12 animals in each group, 36 in total. Three animals from each group were sacrificed and perfused day 15 post disease induction and analysis carried out. Spleens were also harvested and frozen as described in section 3.2.3.0 to examine specific T cell responses on stimulation with MOG 35-55. Three mice from each group were sampled at day 30 and spleens were again harvested and frozen for FACS analysis to be carried out to establish the percentage CD4+, CD8+ and B cells in the total splenocyte population.

4.2.2.5 EAE induction in SJL mice and treatment with rSFV-IFN-β particles on days 5,8,11,12

EAE was induced in 24 SJL mice with freeze-dried SCH from Balb/c mice. Each mouse was immunized with 1mg of the SCH emulsified in the enriched adjuvant as before. 40mg of SCH was dissolved in 6.0ml of PBS, and mixed with 6.0ml of enriched adjuvant in a 20ml plugged syringe to prepare enough mix for 40 mice and allow for loss. Three groups of 8 animals received four intranasal treatments with rSFV10-E-IFN-β particles, rSFV10-E empty particles and TNE buffer alone on days 5, 8, 11 and 12 as described in sections 3.2.2.2 and 3.2.2.6. Clinical disease was graded from day 8 onwards according to the standard neurological scale previously used. Weight was also monitored.

4.2.2.6 Paraffin embedding and sectioning for pathology

As described in section 3.2.2.7.

4.2.2.7 Haematoxylin and eosin staining for routine histology

As described in section 3.2.2.8.

4.2.2.8 Pathological analysis

As described in section 3.2.2.9.

4.2.2.9 Immunohistochemistry on spinal cord sections to detect infiltrating cells

Serial sections of spinal cord mounted on 3-aminopropyltriethoxysilane coated slides were labeled with antibodies specific for CD3 antigen, C45R/B220 antigen, Mac-3 antigen and GFAP to detect infiltrating T cells, B cells, macrophages and astrocytes respectively. Paraffin embedded sections were rehydrated and endogenous peroxidase activity was blocked by treatment with 3% H_2O_2 in 100% methanol for 10 min at room temperature. Antigen retrieval was required to detect the CD3 epitope. Prior to CD3 labeling, sections were immersed in Trilogy (with EDTA) unmasking solution (Cell Marque Corporation; Hot Springs, AR) and heated at high pressure for 3 min in a Cell Marque pressure cooker followed by 5 min cooling. Sections were incubated with the following antibodies overnight at 4°C: rat anti-human CD3 (1:20 dilution), rat anti-mouse B220/C45R (1:150 dilution) and rat anti-mouse Mac-3 (1:35 dilution). A polyclonal rabbit anti-bovine GFAP antibody was used to label astrocytes according to the manufacturer's protocol. Non-specific binding was blocked using 10% NRS or NGS in PBS for 20 min at room temperature. After 30 min incubation with biotinylated rabbit anti-rat or goat anti-rabbit secondary antibody (1:200) at room temperature, Vector Elite ABC HRP kits were used to detect bound primary antibody, according to the manufacturer's instructions using DAB as substrate. Sections were counterstained with haematoxylin, dehydrated and mounted with DPX.

4.2.3.0 Staining of spinal cord sections to detect demyelination

Luxol fast blue staining was employed to detect demyelination in active EAE lesions. Sections were rehydrated in 95% alcohol and stained in luxol fast blue solution overnight at 37°C using a screw-topped plastic coplin jar. Sections were then washed in 95% alcohol for min and rinsed in distilled H_20. Agitating sections for 10 sec in a jar of 0.005% lithium carbonate started differentiation. Differentiation was continued for 30-60 sec in 70% alcohol. All slides were rinsed in distilled water at this stage and the staining was checked with a microscope. The former three steps were repeated until grey and white matter were clearly distinguishable (Nuclei should be colourless and myelin should stand out turquoise on a very pale grey/blue background). Slides were then stained in 0.1% cresyl violet in 1% acetic acid for 10 min and washed in distilled H_20. After a further rinse in 70% alcohol, differentiation was continued in 70% alcohol for approximately 30 sec until only nuclei and nissl substance were purple. Slides were then rinsed quickly in 100% alcohol, cleared and mounted.

4.2.3.1 Morphometric analysis to quantify infiltrating T and B lymphocytes

For morphometric analysis, labeled infiltrating T and B cells were counted using Image Pro Plus software. Three animals from each of the treatment groups, rSFV-IFN-β-treated, rSFV-treated and TNE buffer-treated, each with grade 3+ lesions, were selected and numbers of T and B lymphocytes were counted in serial sections. Positive cells were counted in a minimum of four individual lesions in each animal using the manual tagging option and the average number of T and B cells per lesion were calculated. Cell count data was exported to a statistical analysis programme, Graph Pad Prism 4. Two way ANOVA analysis and Bonferroni post-tests were used for statistical comparison between the treatment groups

4.2.3.2 Splenocyte stimulation assay and T cell responses *ex vivo*

Splenocytes were thawed at 37°C and stimulated with 5 or 10 μg/ml MOG 35-55 peptide for 72 h as described in section 3.2.3.1. Untreated wells and wells treated with 5μg Con A were included as controls. The plate was incubated at 37°C, 5% CO_2 for 72 h. Samples were centrifuged at 14000 rpm (10000g), 4°C to remove cell debris, aliquoted and frozen at –70°C until use. Levels of IFN-γ, IL-10, IL-12 and IL-4 present in stimulated splenocyte supernatant samples were measured using the OptEIA mouse IFN-γ, mouse IL-

10, mouse IL-12 and mouse IL-4 ELISA sets according to the manufacturer's protocol. Two way ANOVA analysis and Bonferroni post-tests were used for statistical comparison between treatment groups.

4.2.3.3 Classification of leucocytes into MHC class II restricted CD4+, class I restricted CD8+ and B cell populations by FACS analysis

Splenocytes taken from animals day 30 post disease induction after treatment on days 5,8,11,12 were labeled with the following antibodies – rat anti-mouse C45R/B220, rat anti-mouse CD4+ and rat anti-mouse CD8+, and FACS analysis was carried out on the labeled splenocytes to identify the percentage of B cells, CD4+ T cells and CD8+ T cells. Splenocytes were counted as previously described in section 3.2.3.1, diluted in PBS + 1% (v/v) NCS and added to wells of a 96 well culture plate at a concentration of 1×10^6 cells per well in 100µl volume. The plate was sealed with a plastic plate sealer and centrifuged at 1500rpm (1365g) for 5 min at 4°C to pellet the cells. The cell supernatant was discarded by flicking off the liquid and the cells were resuspended by vortexing. Cells were then incubated with 50% : 50% PBS + FBS blocking buffer for 10 min at RT after which the cells were centrifuged again, liquid removed and cells resuspended by vortexing. Cells were then incubated with the following antibodies for 1 hr at 4°C - rat anti-mouse C45R/B220, 1:100 dilution, rat anti-mouse CD4+, 1:100 dilution and rat anti-mouse CD8+, 1:100 dilution. After two washes, cells were incubated with biotinylated secondary rabbit anti-rat antibody (1:200), followed by streptavidin-FITC (1:100) to detect bound antibody. All washing steps were carried out using PBS + 1% (v/v) NCS. Control for the antibodies was purified rat IgG2aκ, diluted 1:100. Labelled splenocytes were resuspended in 200µl wash buffer, added to 1ml FACS tubes and volume increased to 1ml with wash buffer. Samples were run on a Becton Dickinson FACScalibur and data was transferred to WinMDI analysis program. Cell percentage data was exported to a statistical analysis programme, Graph Pad Prism 4. One way ANOVA analysis and Bonferroni post-tests were used for statistical comparison between the treatment groups.

4.3 Results

4.3.1 Effect of four rSFV10-E-IFN-β treatments during the effector stage

Preliminary experiments were carried out to refine the time of administration of the rSFV10-E-IFN-β particles. When animals were treated during the effector stage of the disease on days 12, 15, 16 and 17, rSFV-IFN-β particles did prevent disease progression between days 16-26 but this was significant in comparison to the empty particle treated group only ($p<0.01$) which had enhanced severity of EAE compared to the control TNE treated group (Figure 4.1A). Animals receiving rSFV10-E particles experienced greater weight loss overall (Figure 4.1B). Animals were also treated just before and then throughout the effector period on days 5, 8, 11, 13 and 17. In this experiment rSFV10-E-IFN-β treated animals experienced faster recovery than the TNE and empty particle treated animals but only a significant difference was seen in comparison to the clinical scores of the empty particle group (Figure 4.2A). This more rapid recovery time was supported by greater weight gain than in the control groups ($p\leq0.001$) (Figure 4.2B).

4.3.2 Effect of four rSFV10-E-IFN-β treatments before the effector stage

When animals received treatment with rSFV10-E-IFN-β particles just before the effector stage of disease, on days 5, 8, 11 and 12, they experienced reduced disease severity between days 12 and 20 compared to the empty particle and TNE controls (Figure 4.3A). As seen in Figures 4.1 and 4.2, intranasal administration of rSFV10-E empty particles exacerbated disease compared to TNE controls ($p<0.001$). Treatment with rSFV10-E-IFN-β particles at these time points limited disease progression compared to TNE buffer ($p<0.05$), and empty particle controls ($p<0.01$) (Figure 4.3A). All groups experienced increased weight gain after the initial decrease compared to the empty particle controls ($p<0.001$) (Figure 4.3B). Discontinuation of treatment did lead to progression of disease but at a very gradual, less severe rate. A repeat of this experiment confirmed this result.

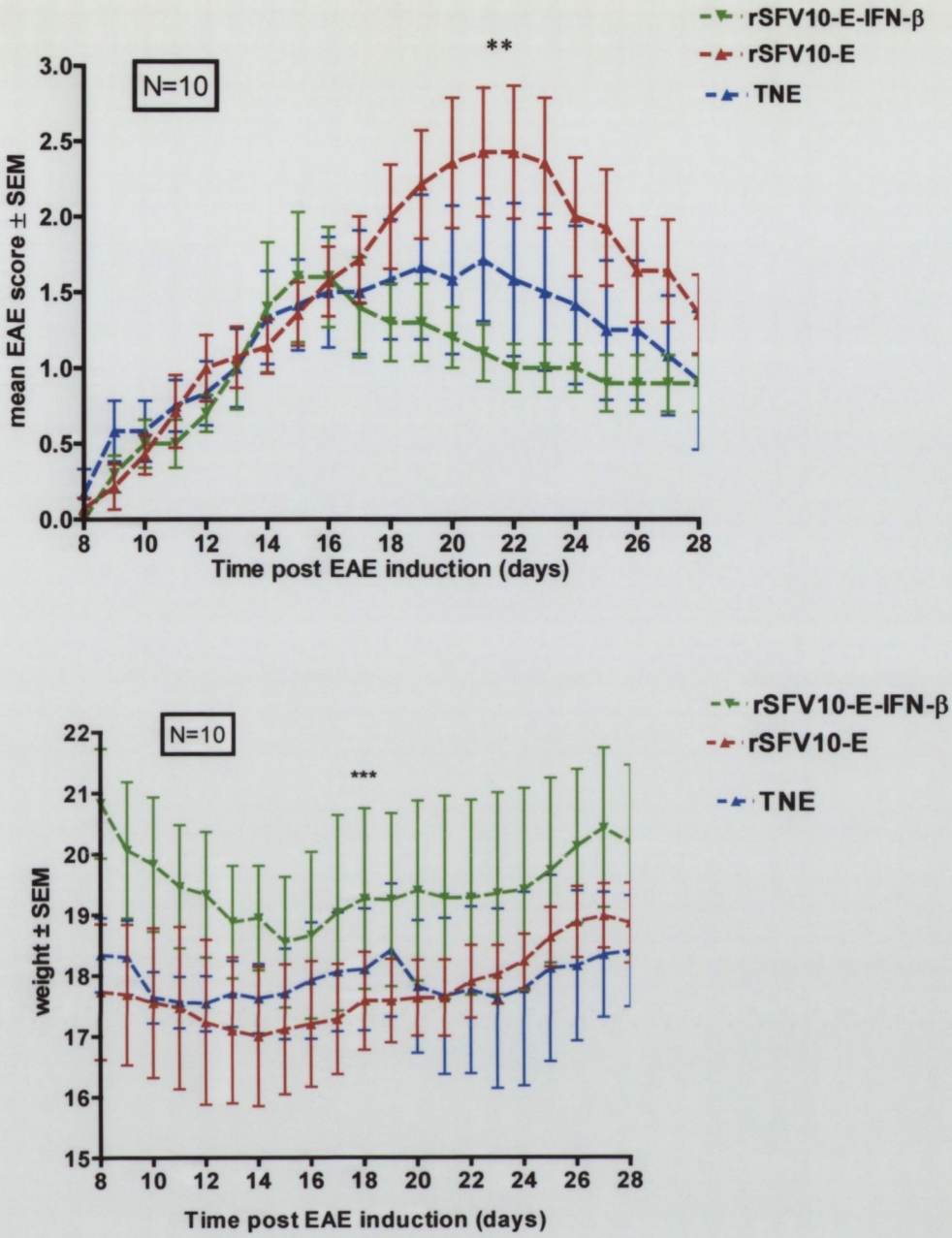

Figure 4.1 The effect of four rSFV-IFN-β treatments during the effector stage on EAE score and weight

Treatment with IFN-β did show some improvement in severity of disease between days 16-26 but this was comparable to the empty particle treated group only ($p<0.01$), no significant difference was seen between the rSFV10-IFN-β group and the TNE controls. Animals receiving rSFV10-E-IFN-β empty particles experienced significantly less weight loss than the rSFV10-E treated and the TNE control groups ($p<0.001$). Statistical analysis was performed using the non-parametric Mann-Whitney test, using Graph Prism 4.0 software.

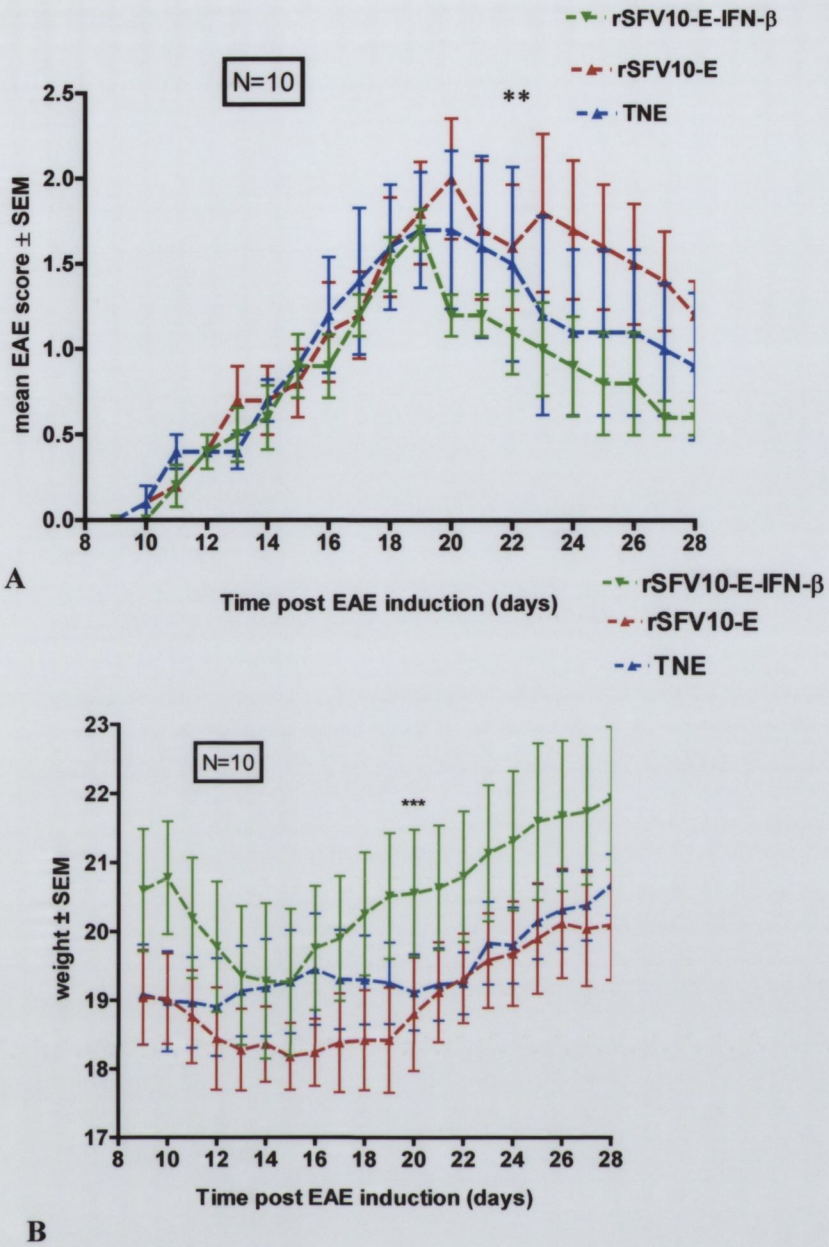

Figure 4.2 The effect of five rSFV10-IFN-β treatments before and during the effector stage on EAE score and weight

Animals treated with rSFV10-E-IFN-β particles did experience a faster recovery than the control groups from day 18 onwards but this was significant in comparison to the empty particle treated group only ($p<0.01$), no significant difference was seen between the rSFV10-E-IFN-β group and the TNE controls. The mice receiving rSFV10-E-IFN-β who experienced faster recovery also experienced greater weight gain from day 18 onwards ($p\leq 0.001$) compared to the control groups. Statistical analysis was performed using the non-parametric Mann-Whitney test, using Graph Prism 4.0 software.

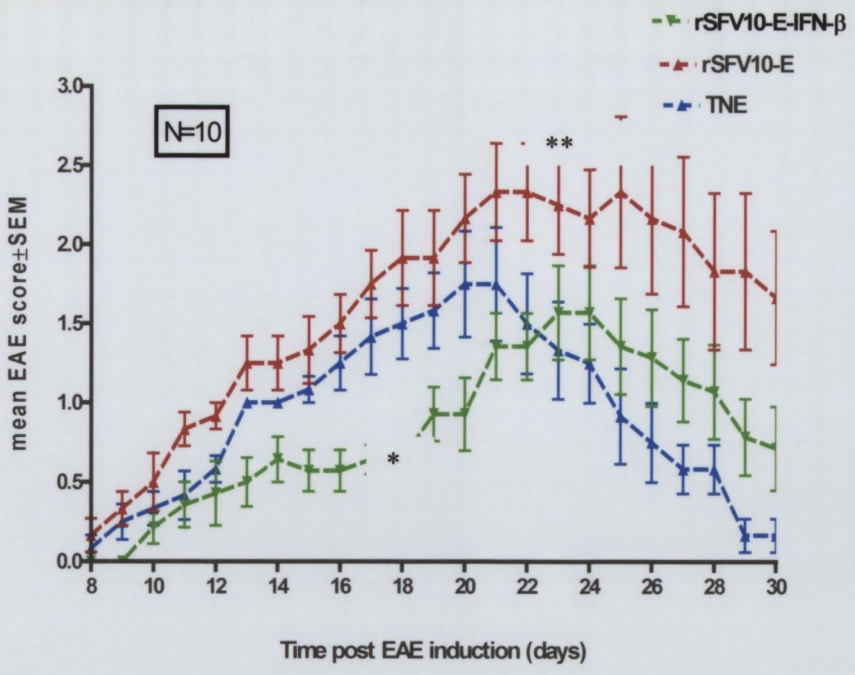

A

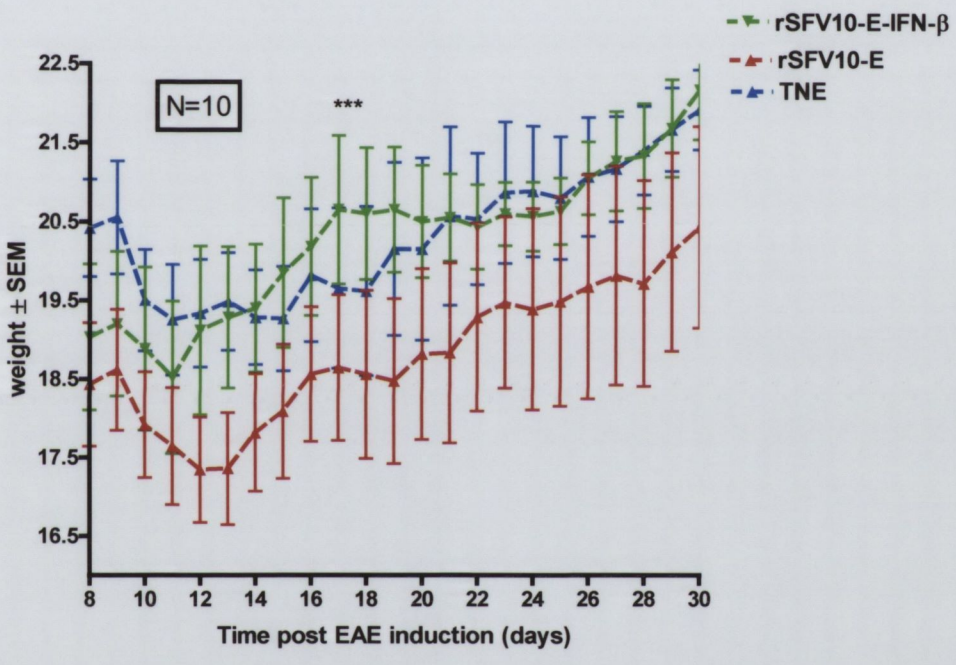

B

Figure 4.3 Effect of four rSFV10-E-IFN-β treatments before the effector stage on EAE score and weight

Animals receiving rSFV10-E-IFN-β particles experienced reduced disease severity between days 12 and 20 compared to the empty particle ($p<0.01$) and TNE controls ($p<0.05$) (A). All animals experienced a gradual increase in weight after the initial decrease with rSFV-IFN-β treated animals experiencing significantly less weight loss than the empty particle treated group ($p<0.001$) (B). Discontinuation of treatment led to progression of disease. Statistical analysis was performed using the non-parametric Mann-Whitney test, using Graph Prism 4.0 software.

4.3.3 Summary of EAE treatments

Table 4.2 summarizes the main findings of these treatment regimes, including the continuous treatment regime discussed in Chapter 3. Continuous treatment with rSFV10-E-IFN-β particles exacerbated disease severity compared to both the TNE ($p<0.05$) and empty particle controls. Administration of empty particle alone also exacerbated the disease model compared to TNE control ($p<0.05$). When less treatments were administered just before and during the effector period on days 5,8,11,13 and 17, rSFV10-E-IFN-β treated animals experienced some improvement in disease, with a maximum EAE score equal to the TNE treated, but this improvement was significant only in comparison to the empty particle treated group ($p<0.05$); no significant difference was seen with the TNE controls. When treatments were targeted towards the effector stage of the disease on days 12,15,16, and 17, rSFV10-E-IFN-β particles did prevent disease progression but again this was significant only in comparison to the empty particle treated group ($p<0.01$), which had enhanced severity of EAE compared to the control TNE treated group. When animals were treated with rSFV10-E-IFN-β particles just before the effector stage of disease, on days 5,8,11 and 12, they experienced a delay in disease onset, lower maximum EAE score compared and significantly lower mean EAE scores compared to both the TNE ($p<0.05$) and empty particle treated animals ($p<0.01$) up to day 20. Again the administration of rSFV10-E empty particles significantly exacerbated disease compared to the TNE controls ($p<0.001$). A repeat of this experiment confirmed the results. Treatment on days 5, 8, 11 and 12 showed a delay in disease onset, lower maximum clinical scores overall and a significant improvement in disease severity up to day 20 in comparison with both TNE and empty particle controls.

Treatment days	Experimental group	EAE mice	Mortality	maximum EAE score (± SEM)	Mean day of onset (± SEM)	P value Vs TNE control	P value vs empty particle control	P value vs TNE control (up to day 20)	P value vs particle control (up to day 20)
3,6,9,12,15, 18,21,24,27	TNE	9/14	3	2.3± 0.7	16.6±1.09	n.a.	0.04*	n.a.	n.s.
	rSFV10-E-IFN-β	10/14	2	3.2± 0.5	15.2±0.93	0.04*	n.s.	n.s.	n.s.
	rSFV10-E	12/14	0	2.8± 0.3	14.0±0.65	0.04*	n.a.	n.s.	n.a.
5,8,11,13,17	TNE	8/10	0	1.7 ± 0.5	16.6±0.84	n.a.	n.s.	n.a.	n.s.
	rSFV10-E-IFN-β	9/10	0	1.7 ± 0.1	16.2±1.29	n.s.	0.048*	n.s.	n.s.
	rSFV10-E	8/10	0	2.0 ± 0.4	16.6±0.87	n.s.	n.a.	n.s.	n.a.
12, 15,16,17	TNE	7/10	0	1.7± 0.5	13.3± 0.90	n.a	n.s.	n.a.	n.s.
	rSFV10-E-IFN-β	8/10	0	1.6 ± 0.3	13.4± 1.10	n.s.	0.006**	n.s.	n.s.
	rSFV10-E	7/10	0	2.4± 0.4	13.6± 0.78	n.s	n.a.	n.s.	n.a.
5,8,11,12	TNE	9/10	0	1.8± 0.4	13.5± 0.75	n.a.	0.0008***	n.a.	n.s.
	rSFV10-E-IFN-β	10/10	0	1.6± 0.3	15.0± 0.80	n.s.	0.0003***	0.046*	0.008**
	rSFV10-E	10/10	0	2.3± 0.5	14.3± 0.86	0.0008***	n.a.	n.s.	n.a.
5,8,11,12 (replicate)	TNE	10/12	0	1.9± 0.3	15.0± 0.89	n.a.	0.0086**	n.a.	n.s.
	rSFV10-E-IFN-β	10/12	0	1.4 ± 0.4	16.4± 1.57	n.s.	0.0002***	0.05*	0.0077**
	rSFV10-E	9/12	0	2.7± 0.4	13.1± 0.92	0.0086**	n.a.	n.s.	n.a.

Table 4.2 Summary of different rSFV-IFN-β treatments on the course of EAE

Continuously treated rSFV10-E-IFN-β animals experienced the highest maximum EAE score. rSFV empty particle treatment exacerbated disease and resulted in an earlier disease onset. Fewer treatments during and through the course of disease on days 12,15,16 and 17 and days 5,8,11,13 and 17 showed some improvement in disease but this was significant in comparison to the empty particle treated only ($p<0.05$). Treatment before the effector stage on days 5,8,11 and 12 proved to be the most effective regime in comparison to the TNE controls ($p<0.05$).

4.3.4 Effect of four rSFV10-E-IFN-β treatments on MOG 35-55 T-cell responses *ex vivo*

Three animals from each group treated with rSFV10-E-IFN-β and controls on days 5, 8, 11 and 12 were anaesthetized and perfused 22 days post disease induction. Specific MOG 35-55 T-cell responses were analyzed on splenocytes taken from these animals. Here a weaker Th1 response was observed with levels not reaching more than 1000 pg/ml (Figure 4.4A), compared to the levels of IFN-γ produced by animals that received continuous treatments (Figure 3.6A). Animals receiving both empty and rSFV10-E-IFN-β particles still produced higher levels of IFN-γ compared to the TNE treated group. rSFV10-E-IFN-β treated animals did produce significantly less IFN-γ than the empty particle treated group at this time point ($p<0.01$). Levels of IL-10 measured were low with no significant differences between the treatment groups (Figure 4.4B). Specific MOG 35-55 T cell responses were also measured in a similar manner in splenocytes taken from animals day 15 p.d.i (Figure 4.5). Overall levels of IFN-γ and IL-10 produced at this time were higher than those produced at day 22 in response to MOG 35-55 stimulation. As before IFN-γ production was higher in rSFV10-E-IFN-β and empty particle treated animals than TNE controls in response to peptide stimulation. rSFV10-E-IFN-β treated animals again produced significantly less than the empty particle treated in response to stimulation with MOG 35-55 ($p<0.01$) (Figure 4.5A). IL-10 levels were again low at this time with no difference seen between the treatment groups (Figure 4.5B). Higher levels of IL-12 were produced from rSFV10-E-IFN-β and empty particle treated animals than from TNE treated animals, with empty particle treated animals producing significantly more IL-12 than TNE treated animals in response to MOG ($p<0.05$) (Figure 4.6A). IL-4 levels were also measured and were low in comparison to the IFN-γ, IL-10 and IL-12 levels. rSFV10-E-IFN-β treated animals did produce more IL-4 than TNE and empty particle controls in response to splenocyte stimulation with MOG 35-55 peptide (Figure 4.6B).

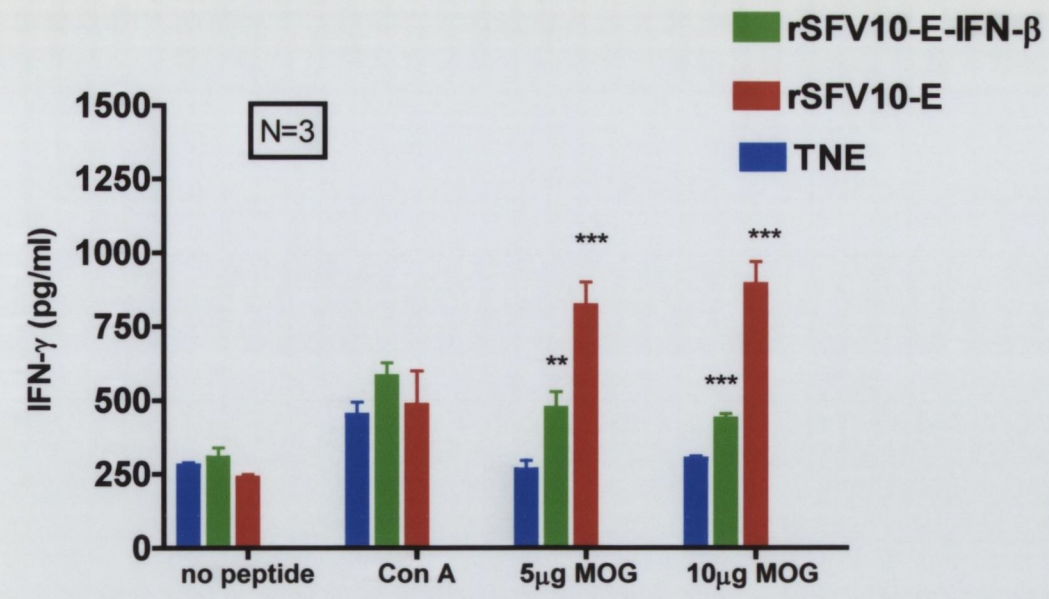

A

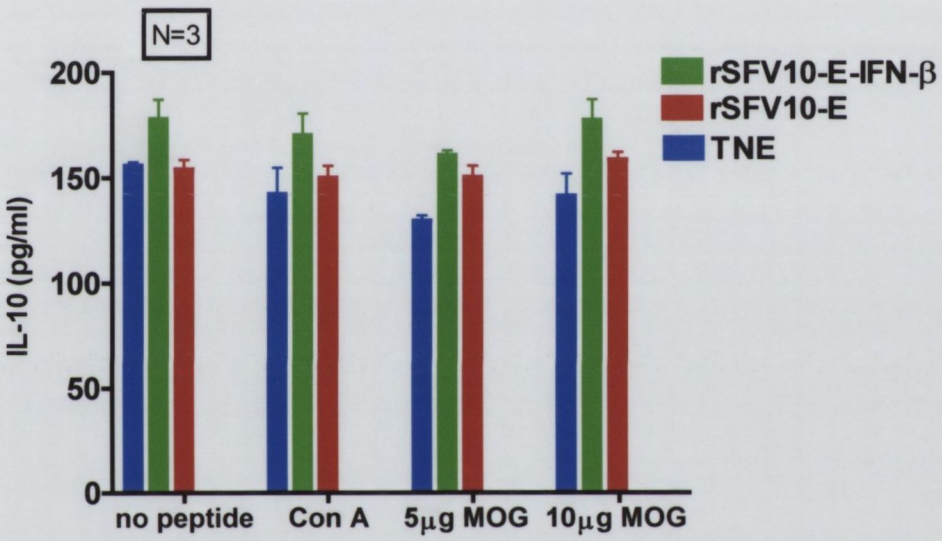

B

Figure 4.4 Production of IFN-γ and IL-10 in response to MOG 35-55 stimulation day 22 p.d.i

This graph shows a trend where more IFN-γ was produced from rSFV10-E-IFN-β and rSFV10-E empty particle treated mice compared to TNE controls after *ex vivo* MOG 35-55 stimulation of splenocytes harvested at day 22 p.d.i. (A). The empty particle controls produced significantly more IFN-γ than the TNE controls ($p<0.001$). rSFV10-E-IFN-β treated animals produced significantly less IFN-γ than empty particle treated mice ($p<0.01$). Minimal levels of IL-10 were produced in response to stimulation with MOG peptide at this time point (B). No difference was seen in the level of IL-10 production between the treatment groups at this time.

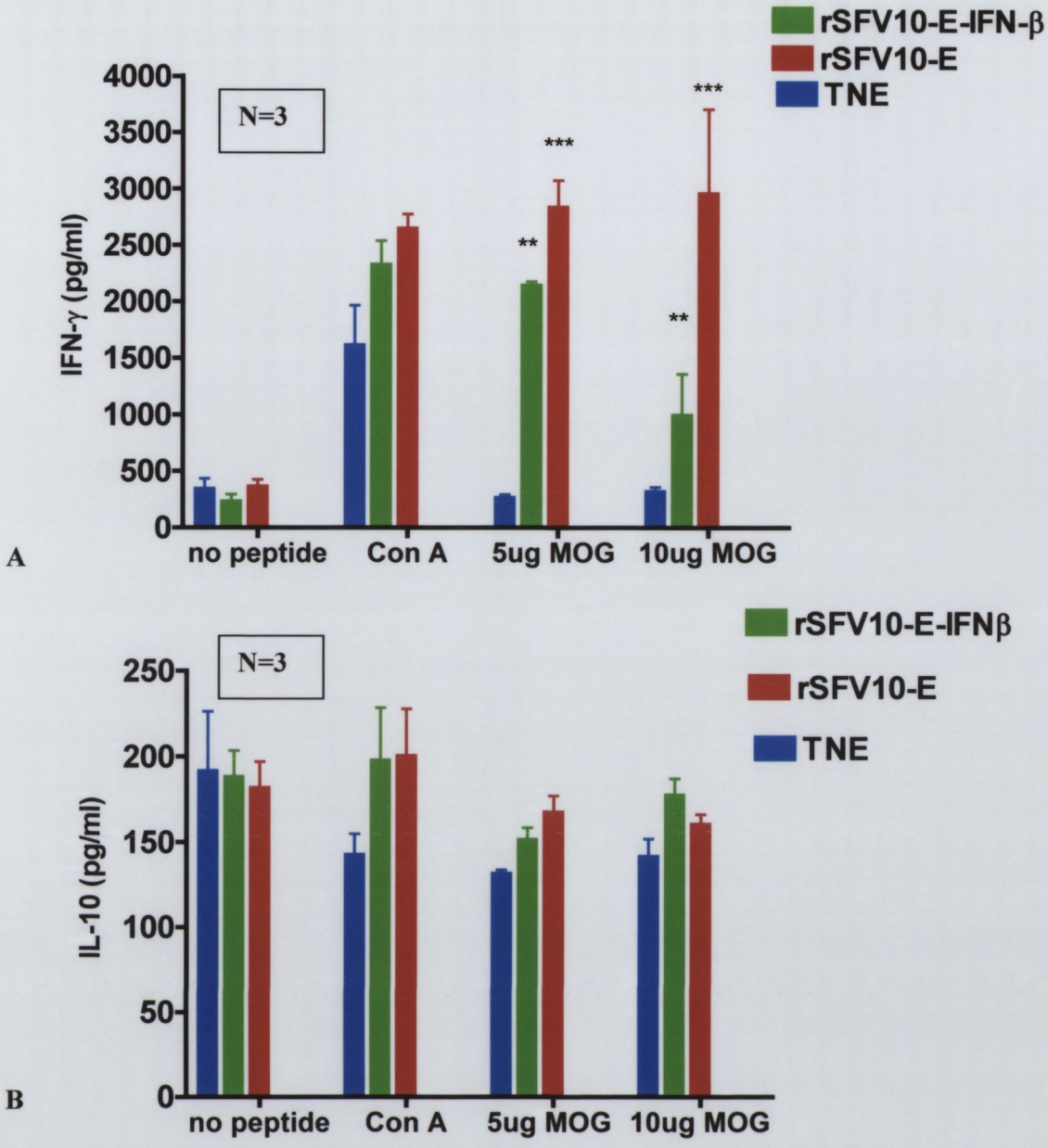

Figure 4.5 Production of IFN-γ and IL-10 in response to MOG 35-55 stimulation day 15 p.d.i

Overall a greater Th1 response was seen on stimulation of splenocytes harvested from animals harvested day 15 p.d.i. with MOG peptide compared to those splenocytes harvested from animals day 22 p.d.i. IFN-γ production was higher in rSFV10-E-IFN-β and empty particle treated animals compared to TNE controls in response to peptide stimulation ($p<0.01$). rSFV10-E-IFN-β treated animals produced less IFN-γ than the empty particle treated animals in response to MOG stimulation, and significantly less in response to 10μg MOG ($p<0.01$) (A). IL-10 levels were again relatively low at this time with no significant differences were seen between the treatment groups (B). Statistical comparison was carried out using Two way ANOVA and Bonferroni post-tests.

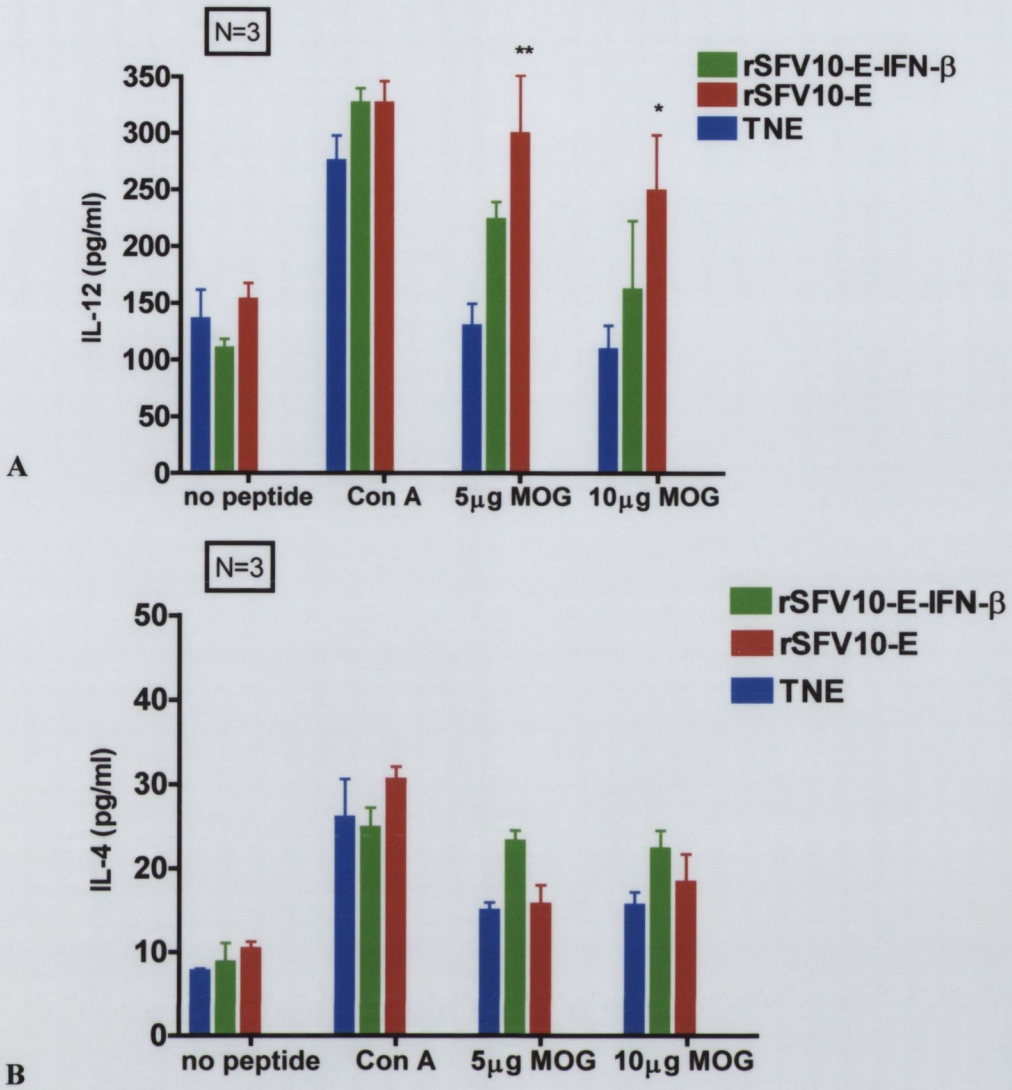

Figure 4.6 Production of IL-4 and IL-12 in response to MOG 35-55 stimulation day 15 p.d.i

Higher levels of IL-12 were produced upon stimulation of splenocytes taken from rSFV10-E-IFN-β treated and empty particle treated animals ($p<0.01$) sampled day 15 p.d.i compared to levels produced by TNE treated controls (A). rSFV10-E treated animals produced the highest levels of IL-12 upon MOG 35-55 stimulation, producing significantly more IL-12 than the TNE controls ($p<0.05$). Levels of IL-4 were also measured but no significant differences were seen between the treatment groups. The main role of IL-4 is in the recovery phase therefore levels would be low day 15 p.d.i when animals are still in the effector stage of disease. 5μg of Con A was added to a well as a positive control in this experiment. Splenocytes from a naïve mouse were included as a negative control for MOG stimulation. Statistical analysis was performed using the non-parametric Mann-Whitney test, using Graph Prism 4.0 software.

4.3.5 Correlation between clinical and pathological scores

Lesions typical of EAE were present in the brains and spinal cords of mice treated with rSFV10-E-IFN-β particles on days 5,8,11,12 and sampled on day 15 or day 22 post disease induction. As expected for this model, lesions were more common and more severe in the spinal cord than in the brain. Lesions were invariably more severe (grade 4 or higher) when both the spinal cord and brain were affected. An overall correlation between clinical score and pathological score was demonstrated at both time points (Table 4.3). Onset of clinical signs commenced on day 15 and is indicated by low clinical scores.

4.3.6 Relative severity of EAE lesions in the spinal cords of rSFV-IFN-β treated and TNE treated animals on day 22 post induction

In all treatment groups EAE lesions were localized in white matter areas and were characterized by myelin vacuolation, axonal degeneration, astrocytic proliferation and infiltrates of lymphocytes, macrophages and neutrophils. Figure 4.7 illustrates the comparison between a typical grade 2 lesion from a rSFV10-E-IFN-β treated animal (A) and the more severe grade 4 lesion from a TNE treated animal (B). Perivascular leucocytic infiltrates are more prominent in (B) than in (A).

4.3.7 Characterization of the EAE lesion

Figure 4.8(A) shows a typical grade 4 lesion in a sagital section of spinal cord from a TNE treated animal. The lesion is characterized by myelin vacuolation, axonal degeneration, astrocytic proliferation and infiltrates of lymphocytes, macrophages and neutrophils. Figure 4.8(B) shows demyelination/myelin vacuolation within this lesion using luxol fast blue staining. Small numbers of T lymphocytes are evenly distributed in areas of myelin vacuolation and in the meninges (Figure 4.8(C)). Densely packed B lymphocytes are located predominantly in perivascular spaces in the meninges (Figure 4.8(D)). Macrophages (Figure 4.8(E)) and large reactive astrocytes (Figure 4.8(F)) are located mainly in areas of myelin vacuolation.

Group sampled day 15 pdi	Mouse no.	Clinical score	Pathology score	Total clinical score	Total pathology score
TNE	1	0.5	1	3	6
	2	1.5	2		
	3	1	3		
rSFV10-E	1	0.5	1	2.5	5
	2	1	2		
	3	1	2		
rSFV10-E-IFN-β	1	0	0	1.0	0
	2	0.5	0		
	3	0.5	0		

Group sampled day 22 pdi	Mouse no.	Clinical score	Pathology Score	Total clinical score	Total pathology score
TNE	1	1	2	7	10
	2	3	4		
	3	3	4		
rSFV10-E	1	1	2	5	9
	2	1.5	3		
	3	2.5	4		
rSFV10-E-IFN-β	1	1	1	3	5
	2	1	2		
	3	1	2		

Table 4.3 Correlation between clinical score and pathology of rSFV10-E-IFN-β treated EAE mice

A direct correlation was seen between EAE scores and pathological scores. rSFV10-E-IFN-β treated animals had lower clinical scores and less severe lesions in the brain and cord. At day 15 lower clinical and pathology scores were observed overall. Animals were only beginning to show symptoms of disease at this time point and minimal myelin and axonal degeneration was present in their spinal cords.

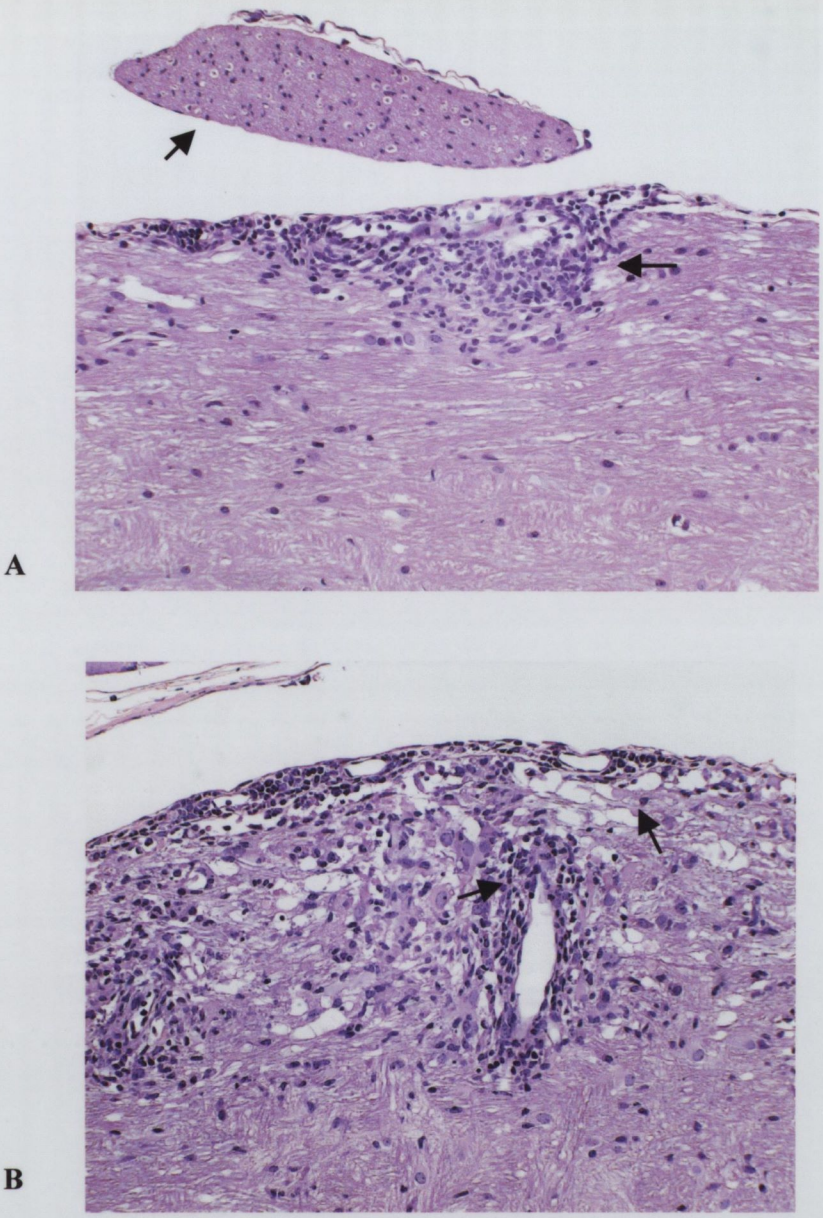

Figure 4.7 Comparison of a type 2 and type 4 EAE lesion in a spinal cord section

A typical type 2 lesion from a rSFV10-IFN-β treated animal is shown in (A) where minimal localised perivascular infiltrate of lymphocytes, macrophages and neutrophils is present in the superificial white matter. A more severe type 4 lesion from a TNE treated animal is shown in (B) where extensive perivascular cuffing, myelin vacuolation and axonal degeneration is present.

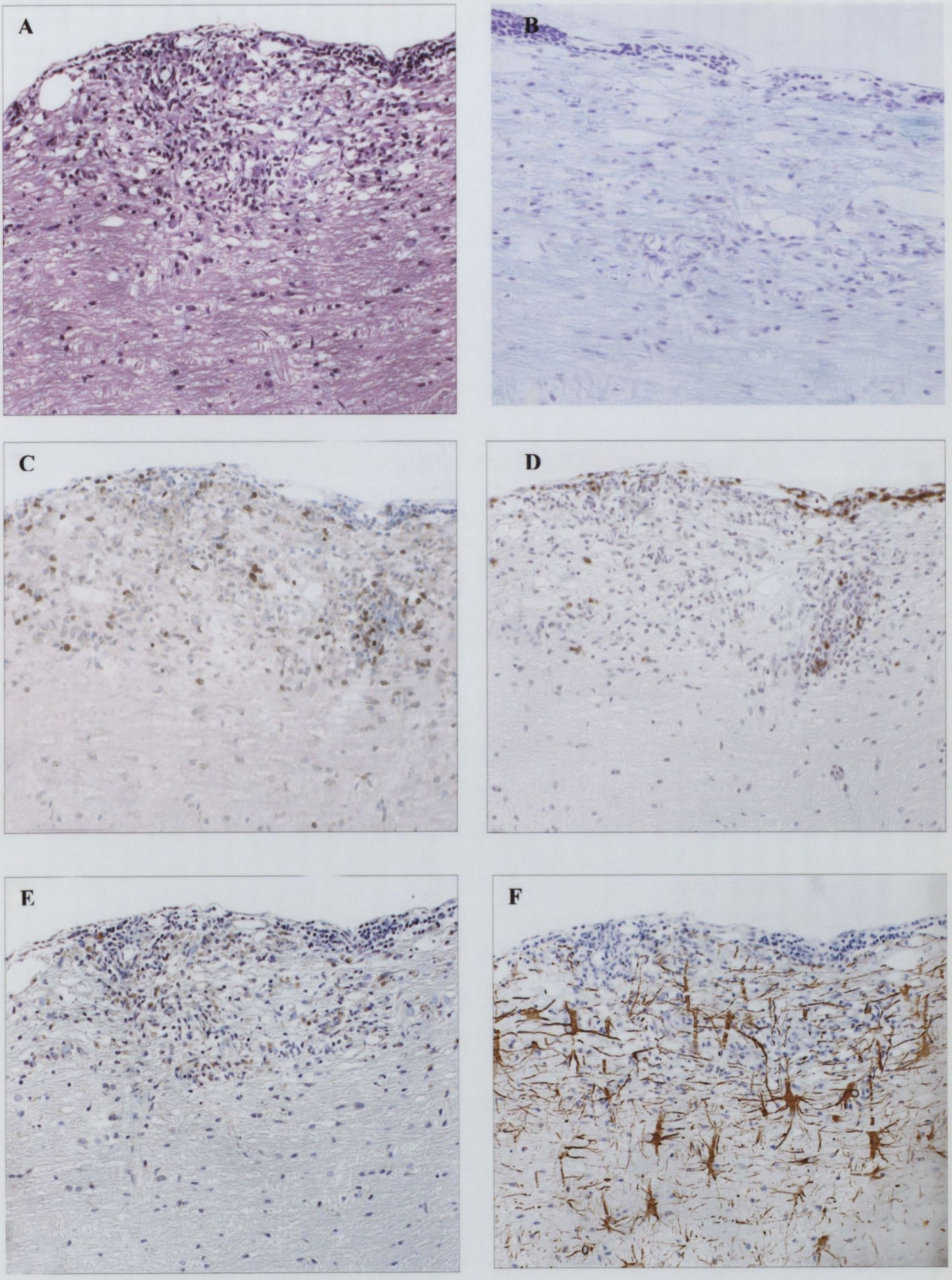

Figure 4.8 Characterisation of a typical EAE lesion on sequential sagital sections of spinal cord

Sequential spinal cord sections from mice perfused day 22 post disease induction were labeled for the following cells: T lymphocytes, B lymphocytes, macrophages and astrocytes using CD3+ antigen marker, C45R/B220 marker, Mac-3 marker and Glial GFAP, respectively. Staining for demyelination was performed using the Luxol Fast Blue method.

(A) a H&E stained section of a typical grade 4 spinal cord lesion from a TNE treated animal selected for characterisation of perivascular lymphocytic infiltration in the meninges and mononuclear cell infiltration in a subpial area of myelin pallor (x200)

(B) luxol fast blue staining for demyelination in the white matter of the same lesion (x400)

(C) T lymphocytic infiltration in both the area of myelin vacuolation and the meninges (x200)

(D) B lymphocytic infiltration mostly in the perivascular spaces in the meninges (x200)

(E) macrophages in the area of myelin vacuolation (x200)

(F) reactive proliferating astrocytes in the adjoining white matter (x200)

4.3.8 Morphometrical analysis of T and B lymphocyte populations

Preliminary observations of the immunohistochemical findings indicated that infiltrating B lymphocytes were fewer in the lesions of animals treated before the effector phase with rSFV10-E-IFN-β than in animals treated with rSFV10-E empty particles and TNE (Figure 4.9A&B). Using three different animals from each treatment group, each with grade 3 lesions, lesions were chosen at random for morphometric analysis of T and B lymphocyte populations. Whereas numbers of infiltrating T-lymphocytes were similar in each of the three treatment groups, significantly fewer ($p<0.01$) B lymphocytes were identified in lesions from animals treated with rSFV10-E-IFN-β than in animals treated with rSFV10-E empty particles and TNE (Figure 4.9C).

4.3.9 FACS analysis to distinguish lymphocytes into MHC class II restricted CD4+ T cells, class 1 restricted CD8+ T cells and B cells

Splenocytes were harvested from animals day 30 post disease induction after treatment with rSFV10-E-IFN-β on days 5,8,11,12 and splenocytes labelled with antibodies specific for B cells, CD4+ cells and CD8+ cells. Significantly higher percentages of CD4+, CD8+ and B cells were found in TNE treated and rSFV10-E-IFN-β treated animals compared to the empty particle treated animals ($p<0.01$) (Figure 4.10). Higher percentages of CD8+ and CD4+ cells constituted the splenocyte population of rSFV10-E-IFN-β treated animals compared to the TNE control group. Little difference was seen between the percentages of the different cell types within the rSFV10-E treated group whereas higher percentages of CD8+ cells were seen in the rSFV10-E-IFN-β and TNE treated groups.

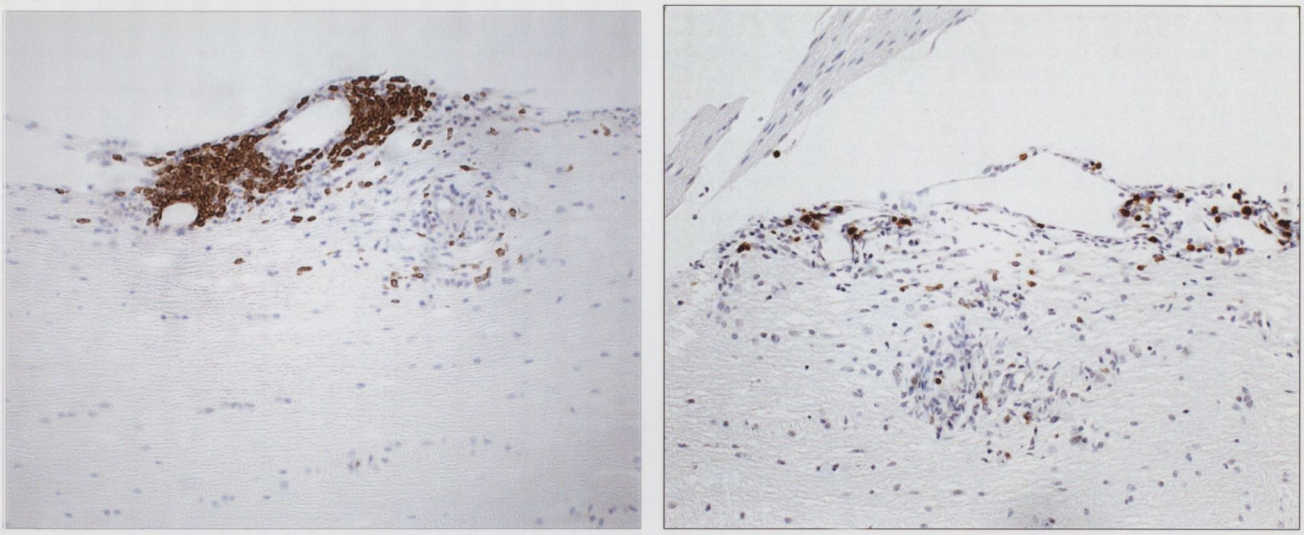

A B

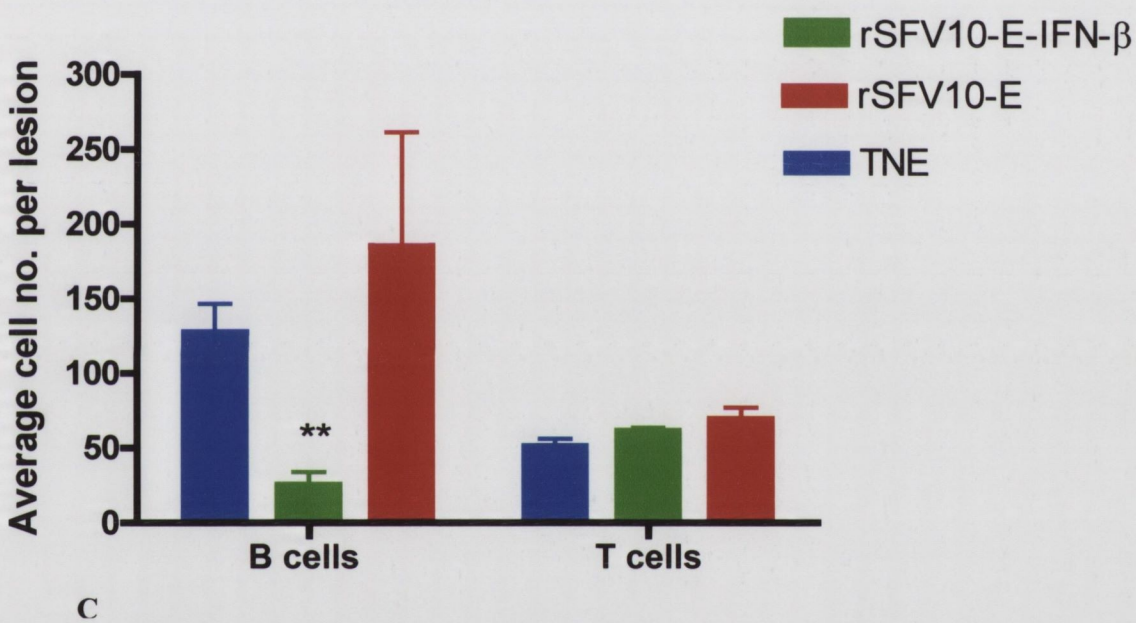

C

Figure 4.9 Comparison of B lymphocytic infiltration in similar spinal cord lesions

From the immunohistochemical labeling performed day 22 post EAE induction it was found that extensive perivascular cuffing of B lymphocytes was present in the lesion of a rSFV10-E empty particle treated animal (A) compared to a similar lesion of a rSFV10-E-IFN-β treated animal where B lymphocytes were more sparsely distributed (B). From morphometrical analysis little difference was seen in the number of infiltrating T lymphocytes between the treatment groups. However, significantly less B cell infiltration was seen in the rSFV10-E-IFN-β treated animals compared to the rSFV10-E empty particle control group ($p<0.01$) (C).

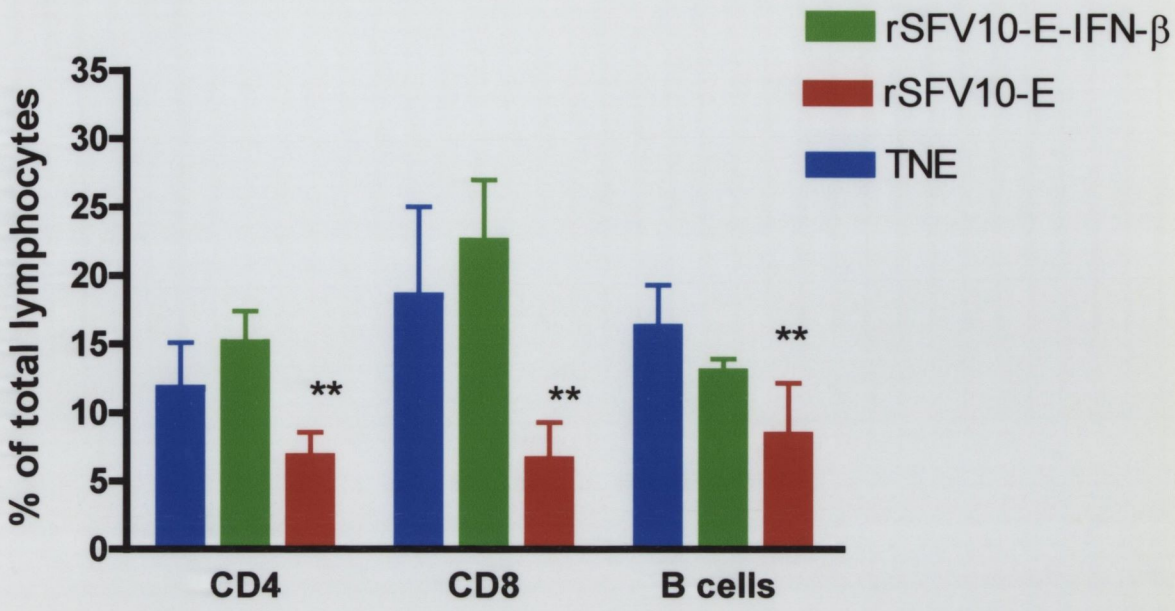

Figure 4.10 FACS analysis of lymphocytes from rSFV10-E-IFN-β particle treated EAE animals in the recovery stage of disease

Significantly lower numbers of CD4+, CD8+ and B cells were found in empty particle treated animals compared to higher percentages in TNE treated and rSFV-IFN-b treated groups ($p<0.01$). A trend was seen where a higher percentages of CD4+ and CD8+ cells were found in the splenocyte population of the rSFV10-E-IFN-β treated animals compared to the TNE treated control animals however this difference was not significant. These animals have all recovered or else are showing signs of recovery. Little difference was seen between the percentages of the different cell types within the rSFV10-E treated animals whereas higher percentages of CD8+ cells were seen in the rSFV10-E-IFN-β and TNE treated groups ($p<0.01$). CD8+ cells are thought to play a role in recovery from EAE.

.

4.4.0 The effect of four rSFV10-E-IFN-β treatments before the effector stage on EAE induced in SJL mice

EAE was induced in SJL mice using spinal cord homogenate. The mice were treated with rSFV10-E-IFN-β particles on days 5,8,11,12 as above. Treatment showed no improvement on the course of the disease with both the rSFV10-E-IFN-β particles and the empty controls making the disease marginally worse (Figure 4.11). All groups including the TNE group experienced severe disease, indicated by higher average clinical scores with an overall maximum EAE score of 3.9 ± 0.3, accompanied by progressive weight loss.

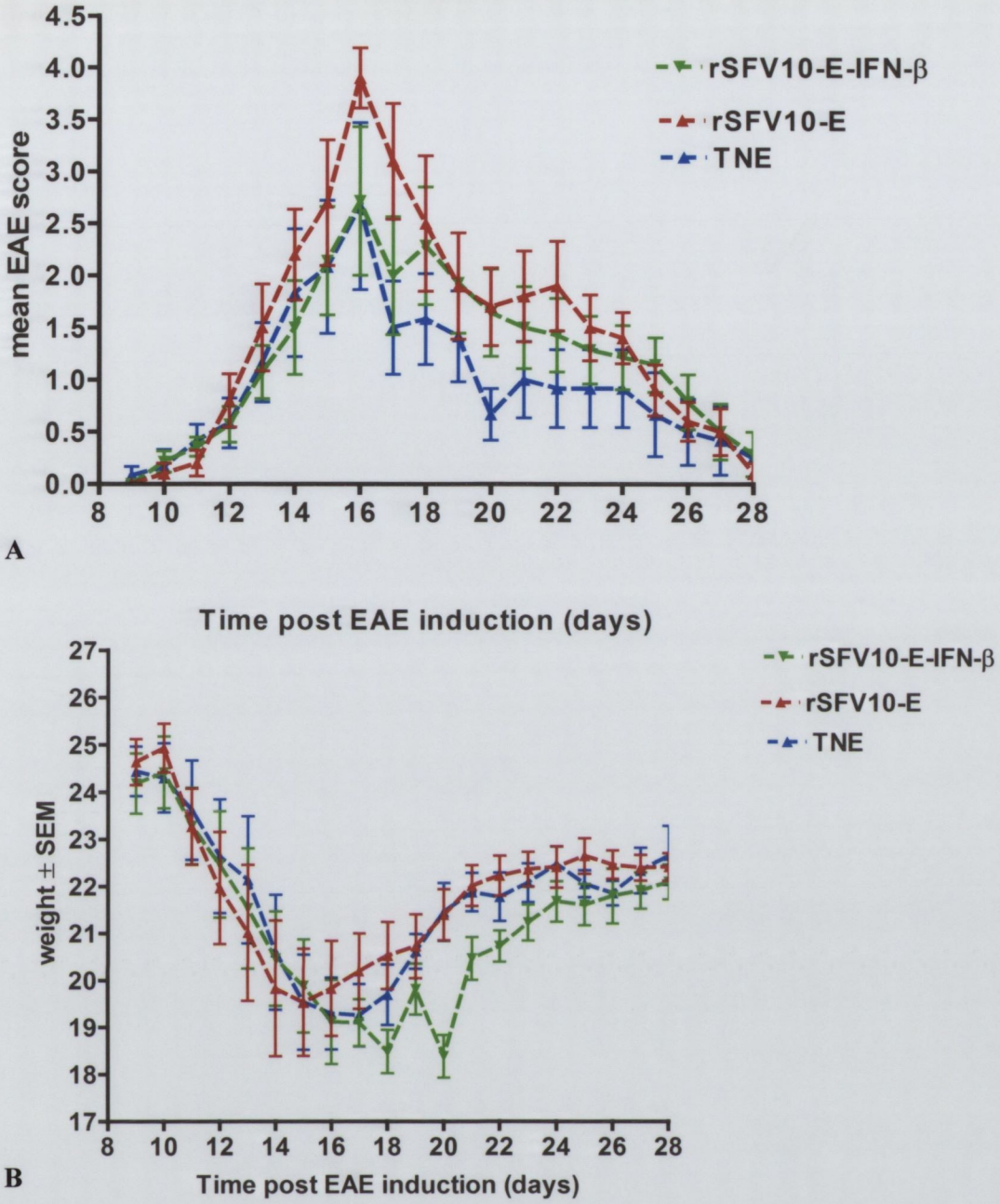

Figure 4.11 Induction and treatment of EAE induced in SJL mice with rSFV-IFN-β

EAE was induced in SJL mice with freeze dried SCH and mice were treated with rSFV10-E-IFN-β particles on days 5,8,11,12. Treatment did not have a beneficial effect on disease. This graph shows a trend where all treatment groups experienced severe disease indicated by high clinical score (A) and (B) correlating weight loss. The data also suggests that the rSFV10-E-IFN-β particles and the empty controls exacerbated disease compared to the TNE controls.

4.4 Discussion

As shown in chapter 3 the potential of rSFV10-E-IFN-β particles to induce an anti-inflammatory Th2 response was insufficient to have an ameliorating effect on EAE, possibly due to the overproduction of IFN-γ. A new treatment regime was therefore devised where treatments were specifically aimed at the effector stage of the disease when the T-cell response to the encephalolithogenic peptide has fully developed and the animals are beginning to show symptoms of disease. Treatment during the effector stage on days 12, 15, 16 and 17 showed some improvement but this was comparable to the empty particle treated animal only ($p<0.01$). Five treatments administered just before and during the effector stage on days 5,8,11,13 and 17 showed that rSFV10-E-IFN-β treated animals recovered more quickly but this again was only comparable to the empty particle treated ($p<0.01$). However, when animals were treated just before the effector stage on days 5, 8, 11 and 12 disease progression was curtailed between days 12 and 20 compared to the TNE controls ($p<0.5$), while control animals continued to worsen ($p<0.01$). Discontinuation of treatment led to a resumption of disease progression though at a slower rate than the control groups. This resumption of disease is consistent with previous studies on the treatment of EAE using rIFN-β protein (Ruuls *et al.*, 1996; van der Meide *et al.*, 1998). A trend was seen where the level of IFN-γ produced by splenocytes from these animals in response to MOG stimulation on day 22 p.d.i was lower than after nine as described in chapter 3. The IFN-γ response was greater when splenocytes harvested from animals day 15 p.d.i were stimulated with MOG *ex vivo*. This increase in IFN-γ induction was most likely due to sampling of this second group of animals within the effector period of disease, when the IFN-γ producing Th1 cells are upregulated. Regardless of the number of treatments the animals received or the stage of disease that the animals were sampled at, splenocytes from rSFV10-E-IFN-β and rSFV10-E treated animals always produced higher levels of IFN-γ in response to MOG stimulation than the TNE treated animals. The empty particle controls produced significantly more ($p<0.001$). The possible beneficial effect that these high levels of IFN-γ may be having on the course of disease, particularly during the induction stage of disease, cannot be ruled out. Previous studies have shown that IFN-γ can elicit a suppressive effect on disease development, either through administration of neutralising anti-IFN-γ monoclonal antibodies or through induction by another Th1 cytokine such as IL-12 (Duong *et al.*, 1994; Gran *et al.*, 2004). From this study however rSFV10-E-IFN-β treated animals produced significantly less IFN-γ than the empty particle

treated mice, indicating that IFN-β may be downregulating the Th1 response. As seen in chapter 3, the level of IL-10 production was minimal, however little or no difference was seen between the rSFV-IFN-β treated group and the control group. Previous studies have shown than IFN-β has the potential in some cases to enhance production of pro-inflammatory cytokines, often resulting in the downregulation of IL-10 (Manetti *et al.*, 1995). In other cases IFN-β has been shown to exert no effect on MOG specific Th2 IL-10 production during the effector stage of EAE (Kawanokuchi *et al.*, 2004). More realistically high IFN-γ levels may be suppressing the IL-10 response, either independently or through the IL-10/IL-12 immunoregulatory circuit, shown to play an important role in EAE (Segal *et al.*, 1998). IL-12 is a potent inducer of IFN-γ production from lymphocytes and NK cells (Trinchieri, 1998; Trinchieri *et al.*, 2003) which suggests that IL-12 is contributing to upregulation of IFN-γ levels which, in turn, are resulting in downregulation of IL-10 levels. Treatment with rSFV10-E-IFN-β is not having an upregulatory effect on IL-10 levels as expected therefore no significant decrease is seen in the IL-12 levels compared to the control groups. In general very low levels of IL-4 were induced. Its main role is in the recovery phase (Khoury *et al.*, 1992), which may explains why low levels are found day 15 p.d.i. when mice are still in the effector phase of disease.

Correlation was observed between the clinical and pathological scores of mice sampled 15 and 22 days after treatment with rSFV10-E-IFN-β particles on days 5,8,11 and 12. Overall, clinical and pathological scores were lower following treatment with rSFV10-E-IFN-β. Clinical and pathological scores were lower in treated and control mice at day 15 p.d.i. when animals were only beginning to show signs of disease. A typical grade 2+ lesion in the superficial white matter of a rSFV10-E-IFN-β treated animal was characterized by localised perivascular infiltrates of lymphocytes, macrophages and neutrophils and contrasted with grade 4+ lesions typical of TNE treated animals which showed extensive perivascular cuffing, myelin vacuolation and axonal degeneration.

Similar improvements in lesion severity have been described previously in different EAE models following treatment with IFN-β (Floris *et al.*, 2002; Ruuls *et al.*, 1996; Yu *et al.*, 1996). SWR × SJL/F mice with EAE showed a delayed progression to clinical disability accompanied by an overall decrease in severity of cellular inflammatory infiltrates and demyelination following s.c. inoculation with IFN-β (Yu *et al.*, 1996). Immunolabelling showed that effector T lymphocytes were mostly found in areas of myelin vacuolation and B cells, whose role in EAE remains controversial, were more

numerous in perivascular spaces of the meninges. Attempts using immunohistochemistry to distinguish the T cells into MHC class II restricted CD4+ and MHC class I restricted CD8+ cells proved unrewarding. Antibodies specific for these cells performed poorly on formalin-fixed paraffin embedded tissues despite the use of epitope unmasking procedures such as trypsinisation and antigen heat retrieval using both citrate buffer and EDTA buffer. Numerous large reactive astrocytes (gliosis) were prominent in areas of white matter vacuolation. Secretion of GM-CSF by the reactive astrocytes probably contributed to the accumulation of macrophages and to the development of demyelination. Intracellular immunolabelling of Th1, Th2, and other regulatory cytokines within the inflammatory lesion should have been carried out to support the *ex vivo* MOG T cell response data. Staining of IL-6, in particular, would have been interesting as IFN-β can upregulate the secretion of IL-6 from reactive astrocytes *in vitro* leading to both pro- and anti-inflammatory responses (Okada *et al.*, 2005). Further immunolabelling of the lesion may also have shown enhanced MHC class II expression on a variety of cell types, mediated by the presence of secreted IFN-β.

Using morphometrical studies, no differences were detected in numbers of T lymphocytes infiltrating lesions in the different treatment groups. However, lesions in rSFV10-E-IFN-β treated animals contained significantly fewer B lymphocytes than similar sized lesions in the control groups. Previous EAE studies have shown conflicting data regarding the role of B cells and the humoral response in EAE. Some studies have shown that B cells are not essential for the development of EAE but possibly play a role in recovery from disease (Wolf *et al.*, 1996). Other studies attribute a protective, regulatory role for B cells in EAE (Fillatreau *et al.*, 2002) and in yet other studies B cells are regarded as having an aggressive effector role (Lyons *et al.*, 1999). Similarly, myelin-reactive antibodies generated during EAE have been shown to play an important role in the development of demyelination (Morris-Downes *et al.*, 2002; Raine *et al.*, 1999). Improvement in EAE has been related to therapy with IFN-β and has been shown to markedly reduce the number of circulating $CD80^+$ B cells which are involved in the Th1 response (Hallal *et al.*, 2003). This finding could, at least in part, explain the results of the present study where fewer numbers of B lymphocytes and milder lesions occurred following treatment with rSFV-IFN-β. Reduced numbers of infiltrating B lymphocytes possibly lead to suppression of the anti myelin antibody response and associated demyelination in these animals.

Further immunological studies examined the percentage of total lymphocytes classified as CD4+, CD8+ and B lymphocytes 30 days after treatment with rSFV-IFN- β The cellular profile for both the TNE and the rSFV-IFN-β treated groups suggests one of recovery. As previously discussed B cells are thought to play a regulatory role in the recovery phase of disease through their ability to produce IL-10 (Fillatreau *et al.*, 2002). When IL-10 deficiency was restricted to B cells only and not T cells, the pro-inflammatory type 1 immune response persisted and mice did not recover. Both TNE and rSFV-IFN-β treated animals have higher percentage B cells than the empty particle treated animals and are in recovery or have fully recovered, while the empty particle treated animals are still displaying symptoms of EAE. A higher percentage of CD4+ T lymphocytes was measured in the splenocytes of the rSFV-IFN-β and TNE treated mice compared to the empty particle treated mice, which also correlates with recovery, as the key IL-10-producing cells within the CNS are the CD4+CD25+ T cell population which are critical to recovery from the disease (McGeachy and Anderton, 2005; McGeachy *et al.*, 2005). CD8+ cells constituted a higher percentage of splenocytes in recovering animals as well. Koh *et al.*, 1992 found that mice deficient for CD8+ cells developed a milder acute EAE, reflected by fewer deaths, but more relapses indicating a possible regulatory role in recovery. Treatment of MS with IFN-β promotes the proliferation of CD8+ cells and therefore the secretion of Th2 cytokines such as TGF-β, leading to improvement in disease (Javed and Reder, 2005). Little is known about the effect of IFN-β on CD8+ cells in EAE.

In conclusion, rSFV-IFN-β particles administered by i.n. inoculation were partially successful in the treatment of EAE only when fewer treatments were administered before the effector stage of disease. This improvement in disease severity was accompanied by improvement in clinical scores and pathology of the lesion, reduced IFN-γ Th1 response to peptide, inhibition of B lymphocytic infiltration into the lesions during the effector stage and increased levels of CD4+, CD8+ and B lymphocytes in recovery. This study showed some important trends but also highlighted some weaknesses. A greater number of animals should have been used in each treatment group to allow for more definite statistical differences to be seen and for further pathological studies, and the EAE experiments which yielded a negative result should have been repeated for confirmation. More immunolabelling should have been carried on spinal cord sections to examine the cytokine balance within the CNS lesion itself and also to establish the effect IFN-β is having on MHC class II expression on immune and CNS cells.

Chapter 5

The effect of co-administered rSFV-IFN-β and rSFV-IL-10 vectors, or rSFV-IFN-β and Cholera Toxin on the course of EAE

5.1 Introduction

One of the possible mechanisms of IFN-β efficacy in MS and EAE is through induction of soluble cytokines such as IL-10 (Byrnes *et al.*, 2002). IL-10 plays an important therapeutic role in both MS and EAE through its ability to inhibit cytokine production by Th1 cells, NK cells and monocyte-macrophages and suppress antigen specific proliferation of Th1 cells (Sagawa *et al.*, 1996). Previous work has shown an upregulation of IL-10 RNA in PBMC cultured with IFN-β *in vitro*, and increased serum and CSF IL-10 protein levels in MS patients after IFNβ-1a injection (Rudick *et al.*, 1998). There have been a number of other studies where IL-10 has been shown to ameliorate or completely suppress the course of EAE (Jerusalmi *et al.*, 2003; Nagelkerken *et al.*, 1997; Rott *et al.*, 1994; Xu *et al.*, 2000; Young *et al.*, 2000), while other studies showed the opposite effect (Cannella *et al.*, 1996; Croxford *et al.*, 1998). IFN-β treatment of different EAE models has resulted in the same upregulatory effect on IL-10 production (Tuohy *et al.*, 2000; Wang *et al.*, 2000; Yasuda *et al.*, 1999). Co-administration of IL-10 with encephalolitogenic MBP 68-86 autoantigen has been shown to suppress EAE in Lewis rats (Xu *et al.*, 2000) but no studies have been done on the co-administration of IL-10 and IFN-β, or any other cytokine, in the treatment of EAE.

CT, a major enterotoxin produced by *Vibrio cholerae*, has become a model immunogen and vaccine adjuvant through its ability to induce Th2 responses to co-administered foreign antigen. Studies have found that immunization of mice with antigen in the presence of CT induces a population of antigen specific CD4+ T cells that produces IL-4, IL-5, IL-6, IL-10 and TNF-α and inhibits the production of IL-12, suppressing the generation of Th1 cells (Lavelle *et al.*, 2004; Lavelle *et al.*, 2003; Williams *et al.*, 1999; Xu-Amano *et al.*, 1994). CT has also been successful in the treatment of autoimmune diseases such as EAE where the oral administration of CT subunit B either before or after disease induction has been shown to prevent EAE in Lewis rats when coupled to minute amounts of MBP (Sun *et al.*, 1996; Sun *et al.*, 2000). Low-dose orally administered CTB-MBP treatment greatly reduced the level of leukocyte infiltration into spinal cord tissue. In a more recent study CT was administered intranasally to treat EAE induced in C57/Bl mice (Yura *et al.*, 2001). Animals received one dose of 32μg of CT in 10μl PBS per nostril on day 7 p.d.i and experienced reduced disease severity as well mortality, and decreased IL-12 and IFN-γ levels.

The work described in this chapter was to co-administer either rSFV10-E-IL-10 particles or CT at the same time as rSFV10-E-IFN-β particles, or 24 h later, by intranasal inoculation in an attempt to boost the Th2 response and improve clinical disease. No previous studies have administered different cytokines simultaneously in the treatment of EAE, either by viral vectors or naked DNA plasmid. Due to the previous success shown in this C57/Bl 6/MOG 35-55 EAE model after treatment with intranasally administered CT, some improvement would be expected upon treatment with rSFV10-E-IFN-β particles and CT. To assess the immunological changes, the specific T cell responses to MOG 35-55, the levels of IFN-γ in the serum and the percentage of CD4+, CD8+ and B cells, which constitute the splenocyte, population was examined. Pathological analysis of the EAE lesions was also performed.

5.2 Materials and methods

5.2.1 Materials

5.2.1.1 SFV expression vectors

The SFV expression vectors, pSFV10-E, pSFV10-E-IFN-β and the split-helper vectors pSFV-Helper S2 and pSFV-Helper CS219A were obtained and used as previously described in section 2.2.1.1. The pSFV1-IL-10 expression vector was kindly donated by Dr. Alan Jerusalmi, former member of the Virology Group, Dept. of Microbiology, Trinity College, Dublin.

5.2.1.2 Molecular reagents

The following primers used for PCR amplification were from MWG Biotech AG (Germany). The restriction sites are shown in italics, Xho1 in the forward primer and Spe1 in the reverse primer :

Murine IL-10 F 5'-AAA*CTCGAG*ATGCCTGGCTCAGCA-3'

Murine IL-10 R 5'-GCC*ACTAGT*CGCTTAGCTTTTCAT-3'

Sequencing primers for the SFV nsP4 region were from Invitrogen (UK).

Nsp 4 F 5'- GCGAAGCTTGCTAACAGTGAAGACAAGC-3'

Nsp4 R 5'-GCCAAGCTTGCTGATGAGTTGCTGCATCT-3'

The following restriction enzymes Xho1, Spe1 and Nru1 were from New England Biolabs (NEB) (MA, USA). dNTP mixture, $MgCl_2$, recombinant RNasin ribonuclease inhibitor, Taq DNA polymerase, Mg^{2+} free polymerase reaction buffer, high efficiency T4 DNA Ligase, ligase buffer, nuclease free water, and lambda DNA marker were from Promega (Wisconsin, USA). The 500bp DNA molecular weight marker was from Roche. A 100bp DNA marker was from New England Biolabs (NEB) (MA, USA). The PCR cleanup, nucleotide extraction and gel extraction kits were from Qiagen Ltd. (West Sussex, UK). Plasmid purification kits for plasmid-preps were from Qiagen Ltd. SP6 RNA polymerase, cloned FPLC pure, $m^7G(5')ppp(5')G$, sodium and nucleoside 5'-triphosphate mix were from Amersham Pharmacia Biotech (Uppsala, Sweden).

5.2.1.3 Cell culture

BHK-21, murine L292 cells and sBHK cells were obtained and cultured as previously described in section 2.2.1.2 and 2.2.2.1.

5.2.1.4 Particle production

Materials for particle production were as described in section 2.2.6.

5.2.1.5 Antibodies

Purified rat anti-mouse IL-10 monoclonal antibody was purchased from BD Pharmingen, UK. Purified rat anti-mouse CD4 (L3T4) monoclonal antibody, purified rat anti-mouse CD8a (Ly-2) monoclonal antibody, purified rat anti-mouse C45R/B220 monoclonal antibody and purified rat IgG2aκ immunoglobulin (isotype control) for FACS analysis were also from BD Pharmingen, UK. Biotinylated rabbit anti-rat (mouse absorbed) secondary antibody, normal rabbit serum and the VECTASTAIN ABC reagents were from Vector Laboratories Inc. (USA). The anti-SFV nsP4 antibody was donated by Dr. Marina Fleeton (Virology group, Dept. of Microbiology, Trinity College). Streptavidin-FITC was purchased from Dako (Denmark).

5.2.1.6 Mice

Specific pathogen free C57/Bl6 mice were purchased from Harlan (Bicester, UK) and were maintained as previously described 2.2.1.3.

5.2.1.7 EAE induction

Materials as previously described in section 3.2.1.3 for induction of EAE in C57/Bl6 mice.

5.2.1.8 Histopathological studies

Materials as previously described in section 3.2.1.6.

5.2.1.9 Splenocyte stimulation assays

Materials as described previously in section 3.2.1.4.

5.2.1.10 FACS analysis

Becton Dickinson FACSCalibur E4687 cytometer and WinMDI (Windows Multiple Document Interface for Flow Cytometry) software program were used for FACS analysis.

5.2.1.11 Enzyme Linked ImmunoSorbant Assay

ELISA sets for the detection of murine IL-10 and IFN-γ were from BD Pharmingen.

5.2.1.12 Miscellaneous

Ethanol:Acetic acid was prepared from 50% ethanol and 50% glacial acetic acid, both from BDH Ltd, UK. H_2O_2, Harris's Haematoxylin and DPX were also purchased from BDH Ltd., UK. DAB substrate came from Sigma (UK). 4% (w/v) paraformaldehyde was made from 20g PFA dissolved in 500ml distilled H_2O. Sodium chloride was from Sigma (UK) and 1M Hepes buffer came from Gibco (UK). High salt buffer (10mM Hepes buffer: 0.5M NaCl) was made from 5ml of 1M Hepes buffer and 50ml of 5M NaCl made up to 500 ml with distilled water. Streptavidin-FITC was purchased from Dako (Denmark). Hard set mounting medium with DAPI came from Vector laboratories Inc. (CA, USA). Whole CT (1×10^5 –1×10^6 units/mg protein) was purchased from Sigma (UK) and was kindly purified using endotoxin removal columns to remove contaminating LPS by Dr. Ed Lavelle, The Immune Regulation Research Group, Dept. of Biochemistry, Trinity College Dublin. XL gold competent cells were from Stratgene (USA). 100ml NZY broth was supplemented with 1.25ml of 1M $MgCl_2$, 1.25ml of 1M $MgSO_4$ and 1ml of 2M glucose for transformation of ultracompetent XL gold cells.

5.2.2 Methods

5.2.2.1 Insert of murine IL-10 into pSFV10-E

See Figure 5.1 for cloning strategy.

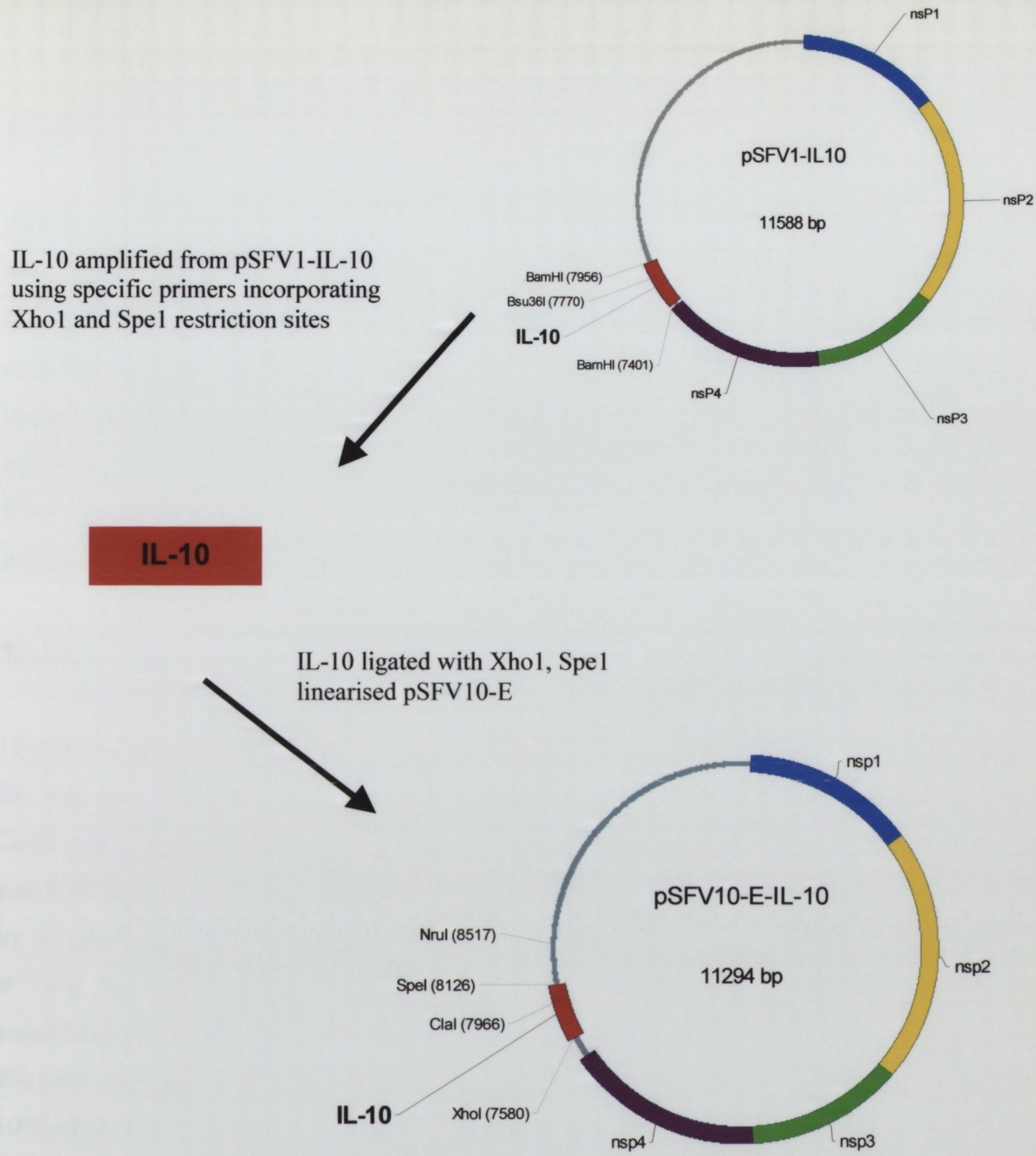

Figure 5.1 Strategy for cloning of IL-10 into pSFV10-E

IL-10 was amplified from pSFV1-IL-10 using specific primers incorporating Xho1 and Spe1 restriction sites and cloned into the more novel pSFV10-E.

5.2.2.1.1 Growth of recombinant rSFV1-IL-10

Competent *E.coli* DH5α cells were prepared and transformed with SFV plasmids, pSFV1-IL-10 and pSFV10-E, as previously described in section 2.2.2.8. Plasmid DNA was isolated from overnight culture broth after inoculation with a transformed *E.coli* colony using Qiagen mini prep kit according to manufacturer's protocol. Plasmid concentration was assessed by mixing a 1μl aliquot of plasmid DNA with 2μl loading buffer and 9μl 1X TBE, and running this on a 0.8% (w/v) agarose gel (0.2g agarose, 2.5μl ethidium bromide (10mg/ml) in 25ml TBE). The concentration of plasmid was estimated from this gel by comparing band intensity with that of the Lambda molecular weight marker [10μl Lambda (Hind111 & EcoR1), 20μl loading buffer, 90μl 1X TBE].

5.2.2.1.2 PCR

Six PCR reactions were carried out to amplify the IL-10 gene from the pSFV1-IL-10 plasmid using new IL-10 F and R primers (Figure 5.2). Each reaction mix contained the following reagents in total 100μl volumes: 0.5μg rSFV1-IL-10 DNA, 0.2mM dNTPs, 2mM $MgCl_2$, 1X Mg^{2+} free polymerase reaction buffer, 1μM forward and reverse primers and 5.0U of Taq DNA Polymerase. Samples were incubated for 2 min at 95°C, followed by 30 cycles of denaturation at 95°C for 30 sec, annealing at 55 °C for 30 sec and extension at 72°C for 4 min. A final extension time of 5 min at 72°C was used and 5μl of the amplified products (5μl PCR prodcut, 2μl loading dye, 15μl 1X TBE) were analyzed on 2% (wt/vol) agarose gel stained with ethidium-bromide (0.5g agarose, 25ml 1X TBE and 10% ethidium bromide).

5.2.2.1.3 Linearisation of pSFV10-E for cloning

Prior to cloning, pSFV10-E was digested with Xho1 and Spe1 restriction enzymes to linearise the plasmid in six reaction mixtures as follows: 10μl plasmid (0.47μg/μl), 5μl 10X buffer 2, 5μl 10X BSA, 2μl (20U) Xho1, 2μl (20U) Spe1 and 26μl H_20. The digested plasmid was analyzed by electrophoresis of 1 μl aliquot of each reaction mixture on a 1.0% (w/v) agarose gel. Nucleotide clean up was then performed on the digested reaction mixtures. Two 50μl reactions were applied to each column and eluted in 30μl nuclease free H_2O, resulting in total volume of 90μl.

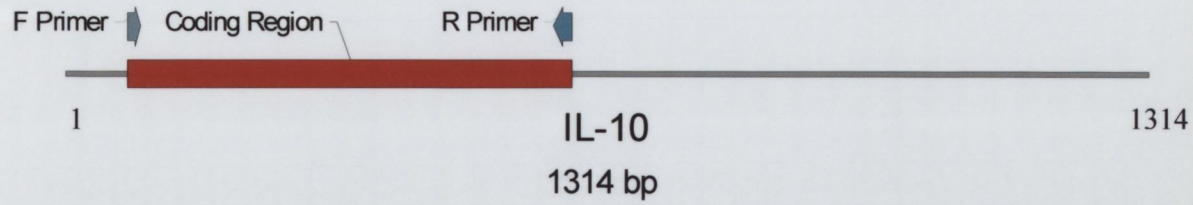

Coding region within the IL-10 gene

atgcctggctcagcactgctatgctgcctgctcttactgactggcatgaggatcagcaggggccagtacagccgggaagacaata
actgcacccacttcccagtcggccagagccacatgctcctagagctgcggactgccttcagccaggtgaagactttctttcaaaca
aaggaccagctggacaacatactgctaaccgactccttaatgcaggactttaagggttacttgggttgccaagccttatcggaaatg
atccagttttacctggtagaagtgatgccccaggcagagaagcatggcccagaaatcaaggagcatttgaattccctgggtgaga
agctgaagaccctcaggatgcggctgaggcgctgtcatcgatttctcccctgtgaaaataagagcaaggcagtggagcaggtga
agagtgattttaataagctccaagaccaaggtgtctacaaggccatgaatgaatttgacatcttcatcaactgcatagaagcatacat
gatgatcaaaatgaaaagctaa

Figure 5.2 IL-10 coding gene sequence

The coding region of the mouse IL-10 gene is a 537 bp sequence, which contains the precursor and mature form of the gene required for production and secretion of protein by cells. The forward primer was designed to include the first 15 nucleotides of this region, as well as an Xho1 restriction site. The reverse primer was designed to include the final 15 nucleotides of the coding region of the IL-10 gene, and a Spe1 restriction site.

5.2.2.1.4 Preparation of the IL-10 insert

Following PCR amplification, IL-10 products were purified using the Qiagen PCR purification protocol, eluted in 30 µl nuclease free water and then digested with Xho1 and Spe1 to create the necessary 'sticky' ends. Digestion mixtures were as follows: 10µl DNA, 26µl H_2O, 5µl buffer 2, 5µl 10X BSA, 20 U Xho1 and 20 U Spe1. After 2 h at 37°C, these digestion reactions were pooled (6 x 50µl) and then further concentrated on a column. 300µl of membrane binding solution was added to the pooled digests. The total 600µl mixture was added to a nucleotide removal column and the column was centrifuged for 1 min at 14,000rpm (10000g). DNA was eluted in 17µl of nuclease free H_2O. 1µl of eluate was quantified on a 1.5% gel, together with 1µl of Xho1, Spe1 linearised pSFV10-E (1µl DNA, 9µl 1X TBE, 2µl loading dye) using 100bp and 500bp DNA ladders.

5.2.2.1.5 Ligation reaction

Linearised pSFV10-E and IL-10 product were mixed at a ratio of 1:10 in a 20µl ligation mixture containing 1 unit T4 high efficiency DNA ligase and 10µl ligase buffer and the mixture incubated overnight at 25°C. This ligation mixture was transformed into XL10 gold ultracompetent cells. These cells provide 20 to 30 fold higher transformation efficiency of ligated DNA. A 90µl volume of cells was added to a pre-chilled 15ml falcon tube on ice, and 4µl of β-mercaptomethanol was then added to the cells. After a 10 min incubation on ice, 9µl of ligation mixture was added to the bacterial mix. The tube was swirled gently and then incubated on ice for another 30 min. The tube was then heat pulsed in a 42°C water bath for 30 sec, after which it was returned to the ice for a further 2 min. 0.9ml of preheated NZY + broth was added and the tube was incubated at 37°C for 1 h with shaking at 225-250 rpm. 200µl of the mixture was plated out on agar plates containing 100µg/ml ampicillin. Plates were incubated overnight at 37°C to allow colony growth. To confirm the presence of insert in the vector, 23 colonies were inoculated into 10ml LB broth containing 100µg/ml ampicillin and incubated on a shaker at 37°C overnight. Plasmids were purified from broth culture using the Qiagen mini-prep kit, and the size compared to pSFV10-E by agarose gel electrophoresis.

5.2.2.1.6 Screening for IL-10 insert

Plasmid mini preps were screened for the presence of IL-10 insert by digestion with Xho1 and Spe1 restriction enzymes, and digests were run on a 2.0% (w/v) agarose gel. Digestions were carried out as follows: 5µl DNA, 2µl 10X BSA, 2µl buffer 2, 0.5µl Xho1, 0.5µl Spe1 and 10µl H_2O. 2µl loading dye was added to the mixture after digestion and ran on a 2% gel with a 500bp ladder. Nine positive clones were obtained in total and four of these were sent for sequencing with the anti-SFV nsP4 sequencing primers to confirm correct sequence.

5.2.2.2 Expression of IL-10 *in vitro*

Expression of IL-10 from rSFV10-E-IL-10 vectors was detected by electroporating 1.5µg of *in vitro* transcribed linearised plasmid into BHK-21 cells and carrying out immunohistochemical labelling to detect IL-10 expression. Immunohistochemical labelling was carried out as previously described in section 2.2.5.3 with purified rat anti-mouse monoclonal IL-10 antibody (1:100 dilution) used to detect IL-10 expression and biotinylated rabbit anti-rat secondary antibody used to detect bound primary antibody (1:200 dilution in rabbit blocking buffer). Labelled cells were visualised with DAB chromogen as before and examined under a bright field microscope (x200).

5.2.2.3 rSFV10-E-IL-10 particle production and titration

High titre rSFV10-E-IL-10 particles were produced as previously described in section 2.2.6 for production of rSFV-IFN-β particles. rSFV10-E-IL-10 vector was linearised with Nru1 restriction enzyme prior to *in vitro* transcription and electroporation into sBHK cells. Viral particles were harvested and titrated as described in sections 2.2.6.4 and 2.2.6.5, using the purified rat anti-mouse IL-10 monoclonal antibody for titration. Particle titres were obtained by examining cells microscopically for the presence of IL-10 using a specific FITC filter. Particle titres were calculated at a magnification of x400 and expressed as IU/ml. The anti-SFV nsP4 antibody was used for titration of SFV empty particle controls as before.

5.2.2.4 Quantification of IL-10 expression from rSFV10-E-IL-10 particles

BHK-21 and L929 cells were cultured as described in section 2.2.2.1 and seeded at a concentration of 1×10^6 cells per well of six well plates in 2ml volume. Both cell lines were infected with rSFV10-E-IL-10 particles and rSFV10-E empty particles at MOIs 1, 10, 100 and mock-infected with TNE buffer, and incubated at 37°C, 5% CO_2 for 24 h. All supernatant samples were then centrifuged at 14,000rpm (10000g) for 5 min, 4°C to remove cell debris, aliquoted and frozen at –70°C until they were assayed for the presence of IL-10. Supernatant samples were tested for the presence of IL-10 by use of a capture ELISA specific for mouse IL-10. Wells of a 96 well plate were coated with 100 µl/well of capture antibody diluted in coating buffer (1:250 dilution), and incubated overnight at 4°C. Wells were washed 3 times with 300µl/well of wash buffer, and plates blocked for 1 h at RT with 200µl/well of assay diluent (10% heat inactivated FBS in PBS). Wells were again washed 3 times with wash buffer, and incubated sealed for 2 h at RT with 100µl/well of either standard IL-10 (serial dilutions in assay diluent) or supernatant samples. Plates were washed as before with 5 total washes, and then incubated sealed for 1 h at RT with 100 µl/well of working detector (detection antibody and avidin-HRP reagent diluted 1:250 in assay diluent). Plates were again washed as before, but with 7 total washes. 100µl/well of TMB substrate was added, and plates incubated at RT in the dark for 30 min, before addition of 50µl stop solution (2N H_2SO_4). Absorbance was read at 450nm within 30 min of adding stop solution.

5.2.2.5 EAE induction

EAE was induced in 91 C57/Bl 6 mice with MOG 35-55 peptide as previously described in section 3.2.2.5. Each mouse was immunized with 100µg of the peptide emulsified in the enriched adjuvant as before. 6.0mg of peptide was dissolved in 9.0ml of PBS, and mixed with 9.0ml of enriched adjuvant in a 20ml plugged syringe, and this was repeated, to prepare enough mix for 120 mice and allow for loss. Immunization was repeated 7 days later and mice also received 200ng of pertussis toxin on days 0,1,7,8 by i.p inoculation. Animals were monitored daily and clinical disease was graded day 8 onwards according to the standard neurological scale previously used. Weight loss was also monitored.

5.2.2.6 Intranasal treatment of EAE with rSFV10-E-IFN-β and rSFV10-E-IL-10 particles, and whole Cholera toxin

On days 5, 8, 11 and 12 post disease induction five groups of 13 animals received intranasal treatment with rSFV10-E-IL-10 particles alone, rSFV10-E-IFN-β particles alone, rSFV10-E-IFN-β particles and rSFV10-E-IL-10 particles together, rSFV10-E empty particles and TNE buffer alone. A further two groups of 13 were treated with rSFV10-E-IFN-β particles and CT, or rSFV10-E particles and CT. For co-administration of rSFV10-E-IL-10 and rSFV10-E-IFN-β particles, each animal was inoculated intranasally with a total of 10^7 IU, each particle vector constituting half the infectious dose, in a volume of 20μl per nostril. Animals receiving combinational treatment with either rSFV10-E-IFN-β or SFV10-E empty particles, and CT toxin, received particle treatments on days 5, 8, 11 and 12 as before in section 4.2.2.4, with CT toxin administered on days 5, 9 and 12. 0.5μg of CT toxin was administered by intranasal inoculation each time in a 20μl volume per nostril. Both rSFV particles and CT was diluted to the required concentrations in TNE buffer, prior to inoculation. Three mice from each group designated for pathological studies were perfused and spleens were excised day 22 post disease induction. Spleens were excised, harvested and frozen as previously described in section 3.2.3.0.

5.2.2.7 Histopathological studies

Paraffin embedding, sectioning and staining were performed by Ms. Alex Whelan-Buckley, and pathological analysis was performed by Prof. Brian Sheahan, Dept. of Veterinary Pathology, University College Dublin. As before, lesions were graded using a semi-quantitative five point system with one plus for isolated focal lesions and five plus for lesions that were diffuse and severe (sections 3.2.2.7, 3.2.2.8, 3.2.2.9) .

5.2.2.8 Splenocytes stimulation assay and serum cytokine levels

Splenocytes taken from mice perfused day 22 were seeded in a 24 well culture plate as previously described in section 3.2.3.1. Cells were stimulated with 5 or 10μg/ml MOG 35-55 peptide, and with 5μg Con A as a positive control for 72 h at 37°C. Cell supernatant was harvested and the levels of IFN-γ and IL-10 present in the supernatant was detected using ELISA sets specific for these cytokines. Blood was also collected from these animals after cardiac puncture by Pasteur pipette and added to 1ml eppendorf tubes. The tubes were incubated at 37°C for 1 h and then centrifuged at 3000rpm (2730g), 4°C to

separate the serum from the red blood cells. The serum was collected and the levels of IFN-γ and IL-10 were measured using ELISA. Statistical analysis was done using two way ANOVA and Bonferroni post-tests (Prism 4.0).

5.2.2.9 FACS analysis

FACS analysis was carried out on splenocytes harvested from each treatment group at day 22. Splenocytes were immunolabeled with antibodies specific for B cells, CD4+ T cells and CD8+ T cells as described in section 4.2.3.2 to distinguish the percentage of each cell type present. The labeled cells were analyzed using a Becton Dickinson FACS caliber E4687 FACS machine and the actual percentage readings were derived using the WinMDI software program for analysis of FACS data. Statistical analysis was done using two way ANOVA and Bonferroni post-tests (Prism 4.0).

5.3 Results

5.3.1 Cloning and expression of IL-10 in pSFV10-E

IL-10 was amplified from rSFV1-IL-10 by PCR (Figure 5.3). The PCR product (537bp + 6 random bases + 12bp for Xho1, Spe1 restriction sites = 555bp) was digested with Xho1 and Spe1 and the resultant product (537bp + 10 bp = 547bp) was ligated with Xho1, Spe1 linearised pSFV10-E to facilitate construction of rSFV10-E-IL-10 (Figure 5.4). Nine rSFV10-E- IL-10 clones were obtained by digestion of multiple plasmid preps with Xho1 and Spe1 (Figure 5.5). Four out of the nine clones were sent for sequencing with SFV nsp4 primers. The resultant sequences were compared with the original coding sequence for mouse IL-10 from GenBank database. A sequence homology of 100% was obtained with the original coding sequence of murine IL-10 for each of the clones (Figure 5.6). IL-10 expression was confirmed in BHK-21 cells transfected by electroporation with *in vitro* transcribed rSFV-IL-10 RNA using immunohistochemistry. Diffuse brown cytoplasmic staining was evident in rSFV10-E-IL-10 electroporated BHK-21 cells 24 h post electroporation (Figure 5.7A). No staining was evident in the PBS electroporated cells or rSFV10-E electroporated cells (Figure 5.7B&C). To quantify the level of IL-10 produced by rSFV10-E-IL-10 particles, BHK-21 and murine L929 cells were infected with rSFV-IL-10 particles at MOIs of 1,10 and 100 and the supernatant harvested after 24 h and tested for the presence of IL-10. High levels of IL-10 expression were detected in both cells lines after rSFV10-E-IL-10 infection (Figure 5.8). Greater expression of IL-10 was found in BHK-21 cells than in L929 cells after 24 h, with levels reaching 1×10^3 ng/ml. Minimal expression was found in both cell lines infected with rSFV10-E particles and mock- infected with TNE.

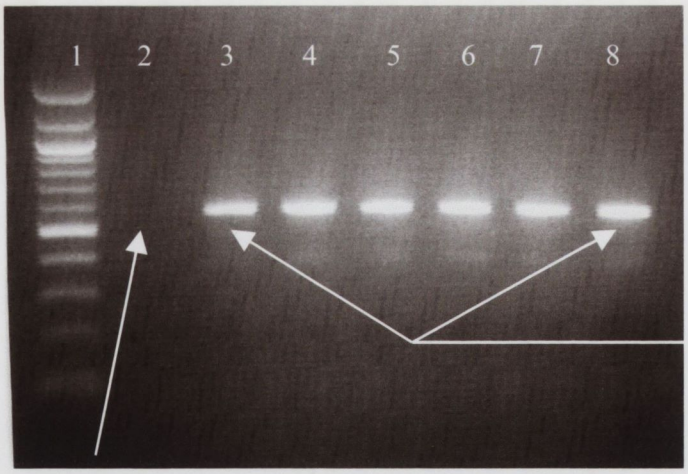

Six IL-10 products, 555bp in size, after PCR of pSFV1-IL-10 using IL-10 specific primers incorporating Xho1 and Spe1 sites

H_2O PCR control - DNA

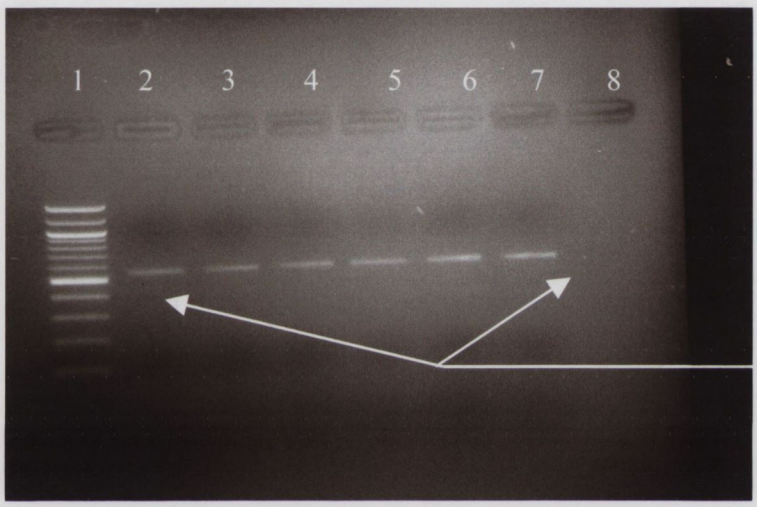

Double Xho1, Spe1 digested IL-10 PCR products (547bp in size) in preparation for pSFV10-E cloning

Figure 5.3 PCR amplification of IL-10 gene from pSFV1-IL-10

5µl of PCR products were run on a 2.0% agarose gel (5µl DNA, 2µl loading dye and 13µl 1X TBE) along with a 100bp marker to ensure the IL-10 gene was successfully amplified (A). IL-10 PCR products were digested with Xho1 and Spe1 to create the correct sticky ends for pSFV10-E cloning. The digests were run on a 2.0% gel prior to pooling and quantification with linearised pSFV10-E (B).

(A) Lane 1: 100bp DNA ladder, Lane 2: H_2O control (no DNA), Lanes 3-8: 5µl IL-10 PCR products amplified from pSFV1-IL-10 (537bp gene + 6 random bp + 12bp for Xho1+Spe1 restriction sites = 555 bp)

(B) (B) Lane 1: 100bp DNA ladder, Lanes 2-7: 1µl Xho1, Spe1 digested IL-10 PCR products (537bp + 10bp = 547bp)

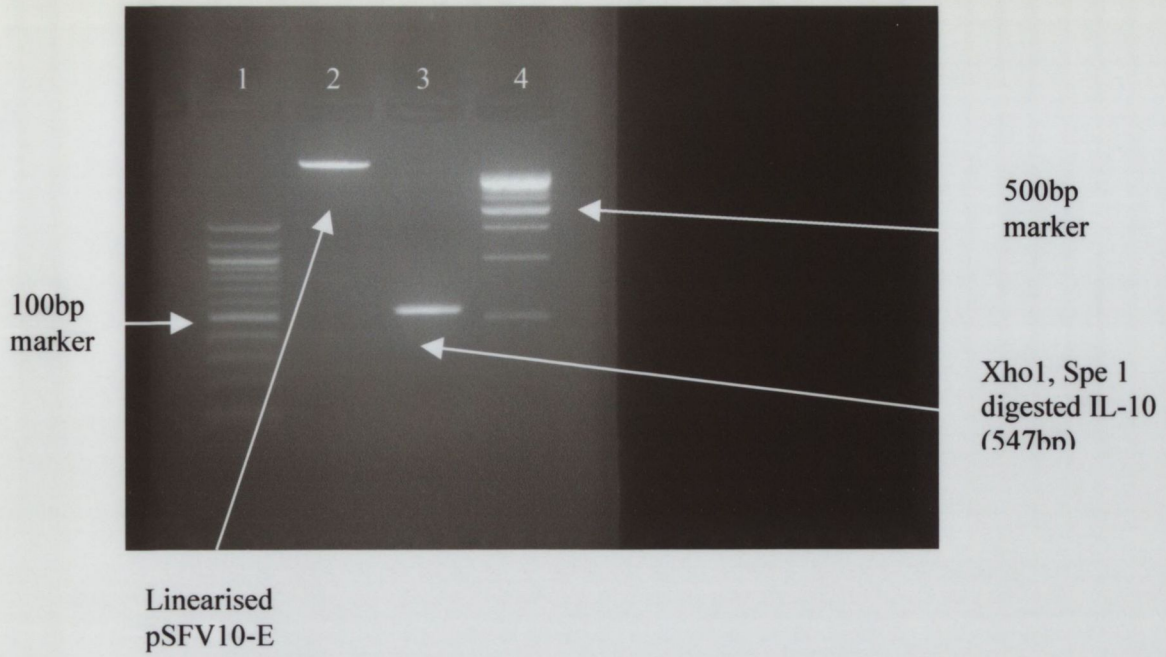

Figure 5.4 Quantification of pSFV10-E plasmid and IL-10 PCR product for ligation

Both pSFV10-E and the IL-10 PCR product were digested with Xho1 and Spe1 restriction enzymes to give the correct 'sticky ends' for ligation. Equal volumes of linearised pSFV10-E and Xho1, Spe1 digested IL-10 were run on a 2.0% agarose gel to allow a ratio to be established for the ligation reaction (1µl DNA, 2µl loading dye and 9µl 1X TBE).

Lane 1: 100bp DNA ladder, Lane 2: 1µl of Xho1, Spe1 linearised pSFV10-E, Lane 3: 1µl of Xho1, Spe1 digested IL-10 (537bp + 10bp site= 547bp), Lane 4: 500bp marker

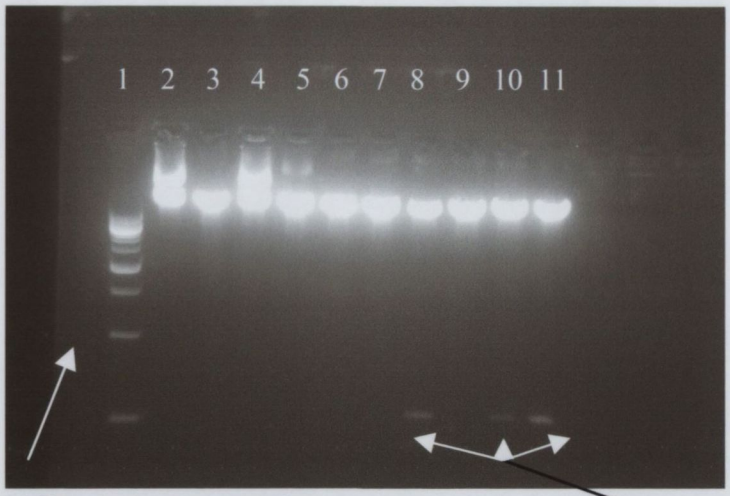

A

500bp marker

Xho 1, Spe 1 digested plasmid preps with IL-10 insert

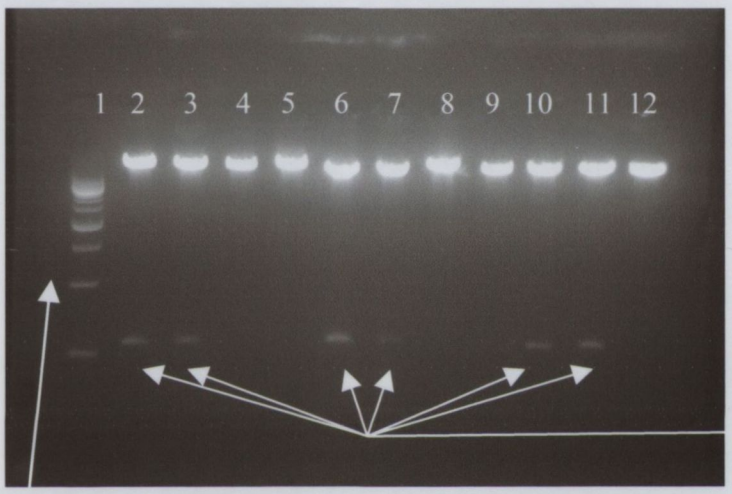

Xho 1, Spe 1 digested plasmid preps with IL-10 insert

B

500bp marker

Figure 5.5 Cloning of IL-10 into pSFV10-E

IL-10 was successfully subcloned from pSFV1 into the enhanced vector pSFV10-E. Nine positive clones were found upon double digestion with Xho1 and Spe1 restriction enzymes. Digests were run on a 2.0% gel to show the IL-10 band of 547bp (537bp gene + 10bp for restriction sites= 547bp).

(A) Lane 1: 500bp DNA ladder, Lanes 8,10 &11: Presence of IL-10 insert in Xho1, Spe1 double digested mini preps, Lanes 2-7 & 9: Xho1, Spe1 digested mini preps without IL-10 insert

(B) Lane 1: 500bp DNA ladder, Lanes 2, 3, 6, 7, 10 & 11 : Presence of IL-10 insert in Xho1, Spe1 double digested mini preps, Lanes 4, 5, 8, 9 & 12: Xho1, Spe1 digested mini preps without IL-10 insert

gi|330436|gb|M11924.1|HS4SUR Epstein-Barr virus B95-8, 12kb shor 61.9 4e-06

Alignments

>gi|6754317|ref|NM_010548.1| Mus musculus interleukin 10 (Il10), mRNA
Length=1314

Score = 1065 bits (537), Expect = 0.0
Identities = 537/537 (100%), Gaps = 0/537 (0%)
Strand=Plus/Plus

```
Query  489   ATGCCTGGCTCAGCACTGCTATGCTGCCTGCTCTTACTGACTGGCATGAGGATCAGCAGG  548
             ||||||||||||||||||||||||||||||||||||||||||||||||||||||||||||
Sbjct  76    ATGCCTGGCTCAGCACTGCTATGCTGCCTGCTCTTACTGACTGGCATGAGGATCAGCAGG  135

Query  549   GGCCAGTACAGCCGGGAAGACAATAACTGCACCCACTTCCCAGTCGGCCAGAGCCACATG  608
             ||||||||||||||||||||||||||||||||||||||||||||||||||||||||||||
Sbjct  136   GGCCAGTACAGCCGGGAAGACAATAACTGCACCCACTTCCCAGTCGGCCAGAGCCACATG  195

Query  609   CTCCTAGAGCTGCGGACTGCCTTCAGCCAGGTGAAGACTTTCTTTCAAACAAAGGACCAG  668
             ||||||||||||||||||||||||||||||||||||||||||||||||||||||||||||
Sbjct  196   CTCCTAGAGCTGCGGACTGCCTTCAGCCAGGTGAAGACTTTCTTTCAAACAAAGGACCAG  255

Query  669   CTGGACAACATACTGCTAACCGACTCCTTAATGCAGGACTTTAAGGGTTACTTGGGTTGC  728
             ||||||||||||||||||||||||||||||||||||||||||||||||||||||||||||
Sbjct  256   CTGGACAACATACTGCTAACCGACTCCTTAATGCAGGACTTTAAGGGTTACTTGGGTTGC  315

Query  729   CAAGCCTTATCGGAAATGATCCAGTTTTACCTGGTAGAAGTGATGCCCCAGGCAGAGAAG  788
             ||||||||||||||||||||||||||||||||||||||||||||||||||||||||||||
Sbjct  316   CAAGCCTTATCGGAAATGATCCAGTTTTACCTGGTAGAAGTGATGCCCCAGGCAGAGAAG  375

Query  789   CATGGCCCAGAAATCAAGGAGCATTTGAATTCCCTGGGTGAGAAGCTGAAGACCCTCAGG  848
             ||||||||||||||||||||||||||||||||||||||||||||||||||||||||||||
Sbjct  376   CATGGCCCAGAAATCAAGGAGCATTTGAATTCCCTGGGTGAGAAGCTGAAGACCCTCAGG  435

Query  849   ATGCGGCTGAGGCGCTGTCATCGATTTCTCCCCTGTGAAAATAAGAGCAAGGCAGTGGAG  908
             ||||||||||||||||||||||||||||||||||||||||||||||||||||||||||||
Sbjct  436   ATGCGGCTGAGGCGCTGTCATCGATTTCTCCCCTGTGAAAATAAGAGCAAGGCAGTGGAG  495

Query  909   CAGGTGAAGAGTGATTTTAATAAGCTCCAAGACCAAGGTGTCTACAAGGCCATGAATGAA  968
             ||||||||||||||||||||||||||||||||||||||||||||||||||||||||||||
Sbjct  496   CAGGTGAAGAGTGATTTTAATAAGCTCCAAGACCAAGGTGTCTACAAGGCCATGAATGAA  555

Query  969   TTTGACATCTTCATCAACTGCATAGAAGCATACATGATGATCAAAATGAAAAGCTAA  1025
             ||||||||||||||||||||||||||||||||||||||||||||||||||||||||
Sbjct  556   TTTGACATCTTCATCAACTGCATAGAAGCATACATGATGATCAAAATGAAAAGCTAA  612
```

Figure 5.6 IL-10 coding region in pSFV10-E-IL-10 sequence analysis

The IL-10 sequence obtained using anti-SFV nsP 4 sequencing primers were blasted against the original IL-10 sequence from the Genbank database. 100% identity of sequence was found with the original sequence. Further restriction analysis and *in vitro* expression studies confirmed expression.

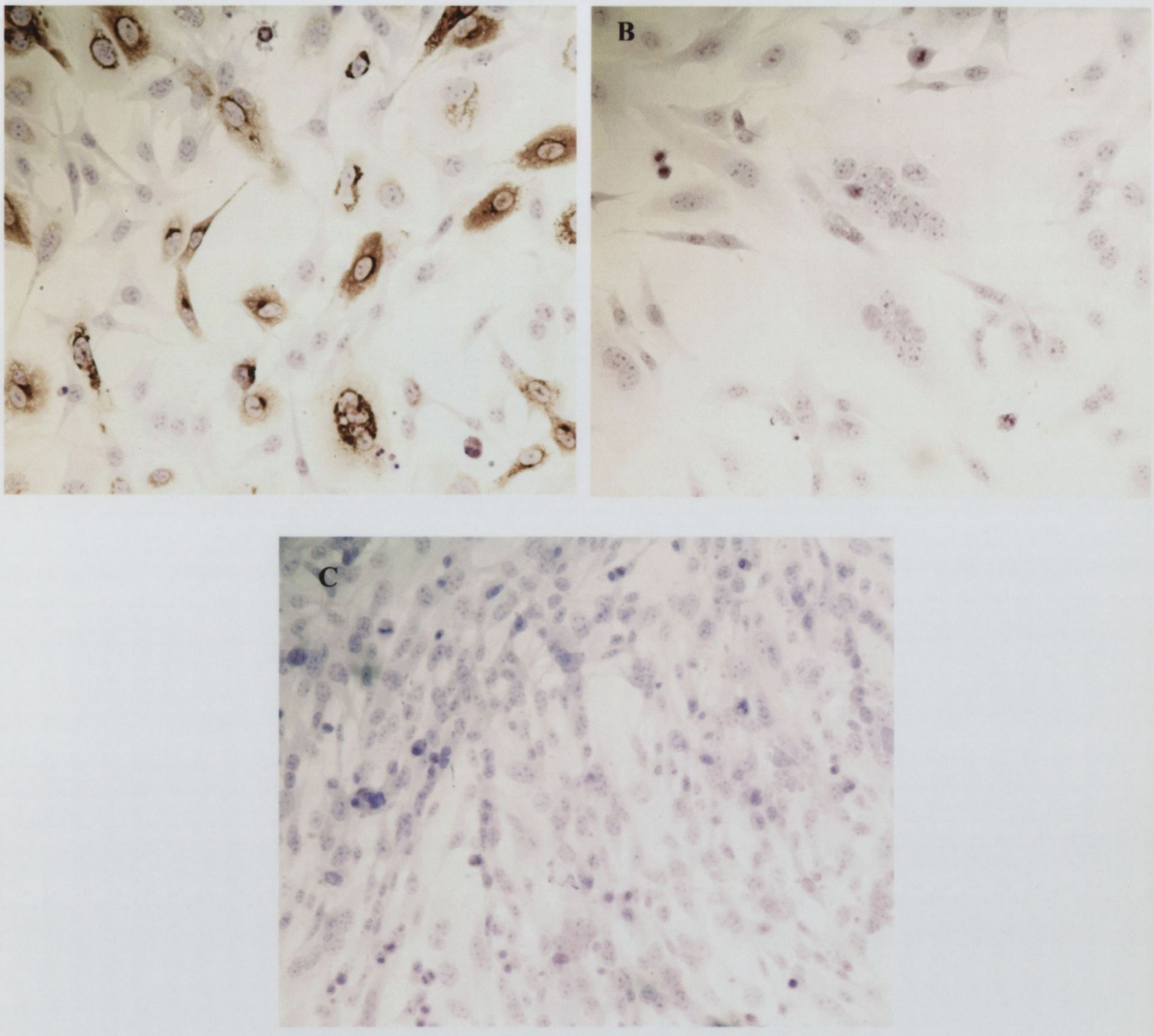

Figure 5.7 Expression of rSFV10-E-IL-10 in BHK-21 cells

rSFV10-E-IL-10 electroporated BHK-21 cells were labelled for the presence of IL-10 using a rat anti-murine IL-10 monoclonal antibody and Vectastain Elite HRP biotin system. Staining was visualised using DAB substrate and slides were counterstained with Haematoxylin Harris and ammonia water. Stained cells were examined using bright field microscopy. Diffuse cytoplasmic staining was evident in the cells electroporated with rSFV10-E-IL-10 (x400) (A). No staining was evident in cells electroporated with RNA from linearised rSFV10-E plasmid or mock-electroporated BHK-21 cells which were included as negative controls (B)&(C), (x400) & (x200) respectively.

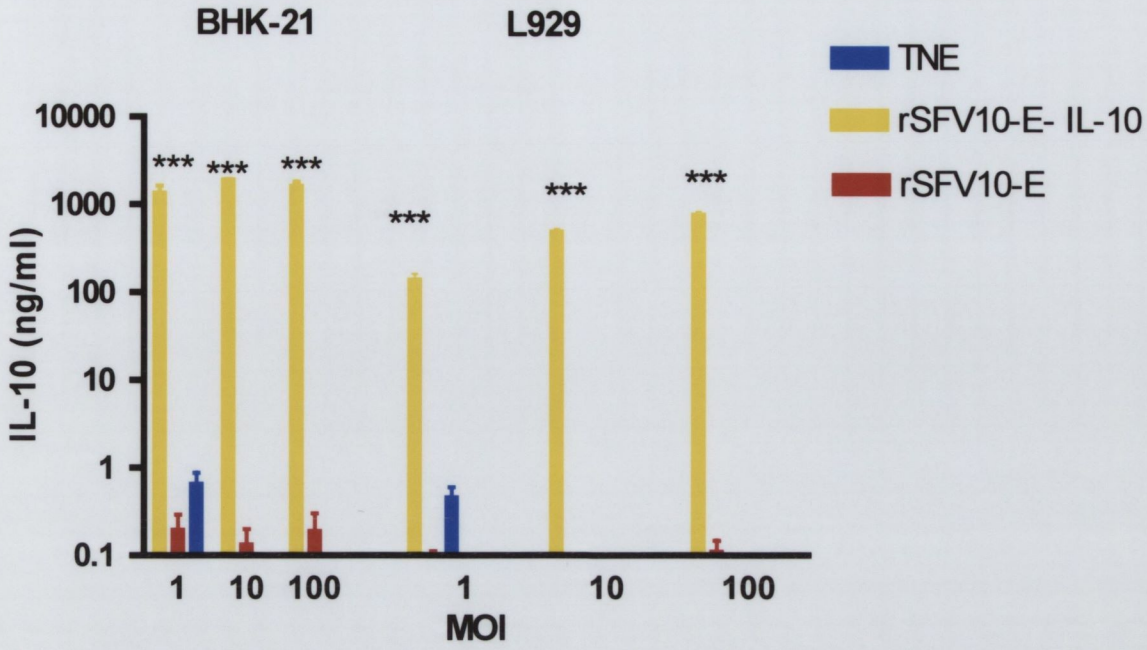

Figure 5.8 Comparison of *in vitro* expression of IL-10 from rSFV10-E-IL-10 particles in different cell lines

Overall rSFV10-E-IL-10 particles produced higher levels of IL-10 expression than rSFV10-E particles in both cell lines at MOIs 1, 10 and 100, with levels reaching $1X10^3$ ng/ml ($p<0.001$). rSFV10-E-IL-10 infected BHK cells produced more IL-10 than rSFV10-E-IL-10 infected L929 cells at all MOIs ($p<0.001$). Mock-infected cells produced minimal levels of IL-10 in both cell lines. Note that the y axis has a logarithmic scale. IL-10 levels were measured in the supernatant of rSFV-IL-10 infected cells using an IL-10 ELISA kit (BD Pharmingen). Concentration was expressed in ng/ml.

5.3.2 Co-administration of rSFV10-E-IFN-β and rSFV10-E-IL-10 particles in the treatment of EAE

EAE was induced in C57/Bl6 mice and five groups of 13 animals were treated with co-administered rSFV10-E-IFN-β and rSFV10-E-IL-10 particles, rSFV10-E-IFN-β particles alone, rSFV10-E-IL-10 particles alone and TNE buffer alone on days 5,8,11,12. Treatment with both rSFV10-E-IFN-β and rSFV10-E-IL-10 particles did slow down disease progression compared to empty particle, rSFV-IL-10 particle and TNE treated mice up to day 19 post disease induction but treatment with rSFV10-E-IFN-β was still more effective showing significant improvement in disease severity compared to the controls ($p<0.01$) (Figure 5.9A). Treatment with rSFV10-E-IL-10 particles alone showed no improvement and enhanced disease severity compared to the TNE control. Discontinuation of treatment with rSFV10-E-IFN-β and rSFV10-E-IL-10 particles and rSFV10-E-IFN-β particles alone led to disease progression. rSFV10-E-IFN-β animals experienced the least amount of weight loss compared to the other groups ($p<0.001$) (Figure 5.9B).

5.3.3 Specific T cells responses to MOG 35-55 *ex-vivo* after rSFV-IFN-β and rSFV-IL-10 treatment

Splenocytes were harvested from mice perfused day 22 post disease induction and T cell responses were measured after MOG 35-55 stimulation. Overall the highest levels of IFN-γ were produced from splencoytes of rSFV10-E animals in response to stimulation (Figure 5.10A). The animals that received both rSFV10-E-IFN-β and rSFV10-E-IL-10 produced levels of IFN-γ comparable to the animals that received individual particle treatments and TNE buffer alone. The double particle treated animals produced marginally more IFN-γ and the rSFV10-E-IFN-β treated produced marginally less. Lower levels of IL-10 were produced overall with no significant differences seen between the treatment groups (Figure 5.10B).

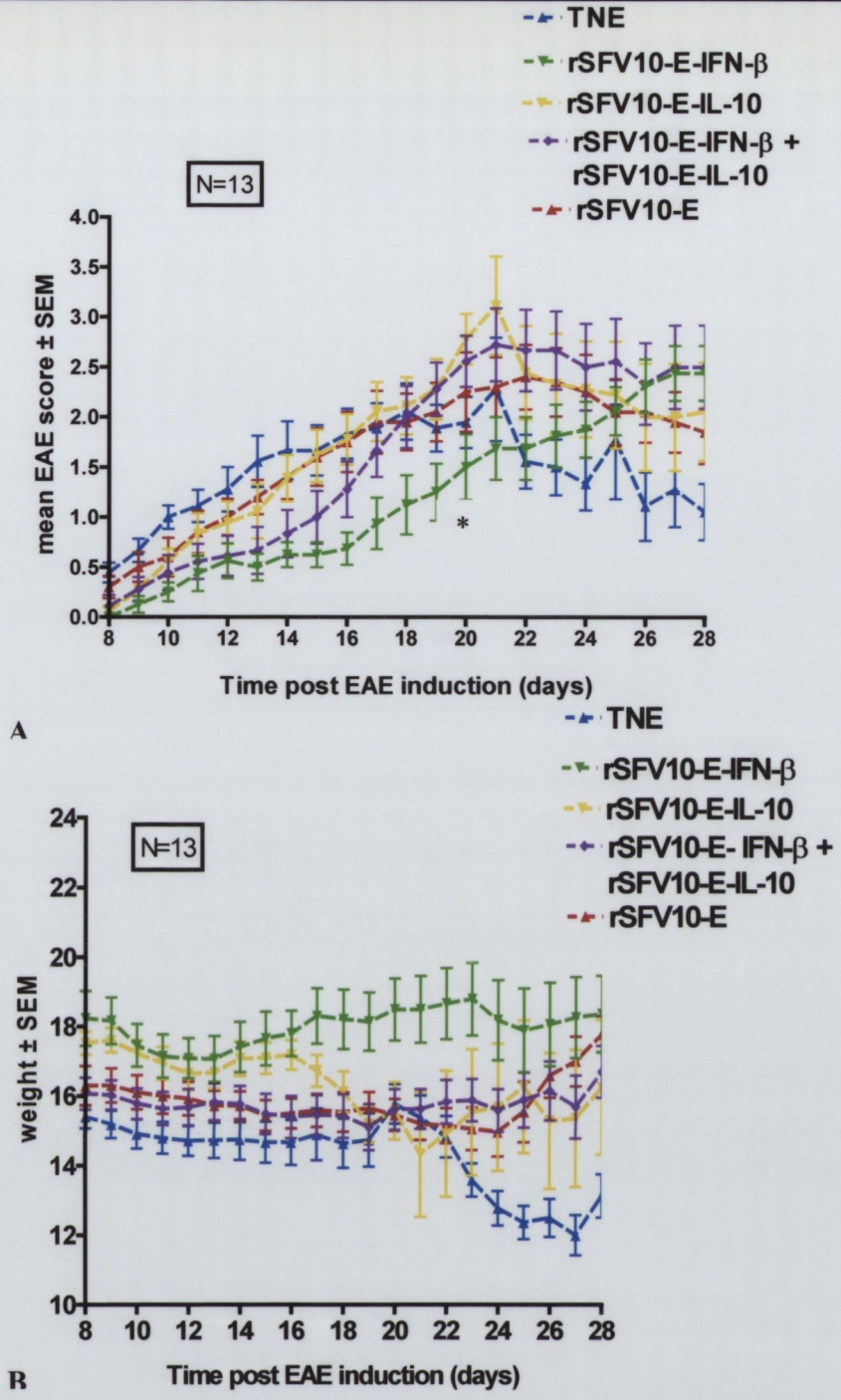

Figure 5.9 Co-administration of rSFV10-E-IFN-β and rSFV10-E-IL-10 in the treatment of EAE

This graph shows a trend where co-treatment with both recombinant vectors improved the disease model compared to the TNE treated and the empty particle control, but treatment with rSFV10-E-IFN-β particles alone still proved more effective. Treatment with rSFV10-E-IL-10 particles alone did not improve disease but actually enhanced severity to a level comparable to the rSFV10-E empty particles. Treatment with rSFV10-E-IFN-β particles significantly improved the disease model compared to the rSFV10-E-IL-10 treated ($p<0.05$) and the empty particle treated animals, and resulted in less weight loss ($p<0.001$).

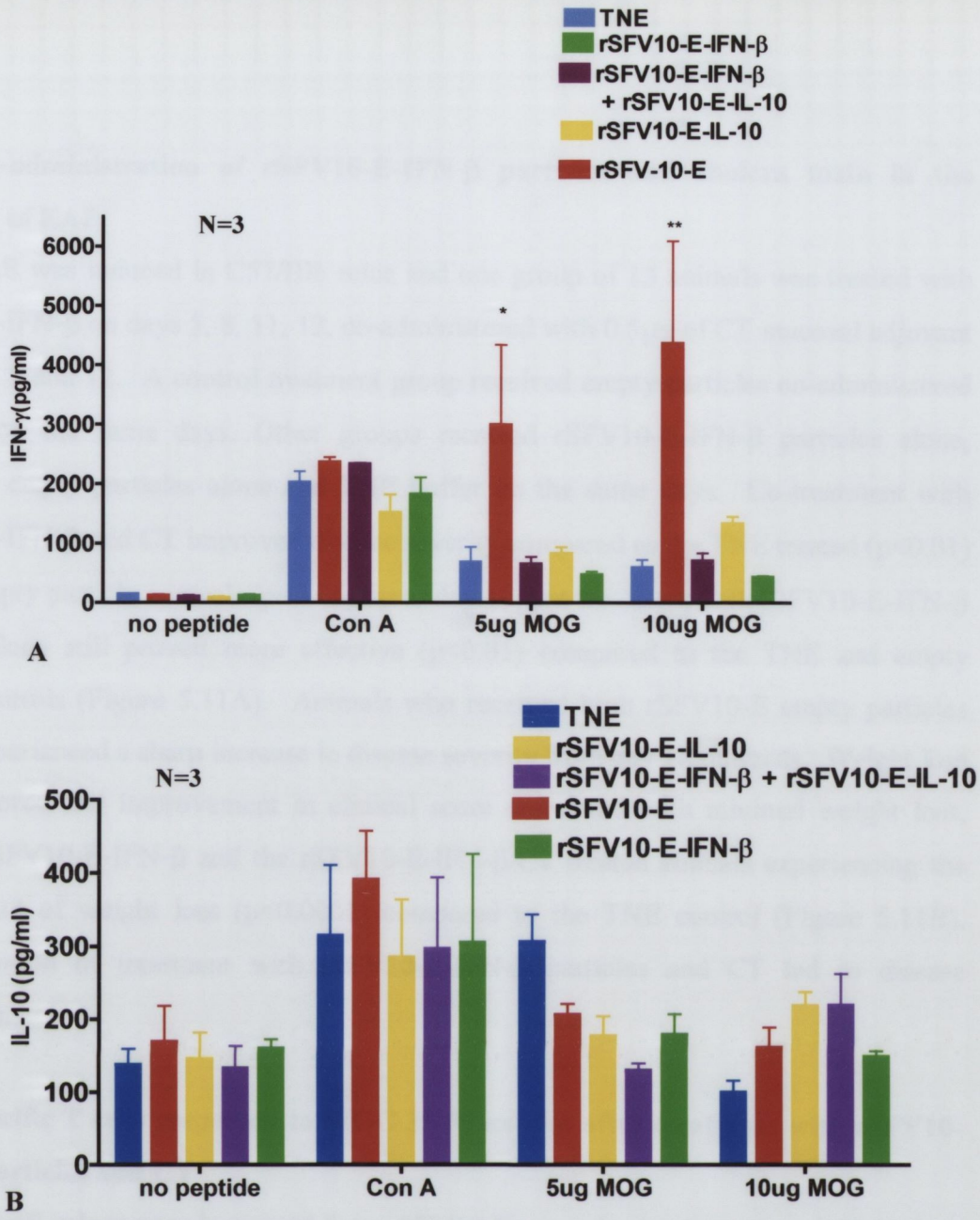

Figure 5.10 The effect of MOG35-55 stimulation on production of IFN-γ and IL-10 from splenocytes *ex vivo*

Overall production of IFN-γ in response to MOG35-55 stimulation was greatest from splenocytes of rSFV10-E empty particle treated animals compared to both the control TNE treated and the other treatment groups ($p<0.05$). The rSFV10-E-IL-10, rSFV10-E-IFN-β and the group that received both particles produced comparable levels of IFN-γ in response to MOG stimulation (A). The levels of IL-10 produced from MOG 35-55 stimulation were measured but no significant difference was seen between the groups (B). Statistical comparison was carried out using Two-way ANOVA and Bonferroni post-tests.

5.3.4 Co-administration of rSFV10-E-IFN-β particles and cholera toxin in the treatment of EAE

EAE was induced in C57/Bl6 mice and one group of 13 animals was treated with rSFV10-E-IFN-β on days 5, 8, 11, 12, co-administered with 0.5μg of CT mucosal adjuvant on days 5, 9 and 12. A control treatment group received empty particles co-administered with CT on the same days. Other groups received rSFV10-E-IFN-β particles alone, rSFV10-E empty particles alone and TNE buffer on the same days. Co-treatment with both rSFV-IFN-β and CT improved disease severity compared to the TNE treated ($p<0.01$) and the empty particle controls ($p<0.05$) up to day 19, but treatment with rSFV10-E-IFN-β particles alone still proved more effective ($p<0.01$) compared to the TNE and empty particle controls (Figure 5.11A). Animals who received both rSFV10-E empty particles and CT experienced a sharp increase in disease severity from day 12 onwards. Weight loss was monitored and improvement in clinical score correlated with minimal weight loss, with the rSFV10-E-IFN-β and the rSFV10-E-IFN-β/CT treated animals experiencing the least amount of weight loss ($p<0.0001$) compared to the TNE control (Figure 5.11B). Discontinuation of treatment with rSFV10-E-IFN-β particles and CT led to disease progression.

5.3.5 Specific T cells responses to MOG 35-55 *ex-vivo* after treatment with rSFV10-E-IFN-β particles and CT

Overall splenocytes harvested from rSFV10-E treated animals produced the highest level of IFN-γ day 22 post disease induction in response to MOG 35-55 stimulation. The rSFV10-E-IFN-β and CT, empty particle and CT and the rSFV10-E-IFN-β treated all produced levels comparable to the TNE buffer treated animals, levels significantly less than those produced by the empty particle treated (Figure 5.12A). The rSFV10-E-IFN-β/CT treated animals produced marginally less IFN-γ than these groups. Overall little difference was seen in the levels of IL-10 produced between the treatment groups but the rSFV10-E-IFN-β/CT treated animals produced the highest levels in response to MOG stimulation (Figure 5.12B).

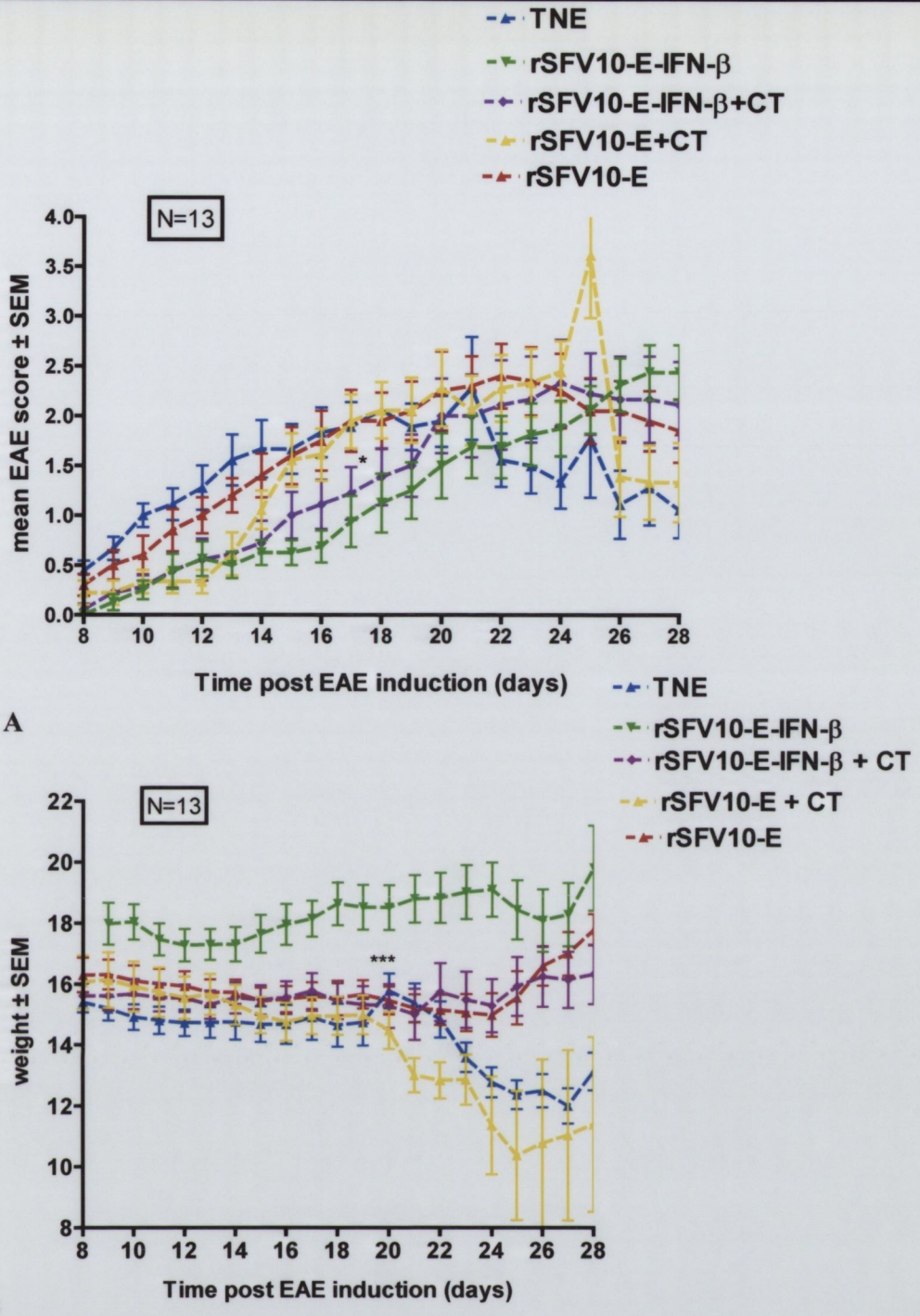

Figure 5.11 Co-administration of rSFV10-E-IFN-β particles and cholera toxin in the treatment of EAE

Co-treatment with both rSFV10-E-IFN-β and CT improved disease severity compared to the TNE treated ($p<0.01$) and the empty particle control ($p<0.05$) up to day 19, but treatment with rSFV10-E-IFN-β particles alone still proved more effective. Discontinuation of treatment led to disease progression. Animals who received rSFV10-E empty particles with CT experienced a sharp increase in disease severity from day 12 onwards. Weight loss was monitored and improvement in clinical score correlated with minimal weight loss. Statistical analysis was performed using the non-parametric Mann-Whitney test, using Graph Prism 4.0 software.

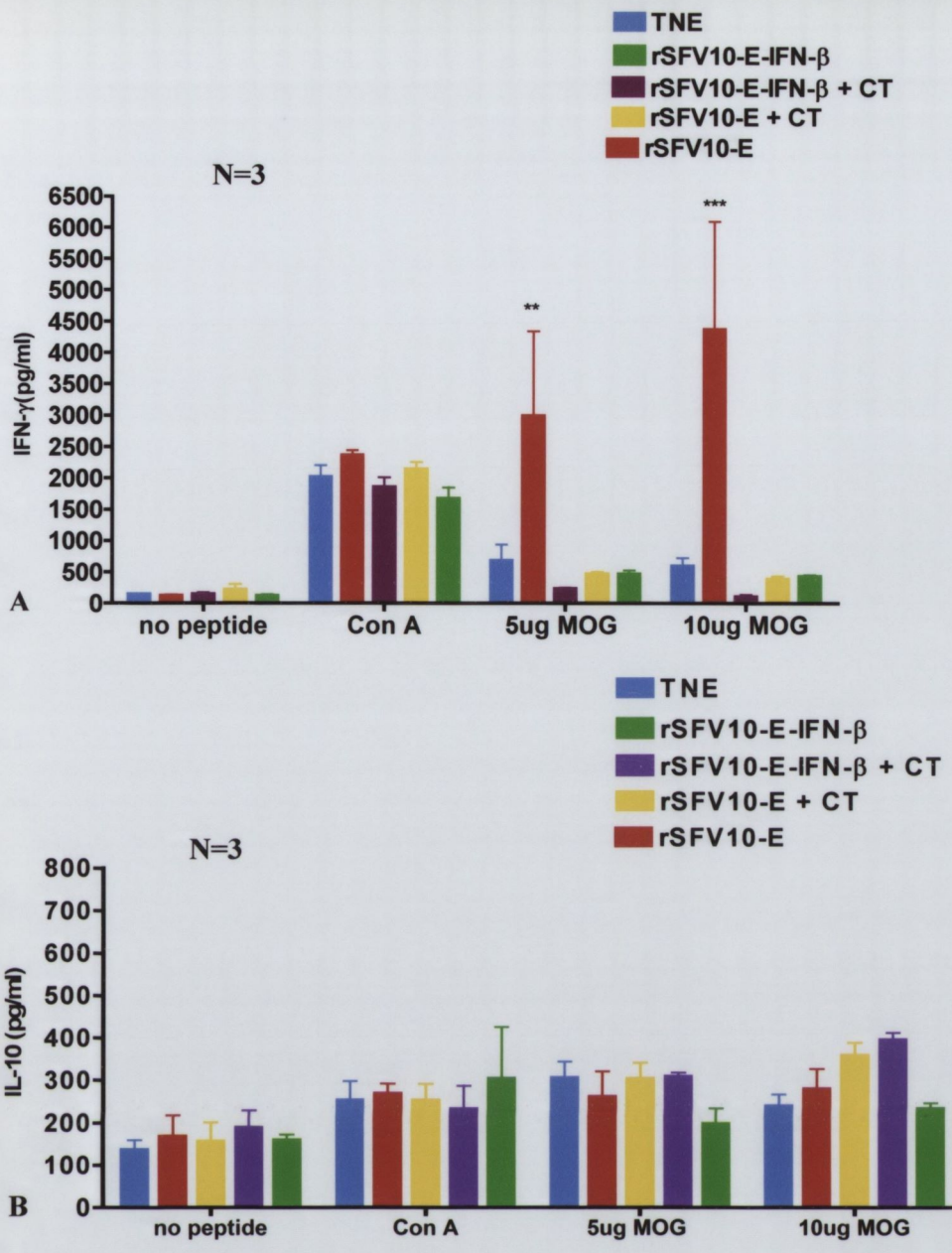

Figure 5.12 The effect of MOG 35-55 stimulation on production of IFN-γ and IL-10 from splenocytes of CT treated animals *ex vivo*

Overall production of IFN-γ in response to MOG35-55 stimulation was greatest from splenocytes of rSFV10-E empty particle treated animals compared to both the control TNE treated and the other treatment groups ($p<0.01$). The rSFV10-E-IFN-β and the groups that received both particles and CT produced comparable levels of IFN-γ in response to MOG stimulation (A). The levels of IL-10 produced from MOG 35-55 stimulation were measured but no significant difference was seen between the groups. A trend was shown where CT treated animals produced marginally more IL-10 than other groups (B). Statistical comparison was carried out using Two-way ANOVA and Bonferroni post-tests.

5.3.6 Summary of EAE treatments

Table 5.1 summarises the main finding from these treatment studies. Overall the animals that received rSFV10-E-IFN-β particles experience the lowest maximum EAE score day 19 post diseases with significant improvement seen in comparison to the TNE and empty particle group. The next most successful treatment was shown in the animals that received both rSFV10-E-IFN-β particles and CT. These animals also experienced a significantly less severe disease than the controls and a lower maximum EAE score than the other groups up to day 19. Treatment with rSFV10-E-IL-10 alone or in conjunction with rSFV10-E-IFN-β particles worsened disease symptoms and delayed recovery. Animals that received rSFV10-E and CT experienced the worse disease overall with a maximum EAE score of 3.6 ±0.6. They experienced earlier disease onset than other groups, exceeded only by the TNE treated animals.

5.3.7 Detection of IFN-γ in the serum of rSFV10-E-IFN-β, rSFV10-E-IL-10 and CT treated animals

The levels of IFN-γ were examined in serum taken from animals perfused day 22 post disease induction after treatment with rSFV10-E-IFN-β, rSFV10-E-IL-10 particles and CT. A trend was seen where more IFN-γ was found in the serum taken from the empty particle treated and the TNE control animals (Figure 5.13). The least amount of IFN-γ was found in the serum taken from the animals treated with both rSFV10-E-IFN-β and CT. Animals that received empty particles and CT also showed lower levels of IFN-γ which were comparable to the levels induced in the rSFV10-E-IFN-β/IL-10 treated animals. The levels of IL-10 in the serum were undetectable.

5.3.8 Pathological analysis of combined treatments

Animals that received both rSFV10-E-IFN-β and rSFV10-E-IL-10 particles showed clinical and pathological scores similar to those seen in animals treated with rSFV10-E-IFN-β alone (Table 5.2). Animals treated with both rSFV10-E-IFN-β particles and CT showed some amelioration in clinical and pathological scores in comparison to the control TNE and empty particle treated mice but little difference occurred compared with mice receiving empty particles and CT. Clinical signs and lesions were most severe in animals treated with rSFV10-E.

Treatment group	No. of deaths	Incidence of EAE	Maximum mean EAE score up to day 19	Maximum mean EAE score up to day 28	Mean day of onset	Compared to TNE control (up to day19)	Comp. to SFV control (up to day 19)
rSFV10-E-IFN-β	0	10/13	1.2 ±0.3	2.4 ± 0.3	17.5 ± 1.3	0.0014**	0.01*
rSFV10-E-IL-10	0	12/13	2.3 ± 0.3	3.1 ± 0.5	14.5 ± 0.7	n.s.	n.s.
rSFV10-E-IFN-β + IL-10	0	12/13	2.3 ± 0.3	2.7 ± 0.4	15.5 ± 1.0	n.s.	n.s.
rSFV10-E + CT	3	12/13	2.0 ± 0.3	3.6 ± 0.6	13.3 ± 0.7	n.s.	n.s.
rSFV10-E-IFN-β + CT	0	12/13	1.5 ± 0.3	2.3 ± 0.4	13.7 ± 1.5	0.0067**	0.049*
TNE	2	12/13	2.0 ± 0.3	2.3 ± 0.5	12.9 ± 0.8	n.a.	n.s
rSFV10-E	0	12/13	2.0 ± 0.3	2.4 ± 0.3	13.9 ± 1.0	n.s.	n.a.

* Probability of the mean EAE score of the treated animals compared to those of the controls
* < 0.05
** <0.01
*** <0.001

n.a. not applicable

n.s. not significant

Table 5.1 Analysis of treatment with rSFV10-E-IFN-β, rSFV10-E-IL-10 and CT

The rSFV10-E-IFN-β and rSFV10-E-IFN-β/CT groups experienced similar maximum EAE scores, when measured up to day 19 or day 28 post EAE induction. Disease progression was curtailed in rSFV10-E-IFN-β treated animals indicated by the latest average day of onset. Overall both groups postponed disease progression (indicated by mean EAE scores) compared to the TNE and empty particle controls up to day 19 ($p<0.05$). Animals that received both rSFV10-E particles and CT experienced the highest maximum EAE score of 3.6 ±0.6. rSFV-IL-10 treated animals and rSFV10-E-IFN-β and rSFV10-E-IL-10 treated animals showed no significant improvement in clinical disease and made disease marginally worse than TNE and empty particle treated groups. The mean day of onset was calculated when animals experienced a clinical score of 1 upwards, as a score of 0.5 was more difficult to assess and more likely to be inaccurate. The maximum mean EAE scores for the TNE and the empty particle control groups were similar and were calculated on days 21 and 22 respectively when the groups experienced most severe disease.

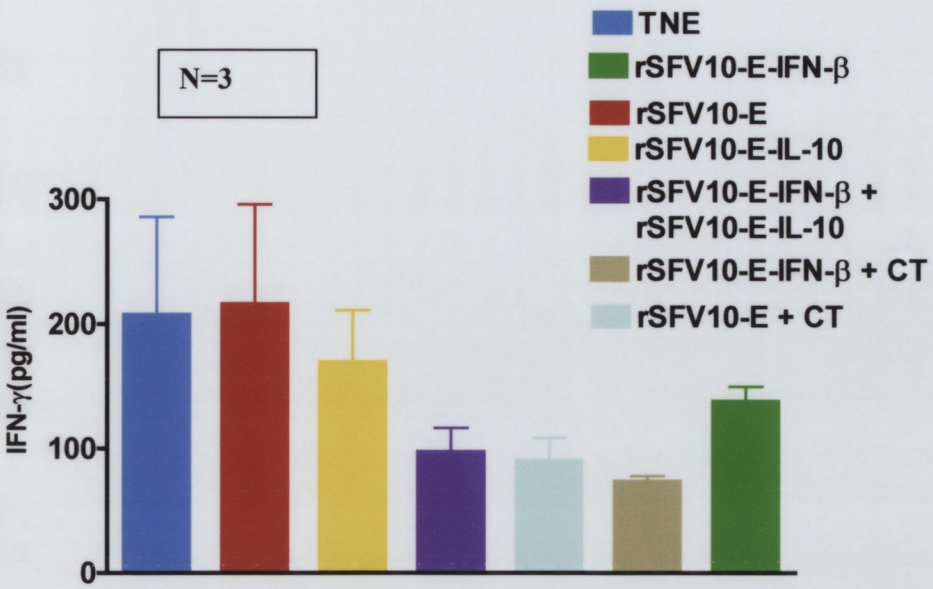

Figure 5.13 Levels of IFN-γ in serum taken from rSFV10-E-IFN-β, rSFV10-E-IL-10 and CT treated animals

The levels of IFN-γ were examined in serum taken from animals perfused day 22 post disease after treatment with rSFV10-E-IFN-β, rSFV10-E-IL-10 particles and CT. A trend was seen where more IFN-γ was found in the serum taken from the empty particle treated and the TNE control animals. The least amount of IFN-γ was found in the serum taken from the animals treated with both rSFV10-E-IFN-β and CT.

Group	#	Clinical score	Pathology score	Total clinical score	Total pathology score
TNE	1	3	3	9.5	10
	2	3	3		
	3	3.5	4		
rSFV10-E	1	4	5	10.5	12
	2	3	4		
	3	3.5	3		
rSFV10-E- IL-10	1	2.5	3	6	9
	2	2	3		
	3	1.5	3		
rSFV10-E + CT	1	1	2	5.5	8
	2	1.5	3		
	3	3	3		
rSFV10-E-IFN-β + CT	1	1	2	5	9
	2	3	4		
	3	1	3		
rSFV10-E- IFN-β + rSFV10-E-IL-10	1	1.5	2	3.5	5
	2	1.5	2		
	3	0.5	1		
rSFV10-E-IFN-β	1	1	1	3	5
	2	1	2		
	3	1	2		

Table 5.2 The effect of combinational treatment with rSFV10-E-IFN-β particles, rSFV10-E-IL-10 particles and CT on clinical score and pathology score of EAE mice

Animals that received both rSFV10-E-IFN-β and rSFV10-E-IL-10 particles experienced lower clinical and pathological scores than the animals treated with rSFV10-E-IL-10 particles alone, but comparable to the scores of the rSFV10-E-IFN-β particle treated animals. Animals that received both rSFV10-E-IFN-β particles and CT did show some improvement in clinical disease and pathology of the lesion in comparison to the control TNE and empty particle treated but little difference was seen in comparison to the animals receiving empty particles and CT. The rSFV10-E animals experienced the most severe clinical disease accompanied by the most severe pathology.

5.3.9 FACS analysis to distinguish lymphocytes into MHC class II restricted CD4+ T cells, MHC class 1 restricted CD8+ T cells and B cells

Splenocytes were harvested from animals day 22 post disease induction after treatment with rSFV10-E-IFN-β and rSFV10-E-IL-10, and co-treatment with rSFV10-E-IFN-β/CT on days 5,8,11,12 and splenocytes labeled with antibodies specific for B cells, CD4+ cells and CD8+ cells. Overall the lowest percentages of these cell types were found in splenocytes of the empty particle control group. As seen in figure 5.14, splenocytes harvested from the rSFV10-E–IFN-β produced more CD4+ and significantly more CD8+ cells ($p<0.01$) than the other groups. In general the other treatment groups produced less CD8+ cells than CD4+ and B cells. The rSFV10-E-IL-10 and the combined treated groups produced the lowest number of CD4+ and CD8+ cells. The combined treated animals, the rSFV10-E-IFN-β and the rSFV10-E-IL-10 treated animals produced similar levels of B cells with the combined treated group producing the highest percentage. Splenocytes of empty particle treated animals produced significantly less B cells than the other groups ($p<0.05$). With co-administered CT, the percentages of CD4+ cells constituting the rSFV10-E-IFN-β/CT treated and the empty particle treated/CT splenocytes were comparable with the rSFV10-E-IFN-β treated groups. The groups who received co-treatment with CT also showed marginally higher percentages of B cells in their splenocytes (Figure 5.15). Overall the lowest percentage of B cells was found in splenocytes of the empty particle control group.

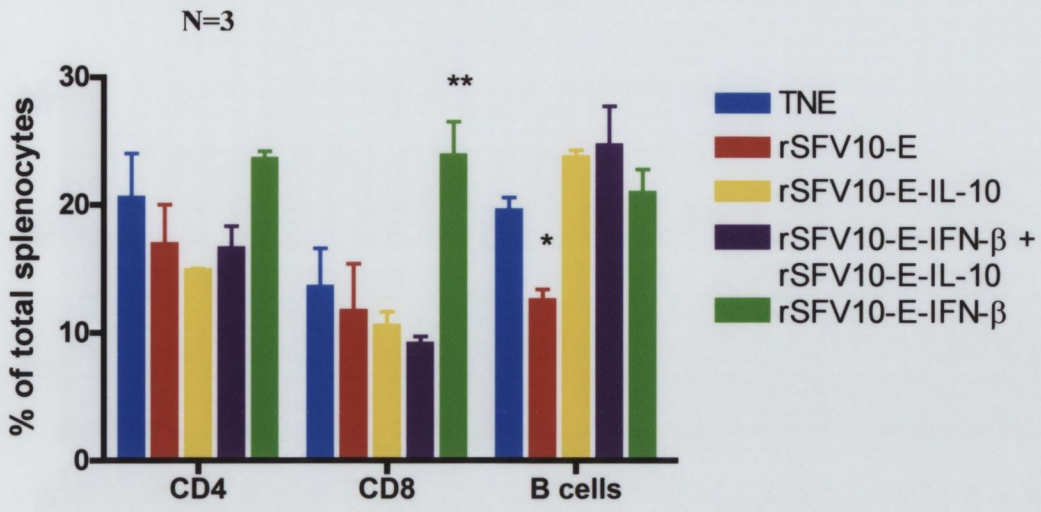

Figure 5.14 FACS analysis of lymphocytes from rSFV10-E-IFN-β and rSFV10-E-IL-10 treated EAE animals

Splenocytes of empty particle treated animals produced significantly less B cells than the other groups ($p<0.05$). Those harvested from the rSFV10-E–IFN-β treated group produced more CD4+ cells, and significantly more CD8+ cells ($p<0.01$) than splenocytes from other groups. In general the other treatment groups produced less CD8+ cells than CD4+ and B cells. The rSFV10-E-IL-10 and the combined treated groups produced the lowest number of CD4+ and CD8+ cells. rSFV10-E-IL-10, rSFV10-E-IFN-β and the combined treated animals produced similar percentages of B cells. The combined treated group produced the highest percentage of B cells. Statistical comparison was carried out using Two-way ANOVA and Bonferroni post-tests.

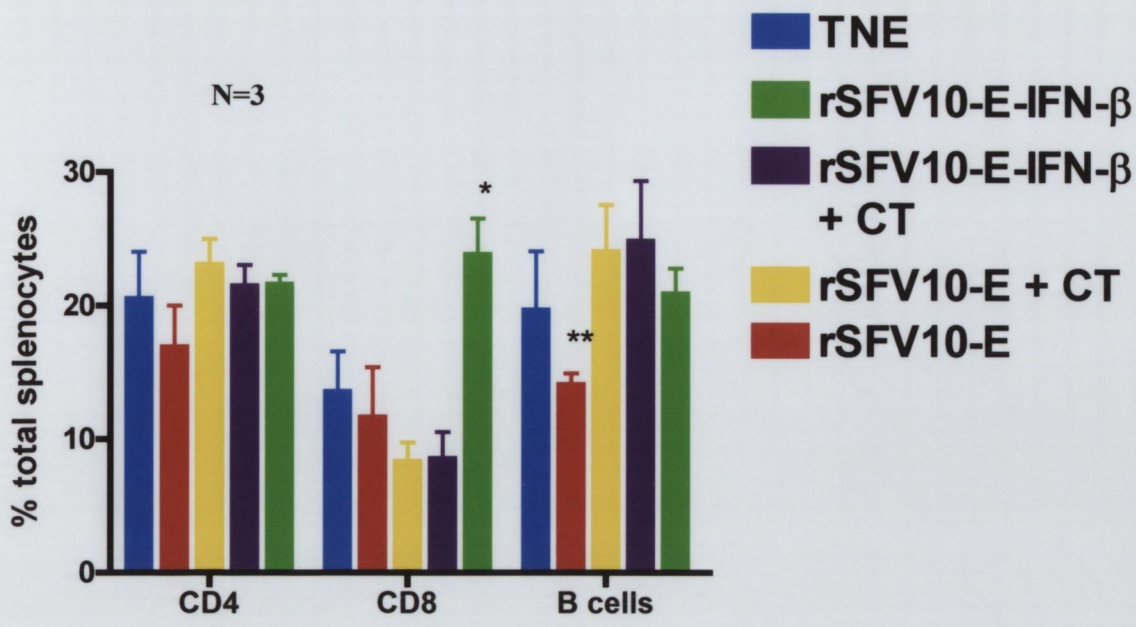

Figure 5.15 FACS analysis of lymphocytes from rSFV10-E-IFN-β and Cholera toxin treated EAE animals

Overall a trend was seen where the lowest percentages of all cell types were found in splenocytes of empty particle treated animals with significantly less B cells than the other groups ($p<0.01$). Overall the highest percentage of CD8+ cells were found in splenocytes of rSFV10-E-IFN-β treated animals ($p<0.05$). The percentage of CD4+ cells was comparable between the rSFV10-E-IFN-β /CT treated, the empty particle treated /CT and the rSFV10-E-IFN-β treated groups. The groups who received co-treatment with CT also showed marginally higher percentages of B cells in their splenocytes. Statistical comparison was carried out using Two-way ANOVA and Bonferroni post-tests.

5.4 Discussion

Although IFN-β and IL-10 have both been successful in the treatment of different models of EAE when administered individually either systemically or via viral vectors, they have never been co-administered or administered with another immunomodulatory cytokine. Due to their ability to upregulate the Th2 response or deviate towards a Th2 it was decided to co-administer both rSFV-IFN-β particles and rSFV-IL-10 particles together on days 5, 8, 11 and 12 which to date has proven to be the most successful treatment. In keeping with this aim of upregulating the overall Th2 response, another treatment regime was decided upon where CT, a well established vaccine adjuvant which induces antigen specific CD4+ T cells to secrete T helper 2 cytokines, was co-administered with rSFV10-E-IFN-β particles (Lavelle *et al.*, 2004; Lavelle *et al.*, 2003; Williams *et al.*, 1999; Xu-Amano *et al.*, 1994). A previous study showed that CT was effective in improving disease severity (Yura *et al.*, 2001). In this study animals received three doses of 0.5μg CT by i.n. inoculation on days 5, 9 and 12 instead of days 5, 8, 11, 12 to avoid any side effects through the administration of CT and PT on the same day. Previous studies had shown that 0.5μg CT is sufficient to induce an immune response (Lavelle *et al.*, 2003).

IL-10 was successfully subcloned from rSFV1-IL-10 vector into the new enhanced rSFV10-E vector. *In vitro* expression studies confirmed diffuse IL-10 cytoplasmic expression in BHK-21 after transfection with rSFV10-E-IL-10 RNA and immunohistochemical labeling for the gene. To quantify the levels of IL-10 expression, BHK-21 and L929 cells were infected with rSFV-IL-10 particles at MOIs of 1, 10 and 100 and the supernatant harvested and tested for the presence of IL-10 by ELISA. Overall, infection with rSFV10-E-IL-10 particles led to greater expression of IL-10 in both BHK-21 and L929 cells than empty particle infected and mock-infected control cells at three different MOIs ($p<0.001$). Infection of BHK-21 cells with rSFV-IL-10 led to greater IL-10 production with levels reaching 1×10^3 ng/ml, approximately 1 log higher than the levels seen in the L929 cells ($p<0.001$). Comparisons can also be made with the *in vitro* expression study performed by Jerusalmi *et al.*, 2003, where infection of both these cell lines with the original rSFV1-IL-10 vector led to much lower levels of secreted IL-10, which did not exceed 16,000 pg/ml. The enhanced vector gave an approximate 50-fold increase in IL-10 production.

Co-treatment with rSFV10-E-IFN-β particles and rSFV10-E-IL-10 particles showed some delay in disease onset up to day 15 but overall no significant difference was

seen with the control TNE and empty particle treated groups. Cessation of treatment led to an increase in disease severity. Animals experienced maximum EAE scores that exceeded those of the control groups resulting in a more severe disease. Treatment with rSFV10-E-IL-10 particles alone showed no improvement in disease and again led to a more severe disease than the rSFV-IFN-β ($p<0.05$). The beneficial action of IL-10 may differ depending on the local cytokine microenvironment produced by the gene-secreting cell types at the time of administration. The vector itself replicates only in the cells of the nasal epithelium and does not enter the CNS as shown by Jerusalmi *et al.*, 2003. We presume that rSFV secreted IL-10 follows the same route of action as IFN-β secreted from rSFV-IFN-β, where the cytokine is carried by axonal transport from the nasal epithelium to the olfactory bulbs, brain and spinal cord by axonal transport. The levels of secreted IL-10 and endogenous IL-10, produced by astrocytes, are insufficient to overcome the Th1 response elicited by the viral vector resulting in disease exacerbation. A previous study has shown that IL-10 failed to treat EAE in a Balb/c model when administered via a replicative HSV type 1 viral vector (Broberg *et al.*, 2001). Similarly an adenoviral vector expressing IL-10 exhibited no beneficial effect in EAE treatment (Croxford *et al.*, 2001). For successful treatment of the EAE model with rSFV10-E-IL-10 particles it may be necessary to treat the animals through out the induction and effector period, on days 5,8,11,13,17 as shown by Jerusalmi *et al.*, 2003 in the treatment of the same EAE model with rSFV1-IL-10. In spite of this lack of improvement on disease course, the specific T cell responses of splenocytes taken from these animals did not show an increased induction of IFN-γ *ex vivo* in response to MOG 35-55 stimulation and in comparison to the empty particle treated, like the rSFV10-E-IFN-β treated, produced significantly less IFN-γ ($p< 0.05$) indicating that the presence of either IL-10 or IFN-β or both is downregulating the Th1 response. rSFV10-E-IL-10 particle treated animals produced marginally more IFN-γ than the co-treated particle group. Little difference was seen in the IL-10 levels. Overall treatment with rSFV10-E-IFN-β on days 5, 8, 11 and 12 remained the most successful treatment with animals experiencing the latest day of disease onset, with the lowest maximum EAE scores up to day 19, with discontinuation of disease leading to a less severe disease than in the rSFV10-E-IL-10 and combined treated groups. The mean day of onset was calculated when animals experienced a clinical score of 1 upwards, as a score of 0.5 was more difficult to assess and more likely to be inaccurate. rSFV10-E-IFN-β and rSFV10-E-IL-10 treated animals showed similar pathology to the rSFV10-E-IFN-β treated animals when perfused on day

22 p.d.i, whereas the rSFV10-E-IL-10 particle treated animals had developed a more severe disease by day 22 which was accompanied by more severe lesions, despite showing an initial delay in disease onset. The maximum mean EAE scores for the TNE and the empty particle control groups were similar, as seen in figures 5.9 and 5.11, and were calculated on days 21 and 22 respectively. TNE and empty particle treated animals showed the most severe pathology overall.

Treatment with CT in combination with rSFV10-E-IFN-β proved to be more effective than treatment with rSFV10-E-IL-10. Treatment did not delay disease onset for as long, but overall animals experienced lower maximum EAE score by day 19 and significantly improved disease severity compared to the TNE ($p<0.01$) and empty particle controls ($p<0.05$). Animals were also treated with CT in combination with empty particles but this regime did not have such promising results, animals had the highest maximum EAE scores overall and the highest number of deaths. The presence of the empty particles is possibly suppressing the beneficial effects of CT through the induction of other Th1 cytokines such as IL-12. Though CT enhances Th2 responses predominantly, it also has the ability to induce IFN-γ production (jones). This may be causing the peak in disease severity seen in the empty particle/CT treated animals. The IFN-γ response from both these groups were significantly lower than the empty particle treated ($p<0.01$) but comparable to the rSFV10-E-IFN-β treated animals. Animals receiving rSFV10-E-IFN-β and CT produced marginally less IFN-γ than the other treatment groups, and more IL-10 but again neither result was significant. It would appear, as discussed before, the presence of the viral vector is automatically upregulating the Th1 response and even though CT has been shown in enhance Th2 responses in previous studies, its ability to overcome the Th1 is not strong enough to see any significant increase in IL-10 production. An insufficient amount of CT may have been administered to overcome this Th1 response but Lavelle *et al.*, 2003 showed that as little as 1.0 μg is capable of inducing a strong Th2 immune response. Three doses of 0.5μg were administered in this study. It would have been beneficial to perform a CT dose response study to see whether the same immune response that was seen by Lavelle *et al.*, 2003 could be established in C57/Bl 6 mice. Both the rSFV10-E-IFN-β particles/CT treated and the rSFV10-E/CT treated animals experienced EAE lesions of similar severity by day 22 when clinical disease has reached a maximum in both groups. Again the rSFV10-E-IFN-β exhibited the least pathology and the TNE and

empty particle treated showed the most. The CT in the brains of the rSFV particle/CT caused treated animals no additional pathology.

As seen in Chapter 4, FACS analysis was carried out to further assess the immune responses of each treatment group by looking at the percentage of CD4+, CD8+ and B lymphocytes day 22 p.d.i. when the TNE animals are showing signs of recovery. As shown in Figure 4.10, rSFV10-E treated animals produced significantly less CD4+, CD8+ and B cells in comparison to the rSFV-IFN-β treated group ($p<0.05$), and the rSFV10-E-IFN-β treated animals produced significantly more CD8+ cells than the TNE group ($p<0.01$) (Figures 5.14 and 5.15). In general CD8+CD28- T suppressor cell activity is persistently low in chronic progressive MS and EAE (Antel *et al.*, 1986; Najafian *et al.*, 2003). Little is known about the effect of IFN-β therapy on these cells in EAE but other studies have shown that in MS, IFN-β enhances these cells leading to improvement in disease (Javed and Reder, 2005). This improvement is due in part to the secretion of TGF-β by these effector cells. TGF-β inhibits the migration of lymphocytes into the CNS *in vivo* (Fabry *et al.*, 1995). rSFV10-E-IL-10 and rSFV10-E-IFN-β/IL-10 treated animals produced a similar percentage of B cells to the rSFV10-E-IFN-β. The role of B cells in MS and EAE remains controversial but they are believed to play a role in disease recovery by production of IL-10 (Fillatreau *et al.*, 2002). In studies where EAE has been successfully treated with IL-10, treatment resulted in an alteration in the cellular phenotype, notably an increase in the numbers of CD8+ T and B cells (Croxford *et al.*, 2001). As there was no significant difference in B cell numbers, the sampling of animals at day 22 may have been too late to see any positive effects. An earlier sampling time point during the effector stage would have been more informative.

CT treated animals produced more CD4+ cells than CD8+ T cells. CT specifically induces CD4+ cells, and CD8+ cells to a lesser extent (Lavelle *et al.*, 2004; Williams *et al.*, 1999). The percentage of B cells constituting the splenocytes of CT treated and rSFV10-E-IFN-β were comparable whereas rSFV10-E treated animals produced significantly less B cells as seen before ($p<0.01$). CT is a powerful oral immunogen and adjuvant which elicits strong IgG and IgA antibody responses, promoting B cell isotype differentiation and ultimately increasing the number of B cells (Lycke and Strober, 1989). To further verify the immunoregulatory characteristics of CT, an ELISA should be performed on serum taken from CT treated EAE animals to measure the IgG and IgA antibody responses.

From this study the introduction of an adjuvant such as CT may be beneficial in the treatment of EAE with rSFV10-E-IFN-β after further experiments to establish the correct dose and frequency of administration are performed. The dose administered may have to be increased or else administered more frequently as a dose of 0.5μg administered three times is insufficient is show any real Th2 response upon stimulation of T cells *ex vivo* with MOG 35-55. Treatment with both rSFV10-E-IFN-β and rSFV10-E-IL-10, and with rSFV10-E-IL-10 alone was disappointing and did not improve the disease model to any great extent, despite showing favourable decreases in IFN-γ levels. This combination of particles may have to be administered during the induction and effector stage of disease if any improvement is to be seen. In both treatment regimes further experiments need to be done to optimize any improvement seen. The administration of rSFV1-IL-10 particles by Jerusalmi *et al.*, 2003 was much more successful in the treatment of the same MOG 35-55 EAE model than either rSFV10-E-IFN-β or rSFV10-E-IL-10 particles alone. The treatment days provided the only difference between the two studies, all other factors, such as mouse strain and age, route of inoculation, clinical grading scale remained constant. Jerusalmi *et al.*, 2003 treated animals on days 5,8,11,13,17 instead of on days 5,8,11 and 12 and showed complete inhibition of disease up until day 20. This is in contrast to our best result where rSFV10-E-IFN-β reduced but did not inhibit disease severity up until day 20. With regard to this study, treatment with rSFV10-E-IFN-β particles alone still remains the most successful treatment option. Despite showing some positive results, this study on combinational treatment has some shortcomings. FACS analysis should have been performed on infiltrating cells of the CNS lesion instead of splenocytes, as these are the cells which are predominantly effected during the course of EAE. It is thought, however, that any effects, either positive or negative, of rSFV-IFN-β treatment on peripheral immune cells will give some indication of changes in the T cell phenotype. Measurement of the overall percentage CD3+ splenocytes would have been helpful in enabling more accurate comparisons to be made between the percentage CD4+ and CD8+ T cells.

Chapter 6

General Discussion

6.0 General discussion

The aim of this study was to examine the effect rSFV vectors expressing IFN-β had on the course of EAE, an animal model of MS. SFV is a neurotropic virus which has been extensively studied as a model of viral neuropathogenesis (Atkins *et al.*, 1990; Donnelly *et al.*, 1997; Gates *et al.*, 1985; Sammin *et al.*, 1999). SFV enters the cells by a number of surface receptors, including HLA molecules such as H2 histocompatibility antigens. Following i.n. infection, the virus follows axonal transport along olfactory tracts from nerve endings in the olfactory mucosa, reaching the CNS via the olfactory bulb. Once there, it infects neurons and oligodendrocytes and proceeds to further infect other areas of the brain (Sammin *et al.*, 1999; Sheahan *et al.*, 1981; Smyth *et al.*, 1990). Virulent strains of SFV induce lethal encephalitis in mice when given i.n. (Atkins *et al.*, 1990). Avirulent strains on the other hand infect neurons at a slower pace allowing for the animals to clear the virus; they do however lead to immune mediated demyelination of the CNS in some mice (Balluz *et al.*, 1993; Sheahan *et al.*, 1981). SFV can also infect other cells outside the CNS. Previous studies have shown that virus multiplies in the spleen, the liver and the lymph nodes as well as the CNS following i.p. infection but only the CNS shows histological lesions (Seamer *et al.*, 1967). Similarly Murphy *et al.*, 1970 showed that multiplication of the virus in the muscle of neonatal mice produces a viremia which leads to invasion of the CNS.

Based on the pathway taken by the virus upon i.n. infection, and its ability to infect a number of cells in the CNS, including neurons and oligodendrocytes, the virus was developed as a vector for gene therapy in the CNS (Atkins *et al.*, 1990; Balluz *et al.*, 1993; Ehrengruber *et al.*, 1999; Glasgow *et al.*, 1997). Original work was done both *in vitro* and *in vivo* uses various types of rSFV vectors to target the CNS (Ehrengruber *et al.*, 2003; Lundstrom and Ehrengruber, 2003; Olkkonen *et al.*, 1993; Vaha-Koskela *et al.*, 2003). More recent work has shown the potential of the SFV split helper system as a gene therapy agent for the CNS. Jerusalmi *et al.*, 2003 showed that a rSFV vector expressing the reporter gene, EGFP, gave high level expression detectable in incoming axons from receptor cells in the olfactory epithelium that terminates in the glomerular area of the olfactory bulbs. Expression occurred in the olfactory bulb as early as one day after i.n. inoculation and continued for up to 10 days, with no detectable pathological damage. No vector RNA was present in any areas of the CNS and could be detected only in the nasal passage of infected animals, suggesting that duration of expression in the CNS is

dependent on the half-life of the protein, and that the viral vector does not enter the CNS. These findings also suggested that transcription and/or replication of the vector RNA was taking place in the cells of the olfactory mucosa, which have the capability to regenerate, as is the case with most upper respiratory infections. Viral RNA persisted for 7 days at the site of inoculation only, which was consistent with previous findings (Morris-Downes *et al.*, 2001). Though the mechanism is not fully understood, expressed protein was carried out to the CNS by axonal transport from the nasal epithelium to the olfactory bulb. When an immunomodulatory cytokine, IL-10, was cloned and expressed from the same rSFV system, similar results were seen. High level expression of the cloned cytokine was shown in the nasal mucosa and olfactory bulbs of mice for up to 7 days after i.n. infection with rSFV-IL-10 vector particles. However, in contrast to EGFP expression, the cloned cytokine was found in higher levels in areas of the brain suggesting that the cytokine is being successfully secreted into the CNS. IL-10 is a classical Th2 cytokine whose main functions include inhibition of IL-12 and suppression of cytokine production by Th1 cells. Intranasal treatment of EAE with these rSFV-IL-10 particles reduced disease severity and pathology of the lesion. From these findings, it was decided to choose another cytokine with similar anti-inflammatory properties and determine the effect expression of this cytokine from rSFV vectors has on the course of EAE. IFN-β was chosen as it is a well established treatment for RRMS with three FDA approved treatments currently available on the market, Betaseron (IFNβ-1b), Rebif (IFNβ-1a) and Avonex (IFNβ-1b). Randomized, placebo controlled clinical trials have shown the efficacy of IFN-β in the treatment of RRMS, when administered alone or in combination with other immunosuppressive agents such as Copaxone (glatiramer acetate) (Jacobs *et al.*, 1996; Lublin *et al.*, 2001; Paty and Li, 1993). Studies on the treatment of different EAE models with IFN-β have been limited and have shown varying degrees of success (Luca *et al.*, 1999; Yasuda *et al.*, 1999; Yu *et al.*, 1996). No previous studies had used IFN-β to treat the MOG 35-55 peptide induced EAE model used in this study. The cytokine has also never been administered by a directly injectable viral vector system, only via a retroviral vector encapsulated within a DNA liposome plasmid. Intracranial inoculation of this DNA encapsulated retroviral vector expressing IFN-β improved disease severity when administered during the effector stage of disease (Triantaphyllopoulos *et al.*, 1998).

IFN activity is usually not detectable in normally growing tissue cultures or in animals. After induction by viruses or dsRNA, IFN-α and IFN-β genes are transcribed and

translated but accumulated mRNAs disappear rapidly. Type 1 IFNs, IFN-α and IFN-β are produced by leucocytes and fibroblasts respectively. A third type 2 IFN or immune IFN, IFN-γ is produced by lymphocytes and macrophages. IFNα/βs are one the first cytokines to be expressed following viral infection but disappear rapidly (Isaacs and Lindenmann, 1957; Isaacs *et al.*, 1957). In this study IFN-β was isolated from the brain RNA of SFV-A7 infected Balb/c mice two d.p.i when detectable levels were present. No detectable levels were found in the spleen at this time or in the brain and spleen at days 4 and 8. Two rSFV systems were used for cloning of IFN-β, pSFV1 and pSFV10-E. pSFV10-E is a more novel plasmid which has been modified to allow enhanced production of heterologous protein. This vector contains a capsid translational enhancer sequence composed of 34 a.a. from the original capsid protein and a 2A autoprotease self cleavage sequence from FMDV (Sjoberg *et al.*, 1994). The heterologous protein is formed as part of a fusion protein with the capsid enhancer protein which is co-translationally cleaved by the autoprotease. This enhanced vector has been used in vaccine and tumour studies due to its ability to produce at least 10 fold more protein than original SFV systems (Chikkanna-Gowda *et al.*, 2005; Daemen *et al.*, 2002; Daemen *et al.*, 2004; Rodriguez-Madoz *et al.*, 2005). In this study, almost 10 fold more IFN–β was expressed from the rSFV10-E-IFN-β vector than from the rSFV1-IFN-β vector on infection of BHK-21 cells at an MOI 10. In general IFN-β levels were highest 36 h.p.i but had decreased by 48 h. Overall infection of L929 cells with both rSFV-IFN-β constructs led to higher production of IFN-β. Studies have shown that L929 and BHK cells produce some endogenous IFN-β upon viral infection (Margolis *et al.*, 1972; Stanwick and Hallum, 1974). This is seen on infection of both cell types with empty particle controls. The presence of virally infected cells is one of the primary intracellular signals for IFN production (Biron, 1998). At this early phase in the study a murine IFN-β ELISA kit was not commercially available therefore levels of secreted IFN-β were measured by a viral inhibition assay. This assay was based on the protective effect elicited by IFN upon infection and is a well established way to measure IFN and ensure biological activity. In our customized assay, L929 cells were first treated with supernatant from rSFV-IFN-β infected cells and then challenged with SFV-A7 at an MOI 1. The percentage of viable cells was measured post challenge by incubation with MTS after which the absorbance was read at a wavelength of 490nm. For quantification of IFN-β within the supernatant, the sample wells were compared with those which contained standard IFN-β of a known concentration. A preliminary experiment had established the

concentration of standard IFN-β which gave 50% protection: 50% CPE upon challenge. This concentration was then included in each experiment and used for comparison with the sample wells. A rat anti-IFN-β mAb was also included in this assay (50ng/well) to ensure that IFN-β alone was exerting the protective effect and not other IFNs. Enhanced IFN-β expression was also seen from the rSFV10-E-IFN-β vector when immunohistochemistry was carried out on rSFV-IFN-β infected cells. Staining was more intense in rSFV10-E-IFN-β infected cells compared to those infected with rSFV1-IFN-β.

Intranasal inoculation was chosen as the treatment route in this study. To date the majority of studies have used the i.c. route of infection for treatment of diseases of the CNS such as EAE, whether or not the immunomodulatory agent is being administered via a viral vector (Broberg *et al.*, 2001; Broberg *et al.*, 2004b; Furlan *et al.*, 1998; Guy *et al.*, 1998). Previous studies have established that the less invasive i.n. route is a more effective and direct route of delivery to the CNS (Broberg *et al.*, 2004a; Jerusalmi *et al.*, 2003). Jerusalmi *et al.* 2003 showed that i.n. delivery of IL-10 in the treatment of EAE was more effective than i.p. or i.m. delivery (Jerusalmi, 2003). Prior to EAE induction and treatment it was important to establish the expression and persistence of IFN-β within the CNS following i.n. infection with rSFV-IFN-β particles. This allowed a treatment regime to be decided upon which gave persistent IFN-β expression throughout the duration of the disease. Overall higher levels of IFN-β were found in the CNS of rSFV10-E-IFN-β treated animals compared to the control animals, confirming IFN-β expression *in vivo*. High levels of IFN-β were seen in the olfactory bulbs of rSFV10-E-IFN-β treated animals 24 h post inoculation. This supports the previous study discussed above which showed high level EGFP or IL-10 expression in the olfactory bulbs of mice as early as 1 day following i.n. inoculation with rSFV-EGFP or rSFV-IL-10 particles (Jerusalmi *et al.*, 2003). IFN-β expression was also found in other parts of the CNS, ensuring successful secretion of the cloned cytokine. High levels were seen in the spinal cord of rSFV-IFN-β treated animals 48 h post inoculation. This suggests a persistence of IFN-β for up to two days post inoculation within the CNS and a route of distribution and action for expressed IFN-β within the CNS. In a similar fashion to expressed EGFP, IFN-β is probably carried from the nasal epithelium to the olfactory bulbs, brain and spinal cord by axonal transport. By 72 h the levels of IFN-β had decreased in both the olfactory bulb and the spinal cord. Low levels of IFN-β were also present in the CNS tissues of rSFV empty particle treated

animals indicating that the presence of viral vector alone is producing endogenous IFN-β at the site of inoculation. Since the vector undergoes transcription and replication in the nasal passage, cells of the nasal epithelium are likely to be producing this endogenous IFN-β in response to rSFV particle infection. A recent study showed a similar result where recombinant SFV infection produced IFN-α/β in cultures of bone marrow-derived murine myeloid DCs (Hidmark *et al.*, 2005). In this study mice received rSFV-EGFP viral particles by i.v. inoculation through the tail vein. Murine DCs were isolated from femurs and tibiae, stimulated with murine GM-CSF and supernatant harvested and measured for the presence of IFNα/β. The IFNα/β response in mice injected with these particles was high and dose dependent. Innate immune responses could also be playing a role in the production of endogenous IFN-β through the activation of TLR 7. TLR7 facilitates the recognition of ssRNA viruses such as influenza and VSV by plasmacytoid DCs and B cells resulting in the activation of costimulatory molecules and production of type 1 IFNs. The effect of SFV infection on cells expressing TLR 7 has not been examined but may be a contributory factor to IFN-β production (Lund *et al.*, 2004).

The majority of clinical trials have shown that IFN-β is most successful in the treatment of RRMS when it is administered frequently and at high doses. Barbero *et al.*, 2004, 2006 showed that treatment of RRMS with IFN-β-1b every-other-day was more effective than once-weekly treatment with IFN-β-1a. Continuous treatment of EAE with high dose IFN-β is also the most effective way of treatment of EAE (Ruuls *et al.*, 1996; Yasuda *et al.*, 1999; Yu *et al.*, 1996). Ruuls *et al.* 1996 showed that daily treatment of EAE in Lewis rats with s.c. injections of high dose rr IFN-β inhibits disease activity with discontinuation of treatment leading to worsening of disease. Thus, together with this evidence and the data describing the duration of IFN-β within the CNS following i.n. inoculation, it was decided to administer frequent rSFV-IFN-β treatments throughout the induction, effector and the recovery stage of disease, starting on day three p.d.i. and every third day after until day 27. The EAE model chosen, the MOG 35-55/C57/Bl6 model, is well established and has shown previous success when treated with rSFV-IL-10 (Jerusalmi *et al.*, 2003). The effector period is generally found between days 12 and 17 in this model. Frequent rSFV-IFN-β treatments did not improve clinical disease as expected but in fact significantly enhanced disease severity in comparison to the TNE controls ($p<0.05$). Studies were performed to examine the overall effect i.n. administration of rSFV-IFN-β

particles had on the host cellular immune response by performing assays on harvested splenocytes *ex vivo*. It is not believed that rSFV particles infect peripheral tissues outside of the CNS nasal epithelium after i.n. inoculation. Replication of the recombinant particles and secretion of the cloned IFN-β at the site of inoculation should induce other cytokine cascades and effect the overall peripheral immune response of the EAE animal. Treatment with rSFV-IFN-β is thought to have evoked a Th1 response, indicated by the enhanced production of IFN-γ from splenocytes of rSFV1-IFN-β and rSFV10-E-IFN-β treated animals in response to stimulation with the MOG 35-55 peptide *ex vivo*. This IFN-γ proliferative response was greater in rSFV-IFN-β treated animals compared to the TNE control and greatest in the rSFV1-IFN-β treated animals ($p<0.01$). IL-10 levels were also measured and indicated some deviation towards a Th2 response in the rSFV-IFN-β treated animals. This anti-inflammatory Th2 response was insufficient to have an ameliorating effect on EAE, possibly due to the overproduction of IFN-γ. Previous studies have shown that the successful or unsuccessful proliferative response of IFN-β treated lymphocytes to priming antigen obviously does not always correlate with an improvement or exacerbation in clinical disease (Luca *et al.*, 1999; Tuohy *et al.*, 2000; Yu *et al.*, 1996). Even when IFN-β was ineffective in treating EAE induced in mice with PLP peptide, it still inhibited PLP139-151 specific proliferative responses (Luca *et al.*, 1999). In some cases IFN-β treatment can result in improvement in clinical disease and inhibition of proliferative response. Continuous IFN-β treatment of EAE induced in SJL mice with MBP reduced disease severity but effectively inhibited the T response to MBP stimulation (Yasuda *et al.*, 1999). In addition to T cell responses to peptide, levels of IFN-γ and IL-10 were also measured in the brains of these animals. No significant difference was seen in these levels between the treatment groups.

Repeated administration of rSFV-IFN-β may be exacerbating the disease model as a result of negative effects that the expressed IFN-β protein is having on CNS cells. As discussed in Chapter 1, IFN-β can enhance expression of MHC class I antigen molecules and, in turn, downregulate MHC class II molecules on a variety of cell types, rendering EAE effector cells more susceptible to lysis by CTL. Any downregulation in MHC class II expression may prevent recombinant virus from entering neighbouring cells as the MHC receptor is required for entry. The presence of expressed IFN-β in the CNS may be even more detrimental to cells through its ability to induce production of 2′-5′-(OAS) and

dsRNA dependent PKR. These enzymes inhibit viral mRNA translation and prevent virus assembly. If recombinant particles cannot be produced for further infection, no IFN-β expression can occur, creating a negative feedback loop. An accumulation of anti-IFN-β antibodies may also be hindering the efficacy of rSFV-IFN-β treatment.

In this first experiment administration of rSFV empty particles alone also exacerbated disease severity by increasing clinical score and weight loss. Wild type avirulent SFV has been shown to potentiate or exacerbate EAE when given peripherally (Eralinna *et al.*, 1996; Mokhtarian and Swoveland, 1987; Wu *et al.*, 1988). Similarly Jerusalmi *et al.*, 2003 found that both rSFV-EGFP and empty particle controls exacerbated clinical disease to a significant level in comparison to the TNE buffer treated animals. This indicates that the rSFV vector, despite no longer retaining any of its structural proteins, is still capable of inducing an immune response. Previous studies have shown that replication deficient HSV and adenoviral vectors are also capable of augmenting the potential for antigen processing and MHC class 1 presentation (Bowers *et al.*, 2003). Immune responses arising from HSV vectors are thought to be as a result of low-level *de novo* viral gene product expression of the intact viral transcription units. Adaptive immunity to adenoviral vectors has also been attributed to low levels of viral gene expression indicated by a reduction of Th2 responses and neutralizing antibodies by E4 deleted vectors. rSFV particle vectors may express similar transcription units leading to the augmentation of the immune response. In our study stimulation of splenocytes from these empty particle control animals *ex vivo* with MOG peptide showed an increased IFN-γ response compared to splenocytes from TNE treated control animals and rSFV-IFN-β treated animals ($p<0.01$), combined with a lower IL-10 response ($p<0.01$). In general SFV vectors have been shown to be successful in inducing humoral and cell-mediated immunity in their role as prototype vaccines (Berglund *et al.*, 1999; Berglund *et al.*, 1998; Colmenero *et al.*, 2001; Morris-Downes *et al.*, 2001). Administration of rSFV RNA by i.m., i.v. or s.c. routes led to significant levels of antigen-specific CTL responses and increased numbers of specific CD8+ T cells, as detected by tetramer binding (Colmenero *et al.*, 2001). In our study the administration of numerous rSFV-IFN-β and empty SFV particle treatments may have primed the immune system to upregulate the pre-existing Th1 inflammatory response typical of EAE. One reason for this upregulation could be due to activation of TLR3 in the presence of rSFV infected cells. A recent study has shown that i.p. or i.v. administration of Vero cells infected with rSFV particle vectors expressing the ovalbumin gene *in vivo* led to

activation of the dsRNA TLR3 on the surface of phagocytosing CD8 + DCs (Schulz *et al.*, 2005). TLR3 signaling augments cross presentation by CD8+ dendritic cells leading to upregulation of co-stimulatory molecules and production of immunomodulatory cytokines such as IFN-γ. Similarly TLR7, as previously discussed, is activated in the presence of ssRNA viruses and may lead to disease exacerbation through the production of Th1 IL-12. Other possible explanations for exacerbation of disease could be due to production of anti-SFV antibodies or to molecular mimicry. Repeated administration of rSFV-IFN-β could be inducing immunity to further vector administration, resulting in reduced efficacy of IFN-β treatments. Molecular mimicry occurs when crossreactivity between microbial antigen and self-antigen initiates the activation of autoaggressive immune responses. In this instance SFV antigens may be crossreacting with murine self-antigens resulting in an autoimmune response.

Due to the negative result for continuous treatment, regimes were designed where fewer rSFV-IFN-β particle treatments were administered, and targeted towards the effector stage of disease, which fell between day 12 and 17 in this EAE model. The rSFV10-E-IFN-β vector had shown more promising results than the rSFV1-IFN-β vector and was chosen as the most suitable vector to continue work with. This vector had induced a stronger Th2 response on stimulation with peptide *ex vivo,* indicated by the increased levels of IL-10 induction. This increased production of IFN-β from rSFV10-E-IFN-β is thought to be leading to a downregulation in the Th1 response and a tendency towards this Th2 response. Treatment of mice through out the effector phase on days 5, 8, 11, 13 and 17 did not show any significant improvement in disease compared to the TNE control. Likewise treatments targeting the late effector stage of disease on days 12, 15, 16 and 17 showed little improvement in comparison to the TNE controls. Treatment before the effector stage on days 5, 8, 11 and 12 proved to be the most effective regime as animals experienced a delay in disease onset, lower maximum EAE scores and significantly lower mean EAE scores compared to both the TNE ($p<0.05$) and empty particle treated animals ($p<0.01$) up to day 20. Discontinuation of treatment led to a resumption of disease progression though at a slower rate than the control groups. This is consistent with previous studies on the treatment of EAE using rIFN-β protein (Ruuls *et al.*, 1996; van der Meide *et al.*, 1998). Splenocytes from these rSFV10-E-IFN-β and rSFV10-E treated animals produced higher levels of IFN-γ in response to MOG stimulation than the TNE treated animals 22 days after disease induction, however these levels were lower than those

induced *ex vivo* after continuous treatment. Higher levels of IFN-γ were induced from splenocytes of animals sampled at the earlier time of 15 days post induction. This was most likely due to sampling of these animals during the effector period of disease, when the IFN-γ producing Th1 cells are upregulated. It is possible that high levels of IFN-γ may have a beneficial effect on the course of disease during the induction stage of disease. In some cases, elimination of IFN-γ worsens EAE by abrogating the termination of the immune response (Krakowski and Owens, 1996). Previous studies have shown that IFN-γ can elicit a suppressive effect on disease development either through induction by another Th1 cytokine such as IL-12 (Gran *et al.*, 2004) or administration of neutralizing antibodies to IFN-γ (Duong *et al.*, 1994; Duong *et al.*, 1992; Lublin *et al.*, 1993). In this study however rSFV10-E-IFN-β treated animals produced significantly less IFN-γ than the empty particle treated mice, indicating that IFN-β may downregulating the Th1 response. As before the IL-10 levels were minimal but at this time point little difference was seen between the treatment groups. High IFN-γ levels may be suppressing the IL-10 response, either independently or through the IL-10/IL-12 immunoregulatory circuit, shown to play an important role in EAE (Segal *et al.*, 1998). IL-12 is a potent inducer of IFN-γ production from lymphocytes and NK cells (Trinchieri, 1998; Trinchieri *et al.*, 2003), which suggests that IL-12 is contributing to upregulation of IFN-γ levels which in turn are resulting in downregulation of IL-10 levels. Studies have shown that IFN-β has the potential to enhance production of inflammatory cytokines leading to downregulation of IL-10 levels (Manetti *et al.*, 1995). In other studies IFN-β is shown to have no significant effect on IL-10 levels (Kawanokuchi *et al.*, 2004). Levels of IL-4 were also measured after *ex vivo* stimulation with MOG peptide. Overall IL-4 levels were found to be low but rSFV10-E-IFN-β treated animals did produce more IL-4 than the control groups. IL-4 is responsible for differentiation of naïve CD4+ cells to Th2 cells and is thought to play a regulatory role in EAE during the recovery phase of disease (Begolka *et al.*, 1998; Khoury *et al.*, 1992). This may explain why low levels are found day 15 post disease induction when mice are still in the effector phase of disease.

In mice EAE pathology is characterized by perivascular lymphocytic and monocytic infiltrates, white matter demyelination, and some limited remyelination (Raine, 1983; Raine, 1984). In our study EAE lesions induced in C57/Bl 6 mice with MOG 35-55 were found in both the brain and spinal cord (mostly in the spinal cord) and were assessed blind according to a five point grading system based on the parameters of EAE. These

parameters included myelin vacuolation, axonal degeneration, leucocytic infiltration and glial activation. Grade 1 lesions were generally small and isolated in the spinal cord whereas grade 5 lesions were diffuse and also found in brain stem areas. In the first experiment involving continuous treatment with rSFV-IFN-β, little difference was seen in the pathology of the lesions between the different treatment groups when examined at two different time points. Clinical and pathological scores correlated in the second experiment where animals that received treatment just before the effector stage of disease experienced less severe disease and weight loss. Animals were perfused day 15 and day 22 post disease induction and overall rSFV-IFN-β treated animals showed lower clinical scores and less severe lesions in the brain and the spinal cord. A grade two lesion showed minimal localized perivascular leucocytic infiltrates whereas a more severe grade four lesion from a TNE treated animal showed extensive perivascular cuffing, myelin vacuolation and axonal degeneration. Similar improvements in pathology of the lesion have been seen in different EAE models after treatment with IFN-β (Floris *et al.*, 2002; Ruuls *et al.*, 1996; Yu *et al.*, 1996). Treatment of EAE induced in (SWR × SJL) F mice with IFN-β by s.c. injection showed a delayed progression to clinical disability accompanied by an overall decrease in severity of cellular inflammatory infiltrates and demyelination (Yu *et al.*, 1996).

Histopathological studies showed infiltration of immune cells but further work was necessary to characterize the phenotypes of these infiltrating cells. Immunohistochemistry was carried out on 4μm sections of sagital spinal cord taken from animals day 22 who had received rSFV-IFN-β particle treatment on days 5,8,11 and 12 as this treatment regime had yielded the most promising result. Effector T lymphocytes were mostly found in the area of myelin vacuolation. It was not possible to distinguish these T lymphocytes into MHC class II restricted CD4+ and class I restricted CD8+ cells as antibodies specific for these cell types did not function on formalin fixed tissue sections, despite the use of epitope unmasking procedures such as trypsinisation and antigen heat retrieval using both citrate buffer and EDTA buffer. The more numerous B cells were found mostly in the perivascular spaces of the meninges. From a qualitative study, extensive perivascular cuffing of B lymphocytes was seen in the lesion of a rSFV10-E empty particle treated animal compared to a similar lesion of a rSFV10-E-IFN-β treated animal where B lymphocytes were more sparsely distributed ($p<0.01$). Morphometric analysis was employed to count the average number of infiltrating T and B lymphocytes in these lesions. No difference was detected in the number of infiltrating T lymphocytes between

the different treatment groups. Lesions in rSFV10-E-IFN-β treated animals contained significantly fewer B lymphocytes than similar sized lesions in the control groups. The role of B cells in EAE remains controversial as they possess both effector and regulatory properties (Fillatreau *et al.*, 2002; Lyons *et al.*, 2002; Lyons *et al.*, 1999; Willenborg and Prowse, 1983). Studies have shown that activated B cells expressing high levels of $CD80^+$ costimulatory protein are involved in activating Th1 cells in MS and EAE. Therapy with IFN-β has been shown to markedly reduce the number of these circulating $CD80^+$ B cells (Genc *et al.*, 1997; Hallal *et al.*, 2003) leading to improvement in clinical disease. This finding could partially explain the beneficial effect of our rSFV10-E-IFN-β treatment on the course of EAE where B cells appear to be involved in an effector role on which IFN-β is exhibiting a downregulatory effect.

Infiltrating macrophages and astrocytes were also immunolabeled and found to be most numerous in areas of myelin vacuolation. The main role for macrophages in these areas of demyelination is in phagocytosis of the myelin debris and presentation of the myelin debris to autoreactive T cells (Dijkstra *et al.*, 1992; Hendriks *et al.*, 2005). Their close proximity to the area of demyelination is due in part to the induction of GM-CSF from astrocytes which adjoin these areas. GM-CSF is a cytokine necessary for growth and differentiation of macrophages, leading to their accumulation at the site of inflammation (Frei *et al.*, 1992). Gliosis was characterized in the lesion by the presence of these large reactive astrocytes which are also involved in anti-inflammatory response through the induction of IL-6 (Eng *et al.*, 1992; Van Wagoner *et al.*, 1999). Studies have shown that IFN-β treatment induces both murine and human primary astrocytes to produce IL-6 (Okada *et al.*, 2005). Further intracellular staining in the CNS lesion to identify cytokine cascades triggered by IFN-β expression would have supported the Th1/Th2 MOG response data. Little is known about the production of endogenous IFN-β in the CNS but it is most likely produced by the resident CNS macrophage or microglial cells (Fujihara *et al.*, 1994). IFN-γ is predominantly secreted by Th1 cells within the inflammatory EAE lesion, whereas Th2 cells, B cells and astrocytes secrete IL-10. Immunostaining of the MHC class I antigen receptor on cells in the CNS lesion would also have helped to establish whether treatment with rSFV-IFN-β is having an upregulatory effect on expression.

To further characterize the immune response involved, FACS analysis was used to examine the percentage of total lymphocytes classified as CD4+, CD8+ and B lymphocytes after successful treatment with rSFV-IFN-β. In this experiment splenocytes

were excised and harvested from animals day 30 p.d.i. It would have been more beneficial to perform FACS analysis on infiltrating CNS and immune cells in the EAE lesion, however it was thought that the effects, either positive or negative, of rSFV-IFN-β treatment on peripheral immune cells would be sufficient to establish any changes in T cell phenotype, and B cell numbers. The cellular profile for both the TNE and the rSFV10-E-IFN-β treated groups suggested one of recovery. In contrast to our morphometric data, both TNE and rSFV10-E-IFN-β treated animals had higher percentage B cells than the empty particle treated animals ($p<0.01$) and were in the recovery phase or had fully recovered, while the empty particle treated animals were still displaying symptoms of EAE. B cells are thought to exhibit a regulatory function in the recovery phase through their ability to produce IL-10. When IL-10 deficiency was restricted to B cells only and not T cells, the pro-inflammatory type 1 immune response persisted and mice did not recover (Fillatreau *et al.*, 2002). A higher percentage of CD4+ and CD8+ lymphocytes were also measured in the splenocytes of rSFV10-E-IFN-β and TNE treated mice compared to the empty particles treated mice, which correlates with recovery. The key IL-10-producing cells within the CNS are the CD4+CD25+ T cell population which are critical to recovery from the disease (Kohm *et al.*, 2002; McGeachy *et al.*, 2005). Expression of the forkhead family transcription factor, foxp3, is required for the development of these regulatory T cells. CD4+CD25+Foxp3+ cells have been shown to limit the risk of EAE arising from T cell receptor crossreactivity or molecular mimicry. Similarly CD8+ cells have been shown to play a role in controlling relapses in late adaptive immune responses (Jiang *et al.*, 1992; Koh *et al.*, 1992). In both MS and EAE, the CD8+CD28+ T suppressor activity is decreased in comparison to normal subjects (Antel *et al.*, 1986; Najafian *et al.*, 2003). Little is known about the effect of IFN-β on these cells in EAE, but treatment of MS with IFN-β enhances CD8+CD28+ T suppressor cell activity leading to an improvement in disease (Javed and Reder, 2005).

To assess the potential of rSFV-IFN-β in the treatment of a different model of EAE, we induced EAE in SJL mice using SCH. This is another well established model of EAE (Morris-Downes *et al.*, 2002). These animals were treated according to the most effective time points to date, before the effector stage of disease on days 5,8,11,12. However rSFV-IFN-β treatment showed no efficacy in the treatment of this model and, in fact, administration of both rSFV-IFN-β and empty particle vectors made the disease marginally worse. Overall this SCH induced EAE proved to mediate a considerably more

severe disease in SJL mice than MOG peptide did in C57/Bl 6 mice. The conclusion was reached that this model was untreatable and not an appropriate model for testing any potential CNS gene therapy option.

In MS clinical trials, continued attempts are being made at improving the efficacy of IFNs by using them in combination with other agents such as statins, immunosuppressive agents and IVIG (Farrell *et al.*, 2005; Lublin *et al.*, 2001; Rudick *et al.*, 2006). Similarly in EAE studies IFN-β has been administered in conjunction with other immunomodulatory reagents such as early pregnancy factor, a secreted protein with immunosuppressive and growth factor properties (Zhang *et al.*, 2000), glucocorticoids such as methylprednisolone which is administered to patients experiencing acute relapses of MS (Schmidt *et al.*, 2001) and minocycline, an tetracycline analogue (Giuliani *et al.*, 2005). Due to their ability to upregulate the Th2 response it was decided to co-administer both rSFV-IFN-β particles and rSFV-IL-10 particles together on days 5,8,11 and 12 which to date has proven to be the most successful treatment. IL-10 was subcloned from the original rSFV1-IL-10 vector constructed by Jerusalmi *et al.* 2003, and expression was confirmed *in vitro*. IL-10 expression was greater in the BHK-21 cell line than in murine L929 cells ($p<0.01$), and when compared to the levels expressed from the original rSFV1-IL-10 vector, the new enhanced vector rSFV10-E-IL-10 produced approximate 50 times more IL-10. In spite of this efficiency of expression of the rSFV vectors *in vitro*, co-administration of rSFV-IFN-β and rSFV-IL-10 particles did not show any significant improvement in comparison to the TNE control animals, though some delay was seen in the average day of disease onset. Animals experienced maximum EAE scores which exceeded those of the control groups resulting in a more severe disease. In contrast to what was seen by Jerusalmi *et al.*, 2003 when treating EAE with rSFV1-IL-10, treatment with rSFV10-E-IL-10 particles alone showed no improvement in disease and led to a more severe disease accompanied by correspondingly severe lesions. Treatment with rSFV1-IL-10 on days 5,8,11,13 and 17 completely inhibited disease up until day 20 and reduced severity of the lesion accordingly. The only difference between these two studies are the days of administration, indicating that successful treatment depends completely on when the rSFV-IL-10 particles are given. More work will have to done to establish a logical reason why IL-10 is more effective at this time points. The beneficial action of IL-10 may differ depending on the local cytokine microenvironment within the CNS at the time of administration. In keeping with previous studies, the clinical outcome of our treatment

study did not correlate with the specific T cell responses *ex vivo* (Luca *et al.*, 1999; Tuohy *et al.*, 2000; Yu *et al.*, 1996). rSFV-IFN-β/rSFV-IL-10 treatment did not show an increased induction of IFN-γ *ex vivo* in response to MOG 35-55 stimulation despite failing to improve disease severity. Like rSFV10-E-IFN-β treated animals, the animals that received combined treatment produced significantly less IFN-γ compared to the empty particle controls, indicating that the presence of either IL-10 or IFN-β or both is downregulating the Th1 response. Endogenous IL-10 may be produced by astrocytes in the CNS, but mostly from infiltrating B cells. From FACS analysis, rSFV10-E-IL-10 and rSFV10-E-IFN-β/rSFV10-E-IL-10 treated animals produced a similar percentage of B cells compared to the rSFV10-E-IFN-β treated group. B cells, as discussed before, are believed to play a role in disease recovery by production of IL-10 (Fillatreau *et al.*, 2002). In studies where EAE has been successfully treated with IL-10, treatment resulted in an alteration in cellular phenotype, notably an increase in the numbers of CD8+ and B cells (Croxford *et al.*, 2001). No increase was seen in CD8+ cells in this study however. This is probably due to the negative outcome of the treatment regime.

Another treatment regime was decided upon where CT, a well established vaccine adjuvant was co-administered with rSFV10-E-IFN-β particles using the best treatment days to date, 5, 8, 11 and 12. The success of CT in the treatment of EAE is due to its ability to induce antigen specific CD4+ T cells to secrete T helper 2 cytokines. This has been well established in vaccine studies (Lavelle *et al.*, 2004; Lavelle *et al.*, 2003; Williams *et al.*, 1999; Xu-Amano *et al.*, 1994). Recent studies have shown that oral administration of CT-B–autoantigen conjugates prevent autoimmune diseases such as EAE by inducing functional tolerance (Sun *et al.*, 1996; Sun *et al.*, 2000). Whole CT has also been successfully used to treat EAE induced in C57/Bl 6 mice with MOG 35-55 (Yura *et al.*, 2001). In this study, animals were treated with 64μg of whole CT by i.n. inoculation. Mice received 32μg CT in 10μl PBS per nostril on day 7 p.d.i. In our study animals received three doses of 0.5μg CT by i.n. inoculation on days 5, 9 and 12 instead of days 5, 8, 11, 12 to avoid any side effects through the inoculation with CT and PT on the same day. This treatment regime proved to be more effective than co-administration of rSFV-IFN-β and rSFV-IL-10 particles. Overall these animals experienced significantly lower mean EAE scores compared to the TNE ($p<0.05$) and empty particle control animals up to day 19 ($p<0.01$), and to the rSFV-IFN-β and rSFV-IL-10 animals. To test the effect of rSFV particles on CT alone, another group of animals received empty particles instead of

rSFV-IFN-β particles, together with CT. These animals experienced the highest maximum EAE scores and number of deaths overall. The presence of the empty SFV particles may be suppressing the beneficial effects of the CT treatment through the induction of Th1 cytokines, whereas the rSFV-IFN-β particles may support it. IFN-γ responses from both the CT groups were significantly lower than from the empty particle treated animals ($p<0.01$), with animals receiving rSFV10-E-IFN-β and CT producing marginally less IFN-γ than the other treatment groups, and more IL-10, though neither result was significant. Both the rSFV10-E-IFN-β particles/CT treated and the rSFV10-E/CT treated animals experienced EAE lesions of similar severity by day 22 when clinical disease has reached a maximum in both groups. No additional pathology was caused in the brains of the rSFV particle/CT treated animals through the administration of CT. FACS analysis showed a trend where both CT treated groups experienced a percentage of B cells in their splenocyte populations marginally higher than those of the rSFV-IFN-β treated, and significantly greater than the empty particle controls. Studies have shown that CT possesses the ability to promote B cell isotype differentiation leading to an upregulation of B cells (Lycke and Strober, 1989). The population of CD4+ cells in CT treated animals also exceeded those of the CD8+ population, as would be expected given the ability of CT to induce a CD4+ T cell response (Lavelle *et al.*, 2004; Lavelle *et al.*, 2003; Williams *et al.*, 1999; Xu-Amano *et al.*, 1994).

In summary, treatment of MOG 35-55 peptide induced EAE was most successful when rSFV-IFN-β particles were administered alone, before the effector stage of disease on days 5,8,11 and 12. This was accompanied by improvement in clinical score and pathology of the lesion, less dramatic weight loss, reduced IFN-γ Th1 response to peptide, inhibition of B lymphocytic infiltration into the lesions during the effector stage and increased levels of CD4+, CD8+ and B lymphocytes in recovery. A trend was seen where the CD8+ cell population of the rSFV-IFN-β treated animals was considerably higher than that of the other treatment groups and the controls, which is not surprising given that IFN-β has been shown to promote the proliferation of MHC class I CD8+ CD28+ T suppressor cells. At these times, the administration of rSFV–IFN-β particles is sufficient to cause some deviation towards a Th2 response without enhancing the pre-existing Th1 response typical of EAE. Co-treatment with rSFV-IL-10 particles did not improve the clinical disease as expected, despite showing favourable T cell responses *ex vivo*. For successful co-treatment with rSFV10-E-IL-10 particles it may be necessary to treat the animals

through out the induction and effector period, on days 5,8,11,13,17 as shown by Jerusalmi *et al.*, 2003 in the treatment of the same EAE model with rSFV1-IL-10. This change in the treatment pattern may prove more effective. Co-treatment with rSFV-IFN-β and CT toxin did show more promising results, with animals experiencing lower maximum EAE scores by day 19 and lower weight loss compared to the controls, but the dose administered needs to be optimised. A dose of 0.5μg administered three times was insufficient is show any real Th2 response upon stimulation ex *vivo*. In spite of the promising results obtained from these treatment studies, there are some fundamental weaknesses in the experimental design of the study. A greater number of animals should have been used in each treatment group to allow for more meaningful statistical analysis of the clinical scores, weights, pathology and *ex vivo* studies. The average number of mice per group was ten but, in hindsight, each group should have contained at least 16 animals, allocating a sufficient number of mice for monitoring of clinical disease and for two sampling time points. Immunological studies should have been performed on the cells of the CNS lesion instead of the peripheral immune cells as these are the cells which mediate the inflammatory response.

After critical analysis of the overall results achieved from this study, treatment of EAE with rSFV vectors expressing IFN-β, or perhaps any cytokine, would not be a realistic option despite their ability to penetrate the BBB and target the CNS directly after i.n. inoculation. Administration of immunomodulatory agents such as cytokines using viral vector systems is complicated since the vectors themselves may evoke potent host immune responses (Bowers *et al.*, 2003). Even in replication deficient viral vector systems some intact genomes encoding ORFs remain, and are capable of augmenting class I host CTL responses. Kristy *et al.* 1998 showed that an HSV vector deleted for an important immediate early (IE) gene encoding an essential transcriptional transactivator, still proved cytotoxic to many cell types in culture. Similarly Johnson *et al.*, 1992 found that complete inhibition or inactivation of all viral IE gene expression was required in the construction of a HSV replication deficient vector expressing Lac Z to avoid CPE. As seen in this study, empty SFV particles, in which the structural genes have been deleted and supplied *in trans* by separate helper vectors, still evoked a strong Th1 response in their host. As discussed above, this response could have happened for many different reasons – production of anti-SFV antibodies, activation of TLRs, molecular mimicry or the presence of SFV transcription units. While this response may be beneficial in the treatment of another disease model, it clearly has a negative impact on EAE. EAE is a classical Th1 disease

therefore administration of rSFV particles will only exacerbate the pre-existing phenotype of the disease, making it difficult to overcome this unwanted response and establish a treatment regime which induces a sufficient Th2 response. When such immune responses are induced, it is difficult to establish whether any beneficial or detrimental effects seen in the disease model are due to the expressed heterologous protein or simply due to the presence of recombinant vector. Most work has been done on the treatment of EAE with HSV and adenoviral vectors using both replication competent and deficient viruses. To date rHSV vector expressing IL-4 has proven to be the most successful treatment when administered intracranially (Broberg *et al.*, 2001; Furlan *et al.*, 1998). Surprisingly this treatment showed no effects on the peripheral immune system when antigen-specific proliferative response and cytokine secretion patterns were examined and is therefore the most likely candidate for an MS clinical trial. Other potential treatments include the i.m. administration of naked DNA plasmids expressing immunomodulators as they are non-immunogenic and non-pathogenic. They can also be repeatedly administered with relatively prolonged periods of expression *in vivo*, ranging from weeks to months after each injection (Piccirillo and Prud'homme, 2003). With regard to IFN-β, i.c. treatment of EAE with a retroviral vector expressing IFN-β proved more successful than i.n. treatment with rSFV-IFN-β. Animals experienced reduced severity of disease after treatment on day 12 but in a similar way to our study, termination of treatment resulted in worsening of disease. This phenomenon was also seen by Ruuls *et al.* 1996, where discontinuation of treatment with rrIFN-β led to disease progression. RRMS patients also experience more frequent relapses if their long term high IFN-β dose is reduced to once-weekly (Barbero *et al.*, 2004). In the majority of previous EAE studies, IFN-β protein was administered systemically with mixed results (Luca *et al.*, 1999; Yasuda *et al.*, 1999). It was found from all these studies that clinical disease outcome does not necessarily correlate with proliferative responses or T cell responses. This supports our study, where positive clinical outcome after treatment on days 5,8,11 and 12 did not correlate with high IL-10 levels. Similarly in the combinational studies with rSFV-IL-10 and whole CT, animals that received rSFV-IL-10 alone or SFV empty particles together with CT experienced severe clinical disease even though they showed favourable IL-10 levels.

Despite the negativity of these EAE results, treatment of MS with viral vectors expressing cytokines may prove more successful than treatment of EAE. EAE is the best animal model of MS available but it can never be considered an exact immunological

replica of the human disease. Firstly EAE is based on a disease which lasts 30 days, with a chronic disease period between days 12-17. In RRMS, patients experience infrequent acute neurological attacks after which they can remain relapse free for years. The course of the human disease is unpredictable and cannot be slotted into a specific time frame. Recent studies have disputed the belief that MS is a CD4 + Th1 disease, believing that CD8+ T cells and the humoral response play a more important effector role than previously thought (Huseby *et al.*, 2001; Lassmann and Ransohoff, 2004; Sun *et al.*, 2001). EAE, on the other hand, is a classical CD4+ Th1 disease, and will never be considered otherwise. Therefore administration of viral vectors expressing immunomodulatory agents such as cytokines could potentially be a lot more effective in the treatment of MS than in EAE, based solely on the immunological differences between the two diseases. The success of IFN-β has been well documented in the treatment of RRMS (Ebers, 1998; Jacobs *et al.*, 1996; Sibley, 1993). This is in contrast to published EAE studies where IFN-β treatment has yielded both positive and negative results. More is known about the mechanism of action of IFN-β in the human disease also (Furlan *et al.*, 2000; Noronha *et al.*, 1993). The most important issue that would need to be addressed before rSFV-IFN-β could be used to treat MS patients is the route of administration. Intranasal inoculation would not be an exceptable route of administration in a clinical trial setting. In MS, the DMAs are generally administered by i.m. or s.c. routes. More work would have to be done to establish a less invasive, more standard route of inoculation. While the results from this study highlight the potential efficacy of rSFV-IFN-β in MS clinical trials, until the immunology and etiology of the disease is fully established, treatment with rSFV vectors should be approached with caution and some level of a skepticism.

In light of the findings from this study, the exploitation of rSFV vectors expressing cytokines such as IFN-β or IL-10 may prove more successful in the field of tumour gene therapy than in the treatment of autoimmune diseases such as MS. Previous studies have shown the success of empty rSFV vectors and rSFV vectors expressing EGFP, IL-12 and p62 –6K SFV structural genes in the treatment of a human lung carcinoma, murine colon carcinoma, and a murine sarcoma (Chikkanna-Gowda *et al.*, 2005; Murphy *et al.*, 2000; Smyth *et al.*, 2005). Of particular interest is the administration of the IL-12 subunits, p35 and p40 via a viral vector in the treatment of a murine sarcoma as IL-12 is itself a potent inducer of the Th1 response (Chikkanna-Gowda *et al.*, 2005). Considering that such a large Th1 response resulted in complete tumour regression in this model, perhaps this is where

the true therapeutic effect of rSFV vectors lies. To date, IFN-β gene therapy with replication-defective adenoviral vectors has shown potential as an effective treatment for some solid tumors such as a human breast cancer xenograft (Qin *et al.*, 1998). In conclusion rSFV-IFN-β or rSFV-IL-10 vectors may not be suitable for treatment of EAE or MS but could yield beneficial, anti-tumoral effects in the field of cancer gene therapy due to their ability to upregulate the Th1 response.

Chapter 7

References

7.0 References

Abbas, A. K., Murphy, K. M., and Sher, A. (1996). Functional diversity of helper T lymphocytes. *Nature* **383**(6603), 787-93.

Abreu, S. L. (1982). Suppression of experimental allergic encephalomyelitis by interferon. *Immunol Commun* **11**(1), 1-7.

Abreu, S. L. (1985). Interferon in experimental autoimmune encephalomyelitis (EAE): effects of exogeneous interferon on the antigen-enhanced adoptive transfer of EAE. *Int Arch Allergy Appl Immunol* **76**(4), 302-7.

Aharoni, R., Teitelbaum, D., Sela, M., and Arnon, R. (1997). Copolymer 1 induces T cells of the T helper type 2 that crossreact with myelin basic protein and suppress experimental autoimmune encephalomyelitis. *Proc Natl Acad Sci U S A* **94**(20), 10821-6.

Ahola, T., and Kaariainen, L. (1995). Reaction in alphavirus mRNA capping: formation of a covalent complex of nonstructural protein nsP1 with 7-methyl-GMP. *Proc Natl Acad Sci U S A* **92**(2), 507-11.

Ahola, T., Laakkonen, P., Vihinen, H., and Kaariainen, L. (1997). Critical residues of Semliki Forest virus RNA capping enzyme involved in methyltransferase and guanylyltransferase-like activities. *J Virol* **71**(1), 392-7.

Aktas, O., Waiczies, S., Smorodchenko, A., Dorr, J., Seeger, B., Prozorovski, T., Sallach, S., Endres, M., Brocke, S., Nitsch, R., and Zipp, F. (2003). Treatment of relapsing paralysis in experimental encephalomyelitis by targeting Th1 cells through atorvastatin. *J Exp Med* **197**(6), 725-33.

Allen, I., and Brankin, B. (1993). Pathogenesis of multiple sclerosis--the immune diathesis and the role of viruses. *J Neuropathol Exp Neurol* **52**(2), 95-105.

Allner, K., Bradish, C. J., Fitzgeorge, R., and Nathanson, N. (1974). Modifications by sodium auro-thio-malate of the expression of virulence in mice by defined strains of Semliki Forest virus. *J Gen Virol* **24**(1), 221-8.

Allsopp, T. E., Scallan, M. F., Williams, A., and Fazakerley, J. K. (1998). Virus infection induces neuronal apoptosis: A comparison with trophic factor withdrawal. *Cell Death Differ* **5**(1), 50-9.

Amor, S., Baker, D., Groome, N., and Turk, J. L. (1993). Identification of a major encephalitogenic epitope of proteolipid protein (residues 56-70) for the induction of experimental allergic encephalomyelitis in Biozzi AB/H and nonobese diabetic mice. *J Immunol* **150**(12), 5666-72.

Amor, S., Groome, N., Linington, C., Morris, M. M., Dornmair, K., Gardinier, M. V., Matthieu, J. M., and Baker, D. (1994). Identification of epitopes of myelin oligodendrocyte glycoprotein for the induction of experimental allergic encephalomyelitis in SJL and Biozzi AB/H mice. *J Immunol* **153**(10), 4349-56.

Amor, S., O'Neill, J. K., Morris, M. M., Smith, R. M., Wraith, D. C., Groome, N., Travers, P. J., and Baker, D. (1996a). Encephalitogenic epitopes of myelin basic protein, proteolipid protein, myelin oligodendrocyte glycoprotein for experimental allergic encephalomyelitis induction in Biozzi ABH (H-2Ag7) mice share an amino acid motif. *J Immunol* **156**(8), 3000-8.

Amor, S., Scallan, M. F., Morris, M. M., Dyson, H., and Fazakerley, J. K. (1996b). Role of immune responses in protection and pathogenesis during Semliki Forest virus encephalitis. *J Gen Virol* **77 (Pt 2)**, 281-91.

Andersson, A., and Karlsson, J. (2004). Genetics of experimental autoimmune encephalomyelitis in the mouse. *Arch Immunol Ther Exp (Warsz)* **52**(5), 316-25.

Andersson, M., Alvarez-Cermeno, J., Bernardi, G., Cogato, I., Fredman, P., Frederiksen, J., Fredrikson, S., Gallo, P., Grimaldi, L. M., Gronning, M., and et al. (1994). Cerebrospinal fluid in the diagnosis of multiple sclerosis: a consensus report. *J Neurol Neurosurg Psychiatry* **57**(8), 897-902.

Andersson, P. B., Waubant, E., Gee, L., and Goodkin, D. E. (1999). Multiple sclerosis that is progressive from the time of onset: clinical characteristics and progression of disability. *Arch Neurol* **56**(9), 1138-42.

Angelucci, F., Mirabella, M., Frisullo, G., Caggiula, M., Tonali, P. A., and Batocchi, A. P. (2005). Serum levels of anti-myelin antibodies in relapsing-remitting multiple sclerosis patients during different phases of disease activity and immunomodulatory therapy. *Dis Markers* **21**(2), 49-55.

Antel, J. P., Bania, M. B., Reder, A., and Cashman, N. (1986). Activated suppressor cell dysfunction in progressive multiple sclerosis. *J Immunol* **137**(1), 137-41.

Argos, P. (1988). A sequence motif in many polymerases. *Nucleic Acids Res* **16**(21), 9909-16.

Arnason, B. G. (1996). Interferon beta in multiple sclerosis. *Clin Immunol Immunopathol* **81**(1), 1-11.

Arnon, R., and Aharoni, R. (2004). Mechanism of action of glatiramer acetate in multiple sclerosis and its potential for the development of new applications. *Proc Natl Acad Sci U S A* **101 Suppl 2**, 14593-8.

Asselin-Paturel, C., Lassau, N., Guinebretiere, J. M., Zhang, J., Gay, F., Bex, F., Hallez, S., Leclere, J., Peronneau, P., Mami-Chouaib, F., and Chouaib, S. (1999). Transfer of the murine interleukin-12 gene in vivo by a Semliki Forest virus vector induces B16 tumor regression through inhibition of tumor blood vessel formation monitored by Doppler ultrasonography. *Gene Ther* **6**(4), 606-15.

Atkins, G. J., and Sheahan, B. J. (1982). Semliki forest virus neurovirulence mutants have altered cytopathogenicity for central nervous system cells. *Infect Immun* **36**(1), 333-41.

Atkins, G. J. (1983). The avirulent A7 Strain of Semliki Forest virus has reduced cytopathogenicity for neuroblastoma cells compared to the virulent L10 strain. *J Gen Virol* **64 (Pt 6),** 1401-4.

Atkins, G. J., Sheahan, B. J., and Dimmock, N. J. (1985). Semliki Forest virus infection of mice: a model for genetic and molecular analysis of viral pathogenicity. *J Gen Virol* **66 (Pt 3),** 395-408.

Atkins, G. J., Sheahan, B. J., and Mooney, D. A. (1990). Pathogenicity of Semliki Forest virus for the rat central nervous system and primary rat neural cell cultures: possible implications for the pathogenesis of multiple sclerosis. *Neuropathol Appl Neurobiol* **16**(1), 57-68.

Atkins, G. J., McQuaid, S., Morris-Downes, M. M., Galbraith, S. E., Amor, S., Cosby, S. L., and Sheahan, B. J. (2000). Transient virus infection and multiple sclerosis. *Rev Med Virol* **10**(5), 291-303.

Baker, D., and Hankey, D. J. (2003). Gene therapy in autoimmune, demyelinating disease of the central nervous system. *Gene Ther* **10**(10), 844-53.

Baker, D., O'Neill, J. K., Gschmeissner, S. E., Wilcox, C. E., Butter, C., and Turk, J. L. (1990). Induction of chronic relapsing experimental allergic encephalomyelitis in Biozzi mice. *J Neuroimmunol* **28**(3), 261-70.

Balachandran, S., Kim, C. N., Yeh, W. C., Mak, T. W., Bhalla, K., and Barber, G. N. (1998). Activation of the dsRNA-dependent protein kinase, PKR, induces apoptosis through FADD-mediated death signaling. *Embo J* **17**(23), 6888-902.

Balluz, I. M., Glasgow, G. M., Killen, H. M., Mabruk, M. J., Sheahan, B. J., and Atkins, G. J. (1993). Virulent and avirulent strains of Semliki Forest virus show similar cell tropism for the murine central nervous system but differ in the severity and rate of induction of cytolytic damage. *Neuropathol Appl Neurobiol* **19**(3), 233-9.

Barbero, P., Bergui, M., Versino, E., Ricci, A., Zhong, J. J., Ferrero, B., Clerico, M., Pipieri, A., Verdun, E., Giordano, L., and Durelli, L. (2006). Every-other-day interferon beta-1b versus once-weekly interferon beta-1a for multiple sclerosis (INCOMIN Trial) II: analysis of MRI responses to treatment and correlation with Nab. *Mult Scler* **12**(1), 72-6.

Barbero, P., Verdun, E., Bergui, M., Pipieri, A., Clerico, M., Cucci, A., Ricci, A., Bergamasco, B., and Durelli, L. (2004). High-dose, frequently administered interferon beta therapy for relapsing-remitting multiple sclerosis must be maintained over the long term: the interferon beta dose-reduction study. *J Neurol Sci* **222**(1-2), 13-9.

Barkhof, F., Karas, G. B., and van Walderveen, M. A. (2000). T1 hypointensities and axonal loss. *Neuroimaging Clin N Am* **10**(4), 739-52 ,ix.

Barna, B. P., Estes, M. L., Jacobs, B. S., Hudson, S., and Ransohoff, R. M. (1990). Human astrocytes proliferate in response to tumor necrosis factor alpha. *J Neuroimmunol* **30**, 239-243.

Barr, D., Kupersmith, M. J., Turbin, R., Bose, S., and Roth, R. (2000). Isolated sixth nerve palsy: an uncommon presenting sign of multiple sclerosis. *J Neurol* **247**(9), 701-4.

Barrett, P. N., Sheahan, B. J., and Atkins, G. J. (1980). Isolation and preliminary characterization of Semliki Forest virus mutants with altered virulence. *J Gen Virol* **49**(1), 141-7.

Barth, B. U., Wahlberg, J. M., and Garoff, H. (1995). The oligomerization reaction of the Semliki Forest virus membrane protein subunits. *J Cell Biol* **128**(3), 283-91.

Beck, R. W., Cleary, P. A., Trobe, J. D., Kaufman, D. I., Kupersmith, M. J., Paty, D. W., and Brown, C. H. (1993). The effect of corticosteroids for acute optic neuritis on the subsequent development of multiple sclerosis. The Optic Neuritis Study Group. *N Engl J Med* **329**(24), 1764-9.

Begolka, W. S., Vanderlugt, C. L., Rahbe, S. M., and Miller, S. D. (1998). Differential expression of inflammatory cytokines parallels progression of central nervous system pathology in two clinically distinct models of multiple sclerosis. *J Immunol* **161**(8), 4437-46.

Benveniste, E. N. (1997). Role of macrophages/microglia in multiple sclerosis and experimental allergic encephalomyelitis. *J Mol Med* **75**(3), 165-73.

Benveniste, E. N., Tang, L. P., and Law, R. M. (1995). Differential regulation of astrocyte TNF-alpha expression by the cytokines TGF-beta, IL-6 and IL-10. *Int J Dev Neurosci* **13**(3-4), 341-9.

Berardelli, P. (1997). Herpesvirus linked to multiple sclerosis. *Science* **278**(5344), 1710.

Berger, T., Rubner, P., Schautzer, F., Egg, R., Ulmer, H., Mayringer, I., Dilitz, E., Deisenhammer, F., and Reindl, M. (2003). Antimyelin antibodies as a predictor of clinically definite multiple sclerosis after a first demyelinating event. *N Engl J Med* **349**(2), 139-45.

Berglund, P., Fleeton, M. N., Smerdou, C., and Liljestrom, P. (1999). Immunization with recombinant Semliki Forest virus induces protection against influenza challenge in mice. *Vaccine* **17**(5), 497-507.

Berglund, P., Smerdou, C., Fleeton, M. N., Tubulekas, I., and Liljestrom, P. (1998). Enhancing immune responses using suicidal DNA vaccines. *Nat Biotechnol* **16**(6), 562-5.

Bernard, C. C. (1976). Experimental autoimmune encephalomyelitis in mice: genetic control of susceptibility. *J Immunogenet* **3**(4), 263-74.

Bernard, C. C., Johns, T. G., Slavin, A., Ichikawa, M., Ewing, C., Liu, J., and Bettadapura, J. (1997). Myelin oligodendrocyte glycoprotein: a novel candidate autoantigen in multiple sclerosis. *J Mol Med* **75**(2), 77-88.

Berti, R., Soldan, S. S., Akhyani, N., McFarland, H. F., and Jacobson, S. (2000). Extended observations on the association of HHV-6 and multiple sclerosis. *J Neurovirol* **6 Suppl 2**, S85-7.

Bettelli, E., Das, M. P., Howard, E. D., Weiner, H. L., Sobel, R. A., and Kuchroo, V. K. (1998). IL-10 is critical in the regulation of autoimmune encephalomyelitis as demonstrated by studies of IL-10- and IL-4-deficient and transgenic mice. *J Immunol* **161**(7), 3299-306.

Billiau, A., Heremans, H., Vermeire, K., and Matthys, P. (1998). Immunomodulatory properties of interferon-gamma. An update. *Ann N Y Acad Sci* **856**, 22-32.

Biron, C. A. (1998). Role of early cytokines, including alpha and beta interferons (IFN-alpha/beta), in innate and adaptive immune responses to viral infections. *Semin Immunol* **10**(5), 383-90.

Bitsch, A., Bahner, D., Wachter, C., Elitok, E., Bogumil, T., Dressel, A., Polak, T., Tumani, H., Weber, F., Poser, S., and Kitze, B. (2004). Interferon beta-1b modulates serum sVCAM-1 levels in primary progressive multiple sclerosis. *Acta Neurol Scand* **110**(6), 386-92.

Bliss, J., Van Cleave, V., Murray, K., Wiencis, A., Ketchum, M., Maylor, R., Haire, T., Resmini, C., Abbas, A. K., and Wolf, S. F. (1996). IL-12, as an adjuvant, promotes a T helper 1 cell, but does not suppress a T helper 2 cell recall response. *J Immunol* **156**(3), 887-94.

Boere, W. A., Benaissa-Trouw, B. J., Harmsen, M., Kraaijeveld, C. A., and Snippe, H. (1983). Neutralizing and non-neutralizing monoclonal antibodies to the E2 glycoprotein of Semliki Forest virus can protect mice from lethal encephalitis. *J Gen Virol* **64 (Pt 6)**, 1405-8.

Bonatti, S. (1982). Biosynthesis and assembly of membrane proteins. *Horiz Biochem Biophys* **6**, 101-22.

Bowers, W. J., Olschowka, J. A., and Federoff, H. J. (2003). Immune responses to replication-defective HSV-1 type vectors within the CNS: implications for gene therapy. *Gene Ther* **10**(11), 941-5.

Bradish, C. J., and Allner, K. (1972). The early responses of mice to respiratory or intraperitoneal infection by defined virulent and avirulent strains of Semliki forest virus. *J Gen Virol* **15**(3), 205-18.

Bradish, C. J., Allner, K., and Fitzgeorge, R. (1975). Immunomodification and the expression of virulence in mice by defined strains of Semliki Forest virus: the effects of cyclophosphamide. *J Gen Virol* **28**(2), 225-37.

Bradish, C. J., Allner, K., and Maber, H. B. (1971). The virulence of original and derived strains of Semliki forest virus for mice, guinea-pigs and rabbits. *J Gen Virol* **12**(2), 141-60.

Bradish, C. J., Fitzgeorge, R., Titmuss, D., and Baskerville, A. (1979). The responses of nude-athymic mice to nominally avirulent togavirus infections. *J Gen Virol* **42**(3), 555-66.

Bright, J. J., Musuro, B. F., Du, C., and Sriram, S. (1998). Expression of IL-12 in CNS and lymphoid organs of mice with experimental allergic encephalitis. *J Neuroimmunol* **82**(1), 22-30.

Broberg, E., Setala, N., Roytta, M., Salmi, A., Eralinna, J. P., He, B., Roizman, B., and Hukkanen, V. (2001). Expression of interleukin-4 but not of interleukin-10 from a replicative herpes simplex virus type 1 viral vector precludes experimental allergic encephalomyelitis. *Gene Ther* **8**(10), 769-77.

Broberg, E. K., Peltoniemi, J., Nygardas, M., Vahlberg, T., Roytta, M., and Hukkanen, V. (2004a). Spread and replication of and immune response to gamma134.5-negative herpes simplex virus type 1 vectors in BALB/c mice. *J Virol* **78**(23), 13139-52.

Broberg, E. K., Salmi, A. A., and Hukkanen, V. (2004b). IL-4 is the key regulator in herpes simplex virus-based gene therapy of BALB/c experimental autoimmune encephalomyelitis. *Neurosci Lett* **364**(3), 173-8.

Bron, R., Wahlberg, J. M., Garoff, H., and Wilschut, J. (1993). Membrane fusion of Semliki Forest virus in a model system: correlation between fusion kinetics and structural changes in the envelope glycoprotein. *Embo J* **12**(2), 693-701.

Brosnan, C. F., Cannella, B., Battistini, L., and Raine, C. S. (1995). Cytokine localization in multiple sclerosis lesions: correlation with adhesion molecule expression and reactive nitrogen species. *Neurology* **45**(6 Suppl 6), S16-21.

Bruck, W., Schmied, M., Suchanek, G., Bruck, Y., Breitschopf, H., Poser, S., Piddlesden, S., and Lassmann, H. (1994). Oligodendrocytes in the early course of multiple sclerosis. *Ann Neurol* **35**(1), 65-73.

Buttke, T. M., McCubrey, J. A., and Owen, T. C. (1993). Use of an aqueous soluble tetrazolium/formazan assay to measure viability and proliferation of lymphokine-dependent cell lines. *J Immunol Methods* **157**(1-2), 233-40.

Byrnes, A. A., McArthur, J. C., and Karp, C. L. (2002). Interferon-beta therapy for multiple sclerosis induces reciprocal changes in interleukin-12 and interleukin-10 production. *Ann Neurol* **51**(2), 165-74.

Calabresi, P. A., Pelfrey, C. M., Tranquill, L. R., Maloni, H., and McFarland, H. F. (1997a). VLA-4 expression on peripheral blood lymphocytes is downregulated after treatment of multiple sclerosis with interferon beta. *Neurology* **49**(4), 1111-6.

Calabresi, P. A., Tranquill, L. R., Dambrosia, J. M., Stone, L. A., Maloni, H., Bash, C. N., Frank, J. A., and McFarland, H. F. (1997b). Increases in soluble VCAM-1 correlate with a decrease in MRI lesions in multiple sclerosis treated with interferon beta-1b. *Ann Neurol* **41**(5), 669-74.

Calabresi, P. A., Tranquill, L. R., McFarland, H. F., and Cowan, E. P. (1998). Cytokine gene expression in cells derived from CSF of multiple sclerosis patients. *J Neuroimmunol* **89**(1-2), 198-205.

Calabresi, P. A., Prat, A., Biernacki, K., Rollins, J., and Antel, J. P. (2001). T lymphocytes conditioned with Interferon beta induce membrane and soluble VCAM on human brain endothelial cells. *J Neuroimmunol* **115**(1-2), 161-7.

Calopa, M., Bas, J., Mestre, M., Arbizu, T., Peres, J., and Buendia, E. (1995). T cell subsets in multiple sclerosis: a serial study. *Acta Neurol Scand* **92**(5), 361-8.

Cannella, B., Cross, A. H., and Raine, C. S. (1991). Adhesion-related molecules in the central nervous system. Upregulation correlates with inflammatory cell influx during relapsing experimental autoimmune encephalomyelitis. *Lab Invest* **65**(1), 23-31.

Cannella, B., and Raine, C. S. (1995). The adhesion molecule and cytokine profile of multiple sclerosis lesions. *Ann Neurol* **37**(4), 424-35.

Castro, M. G., David, A., Hurtado-Lorenzo, A., Suwelack, D., Millan, E., Verakis, T., Xiong, W. D., Yuan, X. P., and Lowenstein, P. R. (2001). Gene therapy for Parkinson's disease: recent achievements and remaining challenges. *Histol Histopathol* **16**(4), 1225-38.

Chabot, S., and Yong, V. W. (2000). Interferon beta-1b increases interleukin-10 in a model of T cell-microglia interaction: relevance to MS. *Neurology* **55**(10), 1497-505.

Chikkanna-Gowda, C. P., Sheahan, B. J., Fleeton, M. N., and Atkins, G. J. (2005). Regression of mouse tumours and inhibition of metastases following administration of a Semliki Forest virus vector with enhanced expression of IL-12. *Gene Ther* **12**(16), 1253-63.

Choi, H. K., Tong, L., Minor, W., Dumas, P., Boege, U., Rossmann, M. G., and Wengler, G. (1991). Structure of Sindbis virus core protein reveals a chymotrypsin-like serine proteinase and the organization of the virion. *Nature* **354**(6348), 37-43.

Clark, H. F., Cohen, M. M., and Lunger, P. D. (1973). Comparative characterization of a C-type virus-producing cell line (VSW) and a virus-free cell line (VH2) from Vipera russelli. *J Natl Cancer Inst* **51**, 645-657.

Clemens, M. J., Hershey, J. W., Hovanessian, A. C., Jacobs, B. C., Katze, M. G., Kaufman, R. J., Lengyel, P., Samuel, C. E., Sen, G. C., and Williams, B. R. (1993). PKR: proposed nomenclature for the RNA-dependent protein kinase induced by interferon. *J Interferon Res* **13**(3), 241.

Colmenero, P., Berglund, P., Kambayashi, T., Biberfeld, P., Liljestrom, P., and Jondal, M. (2001). Recombinant Semliki Forest virus vaccine vectors: the route of injection determines the localization of vector RNA and subsequent T cell response. *Gene Ther* **8**(17), 1307-14.

Colmenero, P., Chen, M., Castanos-Velez, E., Liljestrom, P., and Jondal, M. (2002). Immunotherapy with recombinant SFV-replicons expressing the P815A tumor antigen or IL-12 induces tumor regression. *Int J Cancer* **98**(4), 554-60.

Colton, C. A., Yao, J., Keri, J. E., and Gilbert, D. (1992). Regulation of microglial function by interferons. *J Neuroimmunol* **40**(1), 89-98.

Compston, A. (1997). Genetic epidemiology of multiple sclerosis. *J Neurol Neurosurg Psychiatry* **62**(6), 553-61.

Constantinescu, C. S., Wysocka, M., Hilliard, B., Ventura, E. S., Lavi, E., Trinchieri, G., and Rostami, A. (1998). Antibodies against IL-12 prevent superantigen-induced and spontaneous relapses of experimental autoimmune encephalomyelitis. *J Immunol* **161**(9), 5097-104.

Costa, O., Divoux, D., Ischenko, A., Tron, F., and Fontaine, M. (2003). Optimization of an animal model of experimental autoimmune encephalomyelitis achieved with a multiple MOG(35-55)peptide in C57BL6/J strain of mice. *J Autoimmun* **20**(1), 51-61.

Cross, A. H., Girard, T. J., Giacoletto, K. S., Evans, R. J., Keeling, R. M., Lin, R. F., Trotter, J. L., and Karr, R. W. (1995). Long-term inhibition of murine experimental autoimmune encephalomyelitis using CTLA-4-Fc supports a key role for CD28 costimulation. *J Clin Invest* **95**(6), 2783-9.

Cross, A. H., Trotter, J. L., and Lyons, J. (2001). B cells and antibodies in CNS demyelinating disease. *J Neuroimmunol* **112**(1-2), 1-14.

Croxford, J. L., Triantaphyllopoulos, K., Podhajcer, O. L., Feldmann, M., Baker, D., and Chernajovsky, Y. (1998). Cytokine gene therapy in experimental allergic encephalomyelitis by injection of plasmid DNA-cationic liposome complex into the central nervous system. *J Immunol* **160**(10), 5181-7.

Croxford, J. L., Feldmann, M., Chernajovsky, Y., and Baker, D. (2001). Different therapeutic outcomes in experimental allergic encephalomyelitis dependent upon the mode of delivery of IL-10: a comparison of the effects of protein, adenoviral or retroviral IL-10 delivery into the central nervous system. *J Immunol* **166**(6), 4124-30.

Cua, D. J., Hinton, D. R., and Stohlman, S. A. (1995). Self-antigen-induced Th2 responses in experimental allergic encephalomyelitis (EAE)-resistant mice. Th2-mediated suppression of autoimmune disease. *J Immunol* **155**(8), 4052-9.

Cua, D. J., Groux, H., Hinton, D. R., Stohlman, S. A., and Coffman, R. L. (1999). Transgenic interleukin 10 prevents induction of experimental autoimmune encephalomyelitis. *J Exp Med* **189**(6), 1005-10.

Cua, D. J., Hutchins, B., LaFace, D. M., Stohlman, S. A., and Coffman, R. L. (2001). Central nervous system expression of IL-10 inhibits autoimmune encephalomyelitis. *J Immunol* **166**(1), 602-8.

Daemen, T., Regts, J., Holtrop, M., and Wilschut, J. (2002). Immunization strategy against cervical cancer involving an alphavirus vector expressing high levels of a stable fusion protein of human papillomavirus 16 E6 and E7. *Gene Ther* **9**(2), 85-94.

Daemen, T., Riezebos-Brilman, A., Regts, J., Dontje, B., van der Zee, A., and Wilschut, J. (2004). Superior therapeutic efficacy of alphavirus-mediated immunization against human papilloma virus type 16 antigens in a murine tumour model: effects of the route of immunization. *Antivir Ther* **9**(5), 733-42.

Dandekar, A. A., Anghelina, D., and Perlman, S. (2004). Bystander CD8 T-cell-mediated demyelination is interferon-gamma-dependent in a coronavirus model of multiple sclerosis. *Am J Pathol* **164**(2), 363-9.

Dangond, F. (2002). Molecular Basis of Myelination. *In* "Disorders of Myelin in the Central and Peripheral Nervous systems" (S. F. Pioli, Ed.), pp. 49-50. Butterworth Heinemann, Boston.

de Curtis, I., and Simons, K. (1988). Dissection of Semliki Forest virus glycoprotein delivery from the trans-Golgi network to the cell surface in permeabilized BHK cells. *Proc Natl Acad Sci U S A* **85**(21), 8052-6.

De Simone, R., Giampaolo, A., Giometto, B., Gallo, P., Levi, G., Peschle, C., and Aloisi, F. (1995). The costimulatory molecule B7 is expressed on human microglia in culture and in multiple sclerosis acute lesions. *J Neuropathol Exp Neurol* **54**(2), 175-87.

DeTulleo, L., and Kirchhausen, T. (1998). The clathrin endocytic pathway in viral infection. *Embo J* **17**(16), 4585-93.

Diago, J. I., del Olmo, D., Alcazar, V., Martinez de Icaya, P., Rodriguez, E., and Martinez Montiel, P. (1999). [Thyroid disorders associated with interferon treatment in patients with chronic viral hepatitis or multiple sclerosis]. *Med Clin (Barc)* **113**(2), 50-1.

Dick, A. D., McMenamin, P. G., Korner, H., Scallon, B. J., Ghrayeb, J., Forrester, J. V., and Sedgwick, J. D. (1996). Inhibition of tumor necrosis factor activity minimizes target organ damage in experimental autoimmune uveoretinitis despite quantitatively normal activated T cell traffic to the retina. *Eur J Immunol* **26**(5), 1018-25.

Dijkstra, C. D., De Groot, C. J., and Huitinga, I. (1992). The role of macrophages in demyelination. *J Neuroimmunol* **40**(2-3), 183-8.

Ding, L., Linsley, P. S., Huang, L. Y., Germain, R. N., and Shevach, E. M. (1993). IL-10 inhibits macrophage costimulatory activity by selectively inhibiting the up-regulation of B7 expression. *J Immunol* **151**(3), 1224-34.

Donnelly, S. M., Sheahan, B. J., and Atkins, G. J. (1997). Long-term effects of Semliki Forest virus infection in the mouse central nervous system. *Neuropathol Appl Neurobiol* **23**(3), 235-41.

Dore-Duffy, P., Balabanov, R., Rafols, J., and Swanborg, R. H. (1996). Recovery phase of acute experimental autoimmune encephalomyelitis in rats corresponds to development of endothelial cell unresponsiveness to interferon gamma activation. *J Neurosci Res* **44**(3), 223-34.

Dropulic, B., and Masters, C. L. (1990). Entry of neurotropic arboviruses into the central nervous system: an in vitro study using mouse brain endothelium. *J Infect Dis* **161**(4), 685-91.

Dubuisson, J., and Rice, C. M. (1993). Sindbis virus attachment: isolation and characterization of mutants with impaired binding to vertebrate cells. *J Virol* **67**(6), 3363-74.

Duda, P. W., Schmied, M. C., Cook, S. L., Krieger, J. I., and Hafler, D. A. (2000). Glatiramer acetate (Copaxone) induces degenerate, Th2-polarized immune responses in patients with multiple sclerosis. *J Clin Invest* **105**(7), 967-76.

Duong, T. T., St Louis, J., Gilbert, J. J., Finkelman, F. D., and Strejan, G. H. (1992). Effect of anti-interferon-gamma and anti-interleukin-2 monoclonal antibody treatment on the development of actively and passively induced experimental allergic encephalomyelitis in the SJL/J mouse. *J Neuroimmunol* **36**(2-3), 105-15.

Duong, T. T., Finkelman, F. D., Singh, B., and Strejan, G. H. (1994). Effect of anti-interferon-gamma monoclonal antibody treatment on the development of experimental allergic encephalomyelitis in resistant mouse strains. *J Neuroimmunol* **53**(1), 101-7.

Ebers, G. C., and Sadovnick, A. D. (1994). The role of genetic factors in multiple sclerosis susceptibility. *J Neuroimmunol* **54**(1-2), 1-17.

Ebers, G. C., Sadovnick, A. D., and Risch, N. J. (1995). A genetic basis for familial aggregation in multiple sclerosis. Canadian Collaborative Study Group. *Nature* **377**(6545), 150-1.

Ebers, G. (1998). The PRISMS (Prevention of Relapses and Disability by Interferon beta-1a Subcutaneously in Multiple Sclerosis) Study Group, Randomised double-blind placebo-controlled study of interferon beta-1a in relapsing/remitting multiple sclerosis. *Lancet* **352**, 1498-1504.

Edan, G., and Sabouraud, O. (1991). [Benign forms of multiple sclerosis]. *Rev Prat* **41**(20), 1904-7.

Egg, R., Reindl, M., Deisenhammer, F., Linington, C., and Berger, T. (2001). Anti-MOG and anti-MBP antibody subclasses in multiple sclerosis. *Mult Scler* **7**(5), 285-9.

Ehrengruber, M. U., Lundstrom, K., Schweitzer, C., Heuss, C., Schlesinger, S., and Gahwiler, B. H. (1999). Recombinant Semliki Forest virus and Sindbis virus efficiently infect neurons in hippocampal slice cultures. *Proc Natl Acad Sci U S A* **96**(12), 7041-6

.

Ehrengruber, M. U., Hennou, S., Bueler, H., Naim, H. Y., Deglon, N., and Lundstrom, K. (2001). Gene transfer into neurons from hippocampal slices: comparison of recombinant Semliki Forest Virus, adenovirus, adeno-associated virus, lentivirus, and measles virus. *Mol Cell Neurosci* **17**(5), 855-71.

Ehrengruber, M. U. (2002). Alphaviral gene transfer in neurobiology. *Brain Res Bull* **59**(1), 13-22.

Ehrengruber, M. U., Renggli, M., Raineteau, O., Hennou, S., Vaha-Koskela, M. J., Hinkkanen, A. E., and Lundstrom, K. (2003). Semliki Forest virus A7(74) transduces hippocampal neurons and glial cells in a temperature-dependent dual manner. *J Neurovirol* **9**(1), 16-28.

Embry, A. F., Snowdon, L. R., and Vieth, R. (2000). Vitamin D and seasonal fluctuations of gadolinium-enhancing magnetic resonance imaging lesions in multiple sclerosis. *Ann Neurol* **48**(2), 271-2.

Endoh, M., Tabira, T., and Kunishita, T. (1986). Antibodies to proteolipid apoprotein in chronic relapsing experimental allergic encephalomyelitis. *J Neurol Sci* **73**(1), 31-8.

Eng, L. F., Yu, A. C., and Lee, Y. L. (1992). Astrocytic response to injury. *Prog Brain Res* **94**, 353-65.

Eralinna, J. P., Soilu-Hanninen, M., Roytta, M., Hukkanen, V., Salmi, A. A., and Salonen, R. (1996). Blood-brain barrier breakdown and increased intercellular adhesion molecule (ICAM-1/CD54) expression after Semliki Forest (A7) virus infection facilitates the development of experimental allergic encephalomyelitis. *J Neuroimmunol* **66**(1-2), 103-14.

Ersoy, E., Kus, C. N., Sener, U., Coker, I., and Zorlu, Y. (2005). The effects of interferon-beta on interleukin-10 in multiple sclerosis patients. *Eur J Neurol* **12**(3), 208-11.

Fabry, Z., Topham, D. J., Fee, D., Herlein, J., Carlino, J. A., Hart, M. N., and Sriram, S. (1995). TGF-beta 2 decreases migration of lymphocytes in vitro and homing of cells into the central nervous system in vivo. *J Immunol* **155**(1), 325-32.

Falcone, M., and Bloom, B. R. (1997). A T helper cell 2 (Th2) immune response against non-self antigens modifies the cytokine profile of autoimmune T cells and protects against experimental allergic encephalomyelitis. *J Exp Med* **185**(5), 901-7.

Falcone, M., Rajan, A. J., Bloom, B. R., and Brosnan, C. F. (1998). A critical role for IL-4 in regulating disease severity in experimental allergic encephalomyelitis as demonstrated in IL-4-deficient C57BL/6 mice and BALB/c mice. *J Immunol* **160**(10), 4822-30.

Farrell, R., Heaney, D., and Giovannoni, G. (2005). Emerging therapies in multiple sclerosis. *Expert Opin Emerg Drugs* **10**(4), 797-816.

Favre, D., Studer, E., and Michel, M. R. (1996). Semliki Forest virus capsid protein inhibits the initiation of translation by upregulating the double-stranded RNA-activated protein kinase (PKR). *Biosci Rep* **16**(6), 485-511.

Fazakerley, J. K., and Webb, H. E. (1987). Semliki Forest virus-induced, immune-mediated demyelination: adoptive transfer studies and viral persistence in nude mice. *J Gen Virol* **68 (Pt 2)**, 377-85.

Fazakerley, J. K., Pathak, S., Scallan, M., Amor, S., and Dyson, H. (1993). Replication of the A7(74) strain of Semliki Forest virus is restricted in neurons. *Virology* **195**(2), 627-37.

Ferber, I. A., Brocke, S., Taylor-Edwards, C., Ridgway, W., Dinisco, C., Steinman, L., Dalton, D., and Fathman, C. G. (1996). Mice with a disrupted IFN-gamma gene are susceptible to the induction of experimental autoimmune encephalomyelitis (EAE). *J Immunol* **156**(1), 5-7.

Ferguson, B., Matyszak, M. K., Esiri, M. M., and Perry, V. H. (1997). Axonal damage in acute multiple sclerosis lesions. *Brain* **120 (Pt 3)**, 393-9.

Fernandez, I. M., Snijders, A., Benaissa-Trouw, B. J., Harmsen, M., Snippe, H., and Kraaijeveld, C. A. (1993). Influence of epitope polarity and adjuvants on the immunogenicity and efficacy of a synthetic peptide vaccine against Semliki Forest virus. *J Virol* **67**(10), 5843-8.

Fierz, W., Endler, B., Reske, K., Wekerle, H., and Fontana, A. (1985). Astrocytes as antigen-presenting cells. I. Induction of Ia antigen expression on astrocytes by T cells via immune interferon and its effect on antigen presentation. *J Immunol* **134**(6), 3785-93.

Fillatreau, S., Sweenie, C. H., McGeachy, M. J., Gray, D., and Anderton, S. M. (2002). B cells regulate autoimmunity by provision of IL-10. *Nat Immunol* **3**(10), 944-50.

Fleeton, M. N., Sheahan, B. J., Gould, E. A., Atkins, G. J., and Liljestrom, P. (1999). Recombinant Semliki Forest virus particles encoding the prME or NS1 proteins of louping ill virus protect mice from lethal challenge. *J Gen Virol* **80 (Pt 5)**, 1189-98.

Fleeton, M. N., Liljestrom, P., Sheahan, B. J., and Atkins, G. J. (2000). Recombinant Semliki Forest virus particles expressing louping ill virus antigens induce a better protective response than plasmid-based DNA vaccines or an inactivated whole particle vaccine. *J Gen Virol* **81**(Pt 3), 749-58.

Floris, S., Ruuls, S. R., Wierinckx, A., van der Pol, S. M., Dopp, E., van der Meide, P. H., Dijkstra, C. D., and De Vries, H. E. (2002). Interferon-beta directly influences monocyte infiltration into the central nervous system. *J Neuroimmunol* **127**(1-2), 69-79.

Fox, S. I. (1996). The Nervous System. Fifth ed. *In* "Human Physiology" (C. H. Wheatley, Ed.), pp. 144-148. Wm. C. Brown, Boston.

Frei, K., Bodmer, S., Schwerdel, C., and Fontana, A. (1985). Astrocytes of the brain synthesize interleukin 3-like factors. *J Immunol* **135**(6), 4044-7.

Frei, K., Nohava, K., Malipiero, U. V., Schwerdel, C., and Fontana, A. (1992). Production of macrophage colony-stimulating factor by astrocytes and brain macrophages. *J Neuroimmunol* **40**(2-3), 189-95.

Freund, J., and Dermott, K. M. (1942). Sensitization to horse serum by means of adjuvant. *Proc Soc Exp Biol Med* **49**, 548-553.

Frolova, E., Frolov, I., and Schlesinger, S. (1997). Packaging signals in alphaviruses. *J Virol* **71**(1), 248-58.

Froshauer, S., Kartenbeck, J., and Helenius, A. (1988). Alphavirus RNA replicase is located on the cytoplasmic surface of endosomes and lysosomes. *J Cell Biol* **107**(6 Pt 1), 2075-86.

Fujihara, M., Ito, N., Pace, J. L., Watanabe, Y., Russell, S. W., and Suzuki, T. (1994). Role of endogenous interferon-beta in lipopolysaccharide-triggered activation of the inducible nitric-oxide synthase gene in a mouse macrophage cell line, J774. *J Biol Chem* **269**(17), 12773-8.

Fuller, S. D., Berriman, J. A., Butcher, S. J., and Gowen, B. E. (1995). Low pH induces swiveling of the glycoprotein heterodimers in the Semliki Forest virus spike complex. *Cell* **81**(5), 715-25.

Furlan, R., Poliani, P. L., Galbiati, F., Bergami, A., Grimaldi, L. M., Comi, G., Adorini, L., and Martino, G. (1998). Central nervous system delivery of interleukin 4 by a nonreplicative herpes simplex type 1 viral vector ameliorates autoimmune demyelination. *Hum Gene Ther* **9**(17), 2605-17.

Furlan, R., Bergami, A., Lang, R., Brambilla, E., Franciotta, D., Martinelli, V., Comi, G., Panina, P., and Martino, G. (2000). Interferon-beta treatment in multiple sclerosis patients decreases the number of circulating T cells producing interferon-gamma and interleukin-4. *J Neuroimmunol* **111**(1-2), 86-92.

Furlan, R., Brambilla, E., Ruffini, F., Poliani, P. L., Bergami, A., Marconi, P. C., Franciotta, D. M., Penna, G., Comi, G., Adorini, L., and Martino, G. (2001a). Intrathecal delivery of IFN-gamma protects C57BL/6 mice from chronic-progressive experimental autoimmune encephalomyelitis by increasing apoptosis of central nervous system-infiltrating lymphocytes. *J Immunol* **167**(3), 1821-9.

Furlan, R., Poliani, P. L., Marconi, P. C., Bergami, A., Ruffini, F., Adorini, L., Glorioso, J. C., Comi, G., and Martino, G. (2001b). Central nervous system gene therapy with interleukin-4 inhibits progression of ongoing relapsing-remitting autoimmune encephalomyelitis in Biozzi AB/H mice. *Gene Ther* **8**(1), 13-9.

Furtado, G. C., Olivares-Villagomez, D., Curotto de Lafaille, M. A., Wensky, A. K., Latkowski, J. A., and Lafaille, J. J. (2001). Regulatory T cells in spontaneous autoimmune encephalomyelitis. *Immunol Rev* **182**, 122-34.

Gadient, R. A., and Otten, U. H. (1997). Interleukin-6 (IL-6)--a molecule with both beneficial and destructive potentials. *Prog Neurobiol* **52**(5), 379-90.

Gale, C. R., and Martyn, C. N. (1995). Migrant studies in multiple sclerosis. *Prog Neurobiol* **47**(4-5), 425-48.

Garoff, H., and Simons, K. (1974). Location of the spike glycoproteins in the Semliki Forest virus membrane. *Proc Natl Acad Sci U S A* **71**(10), 3988-92.

Garoff, H., Simons, K., and Renkonen, O. (1974). Isolation and characterization of the membrane proteins of Semliki Forest virus. *Virology* **61**(2), 493-504.

Garoff, H., Simons, K., and Dobberstein, B. (1978). Assembly of the Semliki Forest virus membrane glycoproteins in the membrane of the endoplasmic reticulum in vitro. *J Mol Biol* **124**(4), 587-600.

Garoff, H., Frischauf, A. M., Simons, K., Lehrach, H., and Delius, H. (1980). Nucleotide sequence of cdna coding for Semliki Forest virus membrane glycoproteins. *Nature* **288**(5788), 236-41.

Garoff, H., Huylebroeck, D., Robinson, A., Tillman, U., and Liljestrom, P. (1990). The signal sequence of the p62 protein of Semliki Forest virus is involved in initiation but not in completing chain translocation. *J Cell Biol* **111**(3), 867-76.

Garoff, H., Wilschut, J., Liljestrom, P., Wahlberg, J. M., Bron, R., Suomalainen, M., Smyth, J., Salminen, A., Barth, B. U., Zhao, H., and et al. (1994). Assembly and entry mechanisms of Semliki Forest virus. *Arch Virol Suppl* **9**, 329-38.

Gasser, D. L., Newlin, C. M., Palm, J., and Gonatas, N. K. (1973). Genetic control of susceptibility to experimental allergic encephalomyelitis in rats. *Science* **181**(102), 872-3.

Gates, M. C., Sheahan, B. J., and Atkins, G. J. (1984). The pathogenicity of the M9 mutant of Semliki Forest virus in immune-compromised mice. *J Gen Virol* **65 (Pt 1)**, 73-80.

Gates, M. C., Sheahan, B. J., O'Sullivan, M. A., and Atkins, G. J. (1985). The pathogenicity of the A7, M9 and L10 strains of Semliki Forest virus for weanling mice and primary mouse brain cell cultures. *J Gen Virol* **66 (Pt 11),** 2365-73.

Gay, F. W., Drye, T. J., Dick, G. W., and Esiri, M. M. (1997). The application of multifactorial cluster analysis in the staging of plaques in early multiple sclerosis. Identification and characterization of the primary demyelinating lesion. *Brain* **120 (Pt 8),** 1461-83.

Genc, K., Dona, D. L., and Reder, A. T. (1997). Increased CD80(+) B cells in active multiple sclerosis and reversal by interferon beta-1b therapy. *J Clin Invest* **99**(11), 2664-71.

Gerritse, K., Laman, J. D., Noelle, R. J., Aruffo, A., Ledbetter, J. A., Boersma, W. J., and Claassen, E. (1996). CD40-CD40 ligand interactions in experimental allergic encephalomyelitis and multiple sclerosis. *Proc Natl Acad Sci U S A* **93**(6), 2499-504.

Gilman, S. (1998). Imaging the brain. Second of two parts. *N Engl J Med* **338**(13), 889-96.

Giulian, D., and Lachman, L. B. (1985). Interleukin-1 stimulation of astroglial proliferation after brain injury. *Science* **228,** 497-499.

Giuliani, F., Fu, S. A., Metz, L. M., and Yong, V. W. (2005). Effective combination of minocycline and interferon-beta in a model of multiple sclerosis. *J Neuroimmunol* **165**(1-2), 83-91.

Glasgow, G. M., McGee, M. M., Sheahan, B. J., and Atkins, G. J. (1997). Death mechanisms in cultured cells infected by Semliki Forest virus. *J Gen Virol* **78 (Pt 7),** 1559-63.

Glasgow, G. M., McGee, M. M., Tarbatt, C. J., Mooney, D. A., Sheahan, B. J., and Atkins, G. J. (1998). The Semliki Forest virus vector induces p53-independent apoptosis. *J Gen Virol* **79 (Pt 10),** 2405-10.

Glasgow, G. M., Sheahan, B. J., Atkins, G. J., Wahlberg, J. M., Salminen, A., and Liljestrom, P. (1991). Two mutations in the envelope glycoprotein E2 of Semliki Forest virus affecting the maturation and entry patterns of the virus alter pathogenicity for mice. *Virology* **185**(2), 741-8.

Gomatos, P. J., Kaariainen, L., Keranen, S., Ranki, M., and Sawicki, D. L. (1980). Semliki Forest virus replication complex capable of synthesizing 42S and 26S nascent RNA chains. *J Gen Virol* **49**(1), 61-9.

Gomez de Cedron, M., Ehsani, N., Mikkola, M. L., Garcia, J. A., and Kaariainen, L. (1999). RNA helicase activity of Semliki Forest virus replicase protein NSP2. *FEBS Lett* **448**(1), 19-22.

Gonsette, R. E. (1996). Mitoxantrone immunotherapy in multiple sclerosis. *Mult Scler* **1**(6), 329-32.

Goodkin, D. E., Rudick, R. A., VanderBrug Medendorp, S., Daughtry, M. M., Schwetz, K. M., Fischer, J., and Van Dyke, C. (1995). Low-dose (7.5 mg) oral methotrexate reduces the rate of progression in chronic progressive multiple sclerosis. *Ann Neurol* **37**(1), 30-40.

Goodkin, D. E., Rudick, R. A., VanderBrug Medendorp, S., Daughtry, M. M., and Van Dyke, C. (1996). Low-dose oral methotrexate in chronic progressive multiple sclerosis: analyses of serial MRIs. *Neurology* **47**(5), 1153-7.

Goodman, A. D., Mock, D. J., Powers, J. M., Baker, J. V., and Blumberg, B. M. (2003). Human herpesvirus 6 genome and antigen in acute multiple sclerosis lesions. *J Infect Dis* **187**(9), 1365-76.

Gran, B., Hemmer, B., and Martin, R. (1999). Molecular mimicry and multiple sclerosis--a possible role for degenerate T cell recognition in the induction of autoimmune responses. *J Neural Transm Suppl* **55**, 19-31.

Gran, B., Zhang, G. X., and Rostami, A. (2004). Role of the IL-12/IL-23 system in the regulation of T-cell responses in central nervous system inflammatory demyelination. *Crit Rev Immunol* **24**(2), 111-28.

Grandgirard, D., Studer, E., Monney, L., Belser, T., Fellay, I., Borner, C., and Michel, M. R. (1998). Alphaviruses induce apoptosis in Bcl-2-overexpressing cells: evidence for a caspase-mediated, proteolytic inactivation of Bcl-2. *Embo J* **17**(5), 1268-78.

Granieri, E., and Casetta, I. (1997). Selected reviews common childhood and adolescent infections and multiple sclerosis. *Neurology* **49**(2 Suppl 2), S42-54.

Granieri, E. (2000). Exogeneous factors in the aetiology of multiple sclerosis. *J Neurovirol* **6 Suppl 2**, S141-6.

Greer, J. M., Sobel, R. A., Sette, A., Southwood, S., Lees, M. B., and Kuchroo, V. K. (1996). Immunogenic and encephalitogenic epitope clusters of myelin proteolipid protein. *J Immunol* **156**(1), 371-9.

Griffin, D. E. (1986). Alphavirus pathogenesis and immunity. *In* "The togaviridae and Flaviridae" (M. J. Schlesinger, Ed.), pp. 209-250. Plenum Press, New York.

Gunn, C., Suckling, A. J., and Linington, C. (1989). Identification of a common idiotype on myelin oligodendrocyte glycoprotein-specific autoantibodies in chronic relapsing experimental allergic encephalomyelitis. *J Neuroimmunol* **23**(2), 101-8.

Guy, J., Qi, X., and Hauswirth, W. W. (1998). Adeno-associated viral-mediated catalase expression suppresses optic neuritis in experimental allergic encephalomyelitis. *Proc Natl Acad Sci U S A* **95**(23), 13847-52.

Haahr, S., and Munch, M. (2000). The association between multiple sclerosis and infection with Epstein-Barr virus and retrovirus. *J Neurovirol* **6 Suppl 2**, S76-9.

Hahn, Y. S., Strauss, E. G., and Strauss, J. H. (1989). Mapping of RNA- temperature-sensitive mutants of Sindbis virus: assignment of complementation groups A, B, and G to nonstructural proteins. *J Virol* **63**(7), 3142-50.

Hahn, C. S., and Strauss, J. H. (1990). Site-directed mutagenesis of the proposed catalytic amino acids of the Sindbis virus capsid protein autoprotease. *J Virol* **64**(6), 3069-73.

Hallal, D. E., Farias, A. S., Oliveira, E. C., Diaz-Bardales, B. M., Brandao, C. O., Protti, G. G., Pereira, F. G., Metze, I. L., and Santos, L. M. (2003). Costimulatory molecule expression on leukocytes from mice with experimental autoimmune encephalomyelitis treated with IFN-beta. *J Interferon Cytokine Res* **23**(6), 293-8.

Hanke, T., Barnfield, C., Wee, E. G., Agren, L., Samuel, R. V., Larke, N., and Liljestrom, P. (2003). Construction and immunogenicity in a prime-boost regimen of a Semliki Forest virus-vectored experimental HIV clade A vaccine. *J Gen Virol* **84**(Pt 2), 361-8.

Hardy, P. A., Mazzini, M. J., Schweitzer, C., Lundstrom, K., and Glode, L. M. (2000). Recombinant Semliki forest virus infects and kills human prostate cancer cell lines and prostatic duct epithelial cells ex vivo. *Int J Mol Med* **5**(3), 241-5.

Hardy, W. R., and Strauss, J. H. (1988). Processing the nonstructural polyproteins of Sindbis virus: study of the kinetics in vivo by using monospecific antibodies. *J Virol* **62**(3), 998-1007.

Hartung, H. P., Gonsette, R., Konig, N., Kwiecinski, H., Guseo, A., Morrissey, S. P., Krapf, H., and Zwingers, T. (2002). Mitoxantrone in progressive multiple sclerosis: a placebo-controlled, double-blind, randomised, multicentre trial. *Lancet* **360**(9350), 2018-25.

Hauser, S. L., Doolittle, T. H., Lincoln, R., Brown, R. H., and Dinarello, C. A. (1990). Cytokine accumulations in CSF of multiple sclerosis patients: frequent detection of interleukin-1 and tumor necrosis factor but not interleukin-6. *Neurology* **40**(11), 1735-9.

Hauser, S. L., Fleischnick, E., Weiner, H. L., Marcus, D., Awdeh, Z., Yunis, E. J., and Alper, C. A. (1989). Extended major histocompatibility complex haplotypes in patients with multiple sclerosis. *Neurology* **39**(2 Pt 1), 275-7.

Helenius, A., Morein, B., Fries, E., Simons, K., Robinson, P., Schirrmacher, V., Terhorst, C., and Strominger, J. L. (1978). Human (HLA-A and HLA-B) and murine (H-2K

and H-2D) histocompatibility antigens are cell surface receptors for Semliki Forest virus. *Proc Natl Acad Sci U S A* **75**(8), 3846-50.

Hemmer, B., Fleckenstein, B. T., Vergelli, M., Jung, G., McFarland, H., Martin, R., and Wiesmuller, K. H. (1997). Identification of high potency microbial and self ligands for a human autoreactive class II-restricted T cell clone. *J Exp Med* **185**(9), 1651-9.

Hendriks, J. J., Teunissen, C. E., de Vries, H. E., and Dijkstra, C. D. (2005). Macrophages and neurodegeneration. *Brain Res Brain Res Rev* **48**(2), 185-95.

Hidmark, A. S., McInerney, G. M., Nordstrom, E. K., Douagi, I., Werner, K. M., Liljestrom, P., and Karlsson Hedestam, G. B. (2005). Early alpha/beta interferon production by myeloid dendritic cells in response to UV-inactivated virus requires viral entry and interferon regulatory factor 3 but not MyD88. *J Virol* **79**(16), 10376-85.

Hillert, J., and Olerup, O. (1993). Multiple sclerosis is associated with genes within or close to the HLA-DR-DQ subregion on a normal DR15,DQ6,Dw2 haplotype. *Neurology* **43**(1), 163-8.

Hjelmstrom, P., Juedes, A. E., Fjell, J., and Ruddle, N. H. (1998). B-cell-deficient mice develop experimental allergic encephalomyelitis with demyelination after myelin oligodendrocyte glycoprotein sensitization. *J Immunol* **161**(9), 4480-3.

Hoffman, G. E., Le, W. W., Murphy, A. Z., and Koski, C. L. (2001). Divergent effects of ovarian steroids on neuronal survival during experimental allergic encephalitis in Lewis rats. *Exp Neurol* **171**(2), 272-84.

Hofman, F. M., Hinton, D. R., Johnson, K., and Merrill, J. E. (1989). Tumor necrosis factor identified in multiple sclerosis brain. *J Exp Med* **170**(2), 607-12.

Hogancamp, W. E., Rodriguez, M., and Weinshenker, B. G. (1997). The epidemiology of multiple sclerosis. *Mayo Clin Proc* **72**(9), 871-8.

Hohnoki, K., Inoue, A., and Koh, C. S. (1998). Elevated serum levels of IFN-gamma, IL-4 and TNF-alpha/unelevated serum levels of IL-10 in patients with demyelinating diseases during the acute stage. *J Neuroimmunol* **87**(1-2), 27-32.

Huseby, E. S., Liggitt, D., Brabb, T., Schnabel, B., Ohlen, C., and Goverman, J. (2001). A pathogenic role for myelin-specific CD8(+) T cells in a model for multiple sclerosis. *J Exp Med* **194**(5), 669-76.

Ichikawa, M., Johns, T. G., Adelmann, M., and Bernard, C. C. (1996). Antibody response in Lewis rats injected with myelin oligodendrocyte glycoprotein derived peptides. *Int Immunol* **8**(11), 1667-74.

Inobe, J., Slavin, A. J., Komagata, Y., Chen, Y., Liu, L., and Weiner, H. L. (1998). IL-4 is a differentiation factor for transforming growth factor-beta secreting Th3 cells and oral administration of IL-4 enhances oral tolerance in experimental allergic encephalomyelitis. *Eur J Immunol* **28**(9), 2780-90.

Inobe, J. I., Chen, Y., and Weiner, H. L. (1996). In vivo administration of IL-4 induces TGF-beta-producing cells and protects animals from experimental autoimmune encephalomyelitis. *Ann N Y Acad Sci* **778**, 390-2.

Isaacs, A., and Lindenmann, J. (1957). Virus interference. I. The interferon. *Proc R Soc Lond B Biol Sci* **147**(927), 258-67.

Isaacs, A., Lindenmann, J., and Valentine, R. C. (1957). Virus interference. II. Some properties of interferon. *Proc R Soc Lond B Biol Sci* **147**(927), 268-73.

Issazadeh, S., Kjellen, P., Olsson, T., Mustafa, M., and Holmdahl, R. (1997). Major histocompatibility complex-controlled protective influences on experimental autoimmune encephalomyelitis are peptide specific. *Eur J Immunol* **27**(6), 1584-7.

Itoh, K., and Hirohata, S. (1995). The role of IL-10 in human B cell activation, proliferation, and differentiation. *J Immunol* **154**(9), 4341-50.

Jacobs, L. D., Cookfair, D. L., Rudick, R. A., Herndon, R. M., Richert, J. R., Salazar, A. M., Fischer, J. S., Goodkin, D. E., Granger, C. V., Simon, J. H., Alam, J. J., Bartoszak, D. M., Bourdette, D. N., Braiman, J., Brownscheidle, C. M., Coats, M. E., Cohan, S. L., Dougherty, D. S., Kinkel, R. P., Mass, M. K., Munschauer, F. E., 3rd, Priore, R. L., Pullicino, P. M., Scherokman, B. J., Whitham, R. H., and et al. (1996). Intramuscular interferon beta-1a for disease progression in relapsing multiple sclerosis. The Multiple Sclerosis Collaborative Research Group (MSCRG). *Ann Neurol* **39**(3), 285-94.

Jagelman, S., Suckling, A. J., Webb, H. E., and Bowen, F. T. (1978). The pathogenesis of avirulent Semliki Forest virus infections in athymic nude mice. *J Gen Virol* **41**(3), 599-607.

Jansson, L., Olsson, T., Hojeberg, B., and Holmdahl, R. (1991). Chronic experimental autoimmune encephalomyelitis induced by the 89-101 myelin basic protein peptide in B10RIII (H-2r) mice. *Eur J Immunol* **21**(3), 693-9.

Javed, A., and Reder, A. T. (2005). Therapeutic role of beta-interferons in multiple sclerosis. *Pharmacol Ther*.

Jerusalmi, A. (2003). Ph.D. Trinity College, Dublin.

Jerusalmi, A., Morris-Downes, M. M., Sheahan, B. J., and Atkins, G. J. (2003). Effect of intranasal administration of Semliki Forest virus recombinant particles expressing reporter and cytokine genes on the progression of experimental autoimmune encephalomyelitis. *Mol Ther* **8**(6), 886-94.

Jiang, H., Milo, R., Swoveland, P., Johnson, K. P., Panitch, H., and Dhib-Jalbut, S. (1995). Interferon beta-1b reduces interferon gamma-induced antigen-presenting capacity of human glial and B cells. *J Neuroimmunol* **61**(1), 17-25.

Jiang, H., Zhang, S. I., and Pernis, B. (1992). Role of CD8+ T cells in murine experimental allergic encephalomyelitis. *Science* **256**(5060), 1213-5.

Johnson, K. P., Brooks, B. R., Cohen, J. A., Ford, C. C., Goldstein, J., Lisak, R. P., Myers, L. W., Panitch, H. S., Rose, J. W., and Schiffer, R. B. (1995). Copolymer 1 reduces relapse rate and improves disability in relapsing-remitting multiple sclerosis: results of a phase III multicenter, double-blind placebo-controlled trial. The Copolymer 1 Multiple Sclerosis Study Group. *Neurology* **45**(7), 1268-76.

Johnson, P. A., Miyanohara, A., Levine, F., Cahill, T., and Friedmann, T. (1992). Cytotoxicity of a replication-defective mutant of herpes simplex virus type 1. *J Virol* **66**(5), 2952-65.

Kaariainen, L., Keranen, S., Lachmi, B., Soderlund, H., Tuomi, K., and Ulmanen, I. (1975). Replication of Semliki Forest virus. *Med Biol* **53**(5), 342-51.

Kaluza, G., Lell, G., Reinacher, M., Stitz, L., and Willems, W. R. (1987). Neurogenic spread of Semliki Forest virus in mice. *Arch Virol* **93**(1-2), 97-110.

Kappos, L. (1998). The European Study Group on interferon beta-1b in secondary progressive MS, Placebo-controlled multicentre randomised trial of interferon beta-1b in treatment of secondary progressive multiple sclerosis. *Lancet* **352**, 1491-1497.

Kappos, L., Weinshenker, B., Pozzilli, C., Thompson, A. J., Dahlke, F., Beckmann, K., Polman, C., and McFarland, H. (2004). Interferon beta-1b in secondary progressive MS: a combined analysis of the two trials. *Neurology* **63**(10), 1779-87.

Karp, C. L., Biron, C. A., and Irani, D. N. (2000). Interferon beta in multiple sclerosis: is IL-12 suppression the key? *Immunol Today* **21**(1), 24-8.

Karp, C. L., van Boxel-Dezaire, A. H., Byrnes, A. A., and Nagelkerken, L. (2001). Interferon-beta in multiple sclerosis: altering the balance of interleukin-12 and interleukin-10? *Curr Opin Neurol* **14**(3), 361-8.

Karpus, W. J., and Swanborg, R. H. (1989). CD4+ suppressor cells differentially affect the production of IFN-gamma by effector cells of experimental autoimmune encephalomyelitis. *J Immunol* **143**(11), 3492-7.

Katz, D., Taubenberger, J. K., Cannella, B., McFarlin, D. E., Raine, C. S., and McFarland, H. F. (1993). Correlation between magnetic resonance imaging findings and lesion development in chronic, active multiple sclerosis. *Ann Neurol* **34**(5), 661-9.

Kawanokuchi, J., Mizuno, T., Kato, H., Mitsuma, N., and Suzumura, A. (2004). Effects of interferon-beta on microglial functions as inflammatory and antigen presenting cells in the central nervous system. *Neuropharmacology* **46**(5), 734-42.

Keogh, B., Atkins, G. J., Mills, K. H., and Sheahan, B. J. (2002). Avirulent Semliki Forest virus replication and pathology in the central nervous system is enhanced in IL-12-

defective and reduced in IL-4-defective mice: a role for Th1 cells in the protective immunity. *J Neuroimmunol* **125**(1-2), 15-22.

Keogh, B., Atkins, G. J., Mills, K. H., and Sheahan, B. J. (2003). Role of interferon-gamma and nitric oxide in the neuropathogenesis of avirulent Semliki Forest virus infection. *Neuropathol Appl Neurobiol* **29**(6), 553-62.

Keranen, S., and Kaariainen, L. (1975). Proteins synthesized by Semliki Forest virus and its 16 temperature-sensitive mutants. *J Virol* **16**(2), 388-96.

Keranen, S., and Ruohonen, L. (1983). Nonstructural proteins of Semliki Forest virus: synthesis, processing, and stability in infected cells. *J Virol* **47**(3), 505-15.

Kerschensteiner, M., Gallmeier, E., Behrens, L., Leal, V. V., Misgeld, T., Klinkert, W. E., Kolbeck, R., Hoppe, E., Oropeza-Wekerle, R. L., Bartke, I., Stadelmann, C., Lassmann, H., Wekerle, H., and Hohlfeld, R. (1999). Activated human T cells, B cells, and monocytes produce brain-derived neurotrophic factor in vitro and in inflammatory brain lesions: a neuroprotective role of inflammation? *J Exp Med* **189**(5), 865-70.

Khoury, S. J., Hancock, W. W., and Weiner, H. L. (1992). Oral tolerance to myelin basic protein and natural recovery from experimental autoimmune encephalomyelitis are associated with downregulation of inflammatory cytokines and differential upregulation of transforming growth factor beta, interleukin 4, and prostaglandin E expression in the brain. *J Exp Med* **176**(5), 1355-64.

Khoury, S. J., Akalin, E., Chandraker, A., Turka, L. A., Linsley, P. S., Sayegh, M. H., and Hancock, W. W. (1995). CD28-B7 costimulatory blockade by CTLA4Ig prevents actively induced experimental autoimmune encephalomyelitis and inhibits Th1 but spares Th2 cytokines in the central nervous system. *J Immunol* **155**(10), 4521-4.

Kielian, M., and Helenius, A. (1985). pH-induced alterations in the fusogenic spike protein of Semliki Forest virus. *J Cell Biol* **101**(6), 2284-91.

Kies, M. W., Roboz, E., and Alvord, E. C. J. (1956). Experimental encephalitogenic activity in glycoprotein fraction of bovine spinal cord. *Federation Proc* **15**, 288.

Koh, D. R., Fung-Leung, W. P., Ho, A., Gray, D., Acha-Orbea, H., and Mak, T. W. (1992). Less mortality but more relapses in experimental allergic encephalomyelitis in CD8-/- mice. *Science* **256**(5060), 1210-3.

Kohm, A. P., Carpentier, P. A., Anger, H. A., and Miller, S. D. (2002). Cutting edge: CD4+CD25+ regulatory T cells suppress antigen-specific autoreactive immune responses and central nervous system inflammation during active experimental autoimmune encephalomyelitis. *J Immunol* **169**(9), 4712-6.

Korner, H., and Sedgwick, J. D. (1996). Tumour necrosis factor and lymphotoxin: molecular aspects and role in tissue-specific autoimmunity. *Immunol Cell Biol* **74**(5), 465-72.

Krakowski, M., and Owens, T. (1996). Interferon-gamma confers resistance to experimental allergic encephalomyelitis. *Eur J Immunol* **26**(7), 1641-6.

Krisky, D. M., Wolfe, D., Goins, W. F., Marconi, P. C., Ramakrishnan, R., Mata, M., Rouse, R. J., Fink, D. J., and Glorioso, J. C. (1998). Deletion of multiple immediate-early genes from herpes simplex virus reduces cytotoxicity and permits long-term gene expression in neurons. *Gene Ther* **5**(12), 1593-603.

Kubes, P., and Ward, P. A. (2000). Leukocyte recruitment and the acute inflammatory response. *Brain Pathol* **10**(1), 127-35.

Kuchroo, V. K., Sobel, R. A., Yamamura, T., Greenfield, E., Dorf, M. E., and Lees, M. B. (1991). Induction of experimental allergic encephalomyelitis by myelin proteolipid-protein-specific T cell clones and synthetic peptides. *Pathobiology* **59**(5), 305-12.

Kuchroo, V. K., Das, M. P., Brown, J. A., Ranger, A. M., Zamvil, S. S., Sobel, R. A., Weiner, H. L., Nabavi, N., and Glimcher, L. H. (1995). B7-1 and B7-2 costimulatory molecules activate differentially the Th1/Th2 developmental pathways: application to autoimmune disease therapy. *Cell* **80**(5), 707-18.

Kuroda, Y., and Shimamoto, Y. (1991). Human tumor necrosis factor-alpha augments experimental allergic encephalomyelitis in rats. *J Neuroimmunol* **34**(2-3), 159-64.

Kurtzke, J. F. (1980). Geographic distribution of multiple sclerosis: An update with special reference to Europe and the Mediterranean region. *Acta Neurol Scand* **62**(2), 65-80.

Kurtzke, J. F. (1983). Rating neurologic impairment in multiple sclerosis: an expanded disability status scale (EDSS). *Neurology* **33**(11), 1444-52.

Kurtzke, J. F., Hyllested, K., Heltberg, A., and Olsen, A. (1993). Multiple sclerosis in the Faroe Islands. 5. The occurrence of the fourth epidemic as validation of transmission. *Acta Neurol Scand* **88**(3), 161-73.

Kurtzke, J. F., and Delasnerie-Laupretre, N. (1996). Reflection on the geographic distribution of multiple sclerosis in France. *Acta Neurol Scand* **93**(2-3), 110-7.

Kurtzke, J. F., and Page, W. F. (1997). Epidemiology of multiple sclerosis in US veterans: VII. Risk factors for MS. *Neurology* **48**(1), 204-13.

Kuruganti, P. A., Hinojoza, J. R., Eaton, M. J., Ehmann, U. K., and Sobel, R. A. (2002). Interferon-beta counteracts inflammatory mediator-induced effects on brain endothelial cell tight junction molecules-implications for multiple sclerosis. *J Neuropathol Exp Neurol* **61**(8), 710-24.

Lai, Z., and Brady, R. O. (2002). Gene transfer into the central nervous system in vivo using a recombinanat lentivirus vector. *J Neurosci Res* **67**(3), 363-71.

Laman, J. D., Maassen, C. B., Schellekens, M. M., Visser, L., Kap, M., de Jong, E., van Puijenbroek, M., van Stipdonk, M. J., van Meurs, M., Schwarzler, C., and Gunthert, U. (1998). Therapy with antibodies against CD40L (CD154) and CD44-

variant isoforms reduces experimental autoimmune encephalomyelitis induced by a proteolipid protein peptide. *Mult Scler* **4**(3), 147-53.

Lassmann, H., and Ransohoff, R. M. (2004). The CD4-Th1 model for multiple sclerosis: a critical [correction of crucial] re-appraisal. *Trends Immunol* **25**(3), 132-7.

Lastarza, M. W., Grakoui, A., and Rice, C. M. (1994). Deletion and duplication mutations in the C-terminal nonconserved region of Sindbis virus nsP3: effects on phosphorylation and on virus replication in vertebrate and invertebrate cells. *Virology* **202**(1), 224-32.

Lauer, K. (1995). Environmental associations with the risk of multiple sclerosis: the contribution of ecological studies. *Acta Neurol Scand Suppl* **161**, 77-88.

Lauer, K. (1997). Diet and multiple sclerosis. *Neurology* **49**(2 Suppl 2), S55-61.

Lavelle, E. C., McNeela, E., Armstrong, M. E., Leavy, O., Higgins, S. C., and Mills, K. H. (2003). Cholera toxin promotes the induction of regulatory T cells specific for bystander antigens by modulating dendritic cell activation. *J Immunol* **171**(5), 2384-92.

Lavelle, E. C., Jarnicki, A., McNeela, E., Armstrong, M. E., Higgins, S. C., Leavy, O., and Mills, K. H. (2004). Effects of cholera toxin on innate and adaptive immunity and its application as an immunomodulatory agent. *J Leukoc Biol* **75**(5), 756-63.

Leake, C. J., Varma, M. G., and Pudney, M. (1977). Cytopathic effect and plaque formation by Arboviruses in a continuous cell line (XTC-2) from the toad Xenopuslaevis. *J Gen Virol* **35**, 335-339.

Lehtovaara, P., Ulmanen, I., Kaariainen, L., Keranen, S., and Philipson, L. (1980). Synthesis and processing of Semliki Forest virus-specific nonstructural proteins in vivo and in vitro. *Eur J Biochem* **112**(3), 461-8.

Leonard, J. P., Waldburger, K. E., and Goldman, S. J. (1995). Prevention of experimental autoimmune encephalomyelitis by antibodies against interleukin 12. *J Exp Med* **181**(1), 381-6.

Leonard, J. P., Waldburger, K. E., Schaub, R. G., Smith, T., Hewson, A. K., Cuzner, M. L., and Goldman, S. J. (1997). Regulation of the inflammatory response in animal models of multiple sclerosis by interleukin-12. *Crit Rev Immunol* **17**(5-6), 545-53.

Levine, S., Sowinski, R., Gruenewald, R., and Kies, M. W. (1972). Experimental allergic encephalomyelitis. Production by myelin basic protein adsorbed on particulate adjuvants. *Immunology* **23**(4), 609-14.

Levine, R. A., Gardner, J. C., Fullerton, B. C., Stufflebeam, S. M., Carlisle, E. W., Furst, M., Rosen, B. R., and Kiang, N. Y. (1993). Effects of multiple sclerosis brainstem

lesions on sound lateralization and brainstem auditory evoked potentials. *Hear Res* **68**(1), 73-88.

Levy-Mintz, P., and Kielian, M. (1991). Mutagenesis of the putative fusion domain of the Semliki Forest virus spike protein. *J Virol* **65**(8), 4292-300.

L'Heritier, P. (1970). Drosophila viruses and their role as evolutionary factors. *In* "Evolutionary Biology", pp. 185-209.

Li, D., Traboulsee, A., Abdalla, J., Forrestal, F., and Paty, D. W. (2004). Long-term observational follow-up of the PRISMS cohort: analysis of MRI lesion burden in RRMS patients treated with IFN beta-1a three times weekly (Rebif) Meeting of the American Academy of Neurology. *San Francisco, CA*.

Liblau, R., Steinman, L., and Brocke, S. (1997). Experimental autoimmune encephalomyelitis in IL-4-deficient mice. *Int Immunol* **9**(5), 799-803.

Liljestrom, P., and Garoff, H. (1991). Internally located cleavable signal sequences direct the formation of Semliki Forest virus membrane proteins from a polyprotein precursor. *J Virol* **65**(1), 147-54.

Liljestrom, P., Lusa, S., Huylebroeck, D., and Garoff, H. (1991). In vitro mutagenesis of a full-length cDNA clone of Semliki Forest virus: the small 6,000-molecular-weight membrane protein modulates virus release. *J Virol* **65**(8), 4107-13.

Ling, P. D., Warren, M. K., and Vogel, S. N. (1985). Antagonistic effect of interferon-beta on the interferon-gamma-induced expression of Ia antigen in murine macrophages. *J Immunol* **135**(3), 1857-63.

Linington, C., and Lassmann, H. (1987). Antibody responses in chronic relapsing experimental allergic encephalomyelitis: correlation of serum demyelinating activity with antibody titre to the myelin/oligodendrocyte glycoprotein (MOG). *J Neuroimmunol* **17**(1), 61-9.

Linington, C., Bradl, M., Lassmann, H., Brunner, C., and Vass, K. (1988). Augmentation of demyelination in rat acute allergic encephalomyelitis by circulating mouse monoclonal antibodies directed against a myelin/oligodendrocyte glycoprotein. *Am J Pathol* **130**(3), 443-54.

Linington, C., Berger, T., Perry, L., Weerth, S., Hinze-Selch, D., Zhang, Y., Lu, H. C., Lassmann, H., and Wekerle, H. (1993). T cells specific for the myelin oligodendrocyte glycoprotein mediate an unusual autoimmune inflammatory response in the central nervous system. *Eur J Immunol* **23**(6), 1364-72.

Lobigs, M., and Garoff, H. (1990). Fusion function of the Semliki Forest virus spike is activated by proteolytic cleavage of the envelope glycoprotein precursor p62. *J Virol* **64**(3), 1233-40.

Lobigs, M., Zhao, H. X., and Garoff, H. (1990). Function of Semliki Forest virus E3 peptide in virus assembly: replacement of E3 with an artificial signal peptide

abolishes spike heterodimerization and surface expression of E1. *J Virol* **64**(9), 4346-55.

Loewy, A., Smyth, J., von Bonsdorff, C. H., Liljestrom, P., and Schlesinger, M. J. (1995). The 6-kilodalton membrane protein of Semliki Forest virus is involved in the budding process. *J Virol* **69**(1), 469-75.

Lohse, A. W., Schwerdt, A., Herkel, J., Spahn, T., and Meyer zum Buschenfelde, K. H. (1995). Lack of requirement for CD8+ cells in recovery from and resistance to experimental autoimmune encephalomyelitis. *J Autoimmun* **8**(3), 395-404.

Lubetzki, C., Dubard, T., and Stankoff, B. (1996). [[Therapeutic perspectives in multiple sclerosis]. *Presse Med* **25**(21), 964-6.

Lublin, F. D., Maurer, P. H., Berry, R. G., and Tippett, D. (1981). Delayed, relapsing experimental allergic encephalomyelitis in mice. *J Immunol* **126**(3), 819-22.

Lublin, F. D., Knobler, R. L., Kalman, B., Goldhaber, M., Marini, J., Perrault, M., D'Imperio, C., Joseph, J., Alkan, S. S., and Korngold, R. (1993). Monoclonal anti-gamma interferon antibodies enhance experimental allergic encephalomyelitis. *Autoimmunity* **16**(4), 267-74.

Lublin, F. D., and Reingold, S. C. (1996). Defining the clinical course of multiple sclerosis: results of an international survey. National Multiple Sclerosis Society (USA) Advisory Committee on Clinical Trials of New Agents in Multiple Sclerosis. *Neurology* **46**(4), 907-11.

Lublin, F., Cutter, G., Elfont, R., Khan, O., Lisak, R., and McFarland, H. (2001). A trial to assess the safety of combining therapy with interferon beta-1a and glatiramer acetate in patients with relapsing MS. *Neurology* **56**, 148.

Luca, M. E., Visser, L., Lucas, C. J., and Nagelkerken, L. (1999). IFN-beta modulates specific T cell responses in vitro but does not affect Experimental Autoimmune Encephalomyelitis in the SJL mouse. *J Neuroimmunol* **100**(1-2), 190-6.

Lucchinetti, C. F., Bruck, W., Rodriguez, M., and Lassmann, H. (1996). Distinct patterns of multiple sclerosis pathology indicates heterogeneity on pathogenesis. *Brain Pathol* **6**(3), 259-74.

Lund, J. M., Alexopoulou, L., Sato, A., Karow, M., Adams, N. C., Gale, N. W., Iwasaki, A., and Flavell, R. A. (2004). Recognition of single-stranded RNA viruses by Toll-like receptor 7. *Proc Natl Acad Sci U S A* **101**(15), 5598-603.

Lundstrom, K. (1999). Alphaviruses as tools in neurobiology and gene therapy. *J Recept Signal Transduct Res* **19**(1-4), 673-86.

Lundstrom, K., and Ehrengruber, M. U. (2003). Semliki Forest virus (SFV) vectors in neurobiology and gene therapy. *Methods Mol Med* **76**, 503-23.

Lusa, S., Garoff, H., and Liljestrom, P. (1991). Fate of the 6K membrane protein of Semliki Forest virus during virus assembly. *Virology* **185**(2), 843-6.

Lycke, N., and Strober, W. (1989). Cholera toxin promotes B cell isotype differentiation. *J Immunol* **142**(11), 3781-7.

Lyons, J. A., San, M., Happ, M. P., and Cross, A. H. (1999). B cells are critical to induction of experimental allergic encephalomyelitis by protein but not by a short encephalitogenic peptide. *Eur J Immunol* **29**(11), 3432-9.

Lyons, J. A., Ramsbottom, M. J., and Cross, A. H. (2002). Critical role of antigen-specific antibody in experimental autoimmune encephalomyelitis induced by recombinant myelin oligodendrocyte glycoprotein. *Eur J Immunol* **32**(7), 1905-13.

Maatta, J. A., Kaldman, M. S., Sakoda, S., Salmi, A. A., and Hinkkanen, A. E. (1998). Encephalitogenicity of myelin-associated oligodendrocytic basic protein and 2',3'-cyclic nucleotide 3'-phosphodiesterase for BALB/c and SJL mice. *Immunology* **95**(3), 383-8.

Macnamara, F. N. (1953). The susceptibility of chicks to Semliki Forest virus (Kumba strain). *Ann Trop Med Parasitol* **47**(1), 9-12.

Maimone, D., Gregory, S., Arnason, B. G., and Reder, A. T. (1991). Cytokine levels in the cerebrospinal fluid and serum of patients with multiple sclerosis. *J Neuroimmunol* **32**(1), 67-74.

Margolis, S. A., Oie, H., and Levy, H. B. (1972). The effect of interferon, interferon inducers or interferon induced virus resistance on subsequent interferon production. *J Gen Virol* **15**(2), 119-28.

Markovic-Plese, S., Fukaura, H., Zhang, J., al-Sabbagh, A., Southwood, S., Sette, A., Kuchroo, V. K., and Hafler, D. A. (1995). T cell recognition of immunodominant and cryptic proteolipid protein epitopes in humans. *J Immunol* **155**(2), 982-92.

Martenson, R. E., Deibler, G. E., Kies, M. W., Levine, S., and Alvord, E. C., Jr. (1972). Myelin basic proteins of mammalian and submammalian vertebrates: encephalitogenic activities in guinea pigs and rats. *J Immunol* **109**(2), 262-70.

Martin, D., Near, S. L., Bendele, A., and Russell, D. A. (1995). Inhibition of tumor necrosis factor is protective against neurologic dysfunction after active immunization of Lewis rats with myelin basic protein. *Exp Neurol* **131**(2), 221-8.

Martin, R., and McFarland, H. F. (1995). Immunological aspects of experimental allergic encephalomyelitis and multiple sclerosis. *Crit Rev Clin Lab Sci* **32**(2), 121-82.

Martino, G., and Hartung, H. P. (1999). Immunopathogenesis of multiple sclerosis: the role of T cells. *Curr Opin Neurol* **12**(3), 309-21.

Martino, G., Poliani, P. L., Furlan, R., Marconi, P., Glorioso, J. C., Adorini, L., and Comi, G. (2000a). Cytokine therapy in immune-mediated demyelinating diseases of the central nervous system: a novel gene therapy approach. *J Neuroimmunol* **107**(2), 184-90.

Martino, G., Poliani, P. L., Marconi, P. C., Comi, G., and Furlan, R. (2000b). Cytokine gene therapy of autoimmune demyelination revisited using herpes simplex virus type-1-derived vectors. *Gene Ther* **7**(13), 1087-93.

Martyn, C. N., and Gale, C. R. (1997). The epidemiology of multiple sclerosis. *Acta Neurol Scand Suppl* **169**, 3-7.

Mathiot, C. C., Grimaud, G., Garry, P., Bouquety, J. C., Mada, A., Daguisy, A. M., and Georges, A. J. (1990). An outbreak of human Semliki Forest virus infections in Central African Republic. *Am J Trop Med Hyg* **42**(4), 386-93.

Mathisen, P. M., Yu, M., Johnson, J. M., Drazba, J. A., and Tuohy, V. K. (1997). Treatment of experimental autoimmune encephalomyelitis with genetically modified memory T cells. *J Exp Med* **186**(1), 159-64.

Matsumoto, Y., Ohmori, K., and Fujiwara, M. (1992). Immune regulation by brain cells in the central nervous system: microglia but not astrocytes present myelin basic protein to encephalitogenic T cells under in vivo-mimicking conditions. *Immunology* **76**(2), 209-16.

McDonnell, G. V., and Hawkins, S. A. (1996). Primary progressive multiple sclerosis: a distinct syndrome? *Mult Scler* **2**(3), 137-41.

McGeachy, M. J., and Anderton, S. M. (2005). Cytokines in the induction and resolution of experimental autoimmune encephalomyelitis. *Cytokine* **32**(2), 81-4.

McGeachy, M. J., Stephens, L. A., and Anderton, S. M. (2005). Natural recovery and protection from autoimmune encephalomyelitis: contribution of CD4+CD25+ regulatory cells within the central nervous system. *J Immunol* **175**(5), 3025-32.

McInerney, G. M., Smit, J. M., Liljestrom, P., and Wilschut, J. (2004). Semliki Forest virus produced in the absence of the 6K protein has an altered spike structure as revealed by decreased membrane fusion capacity. *Virology* **325**(2), 200-6.

McIntosh, B. M., Worth, C. B., and Kokernot, R. H. (1961). Isolation of Semliki Forest virus from Aedes (Aedimorphus) argenteopunctatus (Theobald) collected in Portuguese East Africa. *Transfusion (Paris)* **55**, 192-8.

McRae, B. L., Semnani, R. T., Hayes, M. P., and van Seventer, G. A. (1998). Type I IFNs inhibit human dendritic cell IL-12 production and Th1 cell development. *J Immunol* **160**(9), 4298-304.

Meager, A., Parti, S., Leung, H., Woolley, J., Peil, E., Sidhu, S., and Roberts, T. (1987). A two-site sandwich immunoradiometric assay of human lymphotoxin with monoclonal antibodies and its applications. *J Immunol Methods* **104**(1-2), 31-42.

Melancon, P., and Garoff, H. (1986). Reinitiation of translocation in the Semliki Forest virus structural polyprotein: identification of the signal for the E1 glycoprotein. *Embo J* **5**(7), 1551-60.

Melancon, P., and Garoff, H. (1987). Processing of the Semliki Forest virus structural polyprotein: role of the capsid protease. *J Virol* **61**(5), 1301-9.

Mendel, I., Kerlero de Rosbo, N., and Ben-Nun, A. (1995). A myelin oligodendrocyte glycoprotein peptide induces typical chronic experimental autoimmune encephalomyelitis in H-2b mice: fine specificity and T cell receptor V beta expression of encephalitogenic T cells. *Eur J Immunol* **25**(7), 1951-9.

Metsikko, K., and Garoff, H. (1990). Oligomers of the cytoplasmic domain of the p62/E2 membrane protein of Semliki Forest virus bind to the nucleocapsid in vitro. *J Virol* **64**(10), 4678-83.

Milanov, I., Georgiev, D., Kmetska, K., Jordanova, L., and Topalov, N. (1997). Prevalence of multiple sclerosis in Bulgaria. *Neuroepidemiology* **16**(6), 304-7.

Miller, D. H., Rudge, P., Johnson, G., Kendall, B. E., Macmanus, D. G., Moseley, I. F., Barnes, D., and McDonald, W. I. (1988). Serial gadolinium enhanced magnetic resonance imaging in multiple sclerosis. *Brain* **111 (Pt 4)**, 927-39.

Miller, D. J., Bright, J. J., Sriram, S., and Rodriguez, M. (1997). Successful treatment of established relapsing experimental autoimmune encephalomyelitis in mice with a monoclonal natural autoantibody. *J Neuroimmunol* **75**(1-2), 204-9.

Miller, D. J., and Rodriguez, M. (1995). A monoclonal autoantibody that promotes central nervous system remyelination in a model of multiple sclerosis is a natural autoantibody encoded by germline immunoglobulin genes. *J Immunol* **154**(5), 2460-9.

Miller, J. L., and Anders, E. M. (2003). Virus-cell interactions in the induction of type 1 interferon by influenza virus in mouse spleen cells. *J Gen Virol* **84**(Pt 1), 193-202.

Milligan, N. M., Newcombe, R., and Compston, D. A. (1987). A double-blind controlled trial of high dose methylprednisolone in patients with multiple sclerosis: 1. Clinical effects. *J Neurol Neurosurg Psychiatry* **50**(5), 511-6.

Mitchell, G. (1993). Update on multiple sclerosis therapy. *Med Clin North Am* **77**(1), 231-49.

Mokhtarian, F., McFarlin, D. E., and Raine, C. S. (1984). Adoptive transfer of myelin basic protein-sensitized T cells produces chronic relapsing demyelinating disease in mice. *Nature* **309**(5966), 356-8.

Mokhtarian, F., and Swoveland, P. (1987). Predisposition to EAE induction in resistant mice by prior infection with Semliki Forest virus. *J Immunol* **138**(10), 3264-8.

Mokhtarian, F., Wesselingh, S. L., Choi, S., Maeda, A., Griffin, D. E., Sobel, R. A., and Grob, D. (1996). Production and role of cytokines in the CNS of mice with acute viral encephalomyelitis. *J Neuroimmunol* **66**(1-2), 11-22.

Morris, M. M., Dyson, H., Baker, D., Harbige, L. S., Fazakerley, J. K., and Amor, S. (1997). Characterization of the cellular and cytokine response in the central nervous system following Semliki Forest virus infection. *J Neuroimmunol* **74**(1-2), 185-97.

Morris-Downes, M. M., McCormack, K., Baker, D., Sivaprasad, D., Natkunarajah, J., and Amor, S. (2002a). Encephalitogenic and immunogenic potential of myelin-associated glycoprotein (MAG), oligodendrocyte-specific glycoprotein (OSP) and 2',3'-cyclic nucleotide 3'-phosphodiesterase (CNPase) in ABH and SJL mice. *J Neuroimmunol* **122**(1-2), 20-33.

Morris-Downes, M. M., Sheahan, B. J., Fleeton, M. N., Liljestrom, P., Reid, H. W., and Atkins, G. J. (2001). A recombinant Semliki Forest virus particle vaccine encoding the prME and NS1 proteins of louping ill virus is effective in a sheep challenge model. *Vaccine* **19**(28-29), 3877-84.

Morris-Downes, M. M., Smith, P. A., Rundle, J. L., Piddlesden, S. J., Baker, D., Pham-Dinh, D., Heijmans, N., and Amor, S. (2002b). Pathological and regulatory effects of anti-myelin antibodies in experimental allergic encephalomyelitis in mice. *J Neuroimmunol* **125**(1-2), 114-24.

Mossman, S. P., Bex, F., Berglund, P., Arthos, J., O'Neil, S. P., Riley, D., Maul, D. H., Bruck, C., Momin, P., Burny, A., Fultz, P. N., Mullins, J. I., Liljestrom, P., and Hoover, E. A. (1996). Protection against lethal simian immunodeficiency virus SIVsmmPBj14 disease by a recombinant Semliki Forest virus gp160 vaccine and by a gp120 subunit vaccine. *J Virol* **70**(3), 1953-60.

Murphy, A. M., Morris-Downes, M. M., Sheahan, B. J., and Atkins, G. J. (2000). Inhibition of human lung carcinoma cell growth by apoptosis induction using Semliki Forest virus recombinant particles. *Gene Ther* **7**(17), 1477-82.

Murphy, A. M., Sheahan, B. J., and Atkins, G. J. (2001). Induction of apoptosis in BCL-2-expressing rat prostate cancer cells using the Semliki Forest virus vector. *Int J Cancer* **94**(4), 572-8.

Nagelkerken, L., Blauw, B., and Tielemans, M. (1997). IL-4 abrogates the inhibitory effect of IL-10 on the development of experimental allergic encephalomyelitis in SJL mice. *Int Immunol* **9**(9), 1243-51.

Najafian, N., Chitnis, T., Salama, A. D., Zhu, B., Benou, C., Yuan, X., Clarkson, M. R., Sayegh, M. H., and Khoury, S. J. (2003). Regulatory functions of CD8+CD28- T cells in an autoimmune disease model. *J Clin Invest* **112**(7), 1037-48.

Nesbit, G. M., Forbes, G. S., Scheithauer, B. W., Okazaki, H., and Rodriguez, M. (1991). Multiple sclerosis: histopathologic and MR and/or CT correlation in 37 cases at biopsy and three cases at autopsy. *Radiology* **180**(2), 467-74.

Neuhaus, O., Stuve, O., Archelos, J. J., and Hartung, H. P. (2005). Putative mechanisms of action of statins in multiple sclerosis--comparison to interferon-beta and glatiramer acetate. *J Neurol Sci* **233**(1-2), 173-7.

Neuhaus, O., Stuve, O., Zamvil, S. S., and Hartung, H. P. (2004). Are statins a treatment option for multiple sclerosis? *Lancet Neurol* **3**(6), 369-71.

Nieva, J. L., Bron, R., Corver, J., and Wilschut, J. (1994). Membrane fusion of Semliki Forest virus requires sphingolipids in the target membrane. *Embo J* **13**(12), 2797-804.

Nilsson, C., Makitalo, B., Berglund, P., Bex, F., Liljestrom, P., Sutter, G., Erfle, V., ten Haaft, P., Heeney, J., Biberfeld, G., and Thorstensson, R. (2001). Enhanced simian immunodeficiency virus-specific immune responses in macaques induced by priming with recombinant Semliki Forest virus and boosting with modified vaccinia virus Ankara. *Vaccine* **19**(25-26), 3526-36.

Nordstrom, E. K., Forsell, M. N., Barnfield, C., Bonin, E., Hanke, T., Sundstrom, M., Karlsson, G. B., and Liljestrom, P. (2005). Enhanced immunogenicity using an alphavirus replicon DNA vaccine against human immunodeficiency virus type 1. *J Gen Virol* **86**(Pt 2), 349-54.

Noronha, A., Toscas, A., and Jensen, M. A. (1990). Interferon beta augments suppressor cell function in multiple sclerosis. *Ann Neurol* **27**(2), 207-10.

Noronha, A., Toscas, A., and Jensen, M. A. (1992). Contrasting effects of alpha, beta, and gamma interferons on nonspecific suppressor function in multiple sclerosis. *Ann Neurol* **31**(1), 103-6.

Noronha, A., Toscas, A., and Jensen, M. A. (1993). Interferon beta decreases T cell activation and interferon gamma production in multiple sclerosis. *J Neuroimmunol* **46**(1-2), 145-53.

Nygardas, P. T., Gronberg, S. A., Heikkila, J., Joronen, K., Sorsa, T., and Hinkkanen, A. E. (2004). Treatment of experimental autoimmune encephalomyelitis with a neurotropic alphavirus vector expressing tissue inhibitor of metalloproteinase-2. *Scand J Immunol* **60**(4), 372-81.

Okada, K., Kuroda, E., Yoshida, Y., Yamashita, U., Suzumura, A., and Tsuji, S. (2005). Effects of interferon-beta on the cytokine production of astrocytes. *J Neuroimmunol* **159**(1-2), 48-54.

Oksenberg, J. R. (1996). Immunogenetics and heterogeneity in multiple sclerosis. *Ann Neurol* **40**(4), 557-8.

Oksenberg, J. R., and Barcellos, L. F. (2000). The complex genetic aetiology of multiple sclerosis. *J Neurovirol* **6 Suppl 2,** S10-4.

Okuda, Y., Sakoda, S., Bernard, C. C., and Yanagihara, T. (1998). The development of autoimmune encephalomyelitis provoked by myelin oligodendrocyte glycoprotein is associated with an upregulation of both proinflammatory and immunoregulatory cytokines in the central nervous system. *J Interferon Cytokine Res* **18**(6), 415-21.

Olerup, O., and Hillert, J. (1991). HLA class II-associated genetic susceptibility in multiple sclerosis: a critical evaluation. *Tissue Antigens* **38**(1), 1-15.

Oliveira-dos-Santos, A. J., Ho, A., Tada, Y., Lafaille, J. J., Tonegawa, S., Mak, T. W., and Penninger, J. M. (1999). CD28 costimulation is crucial for the development of spontaneous autoimmune encephalomyelitis. *J Immunol* **162**(8), 4490-5.

Olkkonen, V. M., Liljestrom, P., Garoff, H., Simons, K., and Dotti, C. G. (1993). Expression of heterologous proteins in cultured rat hippocampal neurons using the Semliki Forest virus vector. *J Neurosci Res* **35**(4), 445-51.

Owen, K. E., and Kuhn, R. J. (1997). Alphavirus budding is dependent on the interaction between the nucleocapsid and hydrophobic amino acids on the cytoplasmic domain of the E2 envelope glycoprotein. *Virology* **230**(2), 187-96.

Ozawa, K., Suchanek, G., Breitschopf, H., Bruck, W., Budka, H., Jellinger, K., and Lassmann, H. (1994). Patterns of oligodendroglia pathology in multiple sclerosis. *Brain* **117 (Pt 6),** 1311-22.

Palace, J., and Rothwell, P. (1997). New treatments and azathioprine in multiple sclerosis. *Lancet* **350**(9073), 261.

Panitch, H., Miller, A., Paty, D., and Weinshenker, B. (2004). Interferon beta-1b in secondary progressive MS: results from a 3-year controlled study. *Neurology* **63**(10), 1788-95.

Panitch, H. S., Hirsch, R. L., Haley, A. S., and Johnson, K. P. (1987a). Exacerbations of multiple sclerosis in patients treated with gamma interferon. *Lancet* **1**(8538), 893-5.

Panitch, H. S., Hirsch, R. L., Schindler, J., and Johnson, K. P. (1987b). Treatment of multiple sclerosis with gamma interferon: exacerbations associated with activation of the immune system. *Neurology* **37**(7), 1097-102.

Panitch, H. S., and McFarlin, D. E. (1977). Experimental allergic encephalomyelitis: enhancement of cell-mediated transfer by concanavalin A. *J Immunol* **119**(3), 1134-7.

Paolino, E., Fainardi, E., Ruppi, P., Tola, M. R., Govoni, V., Casetta, I., Monetti, V. C., Granieri, E., and Carreras, M. (1996). A prospective study on the predictive value of CSF oligoclonal bands and MRI in acute isolated neurological syndromes for subsequent progression to multiple sclerosis. *J Neurol Neurosurg Psychiatry* **60**(5), 572-5.

Paty, D. W., and Li, D. K. (1993). Interferon beta-1b is effective in relapsing-remitting multiple sclerosis. II. MRI analysis results of a multicenter, randomized, double-blind, placebo-controlled trial. UBC MS/MRI Study Group and the IFNB Multiple Sclerosis Study Group. *Neurology* **43**(4), 662-7.

Peranen, J. (1991). Localization and phosphorylation of Semliki Forest virus non-structural protein nsP3 expressed in COS cells from a cloned cDNA. *J Gen Virol* **72 (Pt 1),** 195-9.

Peranen, J., and Kaariainen, L. (1991). Biogenesis of type I cytopathic vacuoles in Semliki Forest virus-infected BHK cells. *J Virol* **65**(3), 1623-7.

Peranen, J., Takkinen, K., Kalkkinen, N., and Kaariainen, L. (1988). Semliki Forest virus-specific non-structural protein nsP3 is a phosphoprotein. *J Gen Virol* **69 (Pt 9),** 2165-78.

Perrin, P. J., Scott, D., Quigley, L., Albert, P. S., Feder, O., Gray, G. S., Abe, R., June, C. H., and Racke, M. K. (1995). Role of B7:CD28/CTLA-4 in the induction of chronic relapsing experimental allergic encephalomyelitis. *J Immunol* **154**(3), 1481-90.

Pestka, S., Langer, J. A., Zoon, K. C., and Samuel, C. E. (1987). Interferons and their actions. *Annu Rev Biochem* **56,** 727-77.

Peterson, P. K., and Remington, J. S. (2000). "New concepts in the immunopathogenesis of CNS infections." Astrocytes and the neuroimmunological role of IL-6 (E. N. B. a. N. J. V. Wagoner, Ed.) Oxford: Blackwell Science, Malden.

Pettinelli, C. B., and McFarlin, D. E. (1981). Adoptive transfer of experimental allergic encephalomyelitis in SJL/J mice after in vitro activation of lymph node cells by myelin basic protein: requirement for Lyt 1+ 2- T lymphocytes. *J Immunol* **127**(4), 1420-3.

Phalen, T., and Kielian, M. (1991). Cholesterol is required for infection by Semliki Forest virus. *J Cell Biol* **112**(4), 615-23.

Piccirillo, C. A., and Prud'homme, G. J. (1999). Prevention of experimental allergic encephalomyelitis by intramuscular gene transfer with cytokine-encoding plasmid vectors. *Hum Gene Ther* **10**(12), 1915-22.

Piccirillo, C. A., and Prud'homme, G. J. (2003). Immune modulation by plasmid DNA-mediated cytokine gene transfer. *Curr Pharm Des* **9**(1), 83-94.

Poliani, P. L., Brok, H., Furlan, R., Ruffini, F., Bergami, A., Desina, G., Marconi, P. C., Rovaris, M., Uccelli, A., Glorioso, J. C., Penna, G., Adorini, L., Comi, G., t Hart, B., and Martino, G. (2001). Delivery to the central nervous system of a nonreplicative herpes simplex type 1 vector engineered with the interleukin 4 gene protects rhesus monkeys from hyperacute autoimmune encephalomyelitis. *Hum Gene Ther* **12**(8), 905-20.

Porrini, A. M., Gambi, D., and Reder, A. T. (1995). Interferon effects on interleukin-10 secretion. Mononuclear cell response to interleukin-10 is normal in multiple sclerosis patients. *J Neuroimmunol* **61**(1), 27-34.

Porrini, A. M., and Reder, A. T. (1994). IFN-gamma, IFN-beta, and PGE1 affect monokine secretion: relevance to monocyte activation in multiple sclerosis. *Cell Immunol* **157**(2), 428-38.

Poser, C. M. (1995). Viking voyages: the origin of multiple sclerosis? An essay in medical history. *Acta Neurol Scand Suppl* **161**, 11-22.

Poskanzer, D. C., Walker, A. M., Prenney, L. B., and Sheridan, J. L. (1981). The etiology of multiple sclerosis: temporal-spatial clustering indicating two environmental exposures before onset. *Neurology* **31**(6), 708-13.

Prineas, J. W., Kwon, E. E., Goldenberg, P. Z., Ilyas, A. A., Quarles, R. H., Benjamins, J. A., and Sprinkle, T. J. (1989). Multiple sclerosis. Oligodendrocyte proliferation and differentiation in fresh lesions. *Lab Invest* **61**(5), 489-503.

Prud'homme, G. J. (2000). Gene therapy of autoimmune diseases with vectors encoding regulatory cytokines or inflammatory cytokine inhibitors. *J Gene Med* **2**(4), 222-32.

Prud'homme, G. J., and Piccirillo, C. A. (2000). The inhibitory effects of transforming growth factor-beta-1 (TGF-beta1) in autoimmune diseases. *J Autoimmun* **14**(1), 23-42.

Qin, X. Q., Tao, N., Dergay, A., Moy, P., Fawell, S., Davis, A., Wilson, J. M., and Barsoum, J. (1998). Interferon-beta gene therapy inhibits tumor formation and causes regression of established tumors in immune-deficient mice. *Proc Natl Acad Sci U S A* **95**(24), 14411-6.

Raine, C. S. (1983). Multiple sclerosis and chronic relapsing EAE: comparative ultrastructural neuropathology. *In* "Multiple sclerosis" (W. W. Tourtellotte, Ed.), pp. 413-478. Williams & Wilkins, Baltimore.

Raine, C. S. (1984). Biology of disease. Analysis of autoimmune demyelination: its impact upon multiple sclerosis. *Lab Invest* **50**(6), 608-35.

Raine, C. S., Cannella, B., Hauser, S. L., and Genain, C. P. (1999). Demyelination in primate autoimmune encephalomyelitis and acute multiple sclerosis lesions: a case for antigen-specific antibody mediation. *Ann Neurol* **46**(2), 144-60.

Raine, C. S., and Scheinberg, L. C. (1988). On the immunopathology of plaque development and repair in multiple sclerosis. *J Neuroimmunol* **20**(2-3), 189-201.

Raine, C. S., Snyder, D. H., Stone, S. H., and Bronstein, M. B. (1977). Suppression of acute and chronic experimental allergic encephalomyelitis in Strain 13 guinea pigs. A clinical and pathological study. *J Neurol Sci* **31**(3), 355-67.

Raju, R., and Huang, H. V. (1991). Analysis of Sindbis virus promoter recognition in vivo, using novel vectors with two subgenomic mRNA promoters. *J Virol* **65**(5), 2501-10.

Ren, H., Boulikas, T., Lundstrom, K., Soling, A., Warnke, P. C., and Rainov, N. G. (2003). Immunogene therapy of recurrent glioblastoma multiforme with a liposomally encapsulated replication-incompetent Semliki forest virus vector carrying the human interleukin-12 gene--a phase I/II clinical protocol. *J Neurooncol* **64**(1-2), 147-54.

Renno, T., Taupin, V., Bourbonniere, L., Verge, G., Tran, E., De Simone, R., Krakowski, M., Rodriguez, M., Peterson, A., and Owens, T. (1998). Interferon-gamma in progression to chronic demyelination and neurological deficit following acute EAE. *Mol Cell Neurosci* **12**(6), 376-89.

Rep, M. H., Hintzen, R. Q., Polman, C. H., and van Lier, R. A. (1996). Recombinant interferon-beta blocks proliferation but enhances interleukin-10 secretion by activated human T-cells. *J Neuroimmunol* **67**(2), 111-8.

Rep, M. H., Schrijver, H. M., van Lopik, T., Hintzen, R. Q., Roos, M. T., Ader, H. J., Polman, C. H., and van Lier, R. A. (1999). Interferon (IFN)-beta treatment enhances CD95 and interleukin 10 expression but reduces interferon-gamma producing T cells in MS patients. *J Neuroimmunol* **96**(1), 92-100.

Rice, G. P. A. (2001). The use of Betaseron in treatment of MS 17th European Committee for Treatment and Research in Multiple Sclerosis (ECTRIMS). *Dublin, Ireland.*

Rivers, T. M., Sprunt, D. H., and Berry, G. P. (1933). Observations on attempts to produce acute disseminated encephalomyelitis in monkeys. *J Exp Med* **58**, 39-53.

Rizzo, J. F., 3rd, and Lessell, S. (1988). Risk of developing multiple sclerosis after uncomplicated optic neuritis: a long-term prospective study. *Neurology* **38**(2), 185-90.

Robertson, N. P., Fraser, M., Deans, J., Clayton, D., Walker, N., and Compston, D. A. (1996). Age-adjusted recurrence risks for relatives of patients with multiple sclerosis. *Brain* **119 (Pt 2)**, 449-55.

Rodriguez, M., and Scheithauer, B. (1994). Ultrastructure of multiple sclerosis. *Ultrastruct Pathol* **18**(1-2), 3-13.

Rodriguez-Madoz, J. R., Prieto, J., and Smerdou, C. (2005). Semliki forest virus vectors engineered to express higher IL-12 levels induce efficient elimination of murine colon adenocarcinomas. *Mol Ther* **12**(1), 153-63.

Rott, O., Fleischer, B., and Cash, E. (1994). Interleukin-10 prevents experimental allergic encephalomyelitis in rats. *Eur J Immunol* **24**(6), 1434-40.

Ruddle, N. H., Bergman, C. M., McGrath, K. M., Lingenheld, E. G., Grunnet, M. L., Padula, S. J., and Clark, R. B. (1990). An antibody to lymphotoxin and tumor

necrosis factor prevents transfer of experimental allergic encephalomyelitis. *J Exp Med* **172**(4), 1193-200.

Rudick, R. A., Ransohoff, R. M., Lee, J. C., Peppler, R., Yu, M., Mathisen, P. M., and Tuohy, V. K. (1998). In vivo effects of interferon beta-1a on immunosuppressive cytokines in multiple sclerosis. *Neurology* **50**(5), 1294-300.

Ruuls, S. R., de Labie, M. C., Weber, K. S., Botman, C. A., Groenestein, R. J., Dijkstra, C. D., Olsson, T., and van der Meide, P. H. (1996). The length of treatment determines whether IFN-beta prevents or aggravates experimental autoimmune encephalomyelitis in Lewis rats. *J Immunol* **157**(12), 5721-31.

Sadovnick, A. D., Ebers, G. C., Dyment, D. A., and Risch, N. J. (1996). Evidence for genetic basis of multiple sclerosis. The Canadian Collaborative Study Group. *Lancet* **347**(9017), 1728-30.

Sagawa, K., Mochizuki, M., Sugita, S., Nagai, K., Sudo, T., and Itoh, K. (1996). Suppression by IL-10 and IL-4 of cytokine production induced by two-way autologous mixed lymphocyte reaction. *Cytokine* **8**(6), 501-6.

Sakai, K., Zamvil, S. S., Mitchell, D. J., Lim, M., Rothbard, J. B., and Steinman, L. (1988). Characterization of a major encephalitogenic T cell epitope in SJL/J mice with synthetic oligopeptides of myelin basic protein. *J Neuroimmunol* **19**(1-2), 21-32.

Salminen, A., Wahlberg, J. M., Lobigs, M., Liljestrom, P., and Garoff, H. (1992). Membrane fusion process of Semliki Forest virus. II: Cleavage-dependent reorganization of the spike protein complex controls virus entry. *J Cell Biol* **116**(2), 349-57.

Sammin, D. J., Butler, D., Atkins, G. J., and Sheahan, B. J. (1999). Cell death mechanisms in the olfactory bulb of rats infected intranasally with Semliki forest virus. *Neuropathol Appl Neurobiol* **25**(3), 236-43.

Samoilova, E. B., Horton, J. L., and Chen, Y. (1998). Acceleration of experimental autoimmune encephalomyelitis in interleukin-10-deficient mice: roles of interleukin-10 in disease progression and recovery. *Cell Immunol* **188**(2), 118-24.

Santambrogio, L., Crisi, G. M., Leu, J., Hochwald, G. M., Ryan, T., and Thorbecke, G. J. (1995). Tolerogenic forms of auto-antigens and cytokines in the induction of resistance to experimental allergic encephalomyelitis. *J Neuroimmunol* **58**(2), 211-22.

Sariola, M., Saraste, J., and Kuismanen, E. (1995). Communication of post-Golgi elements with early endocytic pathway: regulation of endoproteolytic cleavage of Semliki Forest virus p62 precursor. *J Cell Sci* **108 (Pt 6)**, 2465-75.

Sawicki, D. L., Kaariainen, L., Lambek, C., and Gomatos, P. J. (1978). Mechanism for control of synthesis of Semliki Forest virus 26S and 42s RNA. *J Virol* **25**(1), 19-27.

Sawicki, D. L., and Sawicki, S. G. (1980). Short-lived minus-strand polymerase for Semliki Forest virus. *J Virol* **34**(1), 108-18.

Scallan, M. F., Allsopp, T. E., and Fazakerley, J. K. (1997). bcl-2 acts early to restrict Semliki Forest virus replication and delays virus-induced programmed cell death. *J Virol* **71**(2), 1583-90.

Schmidt, J., Sturzebecher, S., Toyka, K. V., and Gold, R. (2001). Interferon-beta treatment of experimental autoimmune encephalomyelitis leads to rapid nonapoptotic termination of T cell infiltration. *J Neurosci Res* **65**(1), 59-67.

Schulz, O., Diebold, S. S., Chen, M., Naslund, T. I., Nolte, M. A., Alexopoulou, L., Azuma, Y. T., Flavell, R. A., Liljestrom, P., and Reis e Sousa, C. (2005). Toll-like receptor 3 promotes cross-priming to virus-infected cells. *Nature* **433**(7028), 887-92.

Sedgwick, J. D. (1988). Long-term depletion of CD8+ T cells in vivo in the rat: no observed role for CD8+ (cytotoxic/suppressor) cells in the immunoregulation of experimental allergic encephalomyelitis. *Eur J Immunol* **18**(4), 495-502.

Seamer, J., Randles, W. J., and Fitzgeorge, R. (1967). The course of Semliki Forest virus infection in mice. *Br J Exp Pathol* **48**(4), 395-402.

Segal, B. M., Dwyer, B. K., and Shevach, E. M. (1998). An interleukin (IL)-10/IL-12 immunoregulatory circuit controls susceptibility to autoimmune disease. *J Exp Med* **187**(4), 537-46.

Segal, B. M., and Shevach, E. M. (1996). IL-12 unmasks latent autoimmune disease in resistant mice. *J Exp Med* **184**(2), 771-5.

Shaw, M. K., Lorens, J. B., Dhawan, A., DalCanto, R., Tse, H. Y., Tran, A. B., Bonpane, C., Eswaran, S. L., Brocke, S., Sarvetnick, N., Steinman, L., Nolan, G. P., and Fathman, C. G. (1997). Local delivery of interleukin 4 by retrovirus-transduced T lymphocytes ameliorates experimental autoimmune encephalomyelitis. *J Exp Med* **185**(9), 1711-4.

Sheahan, B. J., Barrett, P. N., and Atkins, G. J. (1981). Demyelination in mice resulting from infection with a mutant of Semliki Forest virus. *Acta Neuropathol (Berl)* **53**(2), 129-36.

Shrikant, P., and Benveniste, E. N. (1996). The central nervous system as an immunocompetent organ: role of glial cells in antigen presentation. *J Immunol* **157**(5), 1819-22.

Sibley, W. (1993). The IFNB Multiple Sclerosis Study Group, Interferon beta-1b is effective in relapsing-remitting multiple sclerosis: I. Clinical results of a multicenter, randomized, double-blind, placebo-controlled trial,. *Neurology* **43**, 655-661.

Simmons, R. D., and Willenborg, D. O. (1990). Direct injection of cytokines into the spinal cord causes autoimmune encephalomyelitis-like inflammation. *J Neurol Sci* **100**(1-2), 37-42.

Simons, K., and Garoff, H. (1980). The budding mechanisms of enveloped animal viruses. *J Gen Virol* **50**(1), 1-21.

Singh, I., and Helenius, A. (1992). Role of ribosomes in Semliki Forest virus nucleocapsid uncoating. *J Virol* **66**(12), 7049-58.

Sjoberg, E. M., and Garoff, H. (1996). The translation-enhancing region of the Semliki Forest virus subgenome is only functional in the virus-infected cell. *J Gen Virol* **77 (Pt 6)**, 1323-7.

Sjoberg, E. M., Suomalainen, M., and Garoff, H. (1994). A significantly improved Semliki Forest virus expression system based on translation enhancer segments from the viral capsid gene. *Biotechnology (N Y)* **12**(11), 1127-31.

Skoging, U., Vihinen, M., Nilsson, L., and Liljestrom, P. (1996). Aromatic interactions define the binding of the alphavirus spike to its nucleocapsid. *Structure* **4**(5), 519-29.

Slavin, A., Ewing, C., Liu, J., Ichikawa, M., Slavin, J., and Bernard, C. C. (1998). Induction of a multiple sclerosis-like disease in mice with an immunodominant epitope of myelin oligodendrocyte glycoprotein. *Autoimmunity* **28**(2), 109-20.

Smerdou, C., and Liljestrom, P. (1999). Two-helper RNA system for production of recombinant Semliki forest virus particles. *J Virol* **73**(2), 1092-8.

Smithburn, K. C., and Haddow, A. J. (1944). Semliki Forest virus. Isolation and pathogenic properties. *j immunol* **49**, 141-173.

Smyth, J. M., Sheahan, B. J., and Atkins, G. J. (1990). Multiplication of virulent and demyelinating Semliki Forest virus in the mouse central nervous system: consequences in BALB/c and SJL mice. *J Gen Virol* **71 (Pt 11)**, 2575-83.

Smyth, J. W., Fleeton, M. N., Sheahan, B. J., and Atkins, G. J. (2005). Treatment of rapidly growing K-BALB and CT26 mouse tumours using Semliki Forest virus and its derived vector. *Gene Ther* **12**(2), 147-59.

Snijders, A., Benaissa-Trouw, B. J., Snippe, H., and Kraaijeveld, C. A. (1992). Immunogenicity and vaccine efficacy of synthetic peptides containing Semliki Forest virus B and T cell epitopes. *J Gen Virol* **73 (Pt 9)**, 2267-72.

Soderlund, H. (1973). Kinetics of formation of the Semliki Forest virus nucleocapsid. *Intervirology* **1**(5-6), 354-61.

Soderstrom, M., Ya-Ping, J., Hillert, J., and Link, H. (1998). Optic neuritis: prognosis for multiple sclerosis from MRI, CSF, and HLA findings. *Neurology* **50**(3), 708-14.

Soilu-Hanninen, M., Eralinna, J. P., Hukkanen, V., Roytta, M., Salmi, A. A., and Salonen, R. (1994). Semliki Forest virus infects mouse brain endothelial cells and causes blood-brain barrier damage. *J Virol* **68**(10), 6291-8.

Sriram, S., Mitchell, W., and Stratton, C. (1998). Multiple sclerosis associated with Chlamydia pneumoniae infection of the CNS. *Neurology* **50**(2), 571-2.

Stanwick, T. L., and Hallum, J. V. (1974). Role of interferon in six cell lines persistently infected with rubella virus. *Infect Immun* **10**(4), 810-5.

Stollar, V. (1980). Defective interfering alphaviruses. *In* "The Togaviruses" (R. W. Schlesinger, Ed.), pp. 427-457. Academic Press, New York.

Strauss, J. H., and Strauss, E. G. (1994). "The Alphaviruses: gene expression, replication and evolution." Microbiol. Rev, 58.

Subak-Sharpe, I., Dyson, H., and Fazakerley, J. (1993). In vivo depletion of CD8+ T cells prevents lesions of demyelination in Semliki Forest virus infection. *J Virol* **67**(12), 7629-33.

Sun, D., Newman, T. A., Perry, V. H., and Weller, R. O. (2004). Cytokine-induced enhancement of autoimmune inflammation in the brain and spinal cord: implications for multiple sclerosis. *Neuropathol Appl Neurobiol* **30**(4), 374-84.

Sun, D., Whitaker, J. N., Huang, Z., Liu, D., Coleclough, C., Wekerle, H., and Raine, C. S. (2001). Myelin antigen-specific CD8+ T cells are encephalitogenic and produce severe disease in C57BL/6 mice. *J Immunol* **166**(12), 7579-87.

Sun, J., Link, H., Olsson, T., Xiao, B. G., Andersson, G., Ekre, H. P., Linington, C., and Diener, P. (1991a). T and B cell responses to myelin-oligodendrocyte glycoprotein in multiple sclerosis. *J Immunol* **146**(5), 1490-5.

Sun, J. B. (1993). Autoreactive T and B cells in nervous system diseases. *Acta Neurol Scand Suppl* **142**, 1-56.

Sun, J. B., Olsson, T., Wang, W. Z., Xiao, B. G., Kostulas, V., Fredrikson, S., Ekre, H. P., and Link, H. (1991b). Autoreactive T and B cells responding to myelin proteolipid protein in multiple sclerosis and controls. *Eur J Immunol* **21**(6), 1461-8.

Sun, J. B., Rask, C., Olsson, T., Holmgren, J., and Czerkinsky, C. (1996). Treatment of experimental autoimmune encephalomyelitis by feeding myelin basic protein conjugated to cholera toxin B subunit. *Proc Natl Acad Sci U S A* **93**(14), 7196-201.

Sun, J. B., Xiao, B. G., Lindblad, M., Li, B. L., Link, H., Czerkinsky, C., and Holmgren, J. (2000). Oral administration of cholera toxin B subunit conjugated to myelin basic protein protects against experimental autoimmune encephalomyelitis by inducing transforming growth factor-beta-secreting cells and suppressing chemokine expression. *Int Immunol* **12**(10), 1449-57.

Suomalainen, M., and Garoff, H. (1992). Alphavirus spike-nucleocapsid interaction and network antibodies. *J Virol* **66**(8), 5106-9.

Suzumura, A., Mezitis, S. G., Gonatas, N. K., and Silberberg, D. H. (1987). MHC antigen expression on bulk isolated macrophage-microglia from newborn mouse brain: induction of Ia antigen expression by gamma-interferon. *J Neuroimmunol* **15**(3), 263-78.

Swingler, R. J., and Compston, D. (1986). The distribution of multiple sclerosis in the United Kingdom. *J Neurol Neurosurg Psychiatry* **49**(10), 1115-24.

Takacs, K., Chandler, P., and Altmann, D. M. (1997). Relapsing and remitting experimental allergic encephalomyelitis: a focused response to the encephalitogenic peptide rather than epitope spread. *Eur J Immunol* **27**(11), 2927-34.

Takacs, K., Douek, D. C., and Altmann, D. M. (1995). Exacerbated autoimmunity associated with a T helper-1 cytokine profile shift in H-2E-transgenic mice. *Eur J Immunol* **25**(11), 3134-41.

Takkinen, K. (1986). Complete nucleotide sequence of the nonstructural protein genes of Semliki Forest virus. *Nucleic Acids Res* **14**(14), 5667-82.

Takkinen, K., Peranen, J., and Kaariainen, L. (1991). Proteolytic processing of Semliki Forest virus-specific non-structural polyprotein. *J Gen Virol* **72 (Pt 7)**, 1627-33.

Takkinen, K., Peranen, J., Keranen, S., Soderlund, H., and Kaariainen, L. (1990). The Semliki-Forest-virus-specific nonstructural protein nsP4 is an autoproteinase. *Eur J Biochem* **189**(1), 33-8.

Teige, I., Treschow, A., Teige, A., Mattsson, R., Navikas, V., Leanderson, T., Holmdahl, R., and Issazadeh-Navikas, S. (2003). IFN-beta gene deletion leads to augmented and chronic demyelinating experimental autoimmune encephalomyelitis. *J Immunol* **170**(9), 4776-84.

Tilg, H., Trehu, E., Atkins, M. B., Dinarello, C. A., and Mier, J. W. (1994). Interleukin-6 (IL-6) as an anti-inflammatory cytokine: induction of circulating IL-1 receptor antagonist and soluble tumor necrosis factor receptor p55. *Blood* **83**(1), 113-8.

Tovey, M. G., Begon-Lours, J., and Gresser, I. (1974). A method for the large scale production of potent interferon preparations. *Proc Soc Exp Biol Med* **146**(3), 809-15.

Trapp, B. D., Peterson, J., Ransohoff, R. M., Rudick, R., Mork, S., and Bo, L. (1998). Axonal transection in the lesions of multiple sclerosis. *N Engl J Med* **338**(5), 278-85.

Traugott, U., and Lebon, P. (1988). Interferon-gamma and Ia antigen are present on astrocytes in active chronic multiple sclerosis lesions. *J Neurol Sci* **84**(2-3), 257-64.

Triantaphyllopoulos, K., Croxford, J., Baker, D., and Chernajovsky, Y. (1998). Cloning and expression of murine IFN beta and a TNF antagonist for gene therapy of experimental allergic encephalomyelitis. *Gene Ther* **5**(2), 253-63.

Trinchieri, G. (1998). Interleukin-12: a cytokine at the interface of inflammation and immunity. *Adv Immunol* **70**, 83-243.

Trinchieri, G., Pflanz, S., and Kastelein, R. A. (2003). The IL-12 family of heterodimeric cytokines: new players in the regulation of T cell responses. *Immunity* **19**(5), 641-4.

Tuohy, V. K., Yu, M., Yin, L., Mathisen, P. M., Johnson, J. M., and Kawczak, J. A. (2000). Modulation of the IL-10/IL-12 cytokine circuit by interferon-beta inhibits the development of epitope spreading and disease progression in murine autoimmune encephalomyelitis. *J Neuroimmunol* **111**(1-2), 55-63.

Ulmanen, I., Soderlund, H., and Kaariainen, L. (1976). Semliki Forest virus capsid protein associates with the 60S ribosomal subunit in infected cells. *J Virol* **20**(1), 203-10.

Vaha-Koskela, M. J., Tuittila, M. T., Nygardas, P. T., Nyman, J. K., Ehrengruber, M. U., Renggli, M., and Hinkkanen, A. E. (2003). A novel neurotropic expression vector based on the avirulent A7(74) strain of Semliki Forest virus. *J Neurovirol* **9**(1), 1-15.

van der Meide, P. H., de Labie, M. C., Ruuls, S. R., Groenestein, R. J., Botman, C. A., Olsson, T., and Dijkstra, C. D. (1998). Discontinuation of treatment with IFN-beta leads to exacerbation of experimental autoimmune encephalomyelitis in Lewis rats. Rapid reversal of the antiproliferative activity of IFN-beta and excessive expansion of autoreactive T cells as disease promoting mechanisms. *J Neuroimmunol* **84**(1), 14-23.

van der Veen, R. C., Trotter, J. L., Clark, H. B., and Kapp, J. A. (1989). The adoptive transfer of chronic relapsing experimental allergic encephalomyelitis with lymph node cells sensitized to myelin proteolipid protein. *J Neuroimmunol* **21**(2-3), 183-91.

Van Wagoner, N. J., Oh, J. W., Repovic, P., and Benveniste, E. N. (1999). Interleukin-6 (IL-6) production by astrocytes: autocrine regulation by IL-6 and the soluble IL-6 receptor. *J Neurosci* **19**(13), 5236-44.

van Walderveen, M. A., Barkhof, F., Hommes, O. R., Polman, C. H., Tobi, H., Frequin, S. T., and Valk, J. (1995). Correlating MRI and clinical disease activity in multiple sclerosis: relevance of hypointense lesions on short-TR/short-TE (T1-weighted) spin-echo images. *Neurology* **45**(9), 1684-90.

Venien-Bryan, C., and Fuller, S. D. (1994). The organization of the spike complex of Semliki Forest virus. *J Mol Biol* **236**(2), 572-83.

Vogel, R. H., Provencher, S. W., von Bonsdorff, C. H., Adrian, M., and Dubochet, J. (1986). Envelope structure of Semliki Forest virus reconstructed from cryo-electron micrographs. *Nature* **320**(6062), 533-5.

Voorthuis, J. A., Uitdehaag, B. M., De Groot, C. J., Goede, P. H., van der Meide, P. H., and Dijkstra, C. D. (1990). Suppression of experimental allergic encephalomyelitis by intraventricular administration of interferon-gamma in Lewis rats. *Clin Exp Immunol* **81**(2), 183-8.

Wahlberg, J. M., Boere, W. A., and Garoff, H. (1989). The heterodimeric association between the membrane proteins of Semliki Forest virus changes its sensitivity to low pH during virus maturation. *J Virol* **63**(12), 4991-7.

Wahlberg, J. M., Bron, R., Wilschut, J., and Garoff, H. (1992). Membrane fusion of Semliki Forest virus involves homotrimers of the fusion protein. *J Virol* **66**(12), 7309-18.

Wahlberg, J. M., and Garoff, H. (1992). Membrane fusion process of Semliki Forest virus. I: Low pH-induced rearrangement in spike protein quaternary structure precedes virus penetration into cells. *J Cell Biol* **116**(2), 339-48.

Wahlfors, J. J., Zullo, S. A., Loimas, S., Nelson, D. M., and Morgan, R. A. (2000). Evaluation of recombinant alphaviruses as vectors in gene therapy. *Gene Ther* **7**(6), 472-80.

Waksman, B., and Morrison, L. (1951). Tuberculin type hypersensitivity to spinal cord antigen in rabbits with isoallergic encephalomyelitis. *J. Immunol.* **66**, 421-444.

Waksman, B. H., Porter, H., Lees, M. D., Adams, R. D., and Folch, J. (1954). A study of the chemical nature of components of bovine white matter effective in producing allergic encephalomyelitis in the rabbit. *J Exp Med* **100**, 451-471.

Walther, E. U., Dietrich, E., and Hohlfeld, R. (1996). [Therapy of multiple sclerosis with interferon-beta-1b. Educating the patient and managing side-effects]. *Nervenarzt* **67**(6), 452-6.

Wang, L. Y., and Fujinami, R. S. (1997). Enhancement of EAE and induction of autoantibodies to T-cell epitopes in mice infected with a recombinant vaccinia virus encoding myelin proteolipid protein. *J Neuroimmunol* **75**(1-2), 75-83.

Wang, X., Chen, M., Wandinger, K. P., Williams, G., and Dhib-Jalbut, S. (2000). IFN-beta-1b inhibits IL-12 production in peripheral blood mononuclear cells in an IL-10-dependent mechanism: relevance to IFN-beta-1b therapeutic effects in multiple sclerosis. *J Immunol* **165**(1), 548-57.

Weiner, H. L., Mackin, G. A., Orav, E. J., Hafler, D. A., Dawson, D. M., LaPierre, Y., Herndon, R., Lehrich, J. R., Hauser, S. L., Turel, A., and et al. (1993). Intermittent cyclophosphamide pulse therapy in progressive multiple sclerosis: final report of the Northeast Cooperative Multiple Sclerosis Treatment Group. *Neurology* **43**(5), 910-8.

Weinshenker, B. G. (1995). The natural history of multiple sclerosis. *Neurol Clin* **13**(1), 119-46.

Weinshenker, B. G. (1996). Epidemiology of multiple sclerosis. *Neurol Clin* **14**(2), 291-308.

Weinshenker, B. G., Bass, B., Rice, G. P., Noseworthy, J., Carriere, W., Baskerville, J., and Ebers, G. C. (1989a). The natural history of multiple sclerosis: a geographically based study. 2. Predictive value of the early clinical course. *Brain* **112 (Pt 6)**, 1419-28.

Weinshenker, B. G., Bass, B., Rice, G. P., Noseworthy, J., Carriere, W., Baskerville, J., and Ebers, G. C. (1989b). The natural history of multiple sclerosis: a geographically based study. I. Clinical course and disability. *Brain* **112 (Pt 1)**, 133-46.

White, C. L., Thomson, M., and Dimmock, N. J. (1998). Deletion analysis of a defective interfering Semliki Forest virus RNA genome defines a region in the nsP2 sequence that is required for efficient packaging of the genome into virus particles. *J Virol* **72**(5), 4320-6.

Willems, W. R., Kaluza, G., Boschek, C. B., Bauer, H., Hager, H., Schutz, H. J., and Feistner, H. (1979). Semliki forest virus: cause of a fatal case of human encephalitis. *Science* **203**(4385), 1127-9.

Willenborg, D. O., Fordham, S., Bernard, C. C., Cowden, W. B., and Ramshaw, I. A. (1996). IFN-gamma plays a critical down-regulatory role in the induction and effector phase of myelin oligodendrocyte glycoprotein-induced autoimmune encephalomyelitis. *J Immunol* **157**(8), 3223-7.

Willenborg, D. O., Fordham, S. A., Cowden, W. B., and Ramshaw, I. A. (1995). Cytokines and murine autoimmune encephalomyelitis: inhibition or enhancement of disease with antibodies to select cytokines, or by delivery of exogenous cytokines using a recombinant vaccinia virus system. *Scand J Immunol* **41**(1), 31-41.

Willenborg, D. O., and Prowse, S. J. (1983). Immunoglobulin-deficient rats fail to develop experimental allergic encephalomyelitis. *J Neuroimmunol* **5**(2), 99-109.

Williams, N. A., Hirst, T. R., and Nashar, T. O. (1999). Immune modulation by the cholera-like enterotoxins: from adjuvant to therapeutic. *Immunol Today* **20**(2), 95-101.

Windhagen, A., Newcombe, J., Dangond, F., Strand, C., Woodroofe, M. N., Cuzner, M. L., and Hafler, D. A. (1995). Expression of costimulatory molecules B7-1 (CD80), B7-2 (CD86), and interleukin 12 cytokine in multiple sclerosis lesions. *J Exp Med* **182**(6), 1985-96.

Wolf, S. D., Dittel, B. N., Hardardottir, F., and Janeway, C. A., Jr. (1996). Experimental autoimmune encephalomyelitis induction in genetically B cell-deficient mice. *J Exp Med* **184**(6), 2271-8.

Wu, L. X., Makela, M. J., Roytta, M., and Salmi, A. (1988). Effect of viral infection on experimental allergic encephalomyelitis in mice. *J Neuroimmunol* **18**(2), 139-53.

Xiao, B. G., Bai, X. F., Zhang, G. X., and Link, H. (1998). Suppression of acute and protracted-relapsing experimental allergic encephalomyelitis by nasal administration of low-dose IL-10 in rats. *J Neuroimmunol* **84**(2), 230-7.

Xu, L. Y., Yang, J. S., Huang, Y. M., Levi, M., Link, H., and Xiao, B. G. (2000). Combined nasal administration of encephalitogenic myelin basic protein peptide 68-86 and IL-10 suppressed incipient experimental allergic encephalomyelitis in Lewis rats. *Clin Immunol* **96**(3), 205-11.

Xu-Amano, J., Jackson, R. J., Fujihashi, K., Kiyono, H., Staats, H. F., and McGhee, J. R. (1994). Helper Th1 and Th2 cell responses following mucosal or systemic immunization with cholera toxin. *Vaccine* **12**(10), 903-11.

Yamanaka, R., Zullo, S. A., Ramsey, J., Yajima, N., Tsuchiya, N., Tanaka, R., Blaese, M., and Xanthopoulos, K. G. (2002). Marked enhancement of antitumor immune responses in mouse brain tumor models by genetically modified dendritic cells producing Semliki Forest virus-mediated interleukin-12. *J Neurosurg* **97**(3), 611-8.

Yasuda, C. L., Al-Sabbagh, A., Oliveira, E. C., Diaz-Bardales, B. M., Garcia, A. A., and Santos, L. M. (1999). Interferon beta modulates experimental autoimmune encephalomyelitis by altering the pattern of cytokine secretion. *Immunol Invest* **28**(2-3), 115-26.

Yong, V. W., Chabot, S., Stuve, O., and Williams, G. (1998). Interferon beta in the treatment of multiple sclerosis: mechanisms of action. *Neurology* **51**(3), 682-9.

Yong, V. W., Moumdjian, R., Yong, F. P., Ruijs, T. C. G., Freedman, M. S., Cashman, N., and Angel, J. P. (1991). γ-interferon promotes proliferation of adult human astrocytes in vitro and reactive gliosis in the adult mouse brain in vivo. *Proc Natl Acad Sci U S A* **88**, 7016-7020.

Yoshimura, T., Kunishita, T., Sakai, K., Endoh, M., Namikawa, T., and Tabira, T. (1985). Chronic experimental allergic encephalomyelitis in guinea pigs induced by proteolipid protein. *J Neurol Sci* **69**(1-2), 47-58.

Young, D. A., Lowe, L. D., Booth, S. S., Whitters, M. J., Nicholson, L., Kuchroo, V. K., and Collins, M. (2000). IL-4, IL-10, IL-13, and TGF-beta from an altered peptide ligand-specific Th2 cell clone down-regulate adoptive transfer of experimental autoimmune encephalomyelitis. *J Immunol* **164**(7), 3563-72.

Youssef, S., Stuve, O., Patarroyo, J. C., Ruiz, P. J., Radosevich, J. L., Hur, E. M., Bravo, M., Mitchell, D. J., Sobel, R. A., Steinman, L., and Zamvil, S. S. (2002). The HMG-CoA reductase inhibitor, atorvastatin, promotes a Th2 bias and reverses paralysis in central nervous system autoimmune disease. *Nature* **420**(6911), 78-84.

Yu, M., Nishiyama, A., Trapp, B. D., and Tuohy, V. K. (1996). Interferon-beta inhibits progression of relapsing-remitting experimental autoimmune encephalomyelitis. *J Neuroimmunol* **64**(1), 91-100.

Yudkin, P. L., Ellison, G. W., Ghezzi, A., Goodkin, D. E., Hughes, R. A., McPherson, K., Mertin, J., and Milanese, C. (1991). Overview of azathioprine treatment in multiple sclerosis. *Lancet* **338**(8774), 1051-5.

Yuki, Y., Byun, Y., Fujita, M., Izutani, W., Suzuki, T., Udaka, S., Fujihashi, K., McGhee, J. R., and Kiyono, H. (2001). Production of a recombinant hybrid molecule of cholera toxin-B-subunit and proteolipid-protein-peptide for the treatment of experimental encephalomyelitis. *Biotechnol Bioeng* **74**(1), 62-9.

Yura, M., Takahashi, I., Terawaki, S., Hiroi, T., Kweon, M. N., Yuki, Y., and Kiyono, H. (2001). Nasal administration of cholera toxin (CT) suppresses clinical signs of experimental autoimmune encephalomyelitis (EAE). *Vaccine* **20**(1-2), 134-9.

Zamvil, S., Nelson, P., Trotter, J., Mitchell, D., Knobler, R., Fritz, R., and Steinman, L. (1985). T-cell clones specific for myelin basic protein induce chronic relapsing paralysis and demyelination. *Nature* **317**(6035), 355-8.

Zang, Y. C., Li, S., Rivera, V. M., Hong, J., Robinson, R. R., Breitbach, W. T., Killian, J., and Zhang, J. Z. (2004). Increased CD8+ cytotoxic T cell responses to myelin basic protein in multiple sclerosis. *J Immunol* **172**(8), 5120-7.

Zhang, B., Harness, J., Somodevilla-Torres, M. J., Hillyard, N. C., Mould, A. W., Alewood, D., Love, S. G., Alewood, P. F., Greer, J. M., Cavanagh, A. C., McCombe, P. A., and Morton, H. (2000). Early pregnancy factor suppresses experimental autoimmune encephalomyelitis induced in Lewis rats with myelin basic protein and in SJL/J mice with myelin proteolipid protein peptide 139-151. *J Neurol Sci* **182**(1), 5-15.

Zhang, J., Asselin-Paturel, C., Bex, F., Bernard, J., Chehimi, J., Willems, F., Caignard, A., Berglund, P., Liljestrom, P., Burny, A., and Chouaib, S. (1997). Cloning of human IL-12 p40 and p35 DNA into the Semliki Forest virus vector: expression of IL-12 in human tumor cells. *Gene Ther* **4**(4), 367-74.

Zhang, J., Markovic-Plese, S., Lacet, B., Raus, J., Weiner, H. L., and Hafler, D. A. (1994). Increased frequency of interleukin 2-responsive T cells specific for myelin basic protein and proteolipid protein in peripheral blood and cerebrospinal fluid of patients with multiple sclerosis. *J Exp Med* **179**(3), 973-84.

Zhang, X., Koldzic, D. N., Izikson, L., Reddy, J., Nazareno, R. F., Sakaguchi, S., Kuchroo, V. K., and Weiner, H. L. (2004). IL-10 is involved in the suppression of experimental autoimmune encephalomyelitis by CD25+CD4+ regulatory T cells. *Int Immunol* **16**(2), 249-56.